EARLY DETECTION OF DEMENTIA USING THE HUMAN ELECTROENCEPHALOGRAM

G. T. Henderson

Ph.D.   2004

EARLY DETECTION OF DEMENTIA USING THE HUMAN ELECTROENCEPHALOGRAM

By

GEOFFREY T HENDERSON

A thesis submitted to the University of Plymouth
in partial fulfilment of the degree of

DOCTOR OF PHILOSOPHY

School of Computing, Communication and Electronics
Faculty of Technology

In collaboration with
Department of Neurophysiology
Derriford Hospital
Plymouth

December 2004

Early Detection Of Dementia Using The Human Electroencephalogram

Geoffrey T Henderson

Abstract

Improved life expectancy has led to a significant increase in the number of people in the high-risk age groups that will develop Alzheimer's disease and other dementia. Efforts are being made to develop treatments that slow the progress of these diseases. However, unless a sufferer is diagnosed in the early stages the treatments cannot give the maximum benefit. Therefore, there is an urgent need for a practical, decision support tool that will enable the earliest possible detection of dementia within the large at-risk population.

Current techniques such as Magnetic Resonance Imaging (MRI) that are used to diagnose and assess neurological disorders require specialist equipment and expert clinicians to interpret results. Such techniques are inappropriate as a method of detecting individual subjects with early dementia within the large at-risk population, because everyone within the at-risk group would need to be tested regularly and this would carry a very high cost. Therefore, it is desirable to develop a low cost method of assessment.

This thesis describes research into the use of automated EEG analysis to provide the required testing for dementia. The research begins with a review of previous automated EEG analysis, particularly fractal dimension measures. Initial investigation into the nature of the fractal dimension of the EEG are conducted, including problems encountered when applying fractal measures in affine space. More appropriate fractal methods were evaluated and the most promising of these methods was blind tested using an independent clinical data set. This method was estimated to achieve 67% sensitivity to probable early Alzheimer's disease and 17% sensitivity to vascular dementia (as confirmed by a clinical neurophysiologist from the EEG) with a specificity of 99.9%.

The thesis also describes a fundamental study of the assumed fractal nature of the EEG. It is shown that the fractal nature of the EEG (should it exist at all) is not contributory to the success of fractal dimension measures. From this, it is concluded that the EEG is unlikely to be a fractal. However, the previous success of the fractal methods is important and is likely to be because they detected a related characteristic of the EEG. Two novel methods, which build upon this conclusion and the initial investigations, are reported. The first novel method, applying Allan Variance analysis to the EEG, was unsuccessful but the second method, based on the Probability Density Function of the Zero Crossing Intervals, was more promising. This second method was estimated to achieve 78% sensitivity to probable early Alzheimer's disease and 35% sensitivity to vascular dementia (as confirmed by a clinical neurophysiologist from the EEG) with a specificity of 99.9%. This compares well with a more conventional Alpha/Theta power spectral ratio measure, which was estimated to achieve 50% sensitivity to probable early Alzheimer's disease and 11% sensitivity to vascular dementia with the same data.

The EEG recordings used to assess the methods included artefacts and had no *á priori* selection of elements 'suitable for analysis': This approach gives a good prediction of the usefulness of the techniques, as it would be used in practice. It is noteworthy that the probable Alzheimer's subjects were not previously diagnosed and were therefore in the early stages of exhibiting symptoms.

This thesis also discusses and reports on investigations into subject specific EEG analysis, which may be used as an adjunct to most methods. This analysis moves away from group comparisons that separate individuals into groups (Normal, Alzheimer's, Parkinson's etc.) using indices derived from isolated (snapshot) EEGs and instead compares an EEG to those taken previously from the same subject. It is shown that by looking for trends in indices that arise over time rather than comparing an EEG to what is generally normal within the population the efficacy of a method is improved. In the near future, strategies such as this will become increasingly practical as information technology enabled e-medicine improves.

This research provides a basis for the development of a practical, affordable method, which will detect dementia before there is significant mental decline. Such a method, administered by GPs, for example, as part of a normal check-up, in conjunction with new therapies to slow the progression of dementia could provide many people with years of higher quality life.

Author's Declaration

At no time during the registration for the degree of Doctor of Philosophy has the author been registered for any other University award. This research was funded in part by BAE SYSTEMS.

This Thesis contains approximately 49,500 words.

Publications:

1. Henderson G T, Wu P, Ifeachor E C and Wimalaratna H S K (1998) Subject specific variability of the Fractal Dimension of the Human Electroencephalogram. Proc. Third Int. Conf. On Neural Networks and Expert Systems in Medicine and Healthcare, University of Pisa, pp. 322-330. ISBN 981-02-3611-5.

2. Henderson G T, Ifeachor E C, Wimalaratna H S K, Allen E M and Hudson N R (2000) Prospects for routine detection of dementia using the fractal dimension of the human electroencephalogram. Proc. International Conference on Advances in Medical Signal and Information Processing. Bristol, IEE Conf. Pub. No. 476, pp. 284-289.

3. Henderson G T, Ifeachor E C, Wimalaratna H S K, Allen E M and Hudson N R (2000) Prospects for routine detection of dementia using the fractal dimension of the human electroencephalogram. IEE Proc.-Sci. Meas. Technol., vol. 147 (6), pp. 321-326.

4. Henderson G T, Ifeachor E C, Wimalaratna H S K, Allen E M and Hudson N R (2002) Electroencephalogram-Based methods for routine detection of dementia. Proc. IV International Workshop on Biosignal Interpretation, Polytechnic University Milano, pp. 319-322.

5. Ifeachor E C, Outram N J, Henderson G T, Wimalaratna H S K, Hudson N, Sneyd R, Dong C and Bigan C (2004) Non-linear methods for biopattern analysis: role and challenges, Proc. of the 26th annual international conf. of the IEEE EMBS. San Francisco.

Signed ....

Date ... 8th July 2005

v

Acknowledgements

Table of Contents

List of Figures

List of Tables

List of Abbreviations and Glossary

AD   Alzheimer's Disease

CAT   Computerised Axial Tomography

CDF   Cumulative Density Function

CDROM   Compact Disk Read Only Memory

cps   cycle per second

ECG   Electrocardiogram

EEG   Electroencephalogram

FD   Fractal Dimension

FFT   Fast Fourier Transform

GP   General Practitioner

MRI   Magnetic Resonance Imaging

PC   Personal Computer

PDF   Probability Density Function

PET   Positron Emission Tomography

Ph.D.   Doctor of Philosophy

PSD   Power Spectral Density

rms   root mean square

SD   Standard Deviation

UK   United Kingdom

USA   United States of America

Vol   Volunteer

Chapter 1. Introduction

1.1 Motivations

1.1.1 Early Detection of Dementia

Improved life expectancy [1] has led to a significant increase in the number of people in the high-risk age groups that will develop Alzheimer's disease and other dementia [2]. Some drugs already exist that slow the progression of Cerebrovascular diseases (such as Multi-Infarct) and efforts are being made to develop treatments (such as the Acetylcholinesterase inhibitors; Tacrine, Donepezil and Exelon) which may slow the progress of the Alzheimer's Disease [3], [4]. However, unless a sufferer is diagnosed in the early stages, the treatments, which only slow the development of dementia, cannot give the maximum benefit by extending the time before significant mental decline occurs [5]. A study of Alzheimer's Disease related Cortical Atrophy in the Lancet [6] showed the period between the onset of Alzheimer's disease and meeting the current clinical criteria was between 3 and 5 years. Therefore, there is an urgent need for a practical decision support tool that will enable the earliest detection of dementia within the large population of people at risk.

A further constraint is cost. To illustrate this one may consider current techniques such as Magnetic Resonance Imaging (MRI) and Positron Emission Tomography (PET) that are used to diagnose and assess neurological disorders. These require specialist equipment and expert clinicians to interpret results and are inappropriate as a method of detecting individual subjects with early dementia within the large at-risk population. This is because everyone within the at-risk group would need to be tested regularly and this would carry a high cost.

In summary, it is desirable to develop a low cost method of assessment, which can be carried out quickly by a non-specialist clinician. Such a method, in concert with drugs that slow the progression of Alzheimer's Disease and Cerebrovascular disease, could prolong the symptom free state and give patients an additional number of years of higher quality life.

1.1.2   Other Implications

Success in this area of research could have implications beyond early detection of dementia and provide further clinical benefits for patients, GPs, researchers and clinicians. Some examples are given below:

1.1.2.1   Clinical Care Of Patients with Dementia

An automated method for detecting and quantifying changes that occur as a result of brain dysfunction would allow clinicians to:

- quantify the progression of brain disease; allowing carers, patients and their families to understand the situation and address it appropriately

- assess suitability for specific treatment options

- assess the effectiveness of prescribed treatment

Periodic analysis of the same subject would allow the clinician to understand how a particular patient is progressing relative to previous results (improving, declining, etc.) rather than placing them in an absolute categorisation of level relative to typical normal subjects or typical subjects with dementia.

1.1.2.2 A Test For Safe Driving

Every year many older drivers in the UK are required by their motor insurance company to have a medical examination. Normally, the General Practitioner is asked to certify that they are physically able to drive safely. However, the neurological aspects are difficult because the GP has no effective test for early dementia without referring the patient for further checks. In this situation the GP has to come to a decision based on his subjective opinion whilst recognising the danger presented to the public by a dementing driver and also recognising the negative effect on an older person if their independent mobility is reduced. In these situations a straight forward automated method for detecting and quantifying changes that occur as a result of brain dysfunction would be a welcome aid.

1.1.2.3 Standardisation Of Clinical Results

Human interpretation of the EEG is recognised to have brought benefit to patients but there are benefits to providing a standardised measure that would come from automated analysis. Such a measure would be useful to aid communication between clinicians.

1.1.2.4 Provide A Measure Of General Brain Damage

If it is possible that the use of an automated method for detecting and quantifying changes, which occur as a result of brain dysfunction, it may be extended to quantify the damage done to the brain under some conditions such as microwave irradiation from mobile phone usage or damage from highly physical sports such as boxing.

1.2 Statement of Problem

Analysis of the electrical activity of the brain (the Electroencephalogram or EEG) is seen as a possible way to provide an acceptable and affordable method for early detection of dementia. It is well known that disorders of the brain are accompanied by changes in the EEG and the EEG has long been used in diagnosis of neurological disorders but this generally requires subjective interpretation.

The problem, addressed in this research, is to automate EEG analysis such that early changes due to dementia can be reliably detected before the development of clinically significant mental decline.

Whilst stating this problem, it is necessary to recognise that a great deal of effort has previously been expended in the pursuit of automated EEG analysis and there are few, if any successful automated methods in routine clinical practice.

1.3   Aim and objectives

The aim of this PhD is to contribute to the development an automated EEG analysis method that could be used by non-specialist clinicians (i.e. General Practitioners) to detect the early stages of dementia during routine health checks of older patients. One can envisage in the Doctor's surgery, a hardware module that provides the interface between electrodes on the subjects scalp and desktop PC running some specialist software. To do this, it is necessary to develop an objective, reliable, robust, automated method for detecting and quantifying changes in the EEG that occur as a result of dementia. This is a challenge because the EEG is a complex, non-stationary signal that varies between subjects and is affected by the subjects condition (age, wakefulness, disease, etc.) as well as being affected by stimuli such as light in the eye, sounds applied to the ear or the sensation of pain.

The objectives of this PhD are:

- Critically review published research into automated EEG analysis, particularly in the area of fractal dimension, which appeared to show most promise.

- Develop a mathematically sound fractal dimension method and test it against a given, small sample data set.

- Conduct a blind test of the fractal dimension method on an independent, larger set of data and determine whether the new method is likely to detect dementia in the target, older population before the development of clinically significant mental decline.

- If it is not possible to use the fractal dimension then develop one or more novel method of analysis, which could clearly distinguish between normal and subjects with dementia.

- Examine the subject specific nature of the EEG and determine whether this could help in the detection of dementia and in patient-care.

1.4 Contributions of thesis

This thesis makes the following contributions to knowledge:

- This research demonstrates that previously published methods using the fractal dimension of the EEG are not wholly appropriate because the EEG exists within affine space.

- The performance of a number of fractal dimension methods, which had not previously been applied to the EEG but were appropriate for use with signals that lie in affine space, are investigated, tested and reported in the literature. These methods were developed using a small, pre-existing data set and then blind tested with a new, larger set of independently collected data.

- This research questions the fractal nature of the EEG and demonstrates that the fractal nature of the EEG (should any exists) does not contribute to the success of fractal dimension measures. From this, it is concluded that the EEG is very unlikely to be a fractal. The previous success of fractal methods is due to the detail of the EEG power spectral density and a natural robustness to artefacts.

- A novel method is developed (using the initial small data set) which builds on the previous work during this research using the Allan Variance of the EEG. Results are presented which quantify the capabilities of the new method using the initial small data set. Results are also presented from a larger, blind trial that used data from a hospital EEG database. These results demonstrate that this is not a viable method although the initial indications were good.

- A second novel method is developed using the probability density function of the zero crossing intervals. Results are presented which quantify the capabilities of the new method using the initial small data set. Results are also presented from a larger, blind trial that used data from a hospital EEG database which show that the estimated sensitivity to early probable Alzheimer's disease is 78% and estimated sensitivity to early probable Cerebrovascular disease (confirmed by a clinical neurophysiologist from the EEG) is 35% with a specificity of 99.9%

The majority of the work reported in this Thesis has been published in peer-reviewed conference and journal papers [7], [8], [9] and [10]. A final paper summarising the whole body of work has been submitted to the IEEE transactions journal.

Aside from these contributions to knowledge, the research has led to:

- The production of a large body of software (in Borland Turbo C++ and Microsoft Visual C++) which can access 3 different EEG data formats, display the raw or processed EEG in an easy to use application without the need for en expensive reader station and performs all of the analyses used in this research.

- The collation of a significant database of EEG records that may be used in future work.

1.5   Outline of thesis

This Thesis begins with an introduction (this Chapter) and a background chapter (Chapter 2) which discusses; the current state of knowledge of the Human EEG (section 2.2), fractal theory (in brief, section 2.3), diagnostic performance measures (section 2.4) and the state of the art in Automated EEG analysis (section 0).

Chapter 3 describes detailed investigations into the nature of fractal dimension measures. Fractal dimension measures were chosen because it was felt that these were most likely to contribute to the development of a means of detecting Dementia from the EEG. This Chapter discusses; previously published fractal dimension methods, fractal dimension methods suitable for affine space, subject specific measures, Alpha/Theta ratio determined from the fractal dimension, the time progression of the fractal dimension and the variability of the fractal dimension over the scalp. Section 3.8 records work that questions whether it was right to compute the fractal dimension of the Auto-correlation of the EEG.

Chapter 4 describes a clinical evaluation that tested whether the selected method could provide adequate sensitivity and specificity to be useful in practice. The Chapter begins by describing the preparatory work where method parameters were fixed (otherwise, it could be said that the assessment of the method was not a fair test and that retrospectively applied parameterisation favourably skewed the results). Following this, the main trial is described. Other previously discussed methods and issues are revisited (e.g. subject specific measures).

Following on from the trial, Chapter 5 questions whether the EEG is in-fact a fractal. Based on this conclusion Chapter 6 suggests further methods that may be more appropriate. The results from testing these novel methods are also discussed.

Finally, this Thesis ends with a conclusion and suggestions for future work (Chapter 7) and a list of references (Chapter 8). There are also appendices to describe the software that was written.

Chapter 2.   Background

2.1   Introduction

This chapter describes the background to the research and provides references to other published work.

This thesis is concerned with the early detection of dementia using the Human EEG because the EEG provides a low-cost, practical method of studying brain function and has been used by clinicians for many years to diagnose dementia. This chapter begins, in section 2.2, with a description of the Human EEG; how it is measured, the problems associated with the EEG (such as artefacts), and how clinicians have interpreted the EEG.

The chapter continues, in section 2.3, by describing fractals, chaos and complexity. These subjects, and particularly their application to the Human EEG, are important because concepts adopted from these areas of knowledge have recently been shown to indicate the presence of dementia.

The chapter also discusses diagnostic performance measures in section 2.4.

Finally, section 2.5, provides a brief review of the state of the art in automated EEG analysis (including fractal, chaos and complexity measures).

8

2.2 The Human Electroencephalogram

2.2.1 Introduction

The Electroencephalogram (EEG) is a record of the electrical activity of the brain. This is normally measured from electrodes on the surface of the scalp, although surgically implanted electrodes are sometimes used to provide improved signal strength and localisation. In this research, only recordings taken from the scalp are considered because implanted electrodes would be unacceptably invasive for the early detection of dementia.

Since the EEG was first recorded in 1924, it has become an important clinical tool providing information about the activity of the brain, its condition and possible disease. Research into the nature of the EEG has revealed that it is a complex, non-stationary electrical potential that varies over the surface of the scalp (and throughout the brain). Furthermore, the EEG is affected by the subjects condition (age, wakefulness, disease, etc.) as well as being affected by stimuli such as light in the eye, sounds applied to the ear or the sensation of pain.

2.2.2 Electrode Montage

EEG records used in this research are from electrodes mounted on the scalp using the standard 10/20 system for electrode placement [11] (or the modified Maudsley system, which is similar to the 10/20 system). The 10/20 system is illustrated in Figures 2-1, 2-2 and 2-3 and it uses either 19 or 21 electrodes (sometime electrodes A1 and A2 are not required). Three referencing methods are commonly used:

1. Bipolar: Measurements made between selected pairs of electrodes.

2. Common reference: Measurements taken between electrodes and a reference that is chosen to be least affected by interference, such as the ear lobes (A1 and A2).

3. Common average reference: Measurements taken between electrodes and the mean of the other electrodes used.

9

Using electrodes on the scalp is convenient and non-invasive (unlike electrodes implanted in the brain), but these electrical potentials are small (in the order of 10 to 300 microVolts). Therefore, it is necessary to use accurate, sensitive equipment to measure the EEG signals. These data are normally recorded graphically on long strips of paper or electronically on magnetic media.
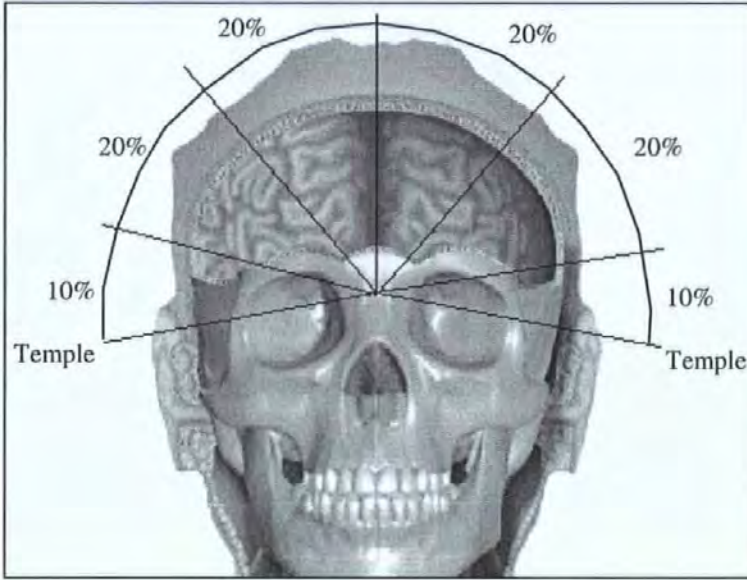
Figure 2-1, Frontal view of electrode placement.
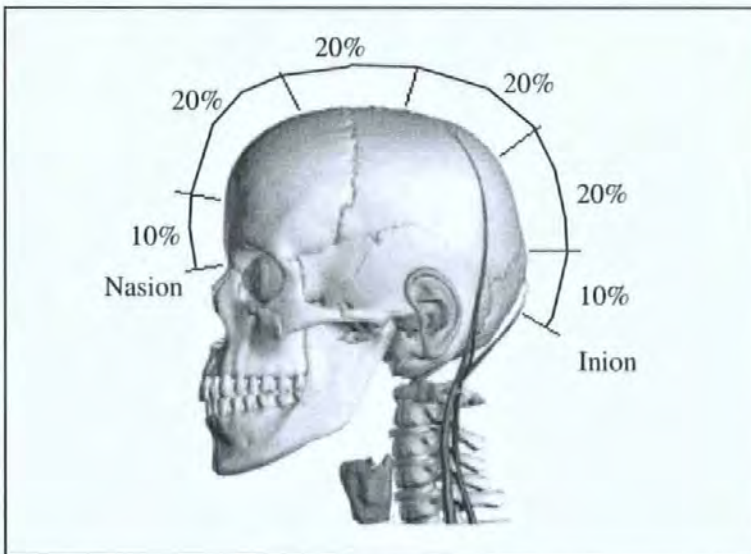
Figure 2-2, Side view of electrode placement.
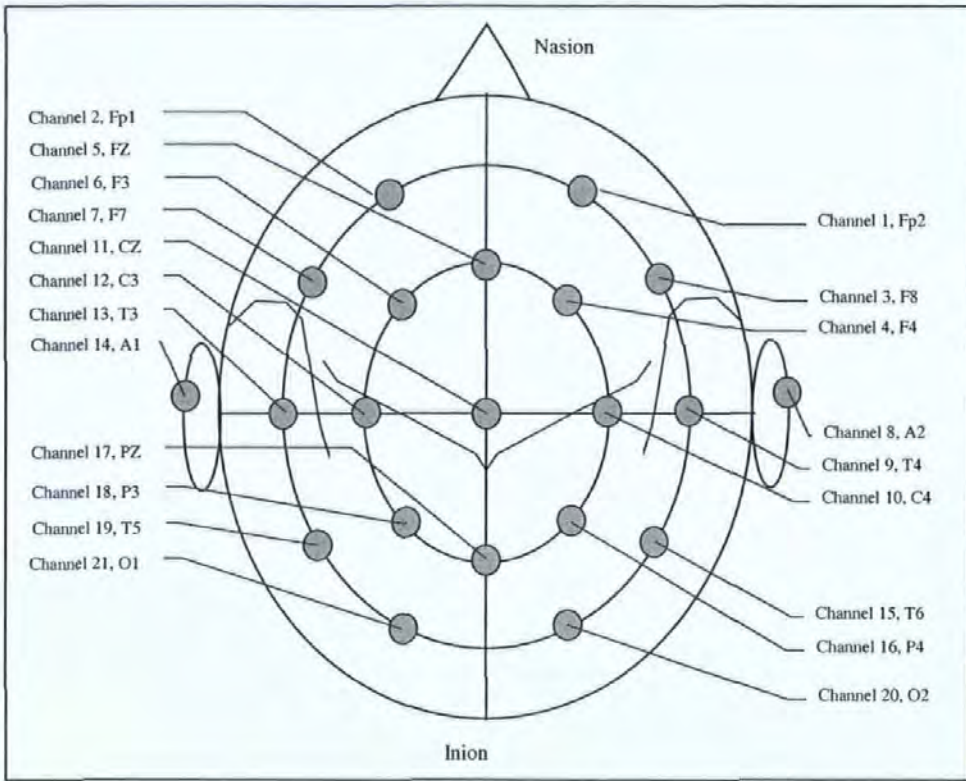
Figure 2-3, Schematic plan view of electrode placement.

A typical display of a 21 electrode common average montage EEG is shown in Figure 2-4.
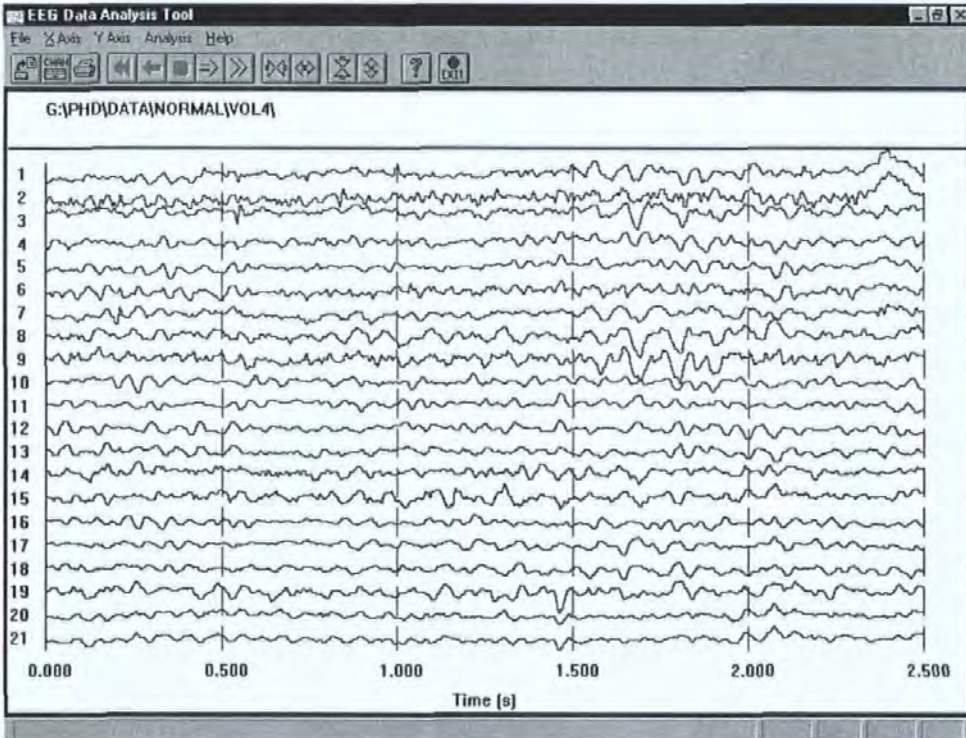
Figure 2-4, Typical EEG display.

11

2.2.3 Artefacts

Artefacts are those signals present in the measured EEG signal that are not of cerebral origin. These originate from a number of sources, both internal and external to the body. Internal sources of artefact are cardiac activity and electrical activity in the muscles of the head (tongue and eye movement or blinking). External sources of artefact may be mains interference or poor, intermittent electrode contact. Artefacts are unhelpful and present significant challenges in EEG analysis.

2.2.4 Human Interpretation

The EEG is normally presented for human interpretation with little pre-processing other than simple band-pass filtering. The EEG is typically drawn on a long strip of paper. This printout and other patient data are studied by a clinician who, using years of training and experience, comes to a diagnosis.

According to Dondey [12], the EEGer interprets an EEG using the following four steps. First, the EEG trace is mentally cut into 'graphic elements'; where 'graphic elements' refer to the elementary patterns that constitute an EEG. Second, based upon the observation of the temporal evolution of potential differences between different pairs of electrodes, one obtains a mental representation of the overall variations observed in the EEG. In the third step, differentiation between artefacts and EEG activity takes place, based on experience. Finally, the significant EEG activities are identified.

Ktonas [13] gives a very good introduction to EEG features and there significance. The most common are:

α activity,   found most strongly in awake relaxed subjects with eyes closed, 8 to 12 cycles per second (cps), quasi-sinusoidal, amplitude 20 to 60μV, strongest in posterior areas of the brain, tends to wax and wane over 1 to 2 seconds forming a 'spindle'.

β activity,   found most strongly in awake attentive subjects, may be present but masked when α activity is present, prominent mainly in central and frontal regions, quasi-sinusoidal, 18 to 24 cps, up to 20μV.

θ activity,   found in drowsy subjects and in some stages of sleep, occurs as bursts of quasi-sinusoidal activity or as single waves, 4 to 7 cps, 50 to 200μV.

δ activity,   found in drowsy subjects and in some stages of sleep, occurs as bursts of quasi-sinusoidal activity or as single waves, 0.5 to 3 cps, 50 to 200μV.

σ spindles,   found in onset of sleep (stage 2), bursts of quasi-sinusoidal activity, 12 to 16 cps.

K complexes, found in onset of sleep (stage 2), single cycle of slow activity, about 1 cps, amplitude distinctly above background.

Spike or Spike-and-Wave. Characteristic of epileptogenic activity, spike has less than 80 milli-second duration, average maximum slope approximately 8μV/milli-second

Slowing.   Disease or injury to the brain causes a slowing of normal activities.

Symmetry.   The healthy human EEG is remarkably symmetrical with respect to the mid-line of the brain in form and spectral content.

It is noted that the effectiveness of EEG analysis is limited because only about one third of the cerebrum can be viewed by non-surgical EEG techniques. Thus, slowly developing lesions, atrophic processes, subdural haematomas, and diseases causing demyelination (loss of myelinated sheath covering the neurones) may produce little or no EEG abnormality. Also, one quarter of all deep cerebral tumours exhibit normal EEG. Diseases such as dementia that affect large areas of the brain are detectable from the EEG. Alzheimer's disease affects all EEG channels in a generalised way although the posterior region is more affected whereas cerebrovascular disease has more defined foci.

2.3 Fractals, Chaos and Complexity

2.3.1 Introduction

The origins of fractal geometry can be traced back to the nineteenth century, but it was in 1975 that the first unifying treatment was given by Benoit B. Mandelbrot [14], a Polish born mathematician. Fractal geometry is the most versatile tool so far discovered for describing and modelling forms that occur in nature; forms that Euclidean geometry cannot describe.

This section introduces the terms "Fractal", "Chaos" and "Complexity", which describe complex, non-linear systems.

2.3.2 Fractals

2.3.2.1 Introduction

Euclidean (and similar) geometries have been used historically to describe mathematically shapes; spheres, quadrilaterals, triangles, hypercubes, etc. However, it was known that shapes that generally occur in nature (terrain, coastlines, trees, etc) have shapes that cannot be described using these "simple" shapes. In the mid-1960s Mandelbrot proposed a way to describe these shapes and named them fractals. The definition of fractal has changed over the years. Mandelbrot, who coined the term, has retracted and replaced his original definition [15]. Now it is generally accepted to refer to a shape whose parts are in some way similar to the whole.

2.3.2.2 An Example

In introducing fractals, it is convenient to begin with an example. This example was conceived by Helge von Koch [17]. The so-called Koch curve may be constructed by taking an equilateral triangle and then on each side add another equilateral triangle to cover the middle third of the line. This is then repeated with smaller and smaller triangles (see Figure 2-5).
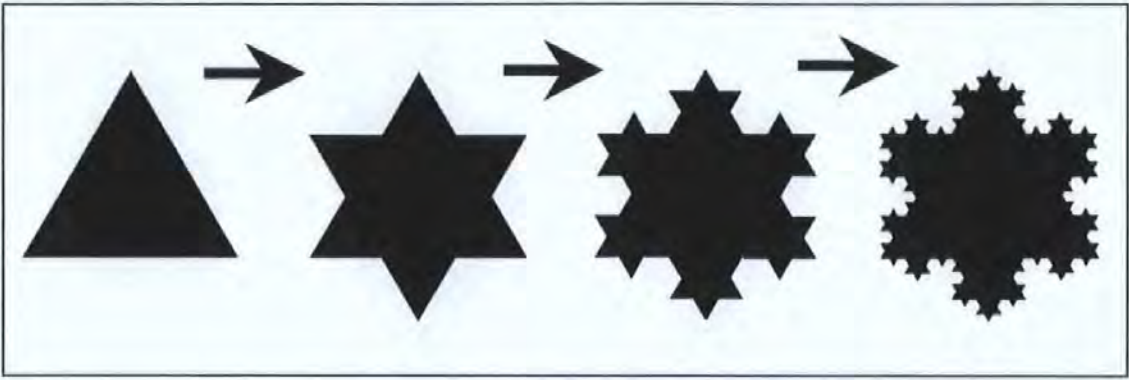
Figure 2-5, Construction of a fractal - the Koch Curve.
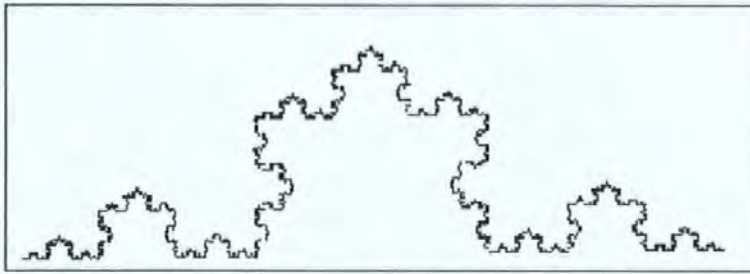
Figure 2-6, Image of one side of the Koch Curve.

The Koch curve reveals an interesting paradox; each time new triangles are added the total length of the outline becomes larger by a factor of 4/3 and therefore the total length of the outline tends to infinity even though the area of the curve remains less than the area of a circle drawn around the original triangle and is therefore finite. Fractal geometry, which was invented to describe shapes such as the Koch curve, it assigns a non-integer (or fractal) dimension. For the Koch curve, the fractal dimension is 1.26.

2.3.2.3   Definition of Fractal Dimension

There are at least 10 definitions of dimension [16], although most are similar. Of these the topological dimension is perhaps the most familiar. Defined in terms of homeomorphisms (permitted topological transformations), it is an integral measure such that finite arcs have a topological dimension of 1, surfaces, 2 and solid bodies 3.

A generally accepted inductive definition of topological dimension is:

If the boundaries of arbitrarily small neighbourhoods of all points in a space are (n-1) dimensional, then the space is n-dimensional. The empty set, and only the empty set, has dimension minus one.

This definition is accurate but difficult to understand. Taking a square as an example, any point within the square has a boundary that is a closed (circular) line. Therefore, a square has one more dimension than a line. Furthermore, any point on the line has a boundary that comprises two points and similarly the boundary to the points is the empty set. Thus, working back to the square; the empty set has dimension -1, the set of points has dimension 0, the line has dimension 1 and the square has dimension 2.

Many of the definitions of dimension (other than topological dimension), and much of Mandelbrot's work on fractals, are based on the Hausdorff dimension, which was first proposed in 1919. A complete definition of the Hausdorff dimension is given by Addison [15]. An overview is given below.

A fractal is characterised by a number of dimensions which is greater than the topological dimension and this dimension need not be integer. To understand the non-integer dimension it is convenient to consider the Koch curve where a single dimension is not sufficient to describe a point on the outline because the length is infinite and 2 dimensions would be too much because the outline does not have an area: Thus the number of dimensions needed to describe it is between 1 and 2 (in fact the dimension is 1.26).

Consider a smooth curve of length L that has a topological dimension D_T of 1. The length of the curve may be estimated by covering it with N small line segments of length δ, where N would be a function of δ. See Figure 2-7. Now is L would be given by:

$$L = \lim_{\delta \to 0}(N(\delta)\delta).$$

(2.1)

16
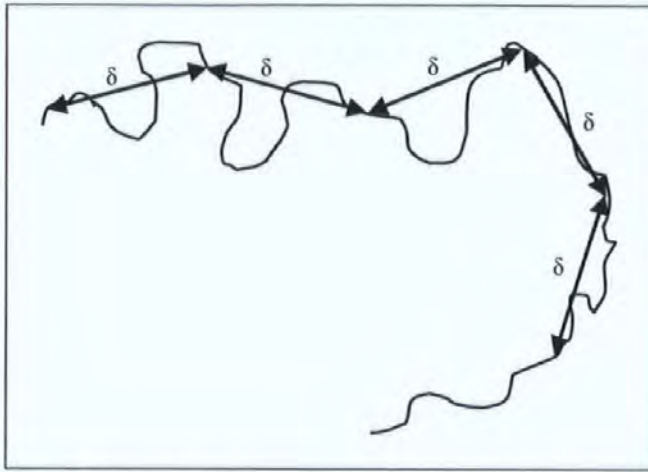
Figure 2-7, Sketch of the divider dimension

Similarly, consider a shape with a topological dimension of two, such as a circle or square, where the area may be estimated by covering it with small squares of side δ. See Figure 2-8.

$$A = \lim_{\delta \to 0}(N(\delta)\delta^2) \tag{2.2}$$
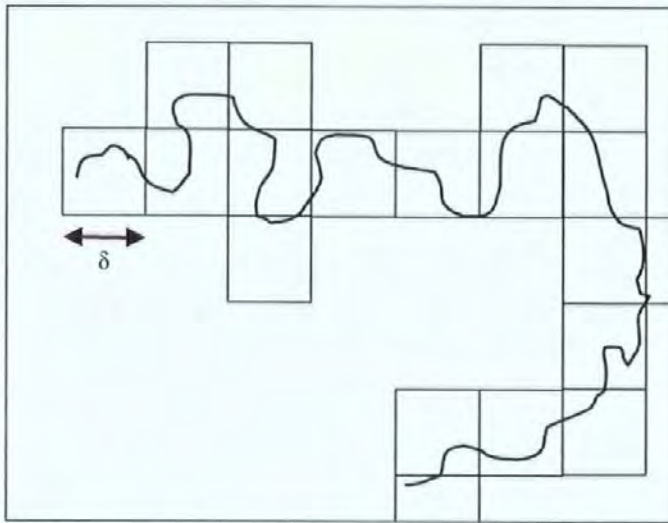
Figure 2-8, Sketch of the Box Dimension.

Thus, the measured quantity (length, area etc.) may be found by covering the shape with small objects that have the same topological dimension. If these objects are covered by small objects of an inappropriate dimension, then the result is either zero or infinite. For example, if we use vanishingly small squares to cover a smooth curve then in the limit the 'area' will be zero. In addition, if we cover a circle with small line segments then in the limit the 'length' will be infinite. We may write a generalised expression for the measured quantity M_d:

$$M_d = \lim_{\delta \to 0}(N(\delta)\delta^d) = \begin{cases} 0 & ,d < D \\ M_{d0} & ,d = D \\ \infty & ,d > D \end{cases}.$$ (2.3)

The value of M_{d0} is not important in this context but the Hausdorff dimension D is of great significance. For a fractal set this dimension (the fractal dimension) obeys the inequality $D_T < D \le D_T + 1$ and is not normally an integer.

2.3.2.4 Computation Of The Fractal Dimension

A coastline is an example of a natural approximation to a fractal [18]; if one steps around a land-sea boundary using N steps of length δ (see Figure 2-7) then N would be found to be a function of the step length, approximately given by:

$$L(\delta) = \delta N(\delta) = L_0 \delta^{D-1}.$$ (2.4)

Here L is the apparent length of the coast, L_0 is a constant and D is the fractal dimension. Using a range of values for δ and measuring the corresponding values for length $L(\delta)$ it is possible to use a least squares (or similar) method to estimate D (which for Norway is about 1.5). This technique of using line segments to cover a fractal with topological dimension of one is known as the Divider Dimension.

An alternative to the Divider Dimension is to cover the coastline with squares (see Figure 2-8); this is the box dimension where the total area A is found to be related to the length of the squares side δ by:

$$A(\delta) = \delta^2 N(\delta) = A_0 \delta^{D-2}.$$ (2.5)

18

Using a range of values for δ and measuring the corresponding values for area $A(\delta)$ it is possible to use a least squares (or similar) method to estimate D.

2.3.3 An Aside Concerning the Geometry of Spaces Containing Fractals

In the preceding discussion of fractals, the implicit assumption has been made that they exist in Euclidean space. A Euclidean space is what most people visualise in their minds eye; where one direction has the same properties as any other direction and there is a defined origin. However, there are a number of alternatives; affine, projective, spherical, inverse, hyperbolic and conformal. The EEG for, example lies in affine space where there is a defined origin but different directions have different units, meanings and properties.

The EEG has 2 dimensions; voltage, which is normally plotted on the y-axis and time, which is normally plotted on the x-axis. Voltage has units of volts, it is an expression of a potential difference (in the electrical sense) between 2 points and the same voltage may be repeated many times within a recording. Time, in contrast, has units of seconds, represents the interval since a reference to the measurement point and there may only be one instance of any value of time within the record. This may seem to be labouring a point but there are important implications for measuring the fractal dimension of an object, such as the EEG, which exist in affine space. For example, the concept of length is meaningless for a diagonal line (which is neither parallel to the voltage axis nor time axis) because voltage and time have different units. These issues are discussed in detail in Chapter 3.

2.3.4 Chaos

2.3.4.1 Linearity And Time-Invariance

To describe Chaos it is convenient to begin by introducing a type of system that is not chaotic - a Linear, Time-Invariance, Dynamical System. The term dynamical means that the system changes with time in a predictable way: An example would be a damped mass on a spring that oscillates when an impulse is applied (see Figure 2-9).
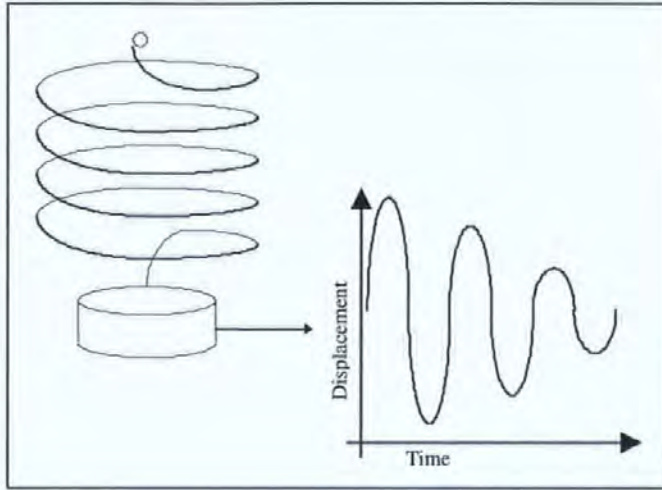
Figure 2-9, A linear, time-invariant system.

The term time-invariant means that the system with the same initial conditions and with the same stimuli will always respond in the same way - in the example this would imply that the mass remains constant and the characteristics of the spring do not change over time. The final term "linear" means that if the input of the system is the sum of several signals then the output will be the sum of the outputs that would be expected from each of the individual input signals.

This description of a linear, time-invariant, dynamical system may be made more mathematically rigorous by noting that the complete condition the system can, at any instant, be described by n real numbers or states that form a vector $x(t)$. In the mass-spring example, the state vector would have two elements that might be the position of the mass and the velocity of the mass. In the general case, the rate of change of these states is a function of the states themselves and external signals (stimulus) that form a vector $u(t)$.

The function of the states that gives their rate of change is linear and time-invariant and therefore may be expressed as a constant matrix F (this is known as the state transition matrix). Furthermore, the observable outputs from the system that form a vector $y(t)$ will be a linear function (described by the constant matrix H - known as the observation matrix) of the states plus some observation noise that is described by a p-vector of noise sources $w(t)$. Summarising this definition in mathematical notation and graphically we have:

$$\dot{x}(t) = F \cdot x(t) + u(t) \tag{2.6}$$

$$y(t) = H \cdot x(t) + w(t) \qquad (2.7)$$
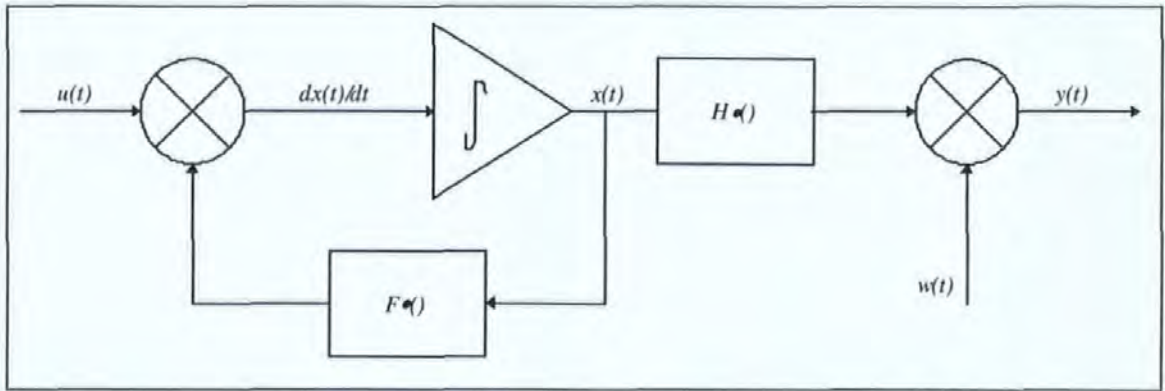
Figure 2-10, Block diagram of a linear time-invariant system.

2.3.4.2   The System Attractor

One way to visualise the dynamics of a system is to consider the behaviour from an initial state $x(t=0)$ with no stimuli applied. The subsequent states $x(t)$ will be a function of the state transition matrix F and $x(t=0)$. It is possible to represent the dynamics of $x(t)$ as a vector field in n-dimensional space (where n is the number of elements in the vector x). The integral curves of the vector field are called trajectories and for the damped mass-spring example the trajectory is a spiral in two-dimensional space:
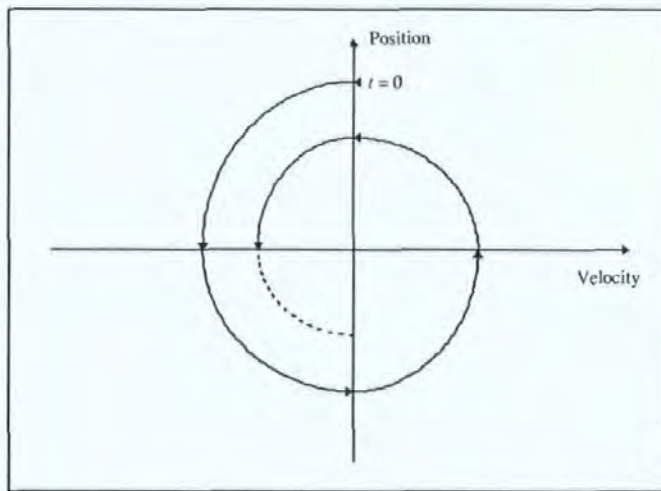
Figure 2-11, Parametric trajectory of the time history of a dynamical system.

In the mass-spring example, the steady state point is at equilibrium but some systems do not come to rest; they have a set of trajectories that describe the steady-state behaviour and these are called the attractor of the system. In the mass-spring example, the attractor is the steady state point. Consider the mass-spring system again, but this time with a motor which causes a steady state oscillation (see Figure 2-12).
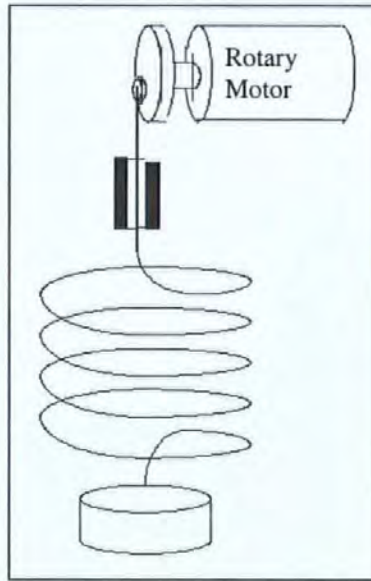
Figure 2-12, Driven mass-spring system.

Now the system trajectories all come to a steady state, which is described by an attractor that is elliptical:
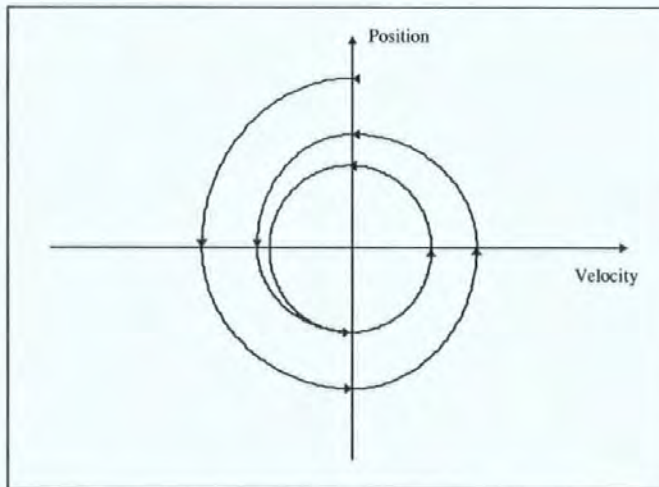
Figure 2-13, Trajectory of driven mass-spring system.

2.3.4.3 Limitations of Linearity and Time-Invariance Assumptions

The theory of linear, time-invariant, dynamical systems has been explored over many years and this has led to very useful tools for systems analysis, state estimation and system control such as the Kalman Filter, Laplace Transforms, etc. However, the major weakness in using linear, time-invariant system theory is that it does not reflect the real world. There are always limits on the assumption of linearity and time-invariance. In the mass-spring example, the spring is only linear over a small range of motion and its characteristics will change with usage. More broadly, this non-linear nature of the world is clear when one considers the mechanisms that drive the atmosphere and the firing of neurones in the brain.

To explore what happens when a system is non-linear we shall use a well known discrete time example [17] which was intended to be a simple description of the evolution of a population taking into account limit food supply:

$$P_{k+1} = rP_k(1-P_k).$$
(2.8)

Where P_k is a number between 0 and 1 that represents the population and r is a constant representing food supply. At low values of r the population becomes extinct (r<1, see Figure 2-14) and at higher levels (1<r<3, see Figure 2-15) it settles on a steady state value. At levels above r=3 the population oscillates initially between 2 levels (see Figure 2-16), then 4 levels (see Figure 2-17), and so on. Finally, the system becomes chaotic (see Figure 2-18).
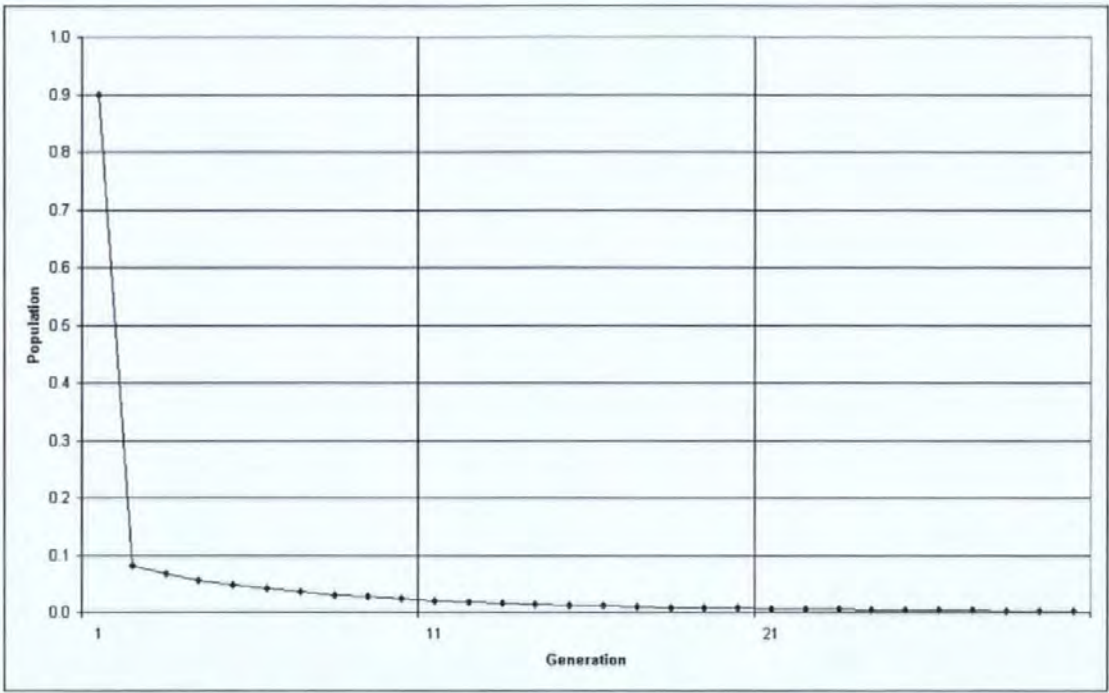
Figure 2-14, Extinction in a dynamic population simulation (r = 0.9).
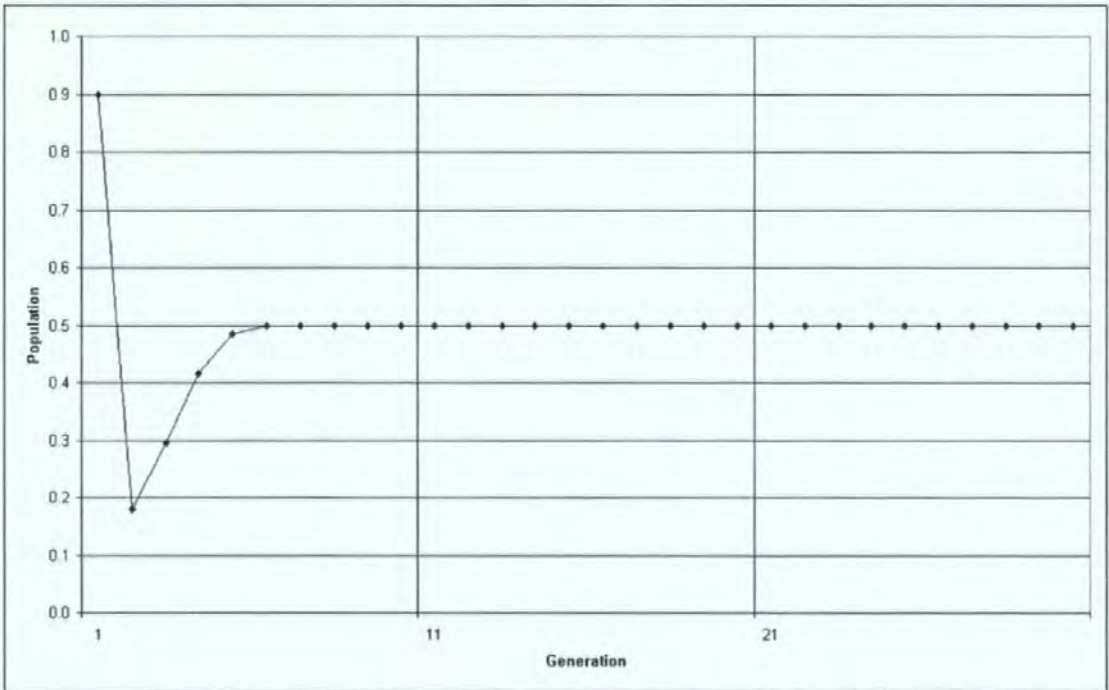
Figure 2-15, Steady state in a dynamic population simulation (r = 2.0).

24
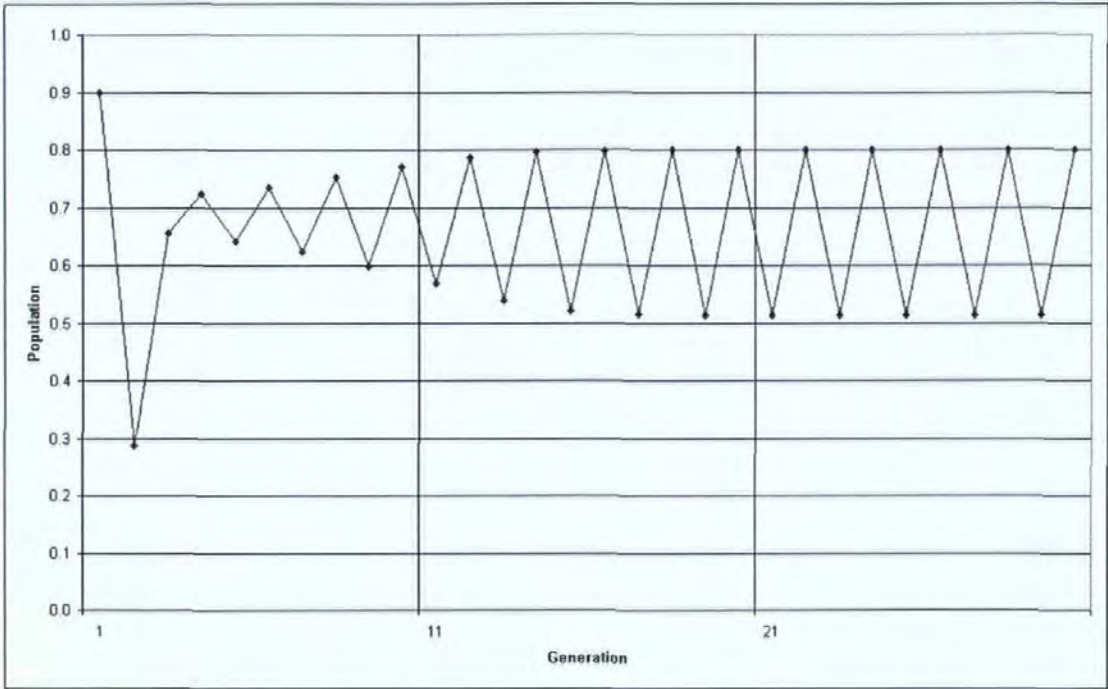
Figure 2-16, Two level oscillation in a dynamic population simulation (r = 3.2).
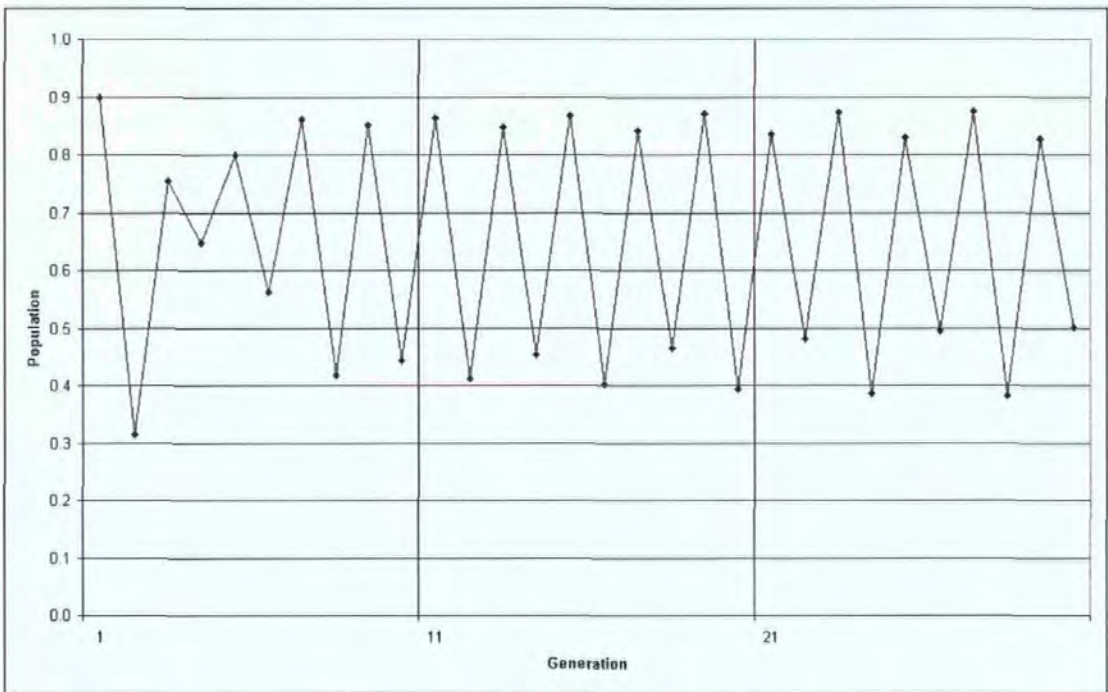
Figure 2-17, Four level oscillation in a dynamic population simulation (r = 3.5).

25
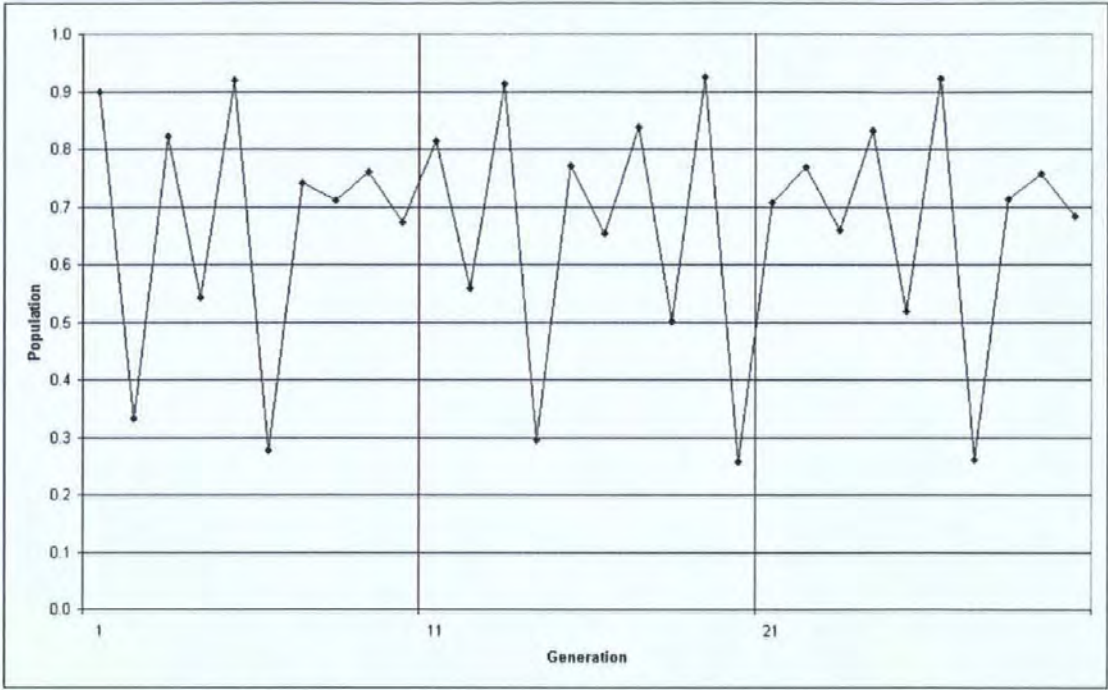
Figure 2-18, Chaos in a dynamic population simulation (r = 3.7).

This complete behaviour is summarised graphically in Figure 2-19 below:

Figure 2-19, Summary of population evolution in a dynamic population simulation.

It may be seen that for higher values of 'r' the system is chaotic. This chaotic system, in common with all chaotic systems, is a predictable system that is non-linear (however not all non-linear systems are chaotic). It is possible to analyse the attractors for chaotic systems and this reveals that the attractors are fractal.

2.3.5 Complexity

To complete this introduction to the terminology of chaos and fractals it is necessary to introduce the term "complex". In this context, the term complex is taken to mean fractal when it is applied to a shape and it is taken to mean chaotic when referring to a time varying signal. The measure of "Dimensional Complexity" is the fractal dimension of the attractor of a chaotic system.

2.4 Diagnostic Performance Measures

2.4.1 General

This thesis is concerned with the development and testing of a novel, EEG-based diagnostic method to detect the early signs of dementia. It is therefore important to measure the quality of the diagnostic decision. This section defines how the performance of a method is measured and defines the terms; Accuracy, Sensitivity, Specificity and Receiver Operating Characteristic. A comprehensive tutorial is given by Metz [19]. This section also discusses the use of statistical extrapolation (i.e. assuming a Gaussian distribution of the results).

The terms positive, negative, true and false are defined in a conventional way. A subject is "positive" if they have the disease in question and "negative" if they do not. Furthermore, a "true" diagnosis is a correct diagnosis and a "false" diagnosis is incorrect.

2.4.2 Accuracy

Any assessment of diagnostic performance requires some comparison with "truth". Perhaps the simplest measure of diagnostic decision quality is the fraction of cases where a correct decision is made. This is accuracy.

There are two main weaknesses of this measure. Firstly, in screening for a relatively rare disease one can be very accurate by simply ignoring all evidence and calling all cases negative. If only 5% of subjects have a disease, a method that simply labelled all cases as negative would have an accuracy of 95%. One might suppose that though this is true, accuracy should be meaningful at least as an index for comparison of diagnostic methods applied to a given population in which disease prevalence is known and fixed. However, this is the second weakness. Two diagnostic modalities can yield equal accuracies but perform differently with respect to the types of correct and incorrect decisions they provide; the incorrect diagnoses from one might be almost all false negative decisions (misses), while those from the other might be nearly all false positives (false alarms), and clearly, the usefulness of these two methods for patient management would be quite different.

2.4.3 Sensitivity and Specificity

To overcome the problems with using a simple accuracy measurement, it is possible to use two terms to describe the performance of a diagnostic method; sensitivity and specificity.

$$\text{Sensitivity} = \frac{[\text{Number of True Positive (TP) decisions}]}{[\text{Number of actual positive cases}]}$$

$$\text{Specificity} = \frac{[\text{Number of True Negative (TN) decisions}]}{[\text{Number of actual negative cases}]}$$

In effect, sensitivity and specificity represent two kinds of accuracy: the first for actual positive cases and the second for actual negative cases. This separation is particularly important because the effects of a false positive and false negative diagnosis may have very different implications in different situations. For example, a false positive may lead to unnecessary surgery. Similarly, a false negative may cause an important drug, which has little detrimental effect on a patient without the disease, not being administered.

Sensitivity and specificity are related to accuracy:

$$\text{Accuracy} = \frac{[\text{Number of True decisions}]}{[\text{Number of cases}]}$$

$$= \text{Sensitivity} \times [\text{Fraction of the study population actually positive}]$$

$$+ \text{Specificity} \times [\text{Fraction of the study population actually negative}]$$

It should also be noted that sensitivity is sometimes described as the True Positive Fraction (TPF) or "hit rate" and specificity is sometimes described as the True Negative Fraction (TNF). Two other useful terms are the False Positive Fraction (FPF), which is also know as "false alarm rate", and the False Negative Fraction (FNF). To summarise;

$$\text{FNF} = 1 - \text{TPF}$$

$$\text{TPF} = \text{"sensitivity"} = \text{"hit rate"}$$

$$\text{FPF} = 1 - \text{TNF}$$

$$\text{FPF} = \text{"false alarm rate"}$$

$$\text{TNF} = \text{"specificity"}$$

2.4.4 Receiver Operating Characteristic

With most methods of analysis, we obtain a metric, such as EEG rms voltage, that must be compared to some threshold to decide if it is normal or abnormal. See Figure 2-20. Clearly, by changing the decision threshold we may alter the proportions of true to false negatives and of true to false positives.
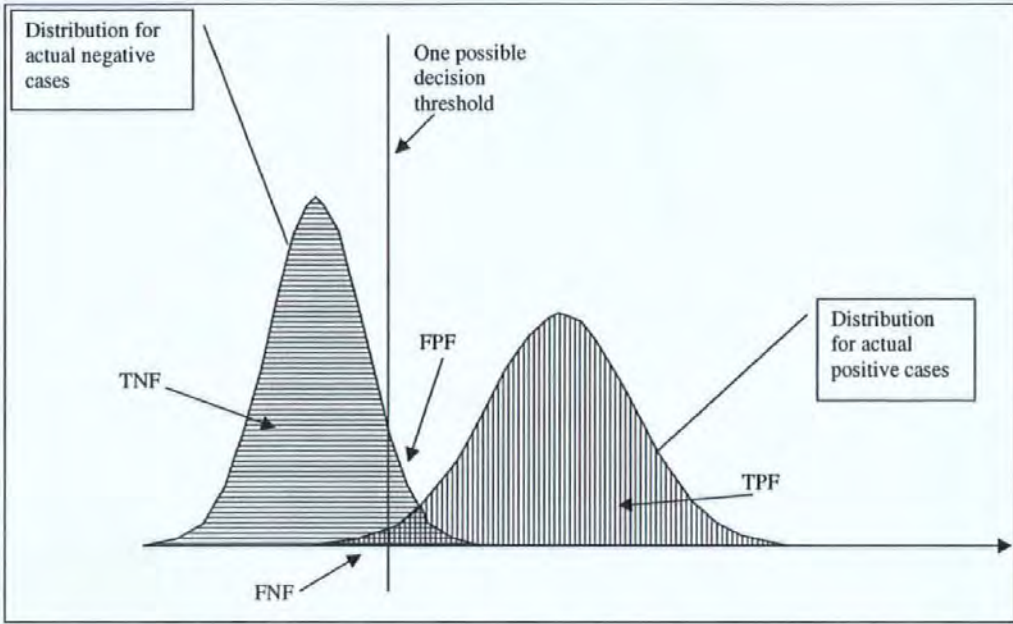
Figure 2-20, Likelihood of positive and negative results against metric.

To see the effect of this we may produce a parametric plot of True Positive Fraction against False Positive Fraction for varying decision thresholds. This plot is called a Receiver Operating Characteristic (ROC) for the diagnostic test, since it describes the inherent detection *characteristics* of the test and since the *receiver* of the test information can *operate* on any point on the curve by using an appropriate decision threshold. A typical plot is shown in Figure 2-21.
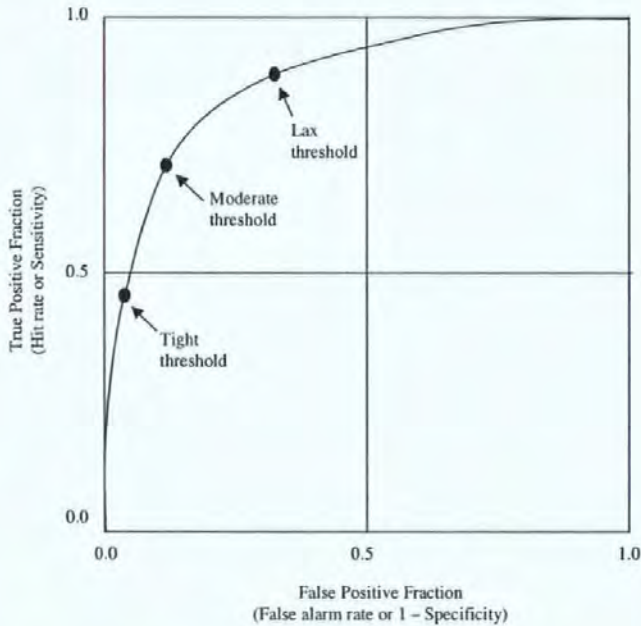
Figure 2-21, Typical Receiver Operating Characteristic.

In this thesis, a decision has been made to choose thresholds such that a specificity of 99.9% is achieved. This is because the diagnostic method would be used as a regular screening for dementia within a large at-risk population and a lack of specificity would cause too many false alarms. The consequence of a false alarm is that a patient would be sent for unnecessary and resource consuming follow up tests. It is felt that 1 in 1000 false alarms would be acceptable. With the threshold set, the sensitivity of the diagnostic method gives a good measure of its practical value and what proportion of sufferers may be helped. The consequence of a false negative (lack of sensitivity) would be that a patient would not receive follow-up and would receive no benefit from the screening.

2.4.5 Discussion of Statistical Extrapolation

In this research, two data sets are used. One is used to develop the method and the other independent set to quantify the performance (sensitivity and specificity) of the method. The population used to quantify performance contains 24 normal subjects, 17 subjects with suspected Alzheimer's Disease and 5 subjects with suspected Vascular Dementia. To estimate the sensitivity of the proposed dementure discriminating metrics the distribution of the metrics from the normal, Alzheimer's and Vascular populations were assumed Gaussian. At the end of the research, this assumption was revisited on the two sets of results for which this thesis makes important claims on sensitivity. These results are:

1. Fractal dimension of the zero-set of the EEG which is claimed to provide discrimination between normal and abnormal EEG during the blind trial using clinical data (see Section 4.3). In this case, the method was estimated to achieve 67% sensitivity to probable early Alzheimer's disease and 17% sensitivity to vascular dementia with a specificity of 99.9%.

2. Alpha/Theta ratio measure derived from the Zero Crossing Interval PDF of the EEG which is claimed to provide discrimination between normal and abnormal EEG during the blind trial using clinical data (see Section 6.3.10). In this case, the method was estimated to achieve 78% sensitivity to probable early Alzheimer's disease and 35% sensitivity to vascular dementia with a specificity of 99.9%.

31

To evaluate the reasonableness of the assumption that the distributions were Gaussian, a null hypothesis was proposed. The null hypothesis was that the results from each population type (normal, Alzheimer's and vascular) over each of the two sets of results (Fractal dimension of the zero-set and Alpha/Theta ratio derived from the Zero Crossing Interval PDF) are from a Gaussian distribution. That is six sets of results. This hypothesis was tested by estimating the skew and kurtosis of each of the sets of results and applying a limit such that none of the skew and kurtosis measures should be greater than twice the standard error of skewness (*ses*) or standard error of kurtosis (*sek*). That is the 95% confidence limit.

The standard error of skewness (*ses*) and standard error of kurtosis (*sek*) may be estimated [20] thus: $ses = \sqrt{6/N}$ and $sek = \sqrt{24/N}$ where N is the number of samples.

The statistics from the 6 sets of results and the standard errors are shown in

	Fractal dimension of the zero set			Alpha/Theta ratio derived from the Zero Crossing Interval		
	Normal population	Alzheimer's population	Vascular population	Normal population	Alzheimer's population	Vascular population
N	24	17	5	24	17	5
Mean	0.679	0.568	0.621	0.761	0.466	0.604
SD	0.029	0.046	0.033	0.063	0.130	0.103
Skew	0.48	-0.07	0.36	0.17	-0.01	-0.28
ses	0.50	0.59	1.10	0.50	0.59	1.10
Skew/ses	**1.0**	**-0.1**	**0.3**	**0.3**	**0.0**	**-0.3**
Kurtosis	-0.77	-0.99	-0.40	-0.57	-0.31	1.49
sek	1.00	1.19	2.19	1.00	1.19	2.19
Kurtosis/sek	**-0.8**	**-0.8**	**-0.2**	**-0.6**	**-0.3**	**0.7**

Table 2-1, Comparison of Skew and Kurtosis with their standard errors for the six most important sets of results in this research.

Therefore, the null hypothesis, that the results from each population type (normal, Alzheimer's and vascular) and each of the two sets of results (Fractal dimension of the zero-set and Alpha/Theta ratio derived from the Zero Crossing Interval PDF) are from a Gaussian distribution, was not rejected when these 12 tests were applied. From this, it is concluded that the distributions are likely to be approximately Gaussian and that the estimates of sensitivity are likely to be unbiased. Thus, it is considered a fair test.

2.5 State of the Art in Automated EEG Analysis

2.5.1 General

EEG data have been subject to interpretation by experienced clinicians for a number of years and it is accepted that this has led to successful diagnosis and treatment of a large number of patients. However, various authors have commented on the disagreement between readers of the same EEG record, due to subjective aspect of EEG interpretation as well as levels of training and experience. This has led to a desire for more precise and universal criteria. Thus, although human interpretation of electrophysiological signals was a great step forward there are benefits to be gained by processing the data further to extract more information and to standardise results.

2.5.2 Artefacts

As previously stated, artefacts are those signals present in the measured EEG signal that are not of cerebral origin. In automated EEG analysis these artefacts present even more of a challenge than they do to an experienced EEGer, this is because the experienced EEGer can recognise and disregard them relatively easily whereas this is a significant challenge for an automated system.

Two approaches to dealing with artefacts in automated EEG are present in the literature. The first is for an expert to recognise and discard segments that contain artefacts before the automated method is applied. This may lead to valid conclusions about the nature of artefact free EEGs but it would not be appropriate for this research as the aim is to introduce a system that does not require specialist involvement. The second method is to apply automated artefact recognition strategies (perhaps using Artificial Neural Networks). This is more appropriate for this research. However, the state of the art in automatic artefact analysis is not sufficiently advanced to be relied upon and therefore, as significant work would be required to validate such a method, it would provide too much of a distraction from the main thrust of the research.

A third alternative, which is not generally used, is to construct a method that is, by its nature, robust to the effect of artefacts. This is the approach taken in this research. Thus, for the analysis pursued in this research the following protocol was generally used:

"For all records, to avoid the possibility of inadvertently or unconsciously selecting data particularly suitable for analysis a predetermined protocol was applied. Data from 60s to 300s from each record was used. This avoids electrical artefacts, which commonly occur at the beginning of a record, and gives a standard 4 minutes of data to analyse. This segment of data, including artefacts, was analysed with no *á priori* selection of elements 'suitable for analysis'. This approach leads to a prediction of the usefulness of the technique, as it would most conveniently be used in practice."

2.5.3 Modelling Human Interpretation

The first attempts at an automated EEG analysis were those of Grass and Gibbs in 1938 [21] and Baldock and Walter in 1946 [22]. Those attempts involved Fourier analysis to extract the frequency content of the human EEG. Work has continued on evaluating the significance of the frequency content of the human EEG; Barlow [23] reported on a system that used mainly power spectral distribution to provide a human readable analysis and diagnosis (no figures are given for the accuracy of this system).

It has been reported [13] that the information taken from a Discrete Fourier Transform differs subtly from that which an EEGer would report. The way a clinician measures frequency content of an EEG pattern is by counting the number of peak-to-trough or peak-to-peak transitions that occur in a unit time. Small irregularities or the existence of sharpness at the peaks of the waves is not reflected into the visual assessment of the frequency content. Other important techniques use amplitude integrators, correlators, period analysis, auto-regression and hybrids of these techniques.

These attempts to automate electrophysiological signal analysis are based on the premise, published by Jansen [24], that "methods that are more likely to succeed attempt to mimic the electroencephalographer". No evidence has been found in the literature to suggest that systems mimicking the EEGer are yet sufficiently accurate and mature for normal clinical situations. This is reinforced by the fact that there are no such systems in common use.

The most promising current research in modelling human interpretation makes use of Fuzzy Logic, which is described, in section 2.5.5 (below).

Some researchers have tried to improve EEG analysis by moving away from modelling human methods and extracting more information from the electrophysiological signals using novel techniques. These new techniques, including polyspectral analysis and parameter extraction based on an analogy with complex systems (dimensional complexity and fractals dimension), are also described in subsequent sections.

2.5.4 Linear Techniques

Linear techniques such as spectral analysis, auto-regression and statistically based comparison with known signal shapes [13] were the first computer based techniques applied to the EEG. This work was successful in that it gave a great insight into the workings of the brain but its diagnostic capabilities were limited.

Linear spectral techniques take a Discrete Fourier Transform of a sampled form of the EEG. This is often mechanised as the Fast Fourier Transform (FFT). In all techniques found in the literature, except Bispectral Analysis (see section 2.5.9), the phase information is discarded and only the Power Spectral Density is used.

A broad spectrum of frequencies are detected when a healthy brain is active and the higher frequencies disappear during certain relaxed states, for example stage 1 sleep. Reduced frequency content relative to a 'healthy normal' whilst awake is a sign of brain dysfunction.

There are many metrics that have been drawn from the Discrete Fourier Transform:

- Alpha power (8 to 12 Hz). Alpha activity tends to show modulation i.e. waxing and waning, over period from 1 to 2 sec, thus forming envelopes (spindles) of activity.

- Beta power (18 to 24 Hz)

- Theta power (4 to 7 Hz)

- Delta power (0.5 to 3 Hz)

- Weighted ratio of low frequency (a x delta + b x theta) to high frequency (c x alpha + d x beta), where a, b, c and d are constants [25]. It is also worth noting that Gotman [25] uses a very easy to understand presentation of a Canonogram.

- 95% Spectral Edge; Frequency at which 95% of signal power lies below

- Power Spectral Median; Frequency at which 50% of signal power lies below

- Relative Delta Power; Ratio of power in delta band to total signal power

Barlow [23] reported on a system that used mainly linear techniques to provide a human readable analysis and diagnosis. No figures are given for the accuracy of this system.

These linear spectral techniques have been explored in depth over many years by many researchers. However, research continues and some success has been reported [26] recently.

2.5.5 Fuzzy Logic

Fuzzy Logic has been developed to describe rules of inference where boundaries are not crisp. As an example we may use the knowledge that reduced frequencies within the human EEG may suggest damage to the brain caused by disease or trauma. Using conventional logic one might propose the rule describing this inference as: If the frequency of α activity in the awake eyes closed state is less than 8Hz then the clinician should be alerted that the EEG is abnormal. This clearly does not distinguish between very low and slightly low (e.g. 0.01Hz and 7.99Hz) whereas it distinguishes greatly between just above and just below 8Hz (e.g.7.99Hz and 8.01Hz). To remain with conventional logic and improve this situation one could propose more complex rules with several boundaries between very low, low, marginal and normal. This leads to a problem of logical complexity: when there are three variables (frequency, amplitude and patient wakefulness) each with four discrete, abstract values there are 64 possible states to map. Fuzzy Logic is a framework within which terms such as "Degree of Normality" may be described by a continuous variable. The graph below illustrates the concept of mapping from α-wave frequency to Degree of Normality:
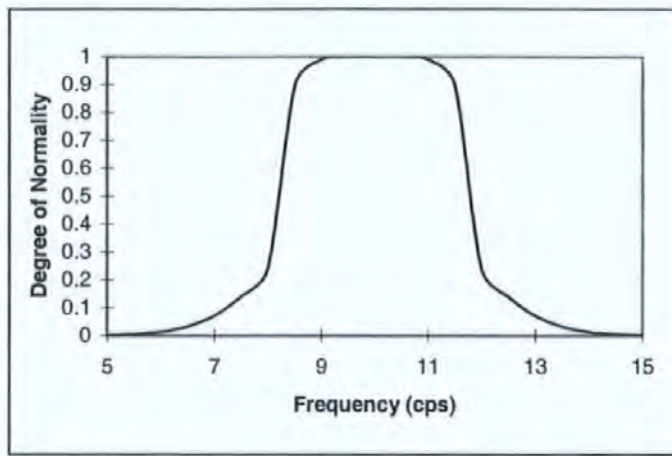
Figure 2-22, Fuzzy definition of alpha activity classification.

To make Fuzzy Logic inference rules, conventional combinational and unitary logic functions are required to be continuous functions. For example, a simple choice for AND may be the multiplication operator. There are several possible sets of operators described in the literature. One study by Riddington *et al* [27] compares the effectiveness of these possible sets of Fuzzy Logic operators for distinguishing EEGs recorded from Alzheimer's Disease sufferers and Normals.

Fuzzy Logic has been used in knowledge based EEG analysis systems [28] that deal with knowledge in a manner akin to human reasoning; that is linguistically (e.g. very normal, somewhat normal, extremely abnormal). This work appears to be relatively successful but the nature of the results used make it difficult to quantify the accuracy.

2.5.6   Artificial Neural Networks

Artificial Neural Networks, commonly referred to simply as Neural Networks, are algorithms which simulate an interconnected network of nodes which are combinational (many to one) devices. These methods are intended to simulate the activity of the Neurones and Axons of the human brain [29]. Their use to simulate human interpretation of the brains output (the EEG) is therefore apt and ironic.

The greatest challenge with Neural Networks is training; the lack of an adequate training algorithm led to a decade of dormancy (1970's) in Neural Network research. Since then, the most important learning algorithms (Error Back Propagation Algorithm, Radial Bias Function and Kohonen Self Organising Map) have been applied to many problems including EEG interpretation.

Training algorithms fall into two types:

1) Supervised learning. The network is presented with a training data set, which comprises many typical inputs and predetermined desired outputs. This data is acted upon by one of a number of learning algorithms (Error Back Propagation, Radial Bias Function etc.) to adapt the network synaptic weights so that the network can approximate and generalise the implied function.

2) Unsupervised learning. The network is presented with a training data set, which comprises typical inputs; there is no predetermined desired output. This data is acted upon by one of a number of self learning algorithms (Competitive Learning, Kohonen's Self Organising Map etc.) to adapt the network synaptic weights so that the network will give a vector output describing its similarity to distinct classes which were found in the training data.

The literature concentrates on the successes, benefits and drawbacks of specific training methods and the abilities of networks so trained to perform useful functions. Neural Networks have been shown particularly good at recognising tumours and other abnormalities in images (Mammograms, Retinal Scans etc.).

Attempts have been made with some success to use Artificial Neural Networks to combine metrics described elsewhere in this report; Pritchard [30] conducted one such study where Delta magnitude, Theta magnitude, Alpha magnitude, Beta magnitude, saturation correlation and dimensional complexity were used to classify Alzheimer's Disease and normal subjects. A sensitivity of 85.7% (12 of 14 AD subjects correctly identified) and a specificity of 96% (24 of 25 controls correctly identified) is claimed – however, this was not a blind trial on independent data.

Neural Networks have also been employed for automatic artefact identification [31]. This is important because in most cases artefacts will have a large detrimental effect on the analysis of the EEG (see section 2.5.2). Note, Kalman Filters [32] and Wavelet transforms [33] have also been used for this task.

During this research, there was some experimentation with Artificial Neural Networks to evaluate the quantity of innovation within the EEG. However, this is not reported, as there was little success.

2.5.7 Dimensional Complexity

The brain is constructed from synapses, neurones, and the like which have responses that are, at the macro level, almost deterministic and non-linear. It has been suggested that the brain could therefore (in a mathematical sense) be chaotic (see section 2.3 for an introduction to fractals, Chaos and Complexity). A further introduction to Chaotic Complexity in humans is given by Bisset [34]: Broadly, for the EEG, a healthy brain exhibits high complexity when it is active. Low complexity, when awake, is a sign of brain dysfunction. Particularly a loss of complexity has been associated with ageing and a loss of the ability to adapt to physiologic stress [35]. A tutorial review of non-linear dynamical (chaotic) analysis of EEGs is given by Pritchard and Duke [36] (the methods discussed involve reconstructing the system attractor and estimating its fractal dimension).

Research in EEG dimensional complexity has evolved from an early work which suggests that human EEG under some conditions may represents deterministic chaos of relatively low dimension [37], through studies measuring the dimension of the strange attractor [38], through to a recent works that has questioned whether the EEG represents a chaotic signal. Finally, Pritchard [39],[40] reported that normal EEG is high dimensional and does not represent low-dimensional chaos. This latter paper suggests that non-linear behaviour could be confused with low-dimensional chaos. A similar point of caution was raised by Sugihara who suggested that one must be very careful to distinguish between chaotic behaviour of a system, sampling errors and noise [41].

39

2.5.8 Fractal Dimension

An alternative measure taken from chaos theory is the fractal dimension of the EEG. It was suggested [42] that the shape of the occipital EEG, as plotted on paper, could be treated as a fractal and that the detected fractal dimension might be used in group comparison studies to differentiate subjects with Alzheimer's Disease from a group of normal subjects. This and further work on the fractal dimension is discussed throughout the remainder of this Thesis.

2.5.9 Polyspectral Analysis

In power spectral estimation, the signal under consideration is processed in such a way that the phase relations between components are lost. The information contained in the power spectrum is essentially that which is present in the auto-correlation sequence; this is sufficient to describe a Gaussian signal completely. However, there are practical situations, including EEG analysis, where it is useful to extract information regarding deviation from Gaussianity and the presence of phase relations. In these situations polyspectra (also known as higher order spectra), defined in terms of higher order statistics ("cumulants") of a signal, are useful. Particular cases of higher order spectra are the third order spectrum also called the Bispectrum which is by definition the Fourier transform of the third order statistics, and the Trispectrum (fourth-order spectrum). A further important statistic is the auto-bicoherence (or simply bicoherence) which represents a normalised Bispectrum.

Other notable higher order statistics are cross-cumulants, cross-bispectrum and cross-bicoherence, which may be invoked to determine the higher order statistics, contained in data where there is more than one signal to be considered.

Higher order statistics provide a way of describing the EEG without the need for prior assumptions as to the nature of the signal. Nikias [43] lists the motivations behind the use of higher order statistics in signal processing as:

1. To suppress additive coloured Gaussian noise

2. To identify non-minimum phase systems or reconstruct non-minimum phase signals

3. To extract information due to deviations from Gaussianity

4. To detect and characterise non-linear properties in signals as well as identify non-linear systems.

Given sufficient data, higher order statistics also provide sufficient information for statistical tests to determine whether a signal is linear and Gaussian.

The subject of Bispectrum Analysis in relation to the human EEG is dominated by Aspect Medical Systems, Inc. who have registered "Bispectral Index" as a trademark [44], [45]. The proprietary nature of Bispectral Index makes it difficult to find out about it. Aspect Medical Systems market an equipment that measures Bispectral Index and this has been used successfully to estimate the level of hypnosis in patients undergoing surgery with various anaesthetics [46], [47], [48], [49], [50], [51], [52], [53] and [54].

A logical extension to this work would be to use polyspectral analysis to extract other information from the human EEG for diagnosis of brain disease.

During this research, there was some experimentation with Higher Order Spectra. However this is not reported as there was little to arise which was novel.

2.5.10 Independent Component Analysis

In Independent Component Analysis (ICA) [55] and Blind Signal Separation (BSS) are related analysis problems that have recently received considerable attention in the machine learning community. In ICA, the EEG is assumed to comprise electrical potentials arising from several sources. Each source (including separate neural clusters, blink artefact, or pulse artefact) projects a unique topography onto the scalp giving rise to so called 'scalp maps'. These maps are mixed according to the principle of linear superposition. ICA attempts to reverse the superposition by separating the EEG into mutually independent scalp maps, or components using statistical methods. The nature and distribution of a set of relevant components is used to infer certain diseases including dementia. ICA has also been used in combination with Artificial Neural Networks to improve efficacy [56].

41

2.5.11 Event Related Potential Analysis

The term "Event Related Potential" refers to electrical potentials (EEGs) that arise as a result of an event such as photic or audio stimulation of the subject. The response of the subject to such events, embedded in the EEG, may be used to study the function of the brain. The ERP are typically analysed and classified using expert systems, Spectral/Bispectral Analysis [59] and Wavelet Analysis [60] to discover their similarity to a normal subject at rest. The degree of deviation from the typical normal subject at rest may then be used to imply the effect of activity or disease.

Interest in Event Related Potential (ERP) analysis has grown recently and these methods are showing promise for the detection of dementia including Alzheimer's Disease [57] and Parkinson's Disease [58].

2.5.12 Alternatives To Automated EEG Analysis

Research into EEG signal analysis must be assessed against the background of significant developments in other related areas: Positron Emission Tomography (PET), Magnetic Resonance Imaging (MRI) and Computerised Axial Tomography (CAT) machines are providing accurate diagnostic information which is superior to that which is derived from EEGs in many areas.

In neurology, PET and MRI provide information for assessing various neurological diseases such as Alzheimer's disease, cerebrovascular disease, Parkinson's disease, Huntington's disease, and Down's Syndrome. Additionally, PET localises epileptic foci for qualifying and identifying the site for surgical intervention. It also allows the characterisation, grading and assessment of possible brain tumour recurrence.

Although scanners are an important element of medical practice, there are still advantages to EEG analysis in some situations. For example it would be impractical to monitor depth of hypnosis with a large scanner in the operating theatre because it would interfere with the surgeons range of movement, whereas automated EEG Bispectral Analysis is no more difficult to accommodate than an Electrocardiogram (ECG) monitor.

A further important factor is affordability. Current techniques such as Magnetic Resonance Imaging (MRI) that are used to diagnose and assess neurological disorders require specialist equipment and expert clinicians to interpret results. Such techniques are inappropriate as a method of detecting individual subjects with early dementia within the large at-risk population, because everyone within the at-risk group would need to be tested regularly and this would carry a very high cost.

2.5.13 Summary Of Automated Analysis Methods

This section has reviewed a number of methods and techniques for EEG analysis; modelling human interpretation, fuzzy logic, artificial neural networks, dimensional complexity and polyspectral analysis. The most striking fact is that, even though significant research has taken place into automatic interpretation of EEGs, none of the techniques, with the exception of Bispectrum Analysis in anaesthesia, is accurate and mature enough to be a significant improvement over human interpretation of specific EEGs. The most important consequence is that there has been little direct benefit to patients, although there is indirect benefit derived from a better understanding of the brain.

Some of the lack of maturity of these methods is made evident by the lack of parameterisation of the methods' efficacies in the literature: Very few of the papers gave estimates of sensitivity and specificity that could be achieved.

2.6 Summary

This chapter has described the background to the research. It has described the Human EEG; how it is measured, the problems associated with the EEG (such as artefacts), and how clinicians have interpreted the EEG especially in diagnosing disease. The chapter also introduced fractals, chaos, complexity, and particularly their application to the Human EEG.

The state of the art in automated EEG analysis was also reviewed. It was shown that (with one exception), even though significant research has taken place into automatic interpretation of EEGs, none of the techniques is accurate and mature enough to be a significant improvement over human interpretation of specific EEGs in clinical practice. The most important consequence being that there has been little direct benefit to patients, although there is indirect benefit derived from a better understanding of the brain.

Chapter 3. Investigation of the Fractal Dimension of Human EEG

3.1 Introduction

This research began with a study of the background material that is discussed in Chapter 2 and this raised a number of questions, which were felt sufficiently important to address in an initial set of investigations. This series of investigations into the previous work on the fractal dimension of the Human EEG and other areas of interest are described in this Chapter.

3.2 Initial Data Set

The initial data used in this research were obtained using a strict protocol. The sampling rate was 256Hz. These data were obtained using the traditional 10-20 system in a Common Reference Montage which was later converted to Common Average and Bipolar Montages in software.

The EEG data were collected from 3 Alzheimer's patients, 3 mixed type (Alzheimer's and multi-infarct dementia) patients, 1 multi-infarct dementia patient and 8 age matched controls (over 65 years of age). All of the age-matched controls had a normal EEG (confirmed by a Consultant Clinical Neurophysiologist). One age-matched control (known as 'vol1') subsequently developed Alzheimer's disease; this record is of particular interest because it is potentially of a subject in transition from 'normal' to Alzheimer's diseased.

Two young volunteers were also used in the study (one male and one female) and their EEGs were confirmed to be normal by a Consultant Clinical Neurophysiologist. The young male (denoted by "X") and the young female (denoted by "Y") had their EEG recorded 3 times at intervals between 7 and 14 days. These recordings give an indication of the variability of a single subject's fractal dimension, which may be compared with the variability between members of the set of normals.

The EEG recordings encompass various states: awake and drowsy with periods of eyes closed and open.

The analysis described in this paper takes the whole recording including artefacts and has no *à priori* selection of elements 'suitable for analysis'. This approach leads to a prediction of the usefulness of the techniques, as they would most conveniently be used in practice.

3.3 Evaluation of Published Fractal Dimension Research

3.3.1 Introduction

The two main sources of published work on the fractal dimension of the Human Electroencephalogram that existed before this research were those by Woyshville and Calabrese [42], and Wu *et al* [61]. These papers are reviewed and discussed in this Chapter. Theoretical consideration and numerical experimentation are used to confirm that both methods have shortcomings. These issues were reported and corrections suggested in a peer reviewed publication [7].

3.3.2 Woyshville and Calabrese

In an early, group comparison study by Woyshville and Calabrese [42] the fractal dimension of the EEG was used to separate subjects with Alzheimer's Disease from a group of normal subjects. The method used to measure the fractal dimension was the Divider Dimension, which is discussed in Section 2.3.2.4.

In this retrospective preliminary investigation from 1994, the occipital EEG changes associated with Alzheimer's disease were examined using the then novel fractal dimension metric. The mean occipital EEG fractal dimension was determined for each of three patient groups representing a spectrum of clinical and EEG pathology: controls, probable AD, and autopsy-confirmed AD. The fractal dimension was significantly reduced in each of the AD groups with respect to the controls ($p<0.001$); and within the AD groups, it was significantly reduced in autopsy-confirmed AD relative to probable AD ($p<0.01$). The fractal dimension findings were said to "parallel the manifest EEG abnormalities in a way that suggested that it had potential clinical utility in metric studies on the EEG, especially when applied to the

dementias". Additionally, as the EEG pathology was particularly well described by the fractal dimension, this was seen as providing further support for a non-linear approach to the background activity of the EEG (see Section 2.5.7 for a comparison with Dimensional Complexity).

When this paper was reviewed and the method was considered in detail, there was a concern that a non-obvious but critical point had been missed; there are problems associated with estimating the fractal dimension of shapes, such as the EEG, that exist in affine space. This issue is introduced in Chapter 2 (Background) at section 2.3.3.

This was confirmed in the literature: as Mandelbrot [62] notes "in the study of isotropic fractals in Euclidean spaces, dimensionalities enter as exponents in expressions of the form $M(R) \propto R^D$ ... However, if the space [in which a record is defined] is not Euclidean but an affine space, in which ... distance along the time axis cannot be compared with distance along the space axis. In such a space, [an interval of length R] cannot be defined, R is meaningless, and D *cannot* enter in as exponent." In the case of an EEG trace, there is no natural scaling between distance along the time axis and distance along the voltage axis. In such a space, a diagonal distance between two points is meaningless and therefore the standard fractal dimension techniques (Divider and Box Dimension) are inappropriate. An exception to this rule would be if a scaling between voltage and time were defined; which it was for Woyshville and Calabrese by the way the EEG had been printed. To demonstrate the effect of the arbitrary choice of scaling on the result, the Divider Dimension method (used by Woyshville and Calabrese) was repeated on data from a single Alzheimer's subject and a single normal subject.

Voltage/Time Scaling (nV/s)	Typical normal subject's fractal dimension	Typical AD subject's fractal dimension
0.04	1.006	1.001
0.08	1.032	1.004
0.16	1.143	1.017
0.31	1.505	1.069
0.6	1.658	1.282
1.3	1.450	1.514
2.5	1.210	1.610
5.0	1.114	1.362
10.0	1.071	1.183

Table 3-1, Variability of Fractal Dimension with Scaling

The table shows that if a scaling of 0.6nV/s is chosen then the Normal subject appears to have a much higher fractal dimension (1.658) than the Alzheimer's subject (1.282). This is the type of clear result that had been reported; fractal dimension for controls of 1.41 and confirmed AD subjects with a fractal dimension of 1.09. However, an issue arises if a scaling of 2.5nV/s is chosen. In this case the previously clear results reverse and cease to give the intuitively correct result. That is the Normal subject appears to have a much lower fractal dimension (1.210) than the AD subject (1.610).

The problem demonstrated above is a direct result of inappropriately applying the Divider Dimension to an object that exists in affine space.

3.3.3   Wu *et al*

3.3.3.1   Introduction

A later study into the use of fractal dimension to analyse the EEG was also published [61]. The method was not published in detail, but fortunately, it was possible to determine the method by reverse engineering the software that had been used. This original code is shown in Appendix A.

This method, as published, was claimed to have achieved 100% separation of normal subjects and patients with dementia. Whilst this is true for the sample of 7 normal subjects and 7 patients with dementia, it would be unlikely to be true on a larger sample. The published results are reproduced below in Table 3-2.

Age matched controls				Subjects with Dementia			
vol2	1.23	vol6	1.21	ad1	1.12	Mix1	1.13
vol3	1.23	vol7	1.21	ad2	1.12	Mix2	1.12
vol4	1.20	vol8	1.20	ad3	1.12	Mix3	1.18
vol5	1.22			mid1	1.13		

Table 3-2, Summary of Published Results.

Although the fractal dimension values are lower for Alzheimer's subjects, there is insufficient data to make a statistically significant statement concerning the sensitivity (probability of correctly identifying subjects with dementia) and specificity (probability of correctly identifying normal subjects) of the method.

The detailed algorithms given below are followed by a commentary (which discusses the probable intent of the software) and a discussion of the method.

3.3.3.2 Detailed Algorithm

In this method, where the sampling rate is assumed to be 256Hz, estimates of fractal dimension D_i, are made for $2 \leq i \leq 6. i \in Z$:

$$D_i = 1 - \frac{\ln(S_i) - \ln(S_0)}{i \ln 2},$$

(3.1)

where:

$$S_i = \sum_{j=0}^{256/2^i} \sqrt{4^i + \frac{k^2 \left(R'_{xx}(j) - R'_{xx}(j+2^i)\right)^2}{R'_{xx}(0)^2}},$$

(3.2)

$$k = 300,$$

(3.3)

and $R'_{xr}(m)$ is based on the auto-correlation of the EEG sampled (256Hz) time series $x(t)$:

$$R'_{xr}(a) = \sum_{b=0}^{255-a} x(b)x(a+b), \quad \forall\, 0 \le a \le 255.$$ (3.4)

Note, k may be expressed in units of sampling interval squared (i.e. $k = 1.526 \times 10^{-5}\, s^2$).

Finally, the highest and lowest of the 5 estimates of fractal dimension (D_i, $2 \le i \le 6, i \in Z$) are discarded and average of the remaining three is taken to be the overall fractal dimension, D.

Although it is not shown in the algorithm description above, there is also a code segment that combines the overall fractal dimension (D) from each 1s segment of data, from each channel into a single fractal dimension for the entire record. A histogram of fractal dimension measures taken from the data-segments is produced and the mode is taken to be the composite measure of fractal dimension for the whole record.

3.3.3.3   Comments on Algorithm

This section is a commentary on the algorithm, which discusses the probable intent of the software.

For this method the step sizes used along the time axis were 4, 8, 16, 32 and 64 samples (expressed as 2^i where $2 \le i \le 6, i \in Z$) and the sampling rate was 256Hz. Therefore, the time steps were 15.6ms, 31.3ms, 62.5ms, 125ms and 250ms.

It may be seen that equation 3.2 calculates the approximate length of the function $R'_{xr}(a)/R'_{xr}(0)$ by using diagonal distances along the function. That is, using Pythagoras' theorem; the diagonal length of each segment is the square root of the sum of the square of the time interval (2^i sampling intervals) and the square of the change in normalised autocorrelation interval $R'_{xr}(a)/R'_{xr}(0)$ over that time interval.

To understand equation 3.1 it is necessary to return to the Divider Dimension. If one assumes that the curve is a fractal then the length of the entire curve, S_i, is given by the equation below (see Section 2.3.2.4).

$$L(\delta) = S_i = \delta N(\delta) = L_0\delta^{D-1} ,$$

(3.5)

where the step size is given by:

$$\delta = 2^iT_s .$$

(3.6)

Therefore,

$$S_i = L_0T_s^{D-1}2^{i(D-1)} .$$

(3.7)

Now, S_0 may be used to estimate the constants:

$$S_0 = L_0T_s^{D-1} .$$

(3.8)

Now, if we divide S_i by S_0 we obtain an equation that may be solved for D:

$$S_i = S_0 2^{i(D-1)} .$$

(3.9)

Taking the natural logarithm of both sides, we obtain:

$$Ln(S_i) = Ln(S_0) + i(D-1)Ln(2) ,$$

(3.10)

$$D_i = 1 - \frac{\ln(S_i) - \ln(S_0)}{i\ln 2} .$$

(3.11)

Thus, an estimate of the fractal dimension of the auto-correlation function has been derived.

3.3.3.4   Discussion of the Method

There are three points to note about this method. Firstly, the fractal dimension of the auto-correlation is estimated instead of the fractal dimension of the raw record; the reason for this is not clear but the option of using the fractal dimension of the auto-correlation in place of the raw data is considered throughout the remainder of this research.

Secondly, the auto-correlation has not been corrected for the number of samples included giving a scaled auto-correlation. It is believed that this is probably an error and results below are reported with and without a correction for this.

Thirdly, it was found that the use of a histogram to form the estimated fractal dimension for the entire record reduced the effects of artefacts and unusual activity on the result. This is thought to be because the number of contaminated segments was small in comparison with the number that were normal and those contaminated segments in general had a highly atypical fractal dimension.

We return to the issue of measuring the fractal dimension in affine space. A version of the Divider Dimension is being estimated in affine space, in a similar way to that used previously (by Woyshville and Calabrese [42]). The problems with this approach have been partially addressed in this method by having fixed step length along the time axis ($\delta = 2^i T_s$), as opposed to fixed diagonal step length over the shape in 2 dimensions, which is normal for the Divider Dimension. The problems with this approach have also been partially addressed by normalising the auto-correlation with respect to the variance ($R'_{xx}(0)$) and using a fixed (but still arbitrary) constant k.

By adjusting this constant, we can see the effect on the results:

Arbitrary scaling Constant, k	Fractal Dimension			
	Normal Subject		Alzheimer's Subject	
	Original method	Corrected auto-correlation	Original method	Corrected auto-correlation
37.5	1.11	1.18	1.04	1.05
75.0	1.15	1.20	1.07	1.09
150	1.21	1.23	1.10	1.12
300	1.23	1.24	1.11	1.11
600	1.23	1.26	1.12	1.12
1200	1.24	1.25	1.12	1.12
2400	1.24	1.25	1.12	1.12
4800	1.24	1.25	1.13	1.12
10^6	1.24	1.25	1.13	1.12

Table 3-3, The Effect Of Scaling Constant On The Results.

With this method, the Dimension measure for the normal subject is greater than that for the Alzheimer's subject, at any reasonable scaling. This is more satisfactory than the ambiguous results produced in the earlier study. It is though interesting to note that the choice of $k=300$ for the scale factor is where the result becomes almost saturated with little further change as the scale factor tends to very large numbers. Interestingly, if we allow the scaling value to tend to infinity then this would give an estimator for fractal dimension:

$$D_i = 1 - \frac{1}{i \ln 2} \cdot \ln \left(\frac{\sum_{j=0}^{256/2^i} |R_{xx}(j) - R_{xx}(j+2^i)|}{\sum_{j=0}^{256} |R_{xx}(j) - R_{xx}(j+1)|} \right). \tag{3.12}$$

It may be seen that this is the equation one would expect if only the vertical distances were considered. This is illustrated in Figure 3-1 where $L(\delta) = \sum |v_j|$.
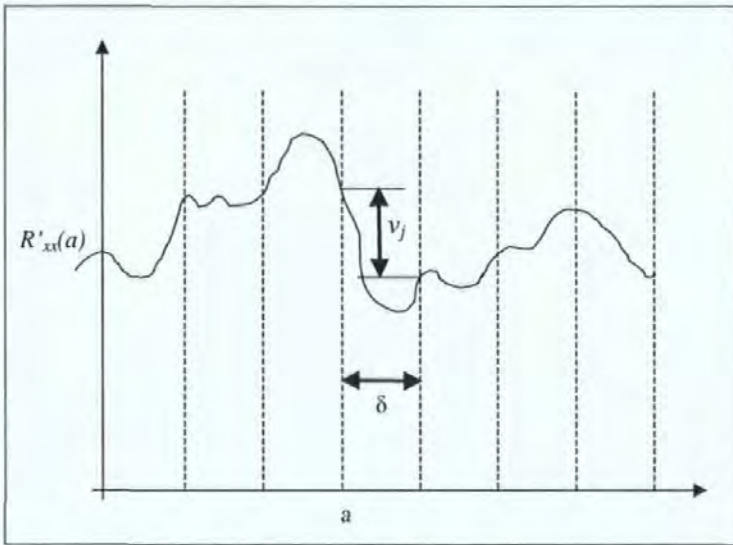
Figure 3-1, A sketch of the fractal dimension as k tends to infinity.

3.4 Fractal Dimension Methods Appropriate to Affine Space

3.4.1 Methods

As both of the published measurements of the fractal dimension of the EEG were not appropriate in affine space, the literature was searched for methods that are more appropriate. A number of methods were discovered in the literature [63] that are suitable for estimating the fractal dimension of shapes in affine space. Two of these methods were selected for use; they are an adapted box dimension and the dimension of the 'zero-set'.

To compute the adapted box dimension we divide the record of duration T into slices of length Δt and note the difference between the maximum and minimum amplitude during each slice (the extent). The mean extent $\varepsilon(\Delta t)$ is computed for a range of Δt (which are exponentially spaced) and the dimension is computed by finding a least squares best fit to the equation below. This is illustrated in Figure 3-2.

$$A(\Delta t) = T\varepsilon(\Delta t) = A_0 \Delta t^{2-D} \tag{3.13}$$
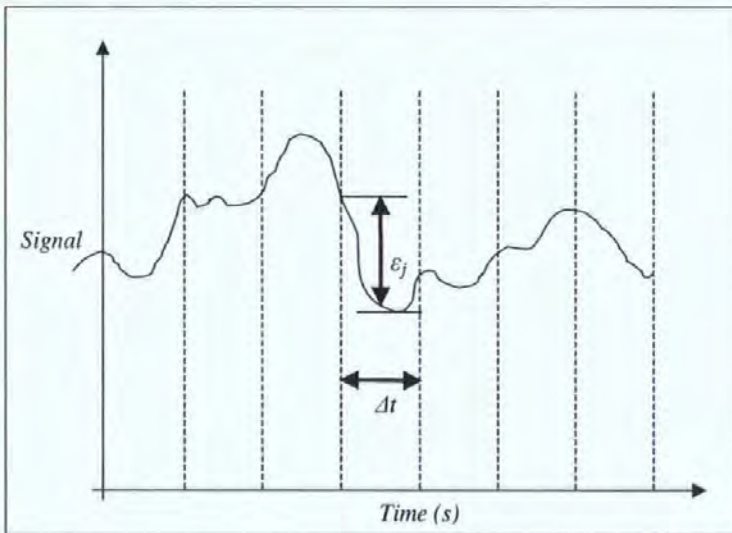
Figure 3-2, A sketch of the adapted box dimension.

This is very similar to Wu's method when it was modified to allow constant k to tend to infinity. The only difference is that the extent (max to min amplitude) is used instead of the difference between the measurement at the beginning and end of the time step.

To compute the dimension of the zero-set we form the set of instances when the record of length T intersects with the time axis. The topological dimension of this set is zero (see Section 2.3.2.3). The length, L, of line necessary to cover all zero-crossings is computed by covering the zero-set with N line segments of length Δt. To compute the fractal dimension of the zero set the length, L, is computed for a range of Δt (which are exponentially spaced) and the dimension is computed by finding a least squares best fit to the equation below. This method is illustrated in Figure 3-3.

$$L(\Delta t) = \Delta t \, N(\Delta t) = L_0 \Delta t^{1-D} \tag{3.14}$$
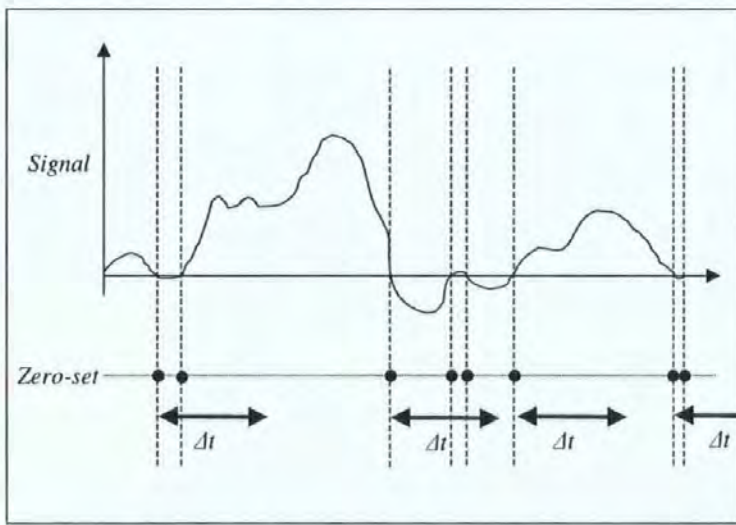
Figure 3-3, A sketch of the dimension of the zero-set.

It was decided to use a histogram of fractal dimension measures from short segments of data as Wu had done, with one change. The change was to use a Gaussian spreading function on the histogram ($\sigma = 0.05$) to avoid noise on the histogram from unduly affecting the result. A typical histogram without Gaussian spreading is shown in Figure 3-4.
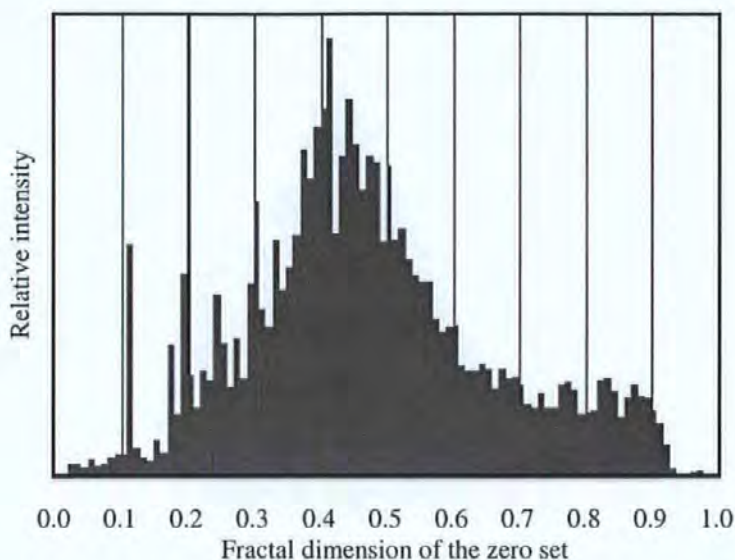
Figure 3-4, Typical histogram of segment fractal dimensions.

3.4.2   Initial Results

The Adapted Box Dimension and Dimension of the Zero Set were each applied to raw EEG data and to the auto-correlation of the EEG data. The results from this work were published in a peer-reviewed paper at the third international Neural Networks and Expert Systems in Medicine conference in Pisa [7]. The data presented below is the fractal dimension for all channels together. The results from the age matched controls (including Vol1 who went on to develop Alzheimer's disease) and the subjects with dementia are shown in Table 3-4 and Table 3-5, respectively.

Record	Raw EEG Data		Auto-correlation of EEG data	
	Adapted Box	Zero-set	Adapted Box	Zero-set
Vol1	1.547	0.564	1.325	0.516
Vol2	1.596	0.562	1.434	0.590
Vol3	1.572	0.560	1.452	0.648
Vol4	1.551	0.561	1.496	0.662
Vol5	1.592	0.562	1.587	0.562
Vol6	1.591	0.561	1.638	0.627
Vol7	1.538	0.564	1.391	0.539
Vol8	1.596	0.616	1.500	0.670
Mean	1.573	0.569	1.478	0.602
Standard Dev'n	0.024	0.019	0.101	0.059

Table 3-4, Results from Age Matched Controls using methods suitable for affine space.

Record	Raw EEG Data		Auto-correlation of EEG data	
	Adapted Box	Zero-set	Adapted Box	Zero-set
AD1	1.560	0.565	1.134	0.323
AD2	1.520	0.560	1.181	0.368
AD3	1.512	0.554	1.183	0.331
MID1	1.483	0.496	1.219	0.384
MIX1	1.533	0.562	1.148	0.324
MIX2	1.442	0.497	1.118	0.270
MIX3	1.608	0.669	1.265	0.438

Table 3-5, Results from subjects with dementia using methods suitable for affine space.

The above data does seem to show that all four fractal methods provide metrics that tend to decrease when dementia is present. However, the separation is not significant in all cases. Specifically, 'MIX3' has a higher fractal dimension than the mean of the normals for both of the metrics based on the raw EEG data. The adapted box dimension and the dimension of the zero-set for the auto-correlation function appear to give a more reliable separation.

It is instructive to plot the distribution of metrics from normal subject (excluding vol1) and then to plot the metrics from subjects with dementia (along with vol1) to illustrate the separation of the 2 groups. Figure 3-5, below, shows such a plot for the zero-set dimension of the auto-correlation function.

Figure 3-6 shows a similar plot for the zero-set dimension of the raw data. In this plot, the normal subjects do not form a cluster that is separated from the subjects with dementia. Thus, these results are clearly worse than the comparable results above, which used the auto-correlation of the EEG. This is disappointing because one has to be suspicious about the use of the auto-correlation function. This suspicion is dealt with in section 3.9.
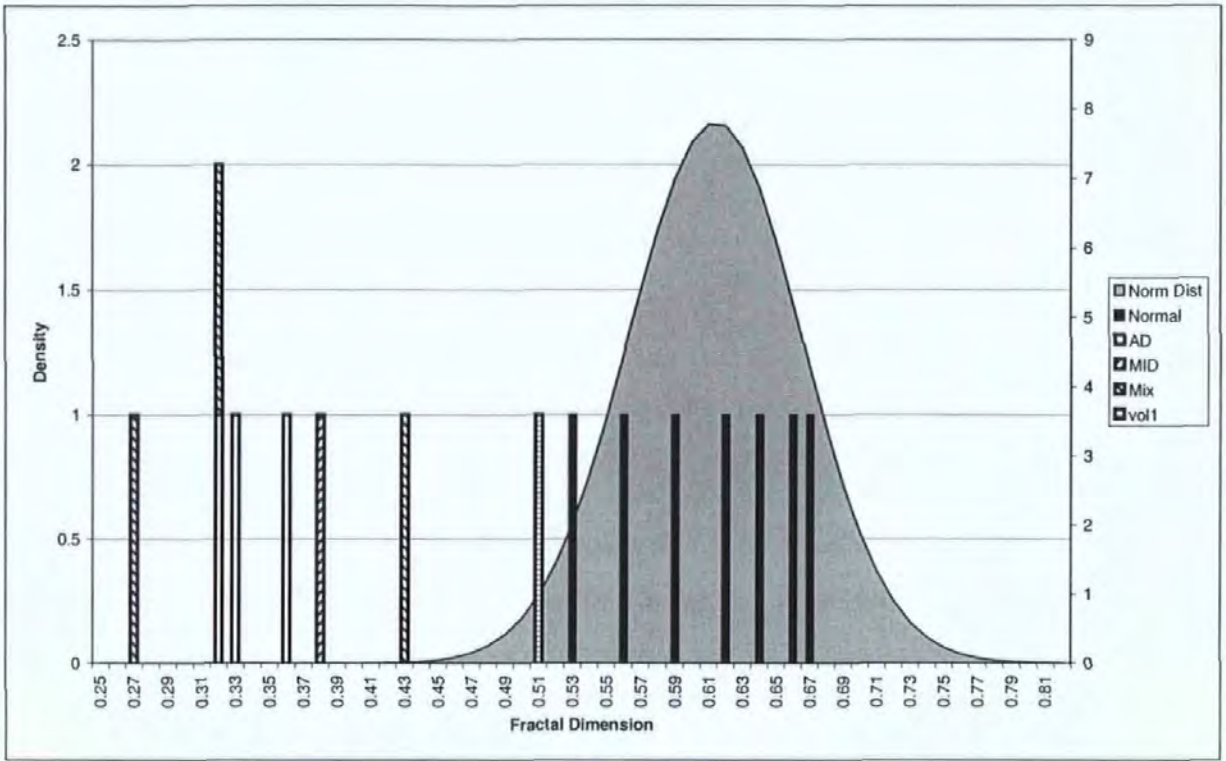
Figure 3-5, Typical histogram of zero set dimension of auto-correlation.
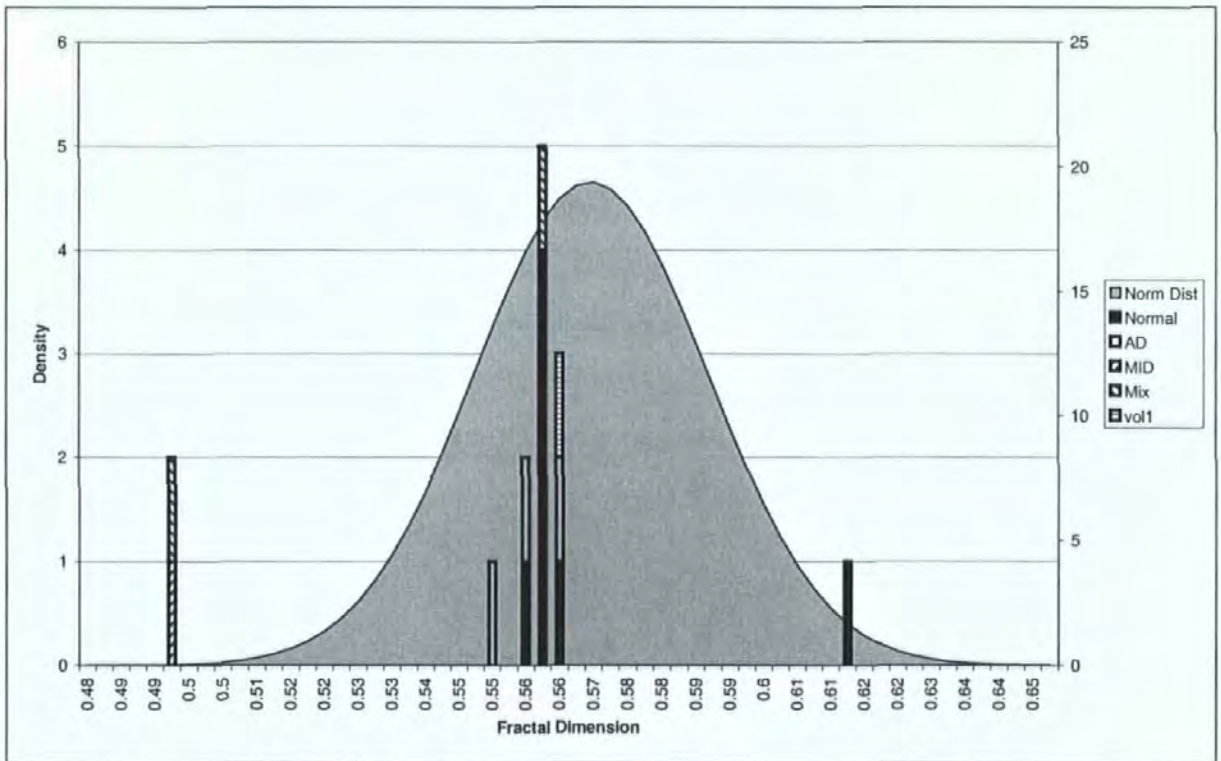
Figure 3-6, Histogram of zero set dimension of raw EEG.

Now we consider the results from the age matched control 'vol1' who was at the time of recording confirmed by a clinician to be 'normal' but went on to develop Alzheimer's Disease. This shows that that the adapted box dimension of the auto-correlation function and the dimension of the zero-set for the auto-correlation function are suspiciously low but not outside the range for normal subjects.

The results from the two young subjects are discussed in section 3.5.

3.4.3 Revised Results

Given these disappointing results, the methods were checked and it was found that changing controlling constants, such as the segment length, affected the results. These effects are dealt with more fully later in this thesis and better results were produced (see below). These better results, produced by tuning parameters, do not represent strong evidence. This is because it is not clear whether the method was working on a specific set of data because the method is tuned to that set of data or because this method tuning will work in general. These concerns were the main reason for conducting the evaluation, with a new, independent set of data, described in Chapter 4.

Record	Raw EEG Data		Auto-correlation of EEG data	
	Adapted Box	Zero-set	Adapted Box	Zero-set
Vol1	1.262	0.639	1.216	0.639
Vol2	1.337	0.703	1.269	0.679
Vol3	1.292	0.676	1.185	0.635
Vol4	1.304	0.688	1.244	0.675
Vol5	1.331	0.703	1.270	0.691
Vol6	1.318	0.693	1.224	0.650
Vol7	1.293	0.678	1.226	0.668
Vol8	1.317	0.678	1.237	0.654
Mean	1.307	0.682	1.234	0.661
Standard Dev'n	0.024	0.020	0.028	0.020

Table 3-6, Revised results from age matched controls.

Record	Raw EEG Data		Auto-correlation of EEG data	
	Adapted Box	Zero-set	Adapted Box	Zero-set
AD1	1.188	0.541	1.043	0.395
AD2	1.237	0.599	1.100	0.528
AD3	1.178	0.523	1.113	0.504
MID1	1.216	0.595	1.133	0.546
MIX1	1.206	0.549	1.040	0.098
MIX2	1.190	0.546	1.072	0.459
MIX3	1.262	0.632	1.096	0.518

Table 3-7, Revised results from subjects with dementia.

Plots of the distribution of results are given in Figure 3-7 (zero set dimension of the auto-correlation) and Figure 3-8 (zero-set dimension of the raw EEG).
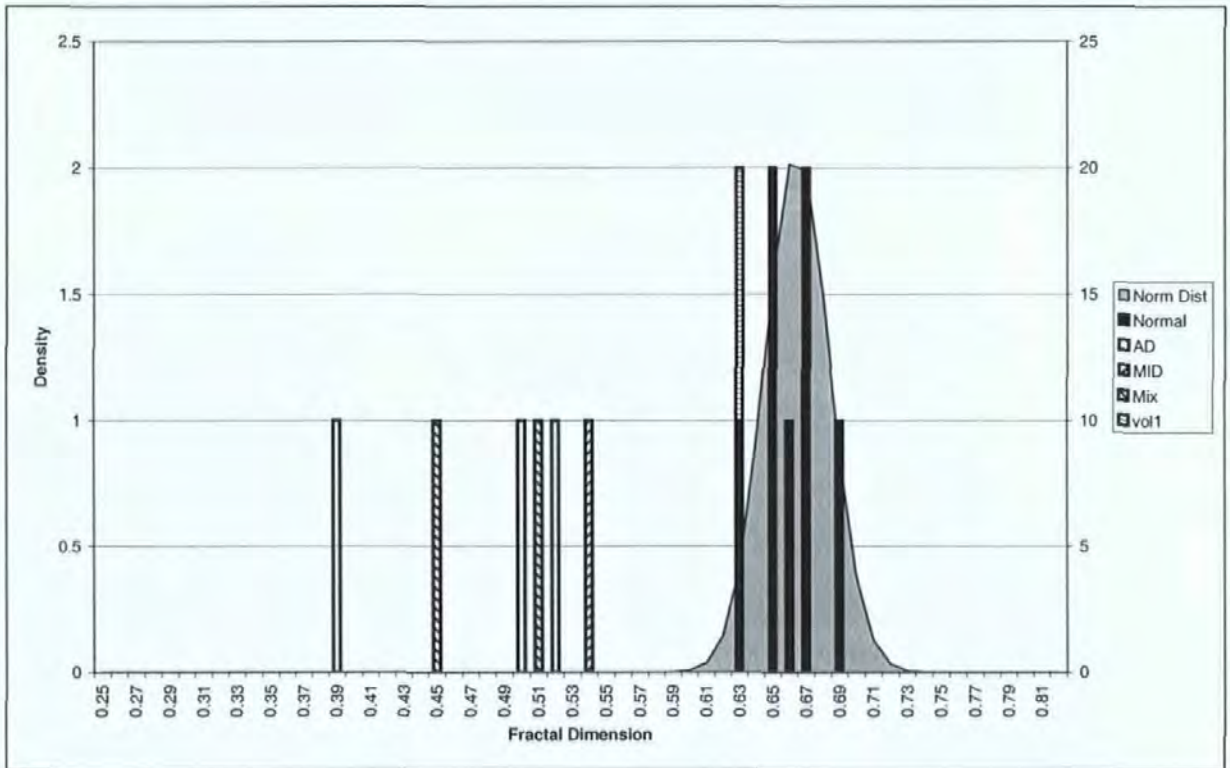
Figure 3-7, Revised histogram of zero set dimension of auto-correlation.
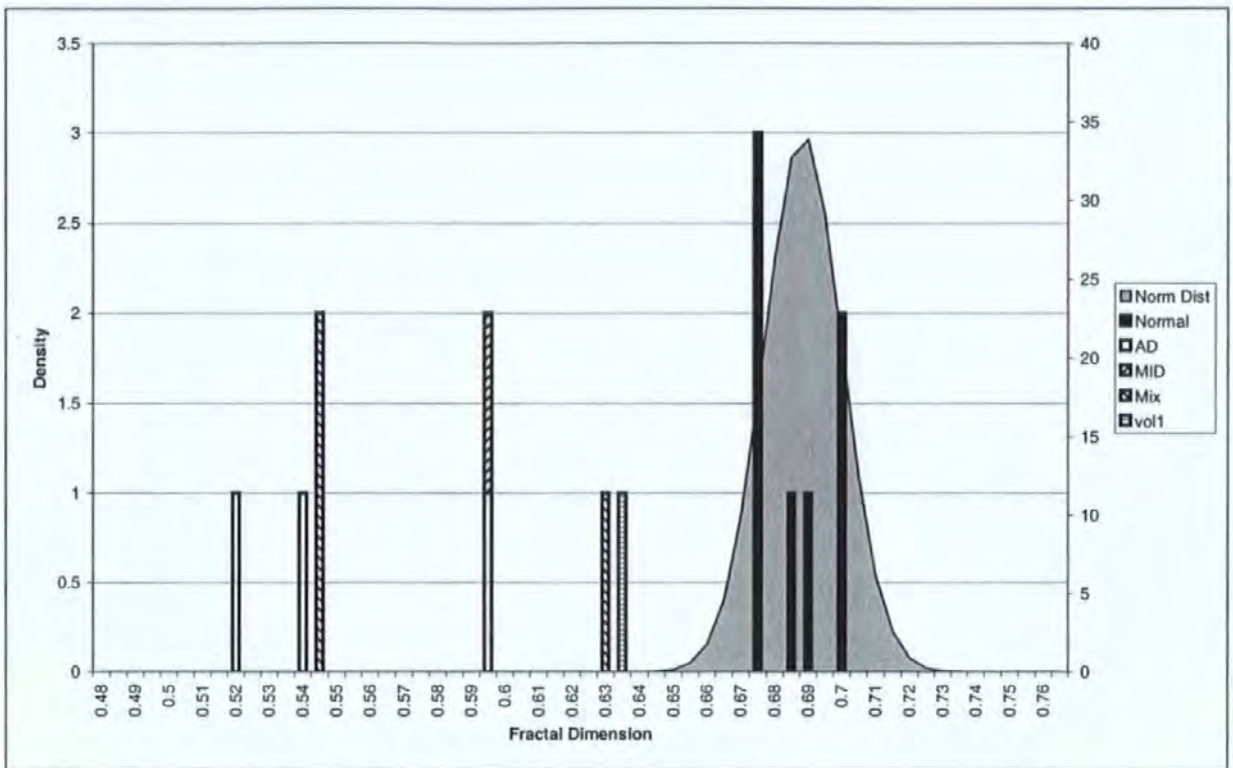
Figure 3-8, Revised histogram of zero set dimension of raw EEG.

It is encouraging to note that, Vol1 (a control who went on to develop Alzheimer's disease) is the lowest of the controls for both of the methods which analysed the raw EEG data.

Unfortunately, there is insufficient data to estimate the skew and kurtosis of the set of fractal dimensions from normal subjects.

3.4.4 Conclusion

This section has described two methods of computing the fractal dimension that are appropriate in affine space and has given results that were achieved when these measures were applied to the EEG (and the auto-correlation of the EEG).

The results provide some weak evidence that these measures may be useful in the early detection of dementia, but because the methods had to be tuned to provide reasonable results it was necessary to conduct a further evaluation on a new, independent set of data. This is described in Chapter 4.

3.5 Subject Specific EEG Analysis

3.5.1 Discussion

If successful, automated EEG analysis has the potential to provide significant benefits but to date, despite significant effort, there has been a general lack of success. It is suggested that this is because research has concentrated on group comparisons, that is, attempting to separate individuals into groups (Normal, Alzheimer's, Parkinson's etc.) using indices derived from isolated (snapshot) EEGs. Improvements in automatic EEG analysis may lie in making the analysis subject specific [64]. That is, comparing an EEG to those taken previously from the same subject: Looking for trends in indices that arise over time rather than comparing an EEG to what is generally normal within the population. In this way, subject specific EEG techniques should be more sensitive. It is hoped consequent improvements in sensitivity will cause automated EEG analysis to fulfil the identified potential.

This concept and some early results have been published in a paper at the Neural Networks and Expert Systems in Medicine conference (NNESMED '98) in Pisa [7].

As an illustration, the figure below shows a hypothetical index measured on a subject who initially falls into a normal population spread. It can be seen that although the subject enters a decline at the onset of disease, it would only be detected by group comparison methods some time later after it falls outside the normal spread.
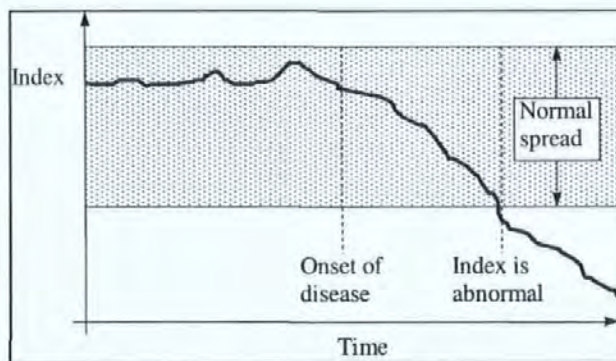
Figure 3-9, Variation of a hypothetical index with time.

The figure above illustrates a fictitious, easily interpreted single index. It is clear from the illustration that population spread plays no part in subject specific EEG analysis, whereas the relative magnitudes and characteristics of measurement noise, normal variation of indices and variations due to disease are of central importance.

When an EEG is analysed and an index (or more than one index) is estimated, the index will be subject to "measurement noise" which is due to short-term variations in the index. For normal subjects the indices will vary over the medium and long term in a characteristic way. What we are looking for is a distinguishable change that implies the onset of disease and a continuing change that gives a measure of disease progression or effect of treatment.

3.5.2 Results and Conclusion

To establish whether this concept merited further investigation the EEG data from the 2 young control subjects (X and Y), which had been recorded 3 times for each subject at 7 to 14 day intervals, was used. The adapted box dimension and the zero-set dimension of the raw EEG data and of the auto-correlation of EEG data were taken, giving a total of 4 measures of fractal dimension. The data presented below is the fractal dimension for all channels together. Table 3-8, below, shows the results from three recordings of each of the two young subjects (known as X and Y).

Record	Raw EEG Data		Auto-correlation of EEG data	
	Adapted Box	Zero-set	Adapted Box	Zero-set
X1	1.564	0.563	1.350	0.536
X2	1.574	0.608	1.385	0.559
X3	1.559	0.564	1.223	0.555
Y1	1.521	0.577	1.273	0.411
Y2	1.519	0.561	1.284	0.425
Y3	1.513	0.558	1.269	0.423

Table 3-8, Results from young subjects.

If one considers the variation from sample to sample from the same subject to be equivalent to measurement noise (or short term variability) on the fractal dimension then one may estimate (all-be-it on a very limited set of data) the population standard deviation for a single subject for each measure (Table 3-9).

Estimated Population Standard Dev^n	Raw EEG Data		Auto-correlation of EEG data	
	Adapted Box	Zero-set	Adapted Box	Zero-set
	0.006	0.020	0.060	0.010

Table 3-9, Variability of results from young subjects.

Table 3-10 presents the data for the age matched controls (repeated from section 3.4.2 for convenience) and the first recording for each of the young normals. For all of the measures, except the zero-set dimension of raw data, the standard deviation among the group of normals is, as expected, larger than the variation for a single subject (Table 3-9). In the case of zero-set dimension of raw data, the standard deviation among the group of normals is not significantly different from the variation for a single subject.

Record	Raw EEG Data		Auto-correlation of EEG data	
	Adapted Box	Zero-set	Adapted Box	Zero-set
vol2	1.596	0.562	1.434	0.590
vol3	1.572	0.560	1.452	0.648
vol4	1.551	0.561	1.496	0.662
vol5	1.592	0.562	1.587	0.562
vol6	1.591	0.561	1.638	0.627
vol7	1.538	0.564	1.391	0.539
vol8	1.596	0.616	1.500	0.670
X1	1.564	0.563	1.350	0.536
Y1	1.521	0.577	1.273	0.411
Mean	1.569	0.570	1.458	0.583
Std Deviation	0.027	0.018	0.114	0.082

Table 3-10, Variability of the population of normal subjects.

It may be noted that young subject 'Y' has a lower than expected fractal dimension on all methods (approximately 2-sigma below the average). Whilst, this is surprising and no reason was found for this, it is still valid to use these data to estimate the magnitude of "measurement noise" within the normal population.

The fractal dimension has also been calculated for the subjects with dementia (Table 3-11):

Record	Raw EEG Data		Auto-correlation of EEG data	
	Adapted Box	Zero-set	Adapted Box	Zero-set
AD1	1.560	0.565	1.134	0.323
AD2	1.520	0.560	1.181	0.368
AD3	1.512	0.554	1.183	0.331
MID1	1.483	0.496	1.219	0.384
MIX1	1.533	0.562	1.148	0.324
MIX2	1.442	0.497	1.118	0.270
MIX3	1.608	0.669	1.265	0.438

Table 3-11, Results from subjects with dementia.

The graph below (Figure 3-10) summarises the results which were obtained using the zero-set dimension of the auto-correlation function and the measured normal variability of the fractal dimension for a single subject as measured on the two young normals (X and Y).
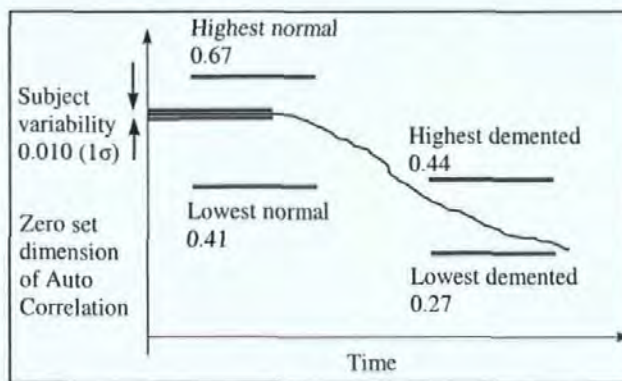
Figure 3-10, Summary of subject specific results showing that this concept could improve early diagnostic efficacy.

The graph demonstrates that the fractal dimension (zero-set) of the auto-correlation function, at this stage of the research, appeared to be a good candidate for use in subject specific detection of dementia. This is because the measured fractal dimension of the EEG is generally lower for a subject with dementia than for normal subject and the variability of a single normal subject's fractal dimension is small in comparison to the variability between members of the set of normals.

3.5.3 Conclusion and Implications

Subject specific analysis of the fractal dimension of the EEG was shown to be an exciting, interesting and useful candidate for early detection of dementia.

It is, however, important to recognise that if this method were adopted then there would be infrastructure requirements with associated costs. In practice, a simple non-subject specific, EEG based method would require a PC, interface box, electrodes and straightforward training for the General Practitioner. Whereas, a subject specific EEG method would require the same plus an information infrastructure which could recall previous results that may have been taken – possibly at another facility. Thus, to be useful and reliable a subject specific measure would require a patients' previous EEG data to follow them and this is not currently a trivial objective to achieve. In the near future, this should become somewhat more achievable with eHealth programs such as Biopattern [65], [66] pressing forward the development of database, internet and computational technologies in pursuit of better health care. Biopattern is a particularly good example to choose, as one of its aims is to develop systems that allow an individual patient's medical data (of many types) to be stored remotely whilst being available quickly for detailed analysis.

3.6 Alpha / Theta Ratio Determined from the Fractal Dimension

3.6.1 Discussion

This section describes the derivation of a metric, which is the ratio of the time that the EEG exhibits Alpha activity to the time that it exhibits Alpha or Theta activity, where classification of alpha or theta like activity is from the Fractal Dimension. This was inspired by a similar metric which has previously been derived from the Power Spectral Density.

Section 3.4.1 describes the measurement of the fractal dimension over short data segments (2s) and constructing a histogram of such results. Then the mode is taken as the composite fractal dimension for the complete record. It is interesting to examine these histograms in more detail. In some cases, the difference between a normal subject and a subject with dementia is very clear. A histogram of the zero-set fractal dimension of the autocorrelation function from a normal and an Alzheimer's subject are shown in Figure 3-12 and Figure 3-11.
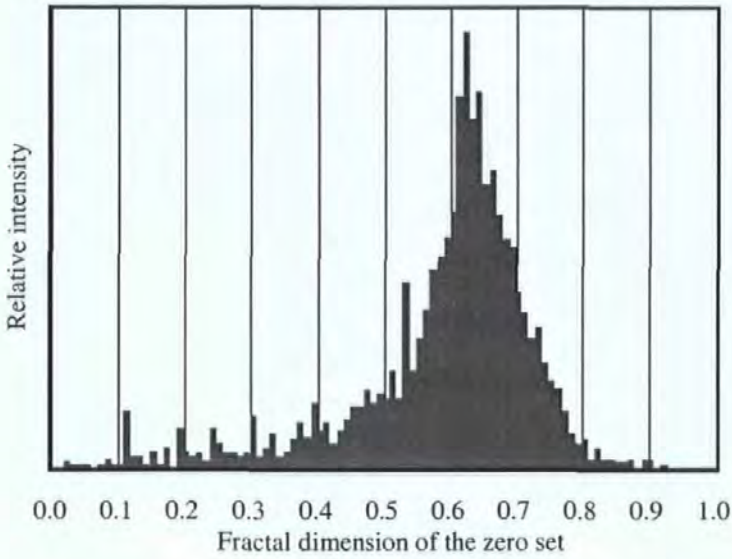
Figure 3-11, Histogram of zero-set dimension of the auto-correlation from Vol2.
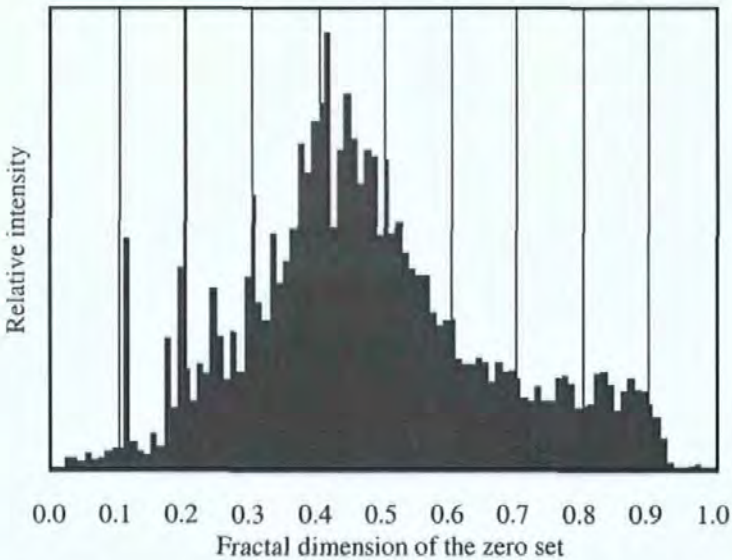
Figure 3-12, Histogram of zero-set dimension of the auto-correlation from AD1.

To better understand the difference between these histograms the signal segments that produced the fractal dimension measures were examined. By observation of the signal segments that produce values of fractal dimension it is possible to show that clearly defined signal types, defined in section 2.2.4, approximately map to certain ranges of values of fractal dimension. These are given in Table 3-12.

	Adapted box dimension of raw data or auto-correlation function	Zero-set dimension of raw data or auto-correlation function
Ocular artefacts	Lower than 1.0	Lower than 0.3
Theta	1.0 to 1.2	0.3 to 0.5
Alpha	1.2 to 2.0	0.5 to 1.0
Beta	Above 2.0	Above 1.0

Table 3-12, Approximate mapping of signal type to fractal dimension

It is necessary to comment on the range of fractal dimension values which are taken to be representative of Beta waves because an adapted box dimension of should be in the range 1 to 2 and the dimension of the zero set should be in the range 0 to 1. However, with the way that the fractal dimension is estimated on short (2s) segments of data there is a possibility of values outside the theoretically valid range occurring. These values occur when the apparent complexity increases at greater magnifications and are eliminated when one estimates the fractal dimension of the whole signal.

Other, less well defined, signals can be classified as having similar fractal dimensions to the clearly defined types and it is possible to determine the density of observations in the Theta, Alpha and Beta ranges directly from the histogram.

It was suggested that a new metric could be used. The metric was the ratio of density in the Alpha range to the sum of the densities in the Alpha and Theta ranges. This metric seems (on the limited data available) capable of differentiating control subjects from subjects with dementia with a wide band between the two groups (see results below). It should be remembered that the entire recording from each subject was used without any pre-selection of segments that we wish to analyse and that this method is relying on pushing the records from artefacts out of the ranges specified for Alpha and Theta.

3.6.2   Results and Discussion

The histograms for all of the initial data set and all four methods are given in Figure 3-13 through Figure 3-33.
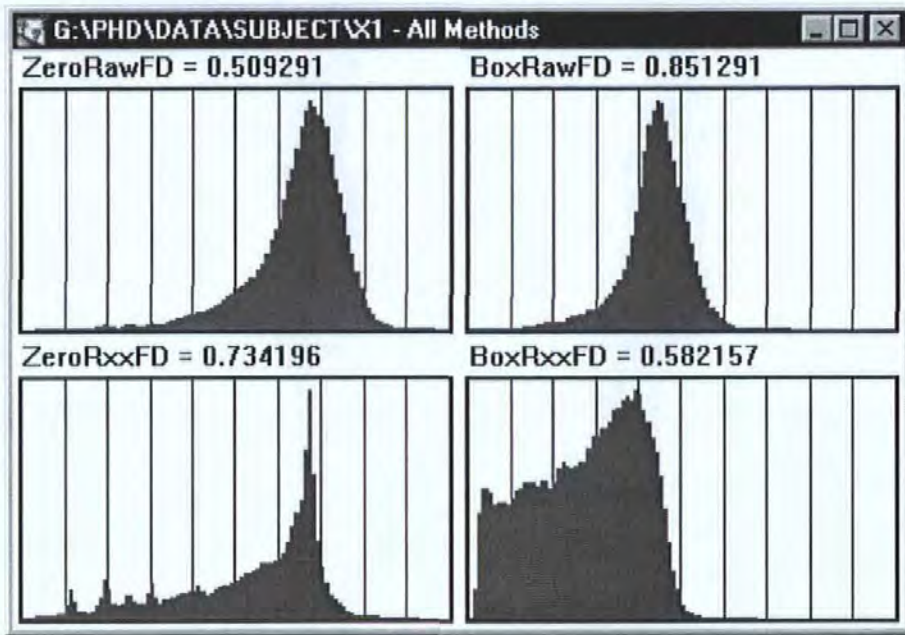
Figure 3-13, Histograms of four fractal measures applied to the EEG of subject X1.
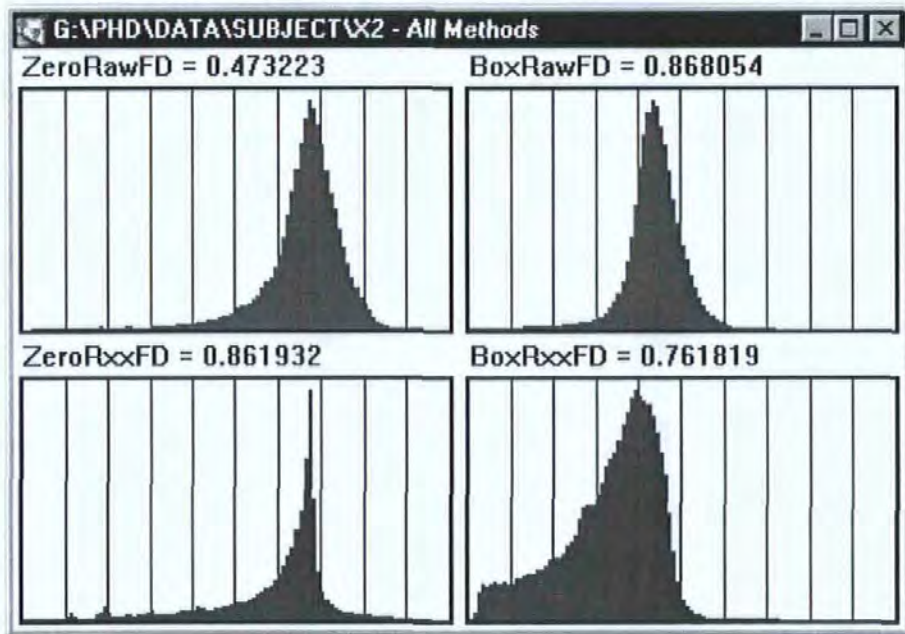
Figure 3-14, Histograms of four fractal measures applied to the EEG of subject X2.
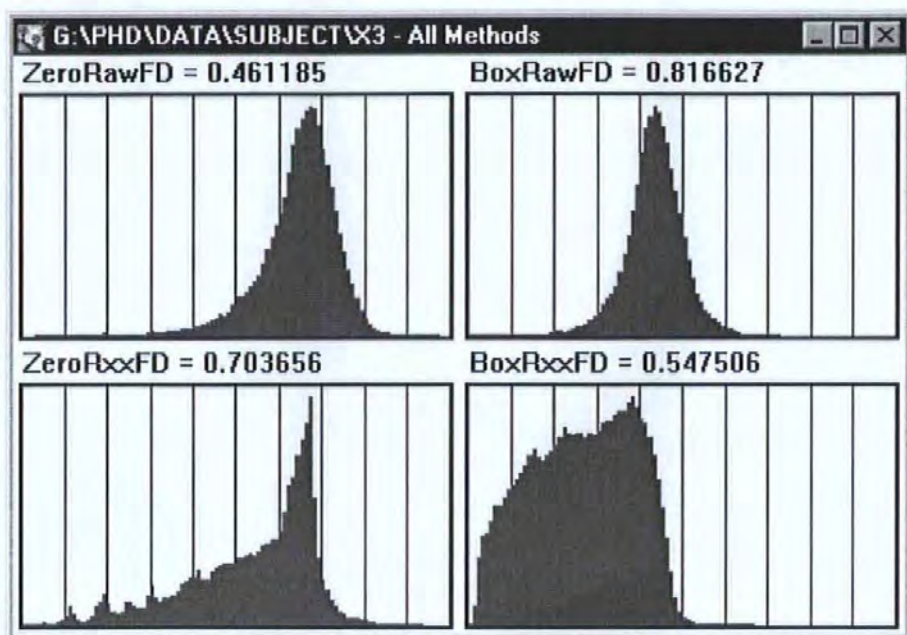
Figure 3-15, Histograms of four fractal measures applied to the EEG of subject X3.
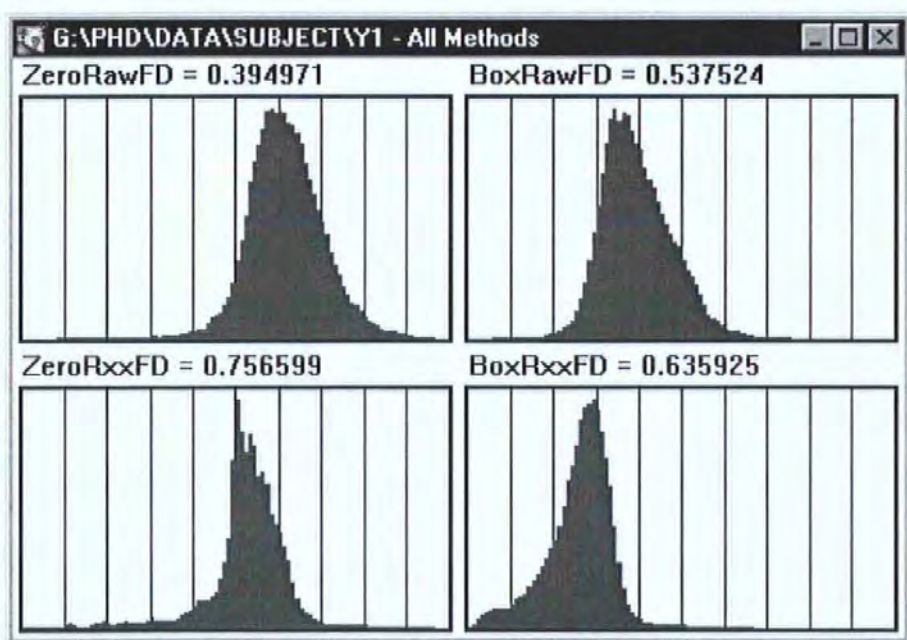
Figure 3-16, Histograms of four fractal measures applied to the EEG of subject Y1.
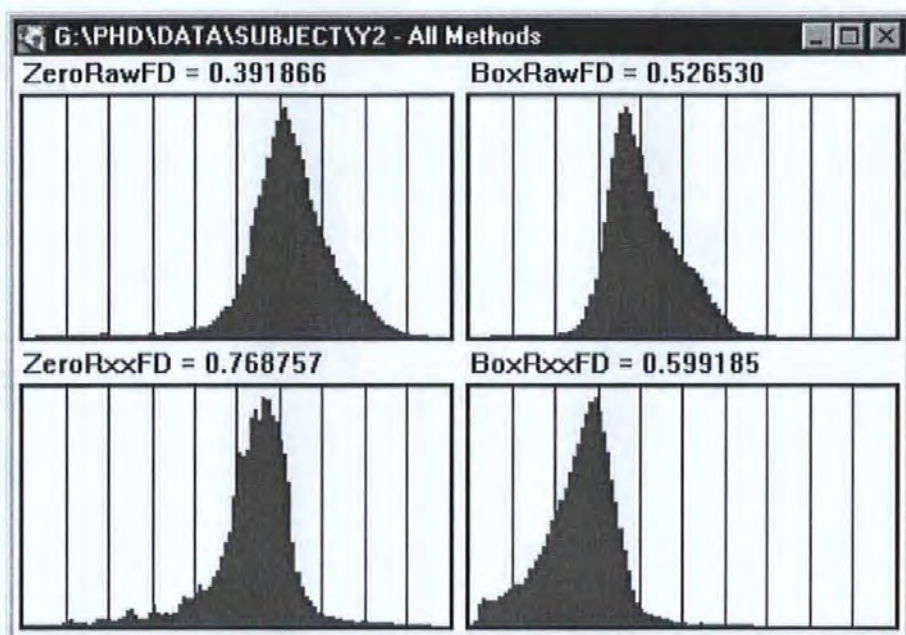
Figure 3-17, Histograms of four fractal measures applied to the EEG of subject Y2.
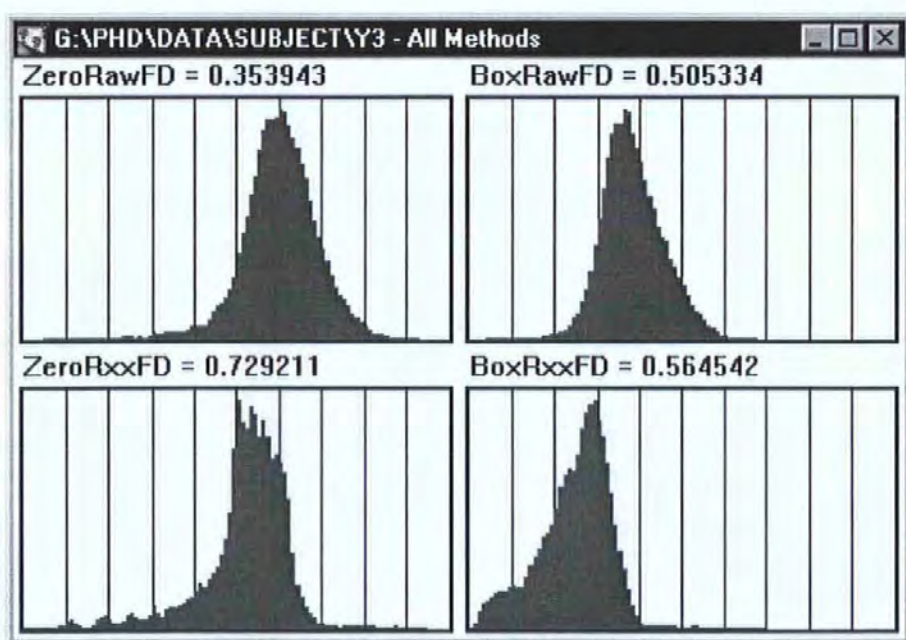
Figure 3-18, Histograms of four fractal measures applied to the EEG of subject Y3.
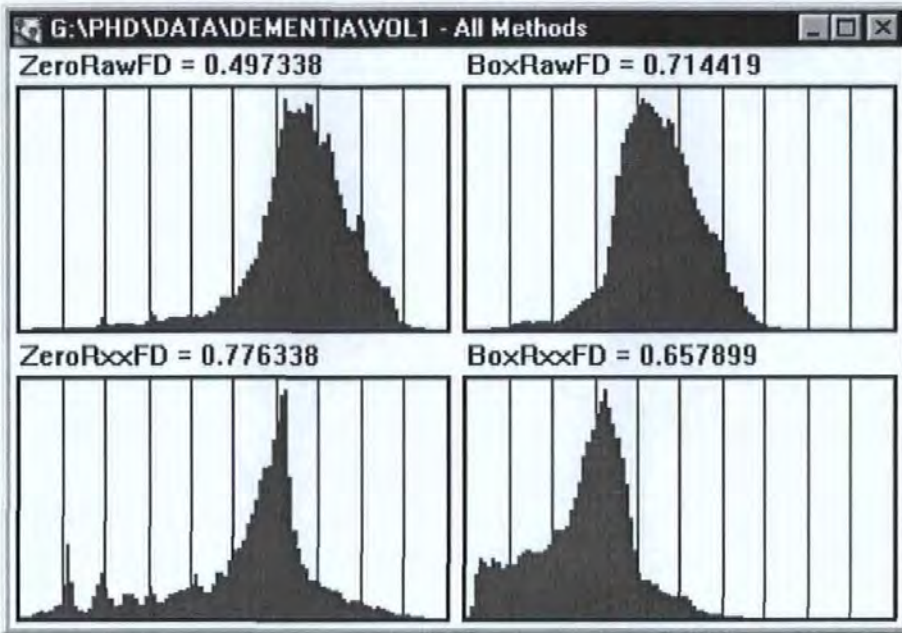
Figure 3-19, Histograms of four fractal measures applied to the EEG of subject Vol1.
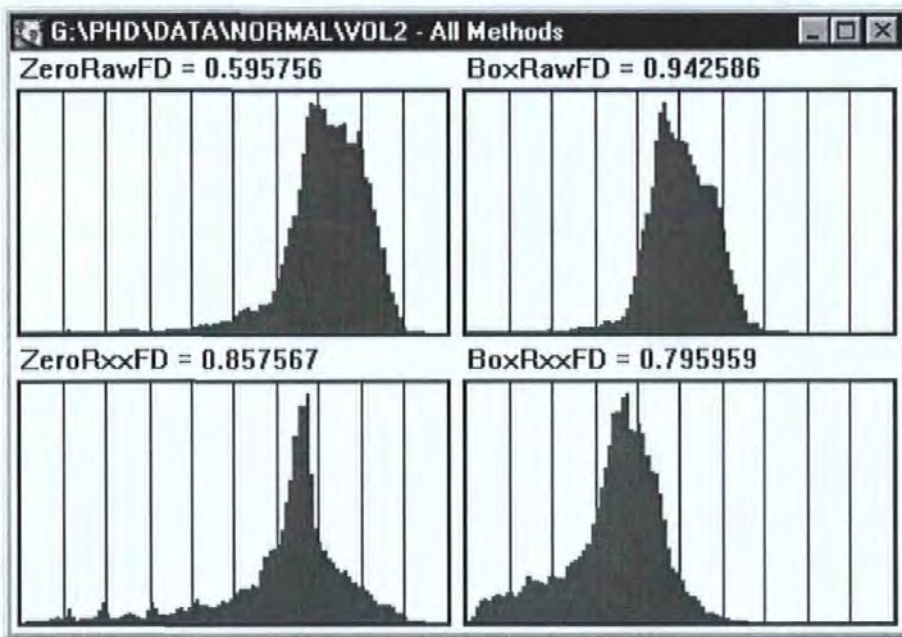
Figure 3-20, Histograms of four fractal measures applied to the EEG of subject Vol2.
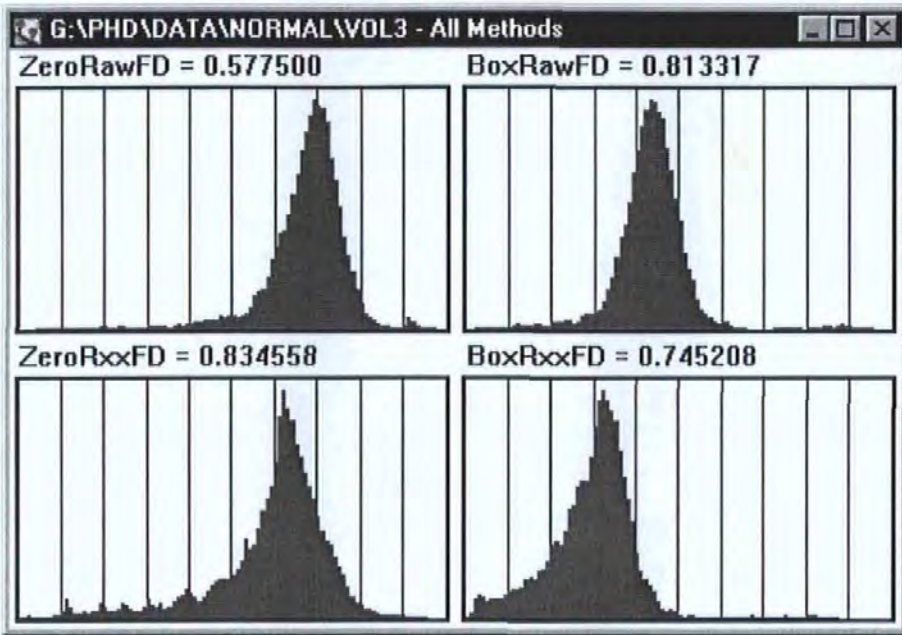
Figure 3-21, Histograms of four fractal measures applied to the EEG of subject Vol3.
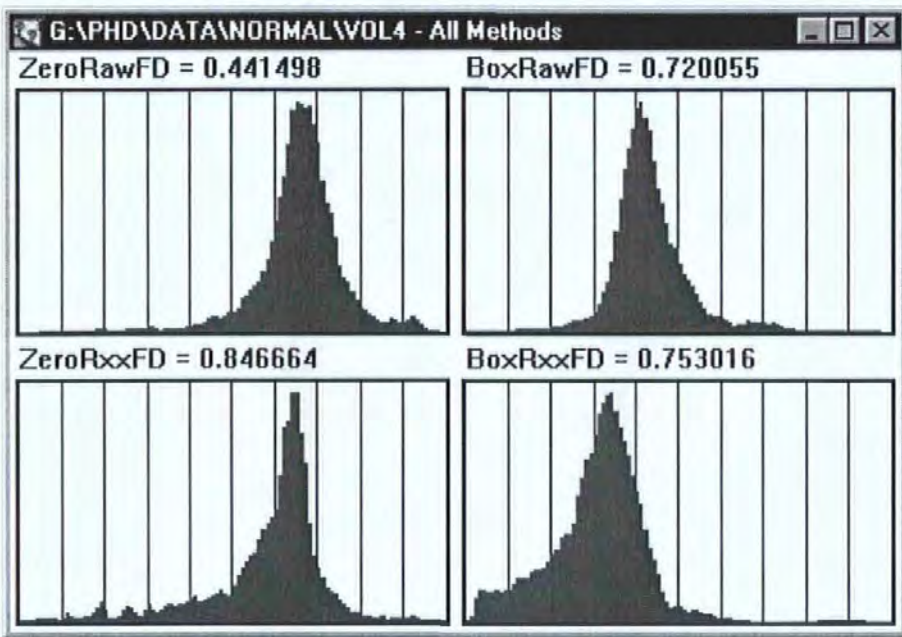
Figure 3-22, Histograms of four fractal measures applied to the EEG of subject Vol4.
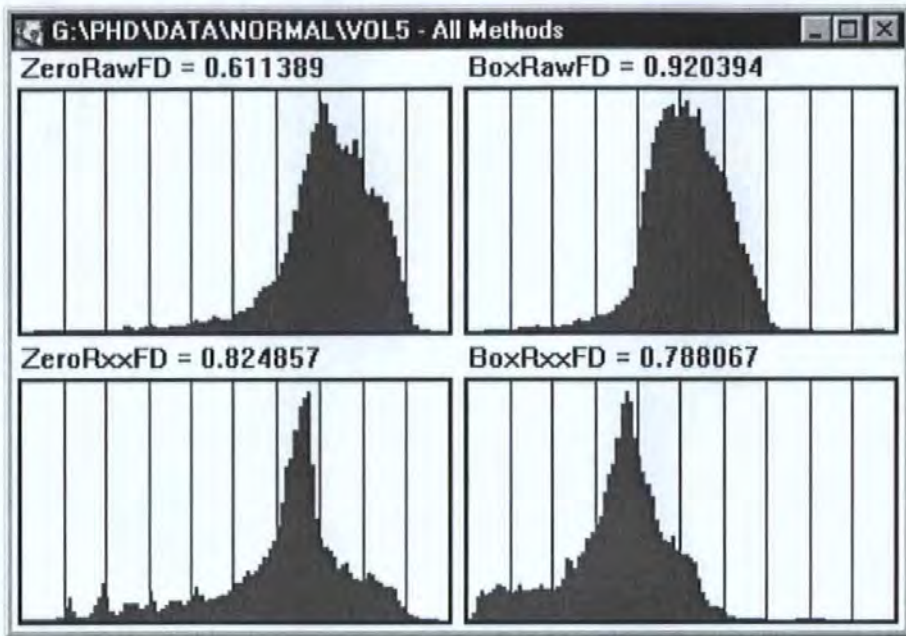
Figure 3-23, Histograms of four fractal measures applied to the EEG of subject Vol5.
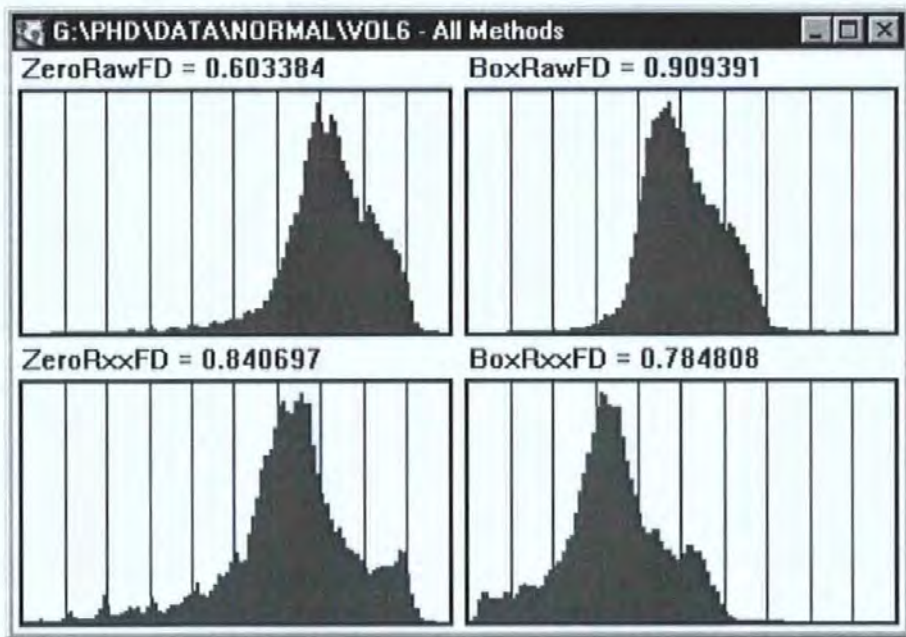
Figure 3-24, Histograms of four fractal measures applied to the EEG of subject Vol6.
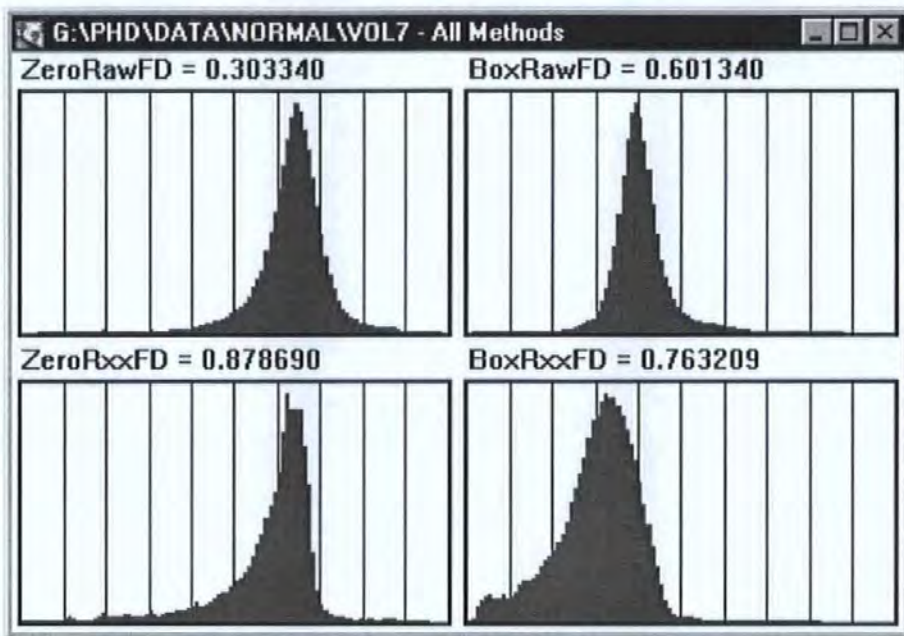
Figure 3-25, Histograms of four fractal measures applied to the EEG of subject Vol7.
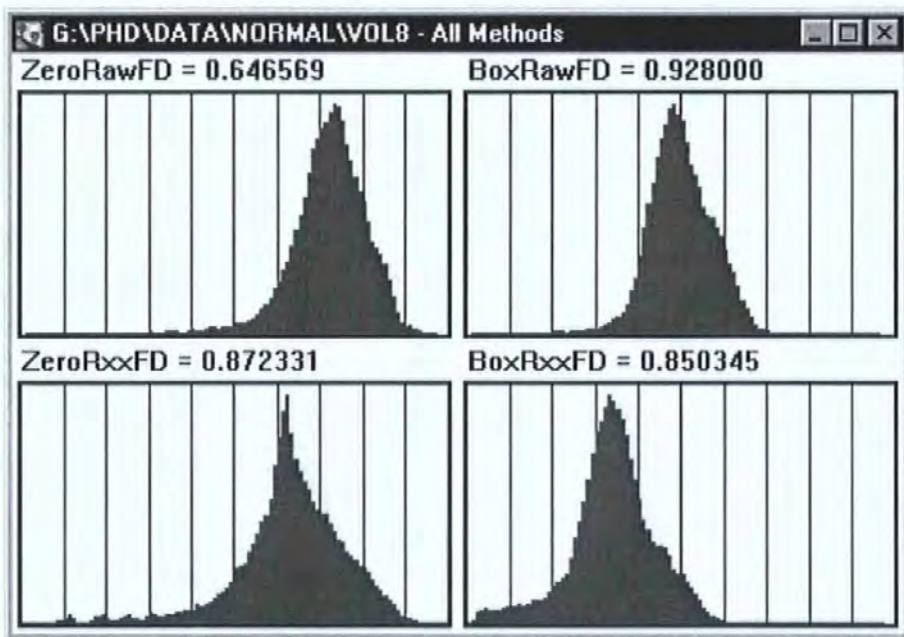
Figure 3-26, Histograms of four fractal measures applied to the EEG of subject Vol8.
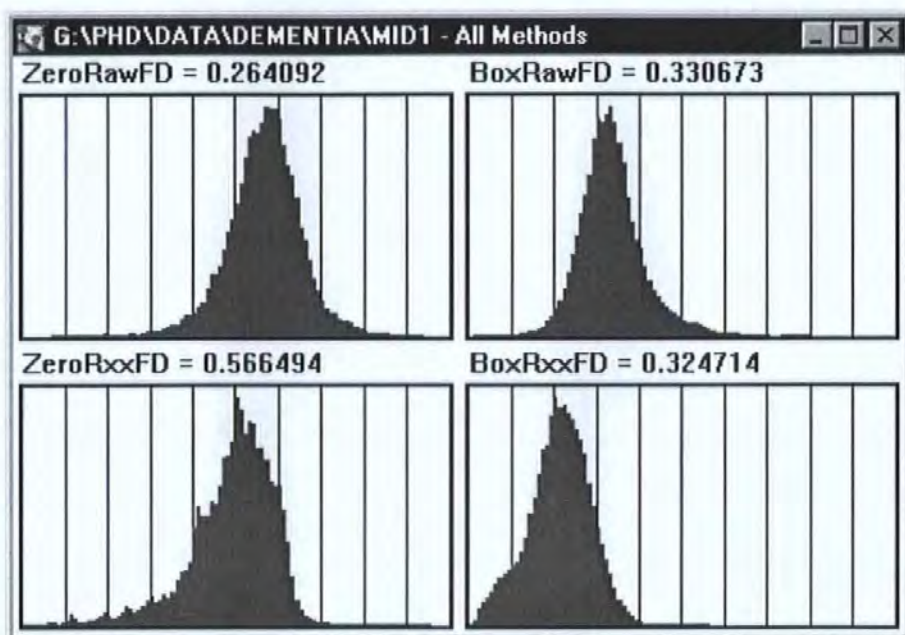
Figure 3-27, Histograms of four fractal measures applied to the EEG of subject MID1.
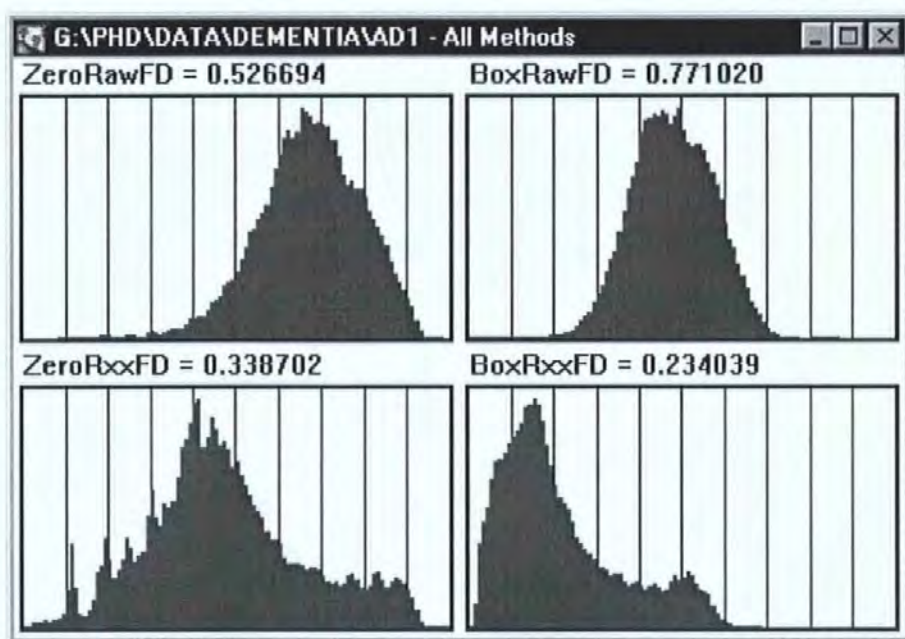
Figure 3-28, Histograms of four fractal measures applied to the EEG of subject AD1.
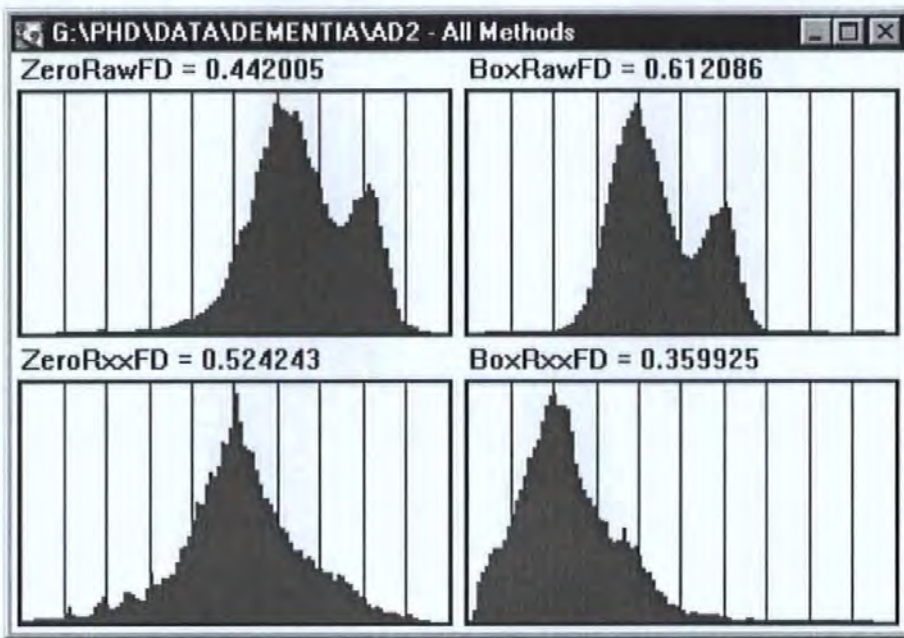
Figure 3-29, Histograms of four fractal measures applied to the EEG of subject AD2.
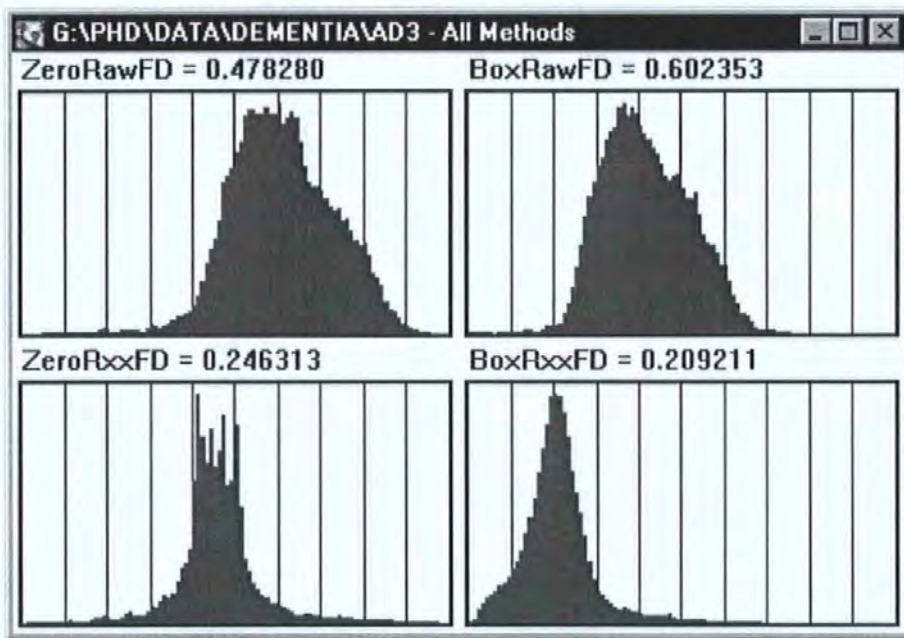
Figure 3-30, Histograms of four fractal measures applied to the EEG of subject AD3.
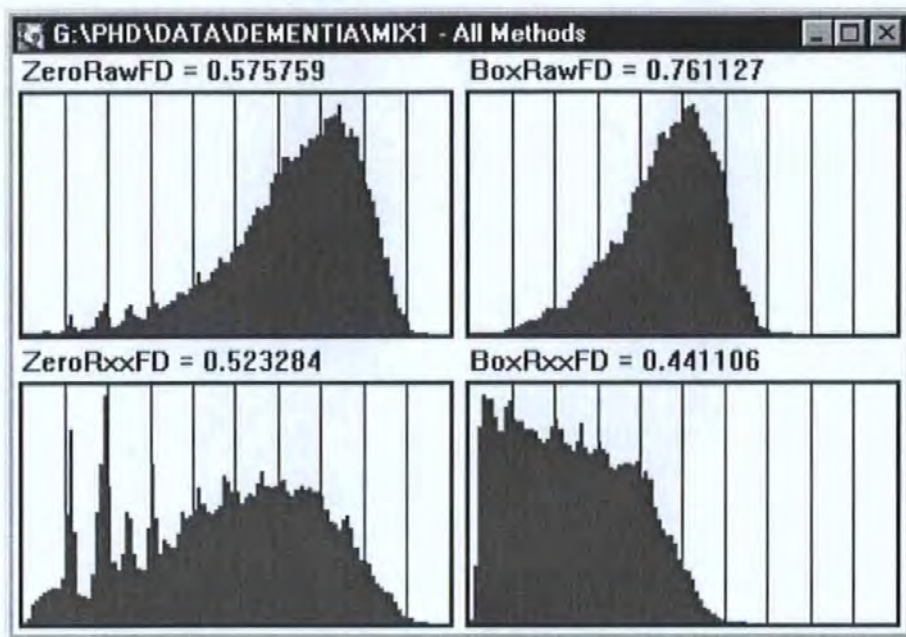
Figure 3-31, Histograms of four fractal measures applied to the EEG of subject Mix1.
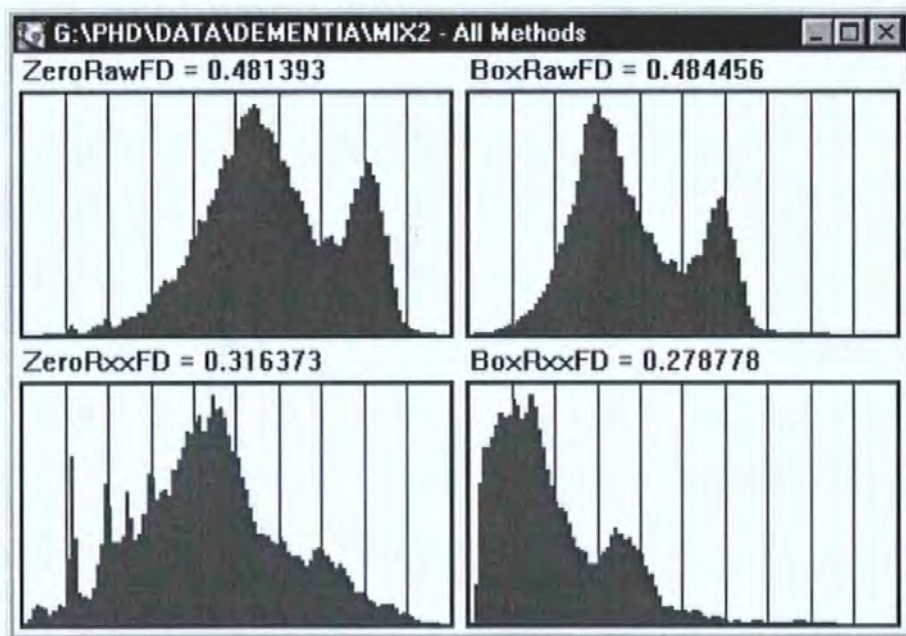
Figure 3-32, Histograms of four fractal measures applied to the EEG of subject Mix2.
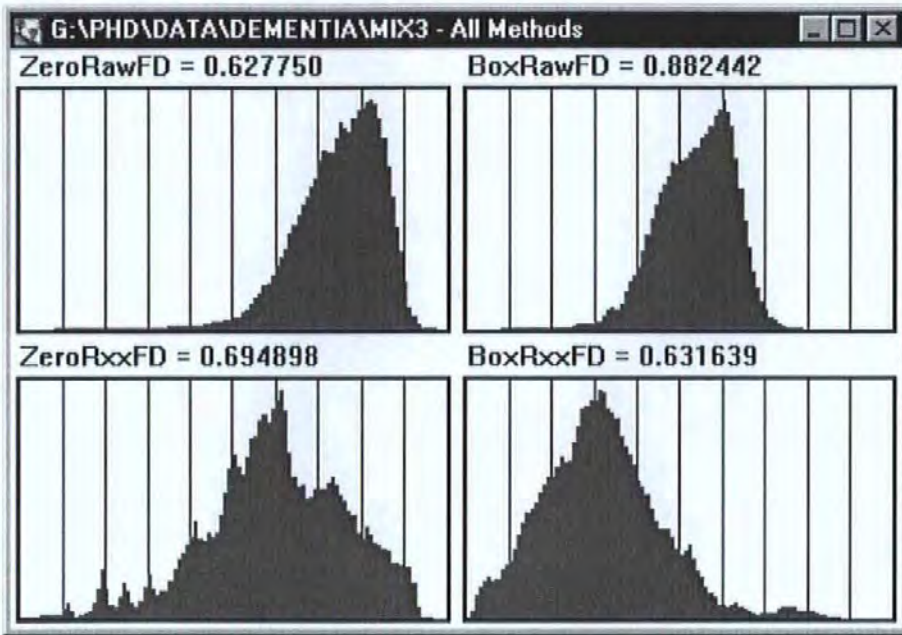
Figure 3-33, Histograms of four fractal measures applied to the EEG of subject Mix3.

The metric (the ratio of density in the Alpha range to the sum of the densities in the Alpha and Theta ranges) was calculated for all four methods and it was found that the most promising came from the Zeros-Set Dimension of the Auto-correlation. This is demonstrated in Table 3-13 and Table 3-14.

		Zero set dimension		Adapted box dimension	
		Raw	Auto-correlation	Raw	Auto-correlation
Age matched controls:	vol2	0.596	0.858	0.943	0.796
	vol3	0.578	0.835	0.813	0.745
	vol4	0.441	0.847	0.720	0.753
	vol5	0.611	0.825	0.920	0.788
	vol6	0.603	0.841	0.909	0.785
	vol7	0.303	0.879	0.601	0.763
	vol8	0.647	0.872	0.928	0.850
Mean		0.540	0.851	0.834	0.783
Standard Deviation		0.123	0.020	0.130	0.035
Age matched control who went on to develop Alzheimer's Disease	vol1	0.497	0.776	0.714	0.658

Table 3-13, Alpha-Theta ratio results for normal subjects.

		Zero set dimension		Adapted box dimension	
		Raw	Auto-correlation	Raw	Auto-correlation
Mixed dementia subjects:	mix1	0.576	0.523	0.761	0.441
	mix2	0.481	0.316	0.484	0.279
	mix3	0.628	0.695	0.882	0.632
Multi-Infarct subjects	mid1	0.264	0.566	0.331	0.325
Alzheimer's Disease subjects	ad1	0.527	0.339	0.771	0.234
	ad2	0.442	0.524	0.612	0.360
	ad3	0.478	0.246	0.602	0.209
"Most normal" subject with dementia		0.628	0.695	0.882	0.632
Difference between "most normal" demented subject and mean normal divided by Std Dev of normal subjects		-0.7	7.9	-0.4	4.3

Table 3-14, Alpha-Theta ratio results for subjects with dementia.

80

For the alpha/theta ratio of the zero set dimension of the auto-correlation function, the difference between the "most normal" subject with dementia (Mix3) and the mean of the normal subjects is 0.156, which is 7.9 times the standard deviation among the normal subjects. This represents (all-be-it on this small data set) a clear differentiation between the normal and subjects with dementia.

Interestingly Vol1 who was passed as normal by a clinician and later developed Alzheimer's Disease is clearly abnormal by this test with a result of 0.776.

The data previously used to investigate the subject specific analysis concept, from the two young controls (X and Y), was reanalysed using this method. The results were a surprise (Table 3-15). X has a spread over three measurements of 0.122, which is more than 6 times the estimated population standard deviation of the age-matched controls. Y, who had less of a spread, was none-the-less surprising because the mean of the results (0.734) was 0.118 less than the mean of the age-matched controls. This difference is just less than 6 times the estimated population standard deviation of the age-matched controls. It would be easy to ignore these data but it was recognised that they provide significant counter evidence to the seemingly strong evidence (above) for the efficacy of this method. It was hypothisised that this could be an age related effect but there was insufficient data to support or reject this.

Young volunteer X	X1	0.785
	X2	0.907
	X3	0.809
Young volunteer Y	Y1	0.751
	Y2	0.750
	Y3	0.702

Table 3-15, Alpha Theta Ratio results for young subjects.

Although the results from X and Y are difficult to explain and the method does not neatly fit the subject specific methodology, it remains an interesting candidate for early detection of dementia. Therefore, results for this metric are produced as a supplement to the evaluation of the other fractal methods using new, independent data described in Chapter 4.

3.7 Time Evolution of the Fractal Dimension

3.7.1 Discussion and Results

Given the preceding discussions of subjects specific measures and a desire to understand better the non-stationary nature of the EEG, it was decided to evaluate how the fractal dimension varies with time. To this end, each of the EEG records was divided into 1-minute intervals and the zero-set fractal dimension of the auto-correlation function was calculated for each. The results for the normal subjects are given in Table 3-16 and the results for the subjects with dementia are given in Table 3-17. These results are also shown graphically in Figure 3-34 and Figure 3-35.

Start Time (s)	FRACTAL DIMENSION OF THE ZERO-SET OF THE AUTO-CORRELATION						
	Vol2	vol3	vol4	vol5	vol6	vol7	vol8
0	0.7531	0.8070	0.8436	0.6300	0.7543	0.7950	0.8103
60	0.8670	0.9121	0.8894	0.9131	0.8690	0.8320	0.8184
120	0.9060	0.8925	0.9153	0.9104	0.8974	0.8511	0.8283
180	0.9154	0.7413	0.9067	0.9229	0.9042	0.8322	0.8294
240	0.9538		0.9312	0.8889	0.8954	0.8446	0.7791
300	0.8338		0.8739	0.6276	0.7568	0.7909	0.8406
360	0.6906		0.7132		0.6029	0.7839	0.8902
420			0.6316			0.9386	0.9155
480						0.8791	0.9188
540						0.8781	0.9197
600						0.9052	0.9051
660						0.9318	0.9032
720						0.9186	0.9248
780						0.9305	0.9237
840						0.9151	0.9172
900						0.9044	

Table 3-16; Time progression of Fractal Dimension in normal subjects.

Start Time (s)	FRACTAL DIMENSION OF THE ZERO-SET OF THE AUTO-CORRELATION						
	Ad1	ad2	ad3	mix1	mix2	mix3	mid1
0	0.6112	0.6922	0.2686	0.5591	0.3595	0.7244	0.6384
60	0.4571	0.5431	0.3029	0.4663	0.3438	0.8459	0.6672
120	0.2575	0.5662	0.3054	0.5642	0.4307	0.7796	0.6122
180	0.2396	0.5166	0.2885	0.5147	0.391	0.7118	0.5855
240	0.2484	0.5584	0.2837	0.5023	0.3532	0.5537	0.5789
300	0.2497	0.5141	0.2927	0.6114	0.3368	0.6838	0.6031
360	0.2541	0.5286	0.2109	0.532	0.3413	0.757	0.5537
420	0.2653	0.5062	0.2543	0.52	0.273	0.7237	0.5251
480	0.3467	0.4495	0.2286	0.5186	0.2698	0.5844	0.5398
540	0.3197	0.4559	0.2328	0.5218	0.2855	0.7205	0.5037
600	0.285	0.4631	0.257	0.4643	0.2063		0.4803
660	0.3792	0.5163		0.5729			
720	0.5161			0.5721			
780	0.4571			0.5861			
840				0.4817			
900							

Table 3-17; Time progression of Fractal Dimension in subjects with dementia.
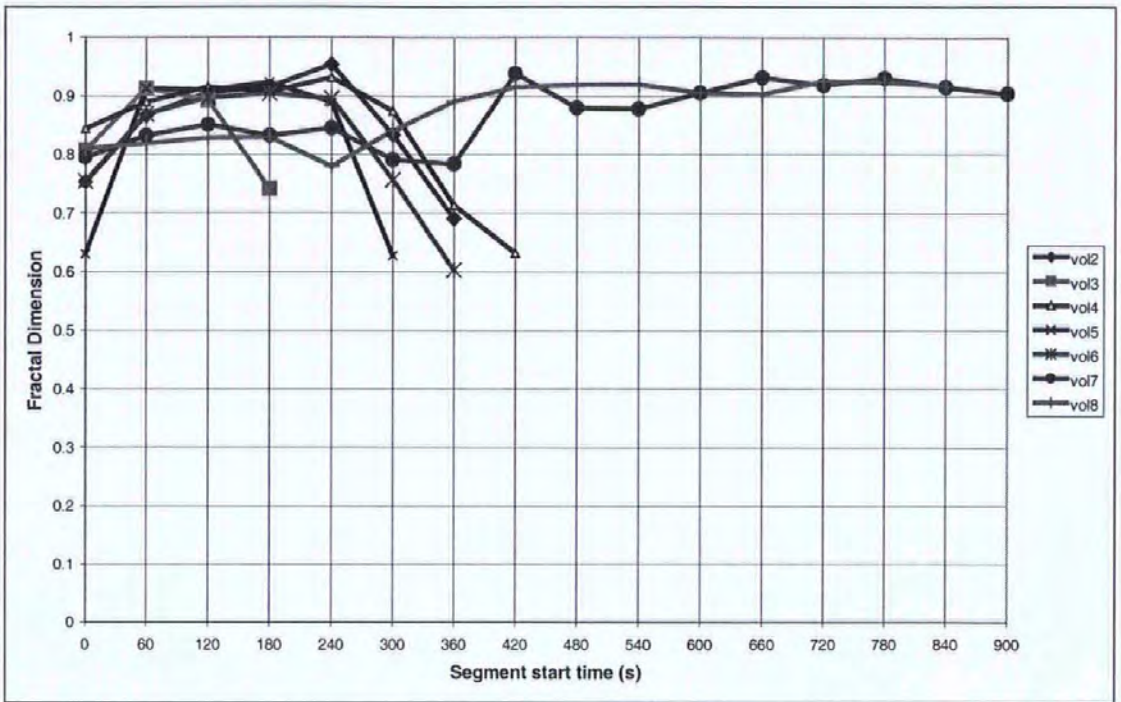
Figure 3-34, Time progression of fractal dimension in normal subjects.
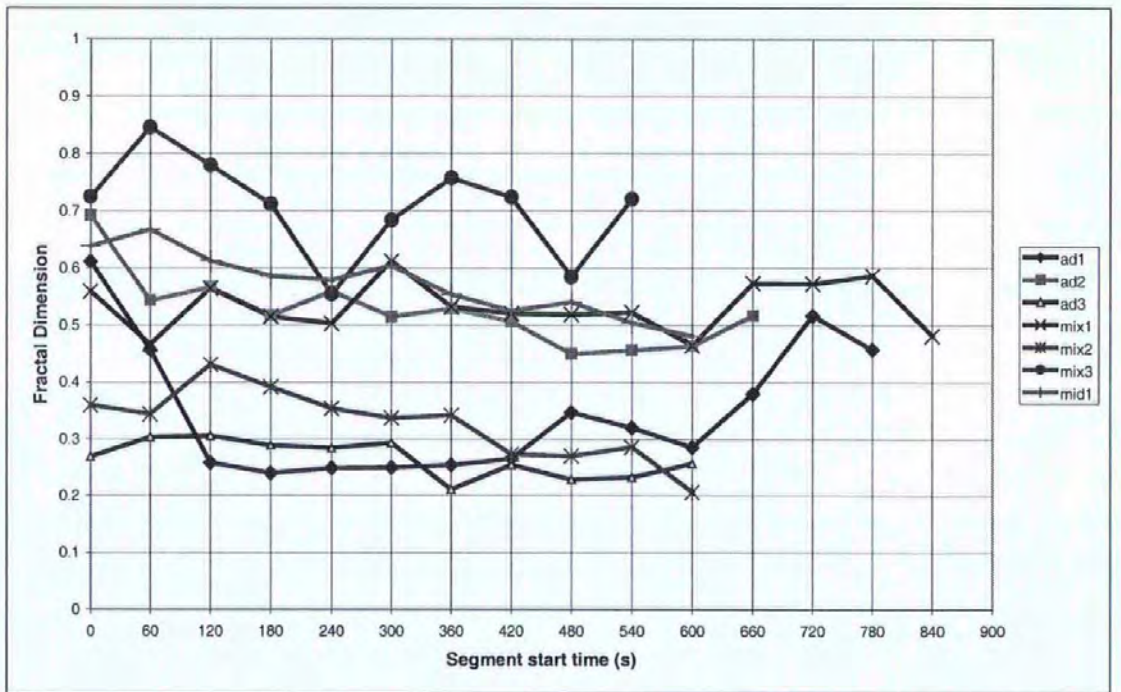
Figure 3-35, Time progression of fractal dimension in subjects with dementia.

3.7.2 Conclusion

It may be seen that the measured fractal dimension (zero-set dimension of the auto-correlation function) is reasonably stable and high for the normal subjects except where they become drowsy toward the end of the recording. The subjects with dementia present a generally lower fractal dimension (as noted previously) and the fractal dimension seems not quite as stable with time as the normals. It is also interesting to note that the subjects with dementia do not seem to enter a drowsy phase before the end of the recording.

3.8 Variability of Fractal Dimension Over the Scalp

3.8.1 Introduction

The efficacy of automated EEG analysis is expected to vary over the scalp for two reasons. Firstly, because the effect of dementia on the EEG varies over the scalp and secondly, because the masking effects of other signals (cerebral in origin and artefacts) varies over the scalp. To investigate the extent of this effect, the fractal dimension was measured independently in all channels and the performance of the method was evaluated for each channel. Section 3.8.2 below describes a method for quantifying the performance of the method and section 3.8.3 contains the results.

3.8.2 Method Evaluation Metric

How well the method works can be quantified by using a "Method Evaluation Metric": As, this research is aimed at analysing an EEG recording to derive an index which is significantly different for normal and subjects with dementia it is important to have a measure that describes how well the index performs this task. We have chosen to measure the performance of a candidate index using, what we have termed, a "Method Evaluation Metric".

To evaluate this metric we begin by calculating the candidate index for all control subjects and subjects with dementia, then the mean and estimated population standard deviation (σ) of the index for the control subjects is recorded (excluding Vol1 who went on to develop Alzheimer's). Finally, the difference between the mean of the index from the controls and the closest index from any of the subjects with dementia (i.e. closest to normal) is divided by σ.

Thus calculated, the Method Evaluation Metric describes how many standard deviations the "most normal" subject with dementia is from the mean of the control subjects. As a guide a 3 is good and 6 is excellent. A similar figure may be produced for Vol1 to see whether there was a significant, previously undetected decline.

An illustrative example is given in Table 3-18, where the index under evaluation is the fractal dimension of the Zero-set of the autocorrelation function. The example shows that it is unlikely that the "most normal" of the subjects with dementia could have come from the population of normals and that Vol1 is hardly distinguishable.

Comment	Subject	Index
Measured index from normal subjects.	Vol2	0.590
	Vol3	0.648
	Vol4	0.622
	Vol5	0.562
	Vol6	0.627
	Vol7	0.539
	Vol8	0.670
Mean	Mean	0.6083
Estimated population Std Dev'n	SD	0.0469
Measured index from subjects with dementia.	AD1	0.323
	AD2	0.368
	AD3	0.331
	MID1	0.384
	MIX1	0.324
	MIX2	0.270
	MIX3	0.438
"Most normal" subject with dementia	MIX3	0.438
Difference from mean normal to "most normal" subject with dementia	Mean–MIX3	0.170
Method evaluation metric. i.e. the difference of mean normal to "most normal" subject with dementia	Mean–MIX3 SD	$3.6\,\sigma$
Control who went on to develop Alzheimer's	Vol1	0.516
Difference from mean normal to Vol1	Mean–Vol1	0.092
Method evaluation metric. i.e. the difference of mean normal to Vol1	Mean–Vol1 SD	$2.0\,\sigma$

Table 3-18, Method evaluation metric.

3.8.3 Results

The results, using the method evaluation metric applied to the four Fractal Dimension methods as they vary over the scalp, are presented graphically below.
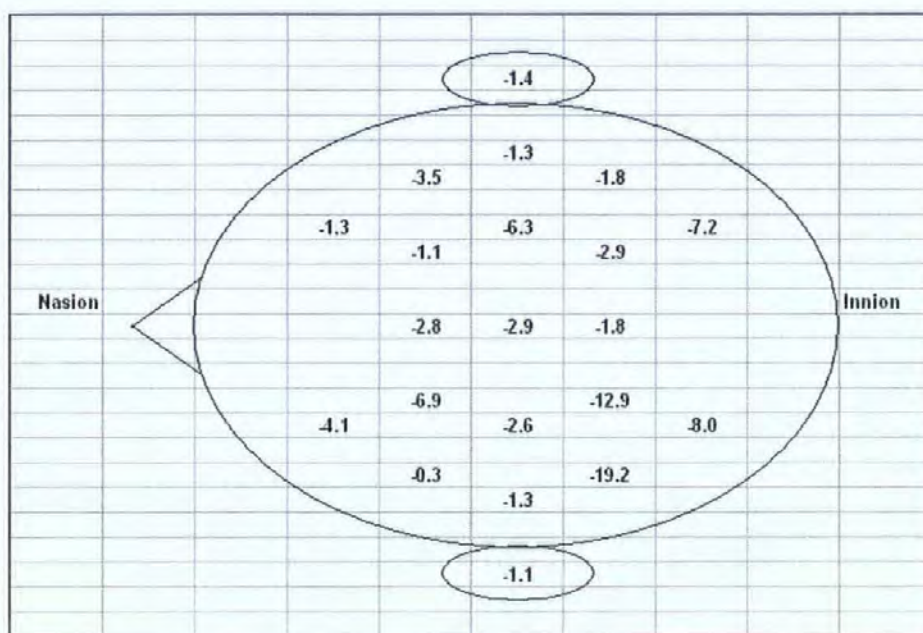
Figure 3-36, Method evaluation metric using the zero-set dimension of the raw data.
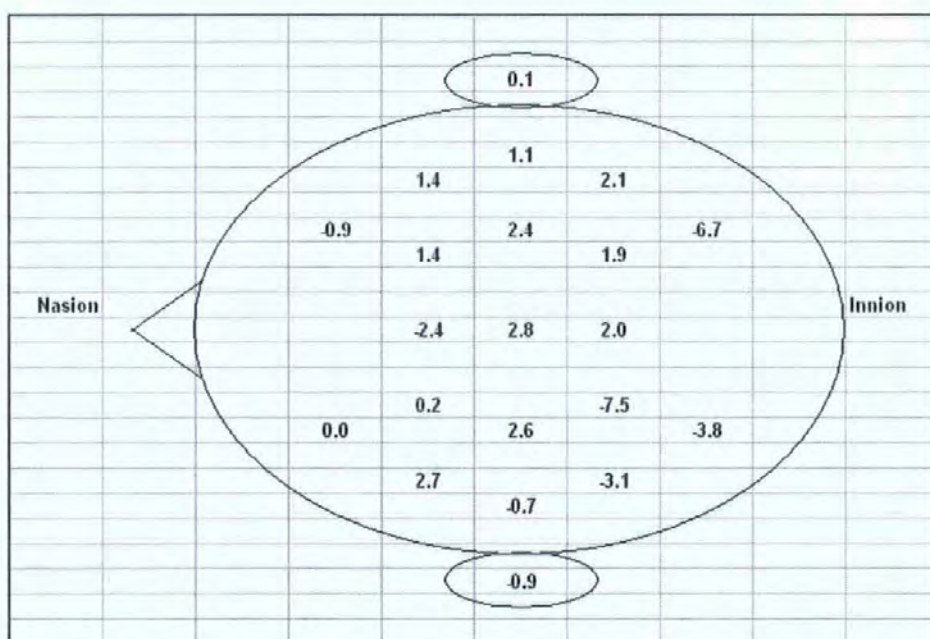
Figure 3-37, Method evaluation metric using the zero-set dimension of the auto-correlation function.
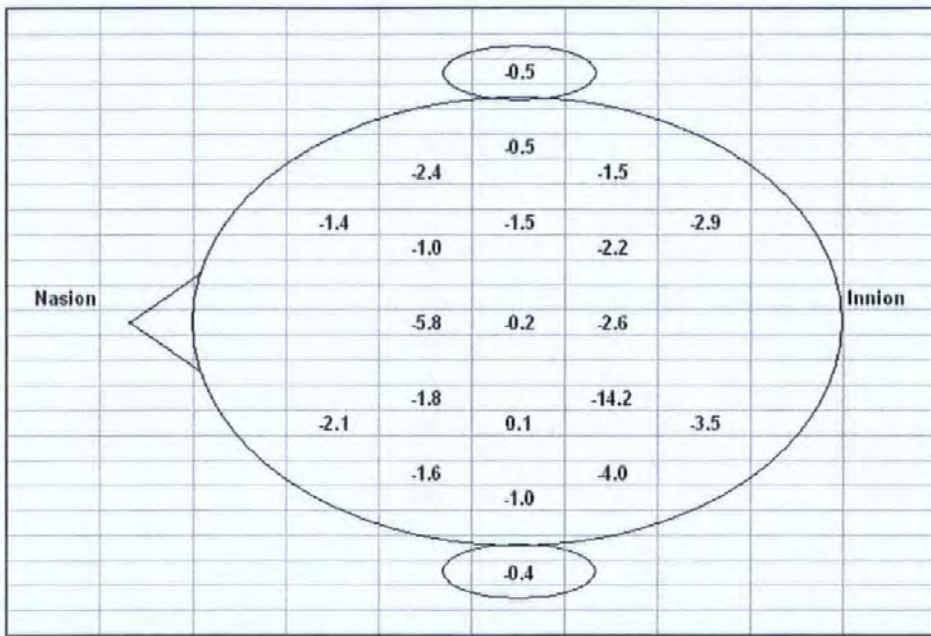
Figure 3-38, Method evaluation metric using the adapted box dimension of the raw data.
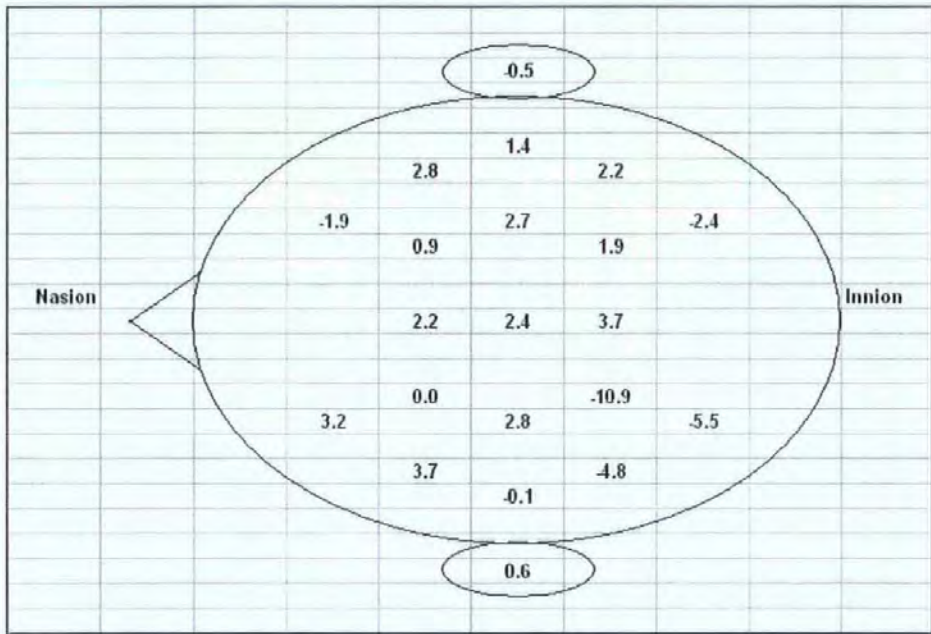
Figure 3-39, Method evaluation metric using the adapted box dimension of the auto-correlation function.

These results are inconclusive, and it was decided to repeat this analysis using the revised methods described in Section 3.4.3.

3.8.4 Revised Results

Given the disappointing results the methods were checked and it was found that changing controlling constants, such as the segment length, affected the results. These effects are dealt with more fully later in this thesis and better results were produced. These tuned methods were used to give the revised results below.
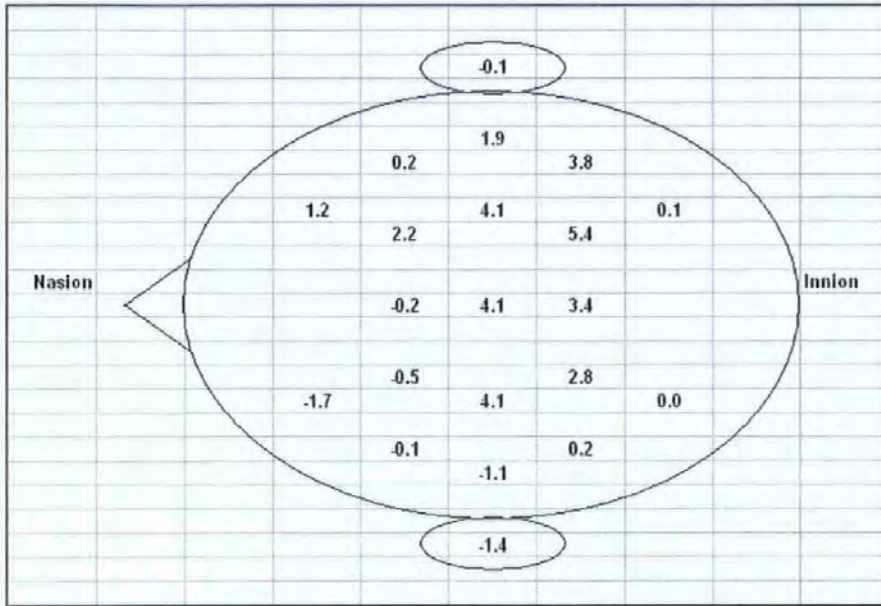
Figure 3-40, Method evaluation metric using the zero-set dimension of the raw data.
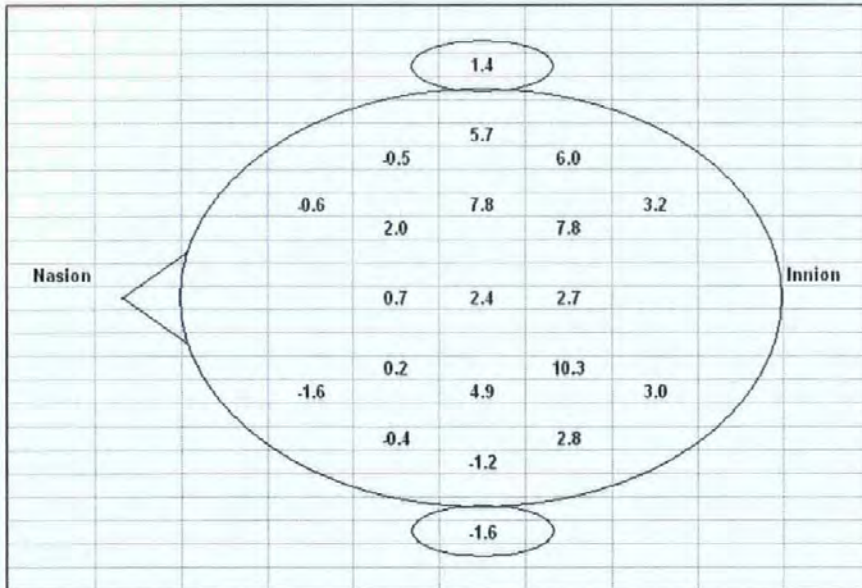
Figure 3-41, Method evaluation metric using the zero-set dimension of the auto-correlation function.
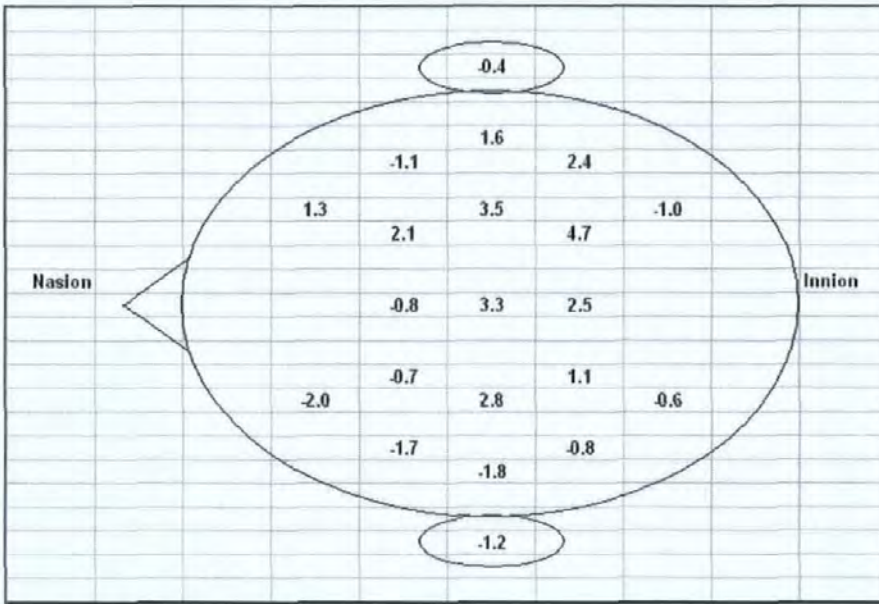
Figure 3-42, Method evaluation metric using the adapted box dimension of the raw data.
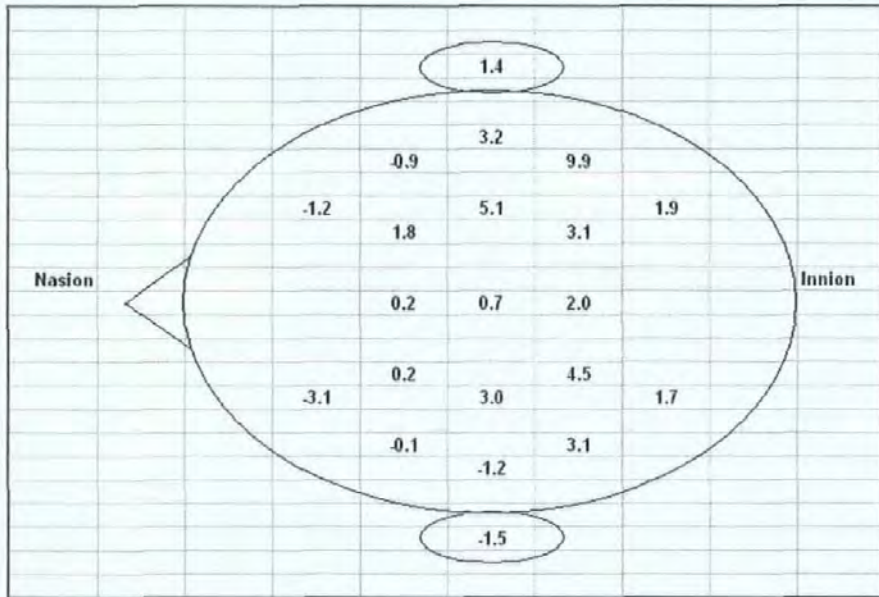
Figure 3-43, Method evaluation metric using the adapted box dimension of the auto-correlation function.

3.8.5 Conclusion

Using the revised method, it was shown that the best separation of subjects with dementia from control subjects was achieved in the central and posterior regions of the scalp. Thus, it has been confirmed that the efficacy of automated EEG analysis does vary over the scalp and this is believed to be for two reasons. Firstly, because the effect of dementia on the EEG varies over the scalp and secondly, because the masking effects of other signals (cerebral in origin and artefacts) varies over the scalp.

Further indications that, in Alzheimer's Disease, the posterior regions of the scalp should provide the earliest evidence for dementia was found in a study of early onset Alzheimer's Disease related Cortical Atrophy in the Lancet [6]. This shows that the earliest atrophy occurs in the posterior region and at the base of the brain.

3.9 Questioning the use of Auto-Correlation

3.9.1 The Question

Inspired by the work of other earlier researchers, the fractal dimension of the auto-correlation function had been used in this research. However, one must ask, "what is the meaning of the fractal dimension of an auto-correlation function?" This is particularly important because these measures seemed, during these initial investigations, to give the best results (although the clinical evaluation in Chapter 4 later showed that this is not the case).

Despite a great deal of thought, the meaning of the fractal dimension of an auto-correlation function could not be envisaged. An interesting alternative is, though, that it has no meaning, but instead happens to give a particular result because of the spectral content of the EEG. It has been shown for example [41] that a non-fractal (i.e. with incoherent phase) can appear to have a measured fractal dimension which is a function of the power spectral density.

3.9.2 Method and Results, Part 1

Initially, the assumption was made that signals on different channels would be, to an extent dependent on the proximity of the electrodes, have similar spectra but different phase/shape. Therefore, it was decided to measure the fractal dimension of the zero-set of the cross-correlation function (between channels) and compare this to the fractal dimension of the zero-set of the auto-correlation.

This analysis was performed on one typical normal subject (vol3) and one typical Alzheimer's subject (AD3). The overall fractal dimension of the zero-set of the auto-correlation for these two subjects were 0.556 and 0.308 respectively. The results below (in Figure 3-44 through Figure 3-47) show these fractal dimensions of cross correlations in graphical form. Note the on-diagonal terms are the fractal dimensions of auto-correlations. Detailed numerical results are in Appendix D. for reference in Table 8-1 through Table 8-4.

From these results, it is clear that the cross-correlations have very similar fractal dimension to the auto-correlation, however it was recognised that this was not a sufficient test because the signals on different channels could still be phase coherent.
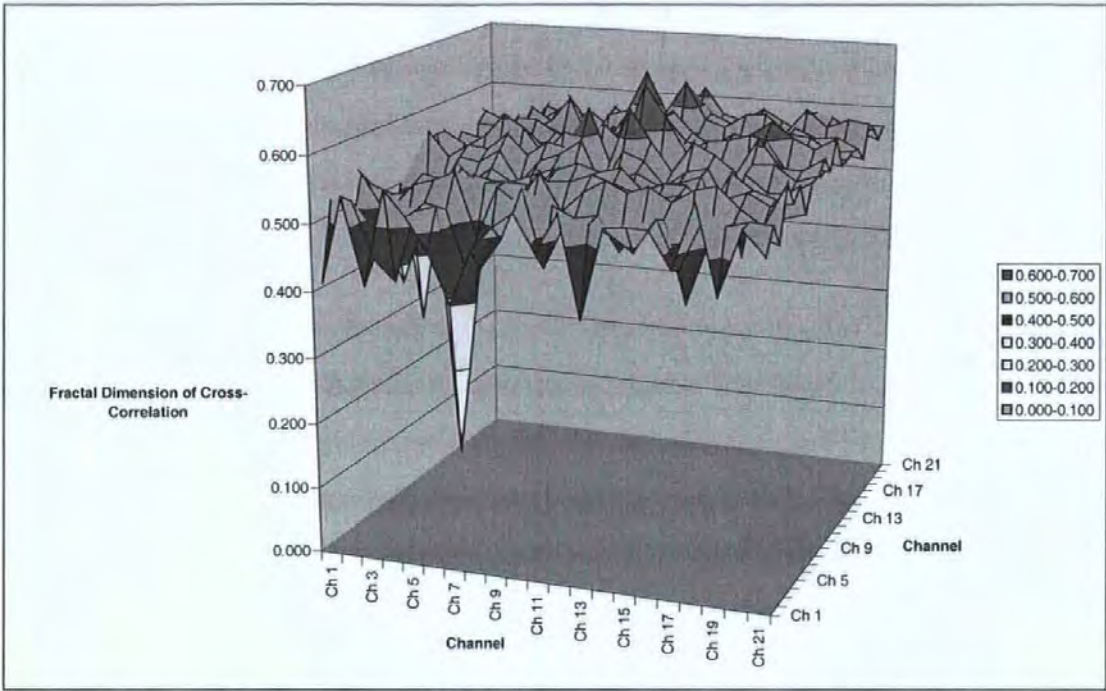
Figure 3-44, 3D representation of the cross-correlation from Vol3.
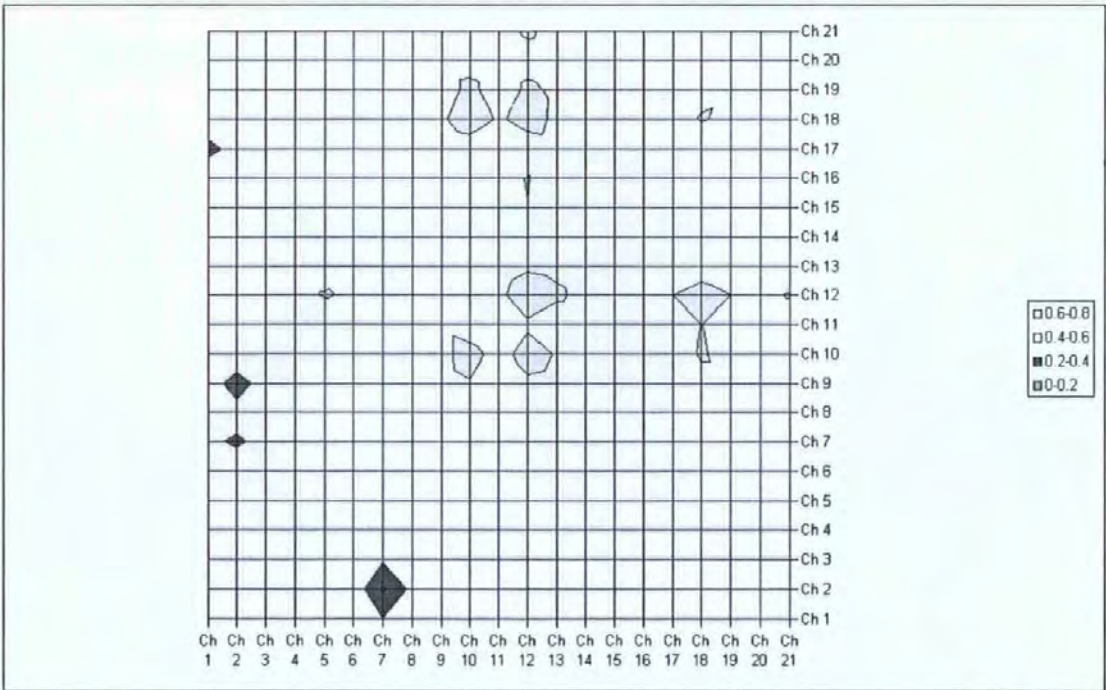
Figure 3-45, Contour map representation of the cross-correlation from Vol3.
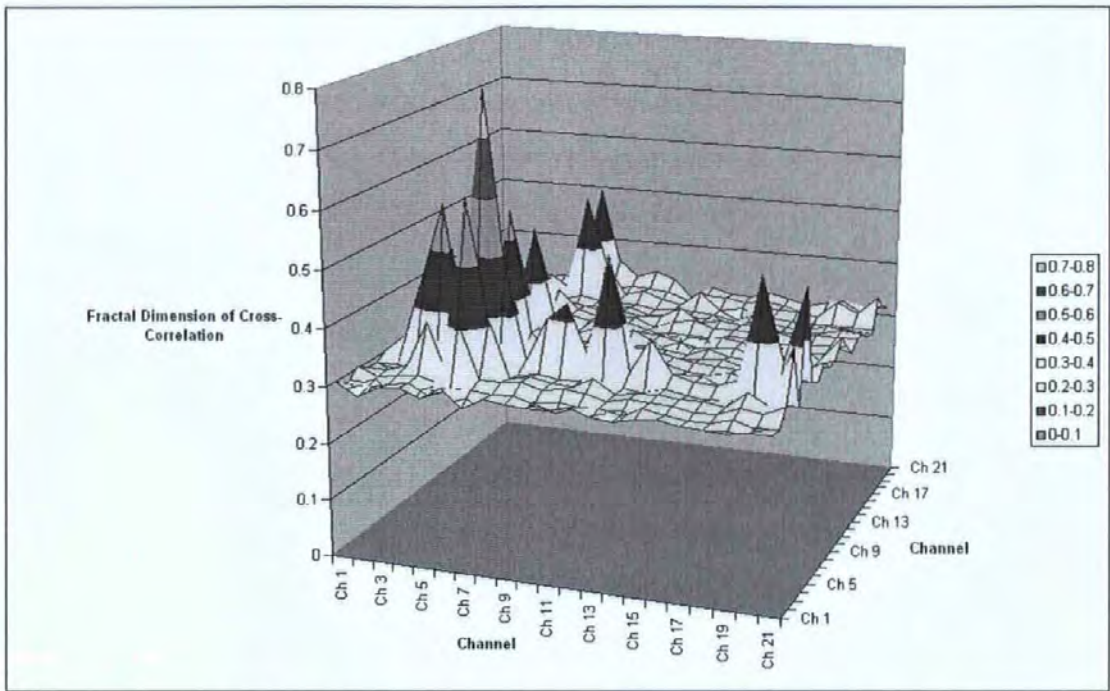
Figure 3-46, 3D representation of the cross-correlation from AD3.
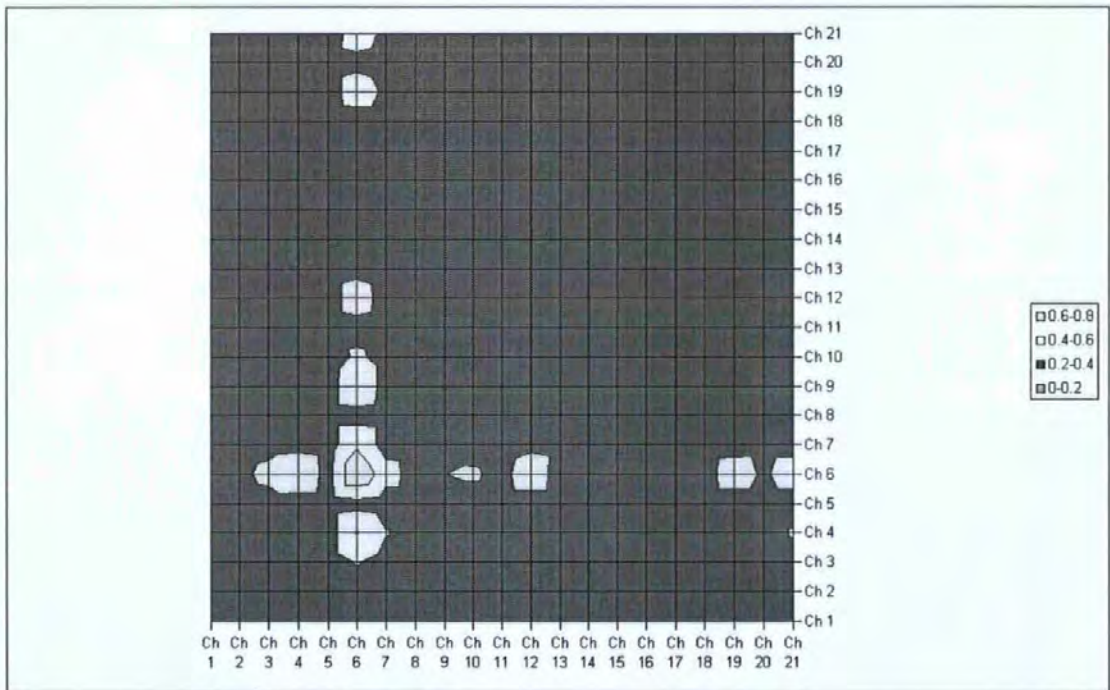
Figure 3-47, Contour map representation of the cross-correlation from AD3.

3.9.3 Method and Results, Part 2

Given the concern that signals on different channels could be phase coherent, it was decided to repeat the analysis. This time, instead of correlating the signal from one channel with the signal from a different channel at the same time, we correlated the signal from one channel with the signal from a different channel at a random different time. Thus, knowing that the EEG is not a stationary signal, we could be sure that any potential phase relationship would be broken. This analysis was again performed on one typical normal subject (vol3) and one typical Alzheimer's subject (AD3).

The results below (in Figure 3-48 through Figure 3-51) show these fractal dimensions of time-incoherent cross-correlations in graphical form. Note the on-diagonal terms are the fractal dimensions of auto-correlations. Detailed numerical results are in Appendix D. for reference in Table 8-5 through Table 8-8.

From these results, it is clear that the time-incoherent cross-correlations have very similar fractal dimension to the auto-correlation (except in the frontal region which is more prone to artefacts).
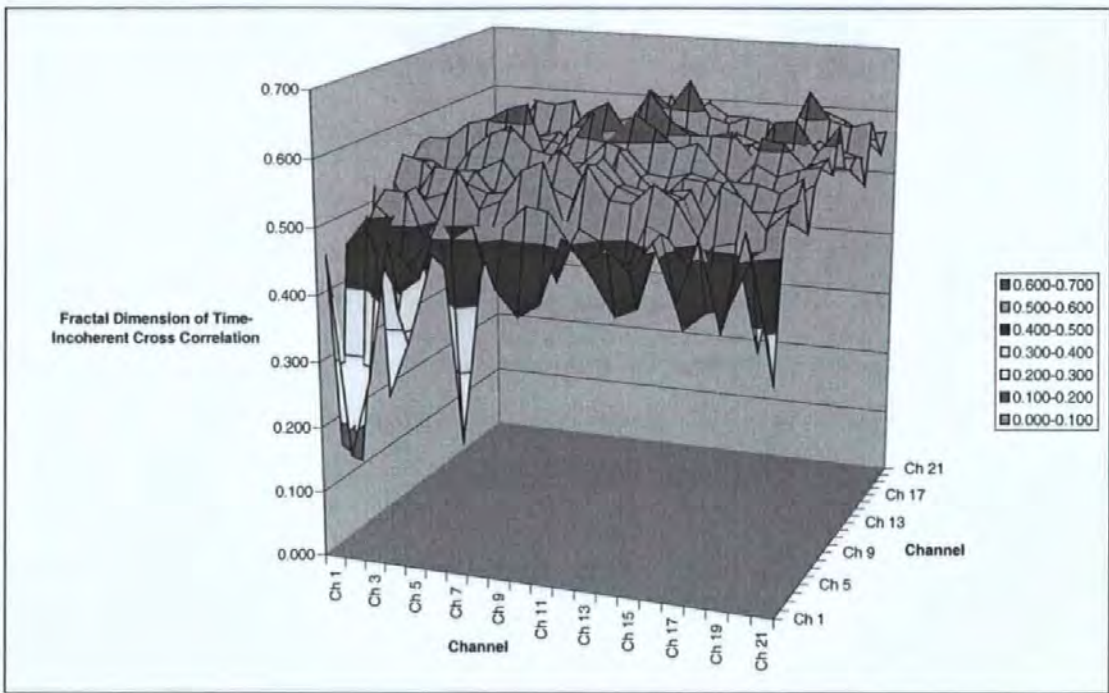
Figure 3-48, 3D representation of the time-incoherent cross-correlation from Vol3.
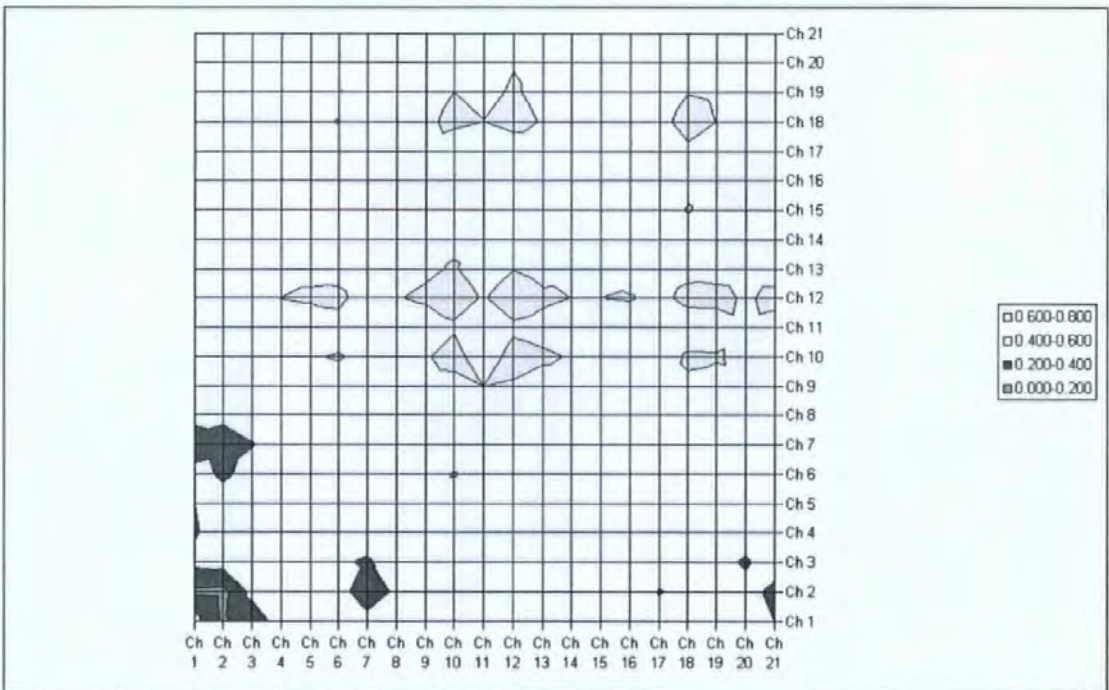
Figure 3-49, Contour map representation of the time-incoherent cross-correlation from Vol3.
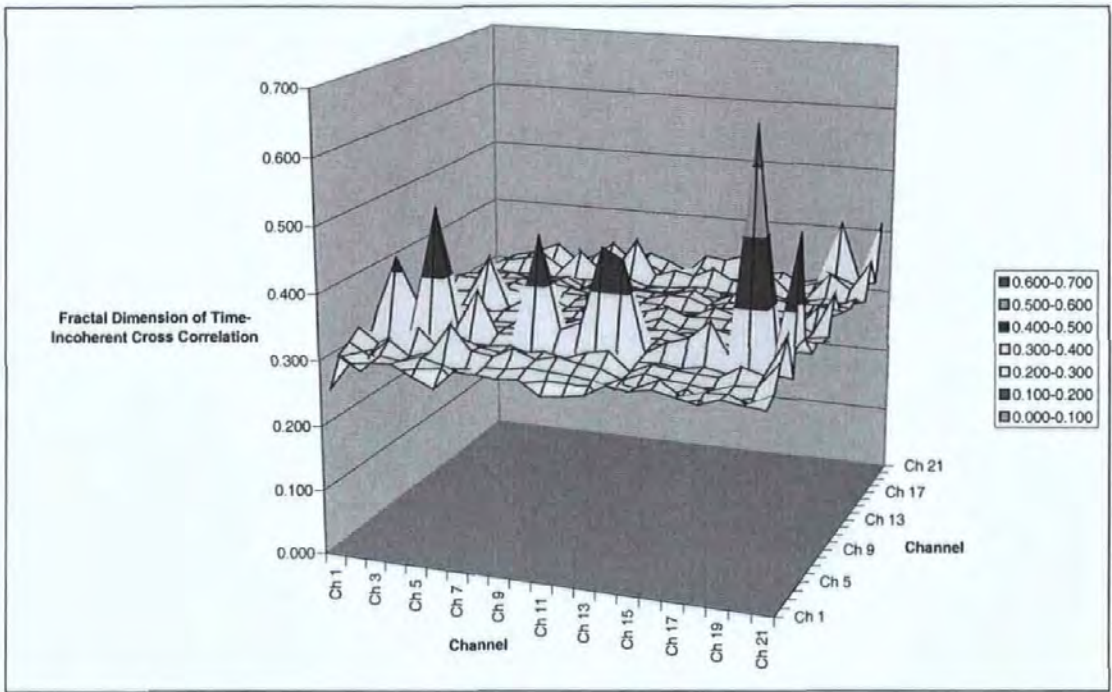
Figure 3-50, 3D representation of the time-incoherent cross-correlation from AD3.
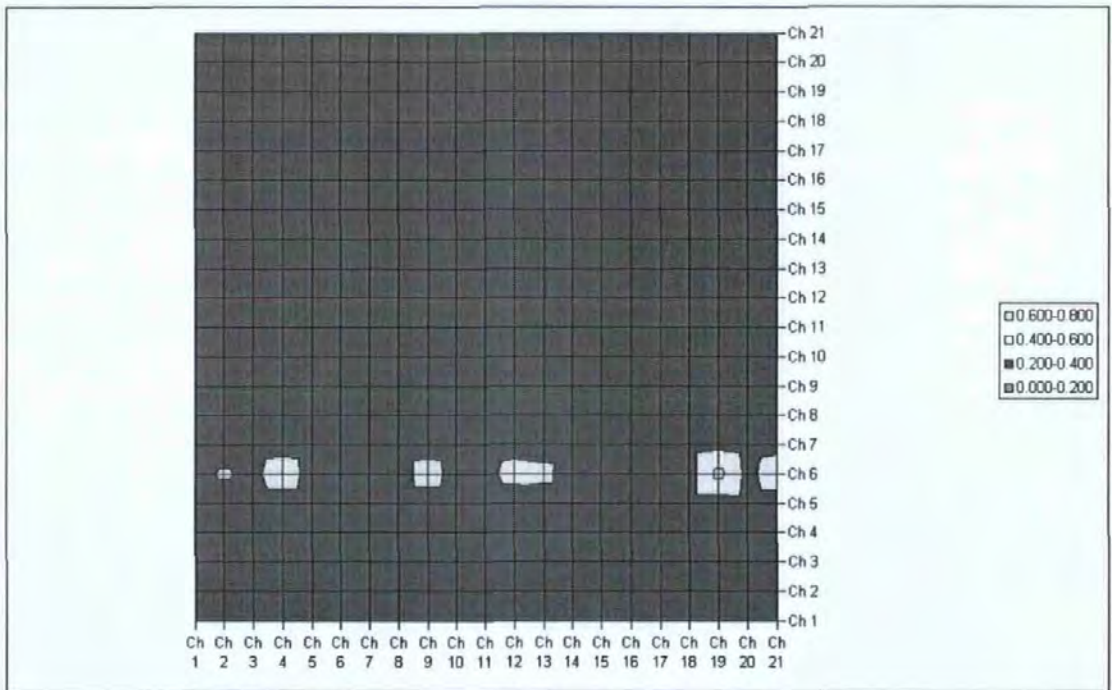
Figure 3-51, Contour map representation of the time-incoherent cross-correlation from AD3.

3.9.4 Method and Results, Part 3

After the experimentation above, it was decided to perform additional analysis on a typical Alzheimer's subject (AD3) and a typical control (Vol3). In this analysis, we varied what correlation was taken and whether phase randomisation was applied. The steps, going further from auto-correlation, are set out in Table 3-19.

Method	Vol3	AD3	Separa-tion
Originally quoted results (up to MEDSIP 2000)	0.648	0.331	0.317
Revised results – new settings	0.557	0.305	0.252
Using cross correlation between all combinations of channels	0.556	0.308	0.248
Using cross correlation with random time intervals	0.558	0.310	0.248
Using auto-correlation with the same phase randomisation in both of the signals. i.e. Ryy where y is a phase randomised x	0.540	0.294	0.246
Using auto-correlation with phase randomisation applied to one signal. i.e. Rxy where y =phase randomised x	0.543	0.301	0.242
Using auto-correlation with different phase randomisation in the signal. i.e. Ryz where y and z = differently phase randomised x	0.536	0.299	0.237

Table 3-19; Zero-Set Dimension of various correlation functions for Vol3 and AD3.

3.9.5 Conclusion

It has been shown that the separation of a typical normal subject from a typical Alzheimer's subject, as measured by the fractal dimension of the zero set of the auto-correlation function, is largely unaffected by replacing the auto-correlation function with a time-incoherent cross correlation function or phase randomised function. This shows that the apparent success of this measure is due to the content of the power spectral density and not to the time domain shape of the waveform.

These results were later taken as evidence that the auto-correlation function is not a fractal and that the fractal dimension measures applied to the auto-correlation function only work because of the spectral content of the EEG. At this stage in the research, the implication that the raw EEG may also not be a Fractal was not recognised, but this was rectified after the Clinical Evaluation by work that is described in Chapter 4.

3.9.6 Frequency Dependence

As an aside, we also briefly investigated whether removing or including specific ranges of frequencies affected the separation.

Method	Vol3	AD3	Separation
Originally quoted results (up to MEDSIP 2000)	0.648	0.331	0.317
Revised results – new settings	0.557	0.305	0.252
ZeroRxx with 0-30Hz components excluded	0.950	0.940	0.010
ZeroRxx with 0-30Hz components only	0.557	0.295	0.262
ZeroRxx with 0-20Hz components only	0.558	0.296	0.262
ZeroRxx with 0-15Hz components only	0.546	0.297	0.249
ZeroRxx with 5-15Hz components only	0.570	0.302	0.268

Table 3-20; Zero-Set Dimension of various the Auto-Correlation functions for Vol3 and AD3.

This appears to show that all of the required information for the method to work is in the frequency range 5Hz to 15Hz. This is consistent with the normal clinical practice of human interpretation of the EEG, where alpha and theta wave intensity is linked to the diagnosis of probably dementia.

3.10 Summary

This research began with a study of the background material, which raised a number of questions. These questions were addressed in an initial set of investigations, which are reported in this chapter.

The two main sources of published work on the fractal dimension of the Human Electroencephalogram that existed before this research were those by Woyshville and Calabrese, and Wu *et al.* These papers were reviewed, particularly from a theoretical standpoint, and numerical experimentation are used to confirm that both methods had shortcomings. In the early, group·comparison study by Woyshville and Calabrese the fractal dimension of the EEG was used to separate subjects with Alzheimer's Disease from a group of normal subjects. However, a critical point had been missed; there are problems associated with estimating the fractal dimension of shapes, such as the EEG, that exist in affine space. The two most significant points for Wu's method were, firstly, the fractal dimension of the auto-correlation is estimated instead of the fractal dimension of the raw record and secondly a version of the divider dimension is estimated in affine space, in a similar way to that used previously by Woyshville and Calabrese.

Two methods, which are appropriate in affine space, were selected from the range of dimension measures found in the literature. The Adapted Box Dimension and Dimension of the Zero Set were each applied to raw EEG data and to the auto-correlation of the EEG data. The results seem to show that all these fractal methods provide metrics that tend to decrease when dementia is present. However, the separation between subjects with dementia and normal subject was not good. It was found that changing controlling constants in the method, such as the segment length, affected the results. Better results were produced by tuning parameters, but this does not represent strong evidence. This is because it is not clear whether the method was working on a specific set of data because the method is tuned to that set of data or because this method tuning will work in general. These concerns were the main reason for conducting the evaluation, with a new, independent set of data, described in Chapter 4.

This chapter also proposed the concept of subject specific analysis of the fractal dimension, which was shown to be an exciting, interesting and useful candidate for early detection of dementia. Subject specific analysis involves comparing an EEG to those taken previously from the same subject: Looking for trends in indices that arise over time rather than comparing an EEG to what is generally normal within the population. Subject specific EEG techniques were shown more sensitive than group comparison based on the same metric. It is noted that if this method were adopted then there would be infrastructure requirements with associated costs for storing and retrieving previous EEG results. In the near future this should become more achievable with eHealth programs which aim is to develop systems that allow an individual patient's medical data (of many types) to be stored remotely whilst being available quickly for detailed analysis.

In these investigations, measurements of fractal dimension over short data segments (2s) were used to construct a histogram of relative likelihood of a fractal dimension value being discovered on any segment and the mode was taken as the composite fractal dimension for the complete record. When the shape of these histograms was studied in more detail, it was observed that that clearly defined signal types (alpha wave, etc.) map approximately to ranges of values of fractal dimension. Other, less well defined, signals can be classified as having similar fractal dimensions to the clearly defined types and it is possible to determine the density of observations in the Theta, Alpha and Beta ranges from the histogram. It was suggested that a new metric could be used. The metric was the ratio of density in the Alpha range to the sum of the densities in the Alpha and Theta ranges. This metric was calculated for all four methods and it was found that the most promising came from the Zeros-Set Dimension of the Auto-correlation. The difference between the "most normal" subject with dementia (Mix3) and the mean of the normal subjects was 30 times the standard deviation among the normal subjects. This represents (all-be-it on this small data set) a clear differentiation between the normal and subjects with dementia. The data previously used to investigate the subject specific analysis concept, from the two young controls was reanalysed using this method and these results provide significant counter evidence to the seemingly strong evidence (above) for the efficacy of this method.

This chapter also reports the study of the time evolution of the fractal dimension. Each of the EEG records was divided into 1-minute intervals and the zero-set fractal dimension of the auto-correlation function was calculated for each. It was shown that the measured fractal dimension (zero-set dimension of the auto-correlation function) is stable and high for the normal subjects except where they become drowsy toward the end of the recording. The subjects with dementia present a generally lower fractal dimension (as noted previously) and the fractal dimension is less stable with time as the normals. It was also noted that subjects with dementia do not seem to enter a drowsy phase before the end of the recording.

The variability of fractal dimension over the scalp was also considered in this chapter. In particular, it was shown that the efficacy of the fractal dimension based methods to separate normal subjects from those with dementia was better in the posterior region of the head. This is believed to be because the effect of dementia on the EEG varies over the scalp and because the masking effects of other signals (cerebral in origin and artefacts) vary over the scalp.

Inspired by the work of other earlier researchers, the fractal dimension of the auto-correlation function had been used in this research. This chapter considered the question "what is the meaning of the fractal dimension of an auto-correlation function?" Despite a great deal of thought, the meaning of the fractal dimension of an auto-correlation function could not be envisaged. It was hypothesised that it has no meaning, but instead happens to give a particular result because of the spectral content of the EEG. It was shown that the separation of a typical normal subject from a typical Alzheimer's subject, as measured by the fractal dimension of the zero set of the auto-correlation function, is largely unaffected by replacing the auto-correlation function with a time-incoherent cross correlation function or phase randomised function. This shows that the apparent success of this measure is due to the content of the power spectral density and not to the time domain shape of the waveform. These results were later taken as evidence that the auto-correlation function is not a fractal and that the fractal dimension measures applied to the auto-correlation function only work because of the spectral content of the EEG. At this stage in the research, the implication that the raw EEG may also not be a Fractal was not recognised, but this was rectified after the Clinical Evaluation.

The final investigation reported in this chapter limited the bandwidth of the EEG to be analysed and demonstrated that all of the required information for the method to work is in the frequency range 5Hz to 15Hz.

Chapter 4. Evaluation of the Fractal Based Methods

4.1 Introduction

The results of the fractal measures investigated in Chapter 3 (and particularly 3.4) provide weak evidence that these measures may be useful in the early detection of dementia. The evidence is considered weak because the methods had to be tuned in order to provide reasonable results. To create strong evidence (or dismiss the weak evidence) it was necessary to conduct a further evaluation on a new, independent set of data. This evaluation is described in this Chapter.

The description of the method evaluation is in five parts. The first is this introduction. The second part (4.2) describes the selection of the method to test and the parameterisation of that method. This is important because post experiment parameterisation will again make the evidence produced less strong. The third part (4.3) describes the data and results from the evaluation. The fourth part (4.4) continues by presenting results that are obtained by applying the other methods considered in the initial investigation (see Chapter 3) to the new data. The final part (4.5) describes the conclusions that are drawn.

4.2 Preparation

4.2.1 Use of the Initial Data Set

The initial data set described in section 3.2 was also used in preparation for the method evaluation. It was used for the selection of which method to test and the parameterisation of that method.

For all records, to avoid the possibility of inadvertently or unconsciously selecting data particularly suitable for analysis a predetermined protocol was applied. Data from 60s to 300s from each record was used. This avoids electrical artefacts, which commonly occur at the beginning of a record, and gives a standard 4 minutes of data to analyse. The EEG recordings encompass various states: awake, hyperventilating, drowsy and alert with periods of eyes closed and open. The analysis described in this paper takes the whole recording including artefacts and has no à priori selection of elements 'suitable for analysis'. This approach leads to a prediction of the usefulness of the techniques, as they would most conveniently be used in practice.

For all data, the recorded sampling rate was downsampled from 256Hz to 128Hz by averaging sets of two consecutive samples for storage reasons.

4.2.2   Choosing a Preferred Method

4.2.2.1   Introduction

With a range of fractal dimension methods and parameters available to choose, it was important to settle on a single, fixed set of parameters before a blind trial, using data recorded in a clinical environment, was conducted. If this had not been done, it could be said that the assessment of the method was not a fair test and that retrospectively applied parameterisation favourably skewed the measured Specificity and Sensitivity. The parameters that needed to be fixed included; the range of lengths used in the Zero Set dimension, the frequency band limiting applied and montage.

4.2.2.2   Selected Parameters

The methods were honed by numerical experimentation to ensure the best chance of good performance. This was found to occur under the following conditions:

1) Montage: Bipolar montage (which exclude the frontal signals); T3-T5, T4-T6, T5-O1, T6-O2, C3-P3, C4-P4, P3-O1, P4-O2 and Cz-Pz, using the minimum fractal dimension across the channel pairs. The choice to use of the minimum fractal dimension over a population of channel pairs rather than the average or mode etc. is due to the nature of the dementia under consideration. Alzheimer's disease shows a generalised slowing over in all regions and minimum, mean or mode would all detect the dementia, but cerebrovascular disease normally has a focus and in the presence of measurement corruption (noise, artefacts, other unrelated effects) the minimum across the channel pairs has the best chance of success. See also Section 3.8, which discusses the variability of the fractal dimension over the scalp.

2) Band limiting; 1Hz to 25Hz. Applied by taking the Fast Fourier Transform and reconstructing the signal from just the required components.

3) Segment length: The raw EEG data were divided into 1 second segments and the estimated fractal dimension from each segment through the entire duration of the recording is plotted on a histogram. The results obtained are almost invariant for segment lengths between 0.5s and 2s. Below 0.5s the results become erratic because of the number of samples is becoming too small compared to the sampling rate employed. With segment lengths greater than 2s the results are affected by the non-stationary nature of the EEG.

4) Taking the fractal dimension from the histogram: the mode of the histogram was taken as the composite measure of fractal dimension for that recording. The strict mode was not used because of a theoretical anomaly if two peaks of equal size occur and because the mode provides no interpolation if there are two similarly sized peaks. The equation used was: $FD = \sum D_i^n FD_i / \sum D_i^n$. Where D_i is the histogram height (density) at fractal dimension estimate FD_i and n is a control constant. When $n=1$ the estimate becomes the mean and when n tends to infinity the estimate tends to the mode. For our experiment $n=4$ was chosen but using strict mode made very little difference.

5) The minimum value for the time interval (denoted by Δt in section 3.4.1) was two 128Hz sampling intervals. The values used for Δt were constrained to be integer numbers of sampling intervals and an approximately exponential distribution was preferred. The intervals used were; 2, 3, 4, 5, 6, 7, 8, 10, 12 15, 18, 22, 27, 33,41, 51 and 63 intervals of 1/128s each.

4.2.2.3   Method Selection

The results under the conditions described above, for the two potential fractal dimension methods applied to the raw EEG record, are shown below in Table 4-1 and Table 4-2. Graphical representations of the separation of the normal group from the subjects with dementia are given in Figure 4-1 and Figure 4-2.

Normal who went onto develop Alzheimer's Disease		
	VOL1	0.64663
Normal		
	VOL2	0.70223
	VOL3	0.70111
	VOL4	0.68458
	VOL5	0.70651
	VOL6	0.68980
	VOL7	0.68876
	VOL8	0.69225
Mean normal		0.69503
Std Dev'n Normal		0.00821
Probable Alzheimer's Disease		
	AD1	0.54797
	AD2	0.60737
	AD3	0.52622
Mean		0.56052
Std Dev'n		0.04201
Vascular and Mixed Dementia		
	MID1	0.58508
	Mix1	0.61497
	MIX2	0.54087
	MIX3	0.63189
Mean		0.59320
Std Dev'n		0.03989

Table 4-1, Fractal Dimension of the Zero Set.

Normal who went onto develop Alzheimer's Disease		
	VOL1	1.28265
Normal		
	VOL2	1.33609
	VOL3	1.31205
	VOL4	1.30633
	VOL5	1.33281
	VOL6	1.32010
	VOL7	1.31023
	VOL8	1.32127
Mean normal		1.31984
Std Dev'n Normal		0.01133
Probable Alzheimer's Disease		
	AD1	1.18772
	AD2	1.24294
	AD3	1.18569
Mean		1.20545
Std Dev'n		0.03248
Vascular and Mixed Dementia		
	MID1	1.20300
	Mix1	1.23986
	MIX2	1.16180
	MIX3	1.26674
Mean		1.21785
Std Dev'n		0.04560

Table 4-2, Adapted Box Dimension.
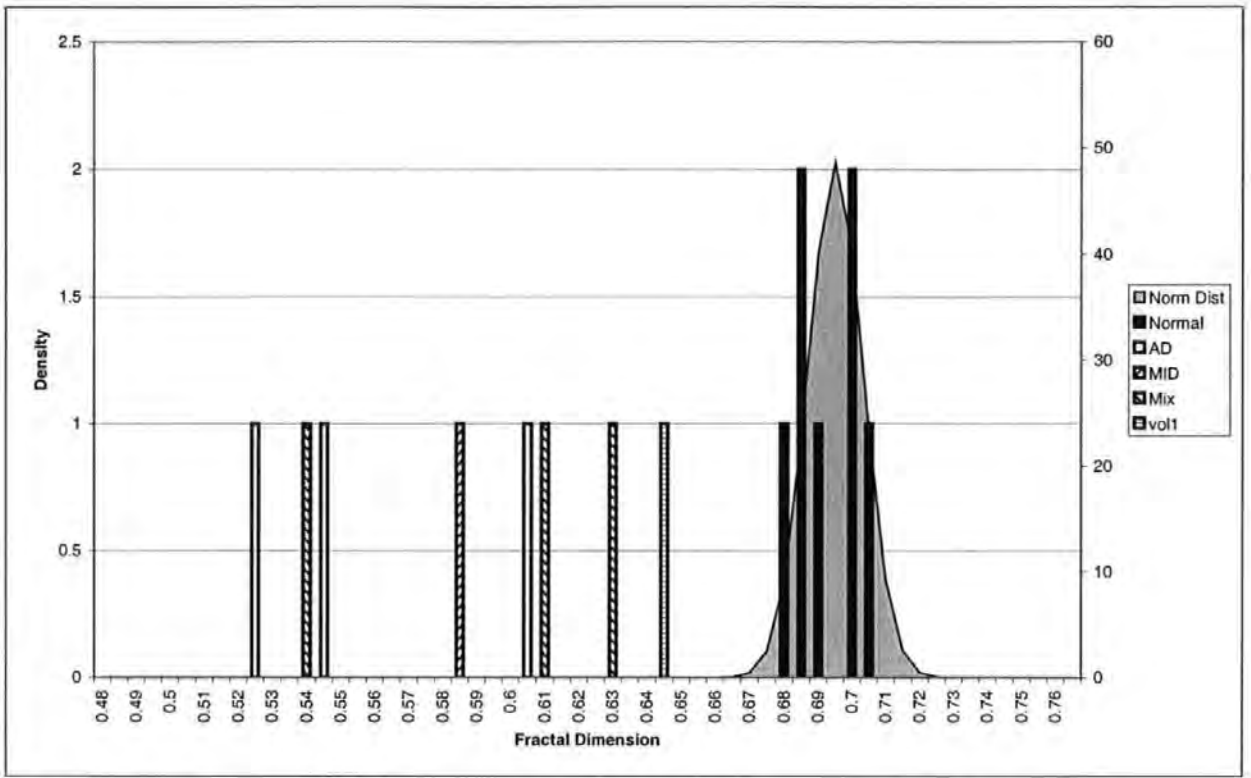
Figure 4-1, Distribution of the zero set dimension of raw EEG.
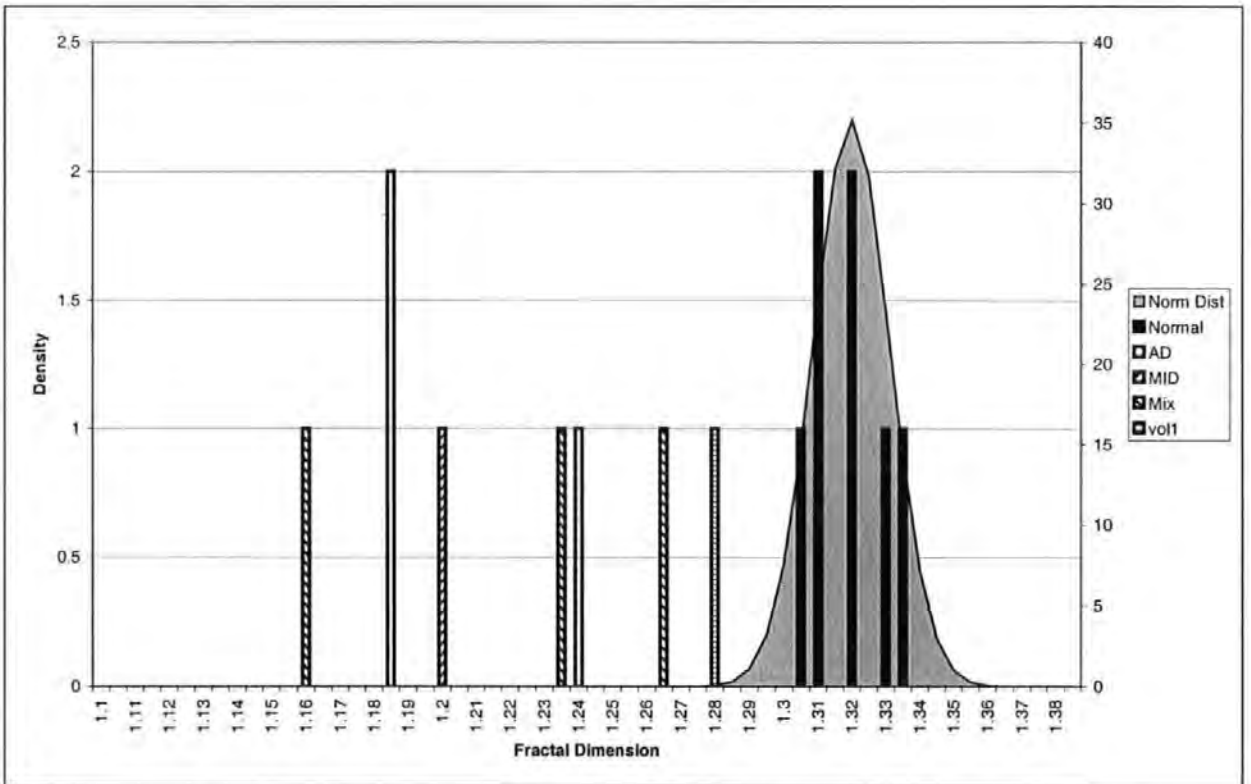

Figure 4-2, Distribution of the adapted box dimension of raw EEG.

From these results and assuming a Normal distribution to the results, it is possible to estimate the efficacy of the method in detecting dementia.

For the fractal dimension of the Zero-Set, if one were to demand a specificity of 99.9% then a result would be considered abnormal if it were less than 0.6697. This implies a sensitivity to Alzheimer's disease of 99.5% and a sensitivity to vascular (or mixed) dementia of 97.2%. Furthermore, the Normal who went on to develop Alzheimer's disease (Vol1) would have been flagged as abnormal (before it was detected by a clinician).

Similarly, for the Adapted Box Dimension, if one were to demand a specificity of 99.9% then a result would be considered abnormal if it were less than 1.2848. This implies a sensitivity to Alzheimer's disease of 99.3% and a sensitivity to Vascular (or mixed) of 92.9%. Furthermore, the Normal who went on to develop Alzheimer's disease (Vol1) would have been flagged as slightly abnormal (before it was detected by a clinician). It can also be shown that this is a statistically significant effect; $p < 0.0001$ for both methods.

Turning to the fractal dimension methods as applied to the auto-correlation function:

Normal who went onto develop Alzheimer's Disease		
	VOL1	0.64272
Normal		
	VOL2	0.69940
	VOL3	0.68227
	VOL4	0.67962
	VOL5	0.69564
	VOL6	0.65165
	VOL7	0.67992
	VOL8	0.66044
Mean normal		0.67842
Std Dev'n Normal		0.01730
Probable Alzheimer's Disease		
	AD1	0.41161
	AD2	0.53139
	AD3	0.50340
Mean		0.48213
Std Dev'n		0.06266
Vascular and Mixed Dementia		
	MID1	0.57662
	Mix1	0.15324
	MIX2	0.44142
	MIX3	0.55128
Mean		0.43064
Std Dev'n		0.19402

Table 4-3, Fractal Dimension of the Zero Set applied to the Auto-Correlation Function.

Normal who went onto develop Alzheimer's Disease		
	VOL1	1.24411
Normal		
	VOL2	1.27393
	VOL3	1,23458
	VOL4	1.24752
	VOL5	1.27693
	VOL6	1.25552
	VOL7	1.25311
	VOL8	1.24804
Mean normal		1.25566
Std Dev'n Normal		0.01506
Probable Alzheimer's Disease		
	AD1	1.05558
	AD2	1.10981
	AD3	1.12675
Mean		1.09738
Std Dev'n		0.03718
Vascular and Mixed Dementia		
	MID1	1.12465
	Mix1	1.03798
	MIX2	1.06776
	MIX3	1.12030
Mean		1.08767
Std Dev'n		0.04202

Table 4-4, Adapted Box Dimension applied to the Auto-Correlation Function.

From these results and again assuming a Normal distribution to the results, it is possible to estimate the efficacy of the method in detecting dementia.

For the fractal dimension of the Zero-Set applied to the auto-correlation function; if one were to demand a specificity of 99.9% then a result would be considered abnormal if it were less than 0.62497. This implies a sensitivity to Alzheimer's disease of 98.9% and a sensitivity to Vascular (or mixed) of 84.2%. Furthermore, the Normal who went on to develop Alzheimer's disease (Vol1) would not have been flagged as abnormal.

Similarly, for the Adapted Box Dimension applied to the auto-correlation function; if one were to demand a specificity of 99.9% then a result would be considered abnormal if it were less than 1.2091. This implies a sensitivity to Alzheimer's disease of 99.9% and a sensitivity to Vascular (or mixed) of 99.8%. Furthermore, the Normal who went on to develop Alzheimer's disease (Vol1) would not have been flagged as abnormal.

Table 4-5 summarises the four methods detailed above (with 99.9% specificity):

Method	Zero Set	Adapted Box	Zero Set of Auto-correlation	Adapted Box of Auto-correlation
Mean Normal	0.6950	1.3198	0.6784	1.2557
SD Normal	0.0082	0.0113	0.0173	0.0151
Limit of what is considered normal	0.6697	1.2848	0.6250	1.209
Mean AD	0.5605	1.2055	0.4821	1.0974
SD AD	0.0420	0.0325	0.0627	0.0372
Sensitivity to AD	99.5%	99.3%	98.9%	99.9%
Mean vascular	0.5932	1.2179	0.4306	1.0877
SD vascular	0.0399	0.0456	0.1940	0.0420
Sensitivity to vascular	97.2%	92.9%	84.2%	99.8%

Table 4-5, Summary of results using development data set.

These results suggest that the Adapted Box Dimension applied to the auto-correlation function was the best of the four methods. However, because of the concern over the use of the fractal dimension of the auto-correlation function, it was decided to select the fractal dimension of the zero-set of the raw EEG data as the preferred method. The main concern was that constructing the auto-correlation function removes phase information from the signal and a fractal with the phase information removed is no longer a fractal (see also Section 3.8). Thus, measuring the fractal dimension of a non-fractal was incongruous. It is noted, however, that fractal measures may be applied to a non-fractals and useful results extracted. This concern lead, in time, to an investigation into whether the EEG was a fractal (reported in Chapter 5). Notwithstanding the previous argument, results from all methods are reported in Section 4.4.1.

4.3 Trial of Preferred Method

4.3.1 Evaluation Data Set

The data used for this evaluation were obtained from Derriford Hospital and had been collected using normal hospital practices. The EEG recordings encompass various states: awake, drowsy and alert with periods of eyes closed and open. Within this data set, there were 24 normal records, 17 probable Alzheimer's disease and 5 probable Vascular Dementia. This data set did not reuse any of the development data set. These data were obtained using the modified Maudsley system, which is similar to the traditional 10-20 system. The classification of the records between normal and Alzheimer's disease was taken from the written hospital diagnosis sheets. It is noteworthy that the probable Alzheimer's subjects were not previously diagnosed and were therefore in the early stages of exhibiting symptoms; in fact some of these subjects were not referred for dementia diagnosis but came in for investigation of seizures et cetera.

For all records, to avoid the possibility of inadvertently or unconsciously selecting data particularly suitable for analysis a predetermined protocol was applied. Data from 60s to 300s from each record was used. This avoids electrical artefacts, which commonly occur at the beginning of a record, and gives a standard 4 minutes of data to analyse. This segment of data including artefacts was analysed with no *á priori* selection of elements 'suitable for analysis'. This approach leads to a prediction of the usefulness of the technique, as it would most conveniently be used in practice.

For all data, the recorded sampling rate was 256Hz reduced to 128Hz for analysis by averaging sets of 2 consecutive samples (for storage reasons).

4.3.2 Results from the Preferred Method

The results obtained by applying the preferred method to the evaluation data set are presented in Table 4-6. A graphical representation of the distribution of results is given in Figure 4-3. The results are summarised in Table 4-7. Finally, detailed results over all channels of all subjects are given in Table 8-9 through Table 8-12.

	Normal	Alzheimer's	Vascular
Results	0.6436	0.5737	0.6203
	0.6461	0.5725	0.6357
	0.7173	0.6186	0.5810
	0.6799	0.5540	0.6673
	0.6662	0.5796	0.5993
	0.6428	0.5216	
	0.6714	0.5799	
	0.6443	0.5587	
	0.6581	0.6088	
	0.6706	0.4969	
	0.6904	0.5162	
	0.6963	0.6336	
	0.7028	0.5921	
	0.7076	0.5072	
	0.6527	0.5973	
	0.6794	0.5042	
	0.7147	0.6472	
	0.6547		
	0.7112		
	0.7443		
	0.6473		
	0.7201		
	0.6611		
	0.6812		
Number of samples	24	17	5
Mean	0.6793	0.5684	0.6207
SD	0.0293	0.0464	0.0333

Table 4-6, Detail of results (by subject) from preferred method applied to evaluation data set.
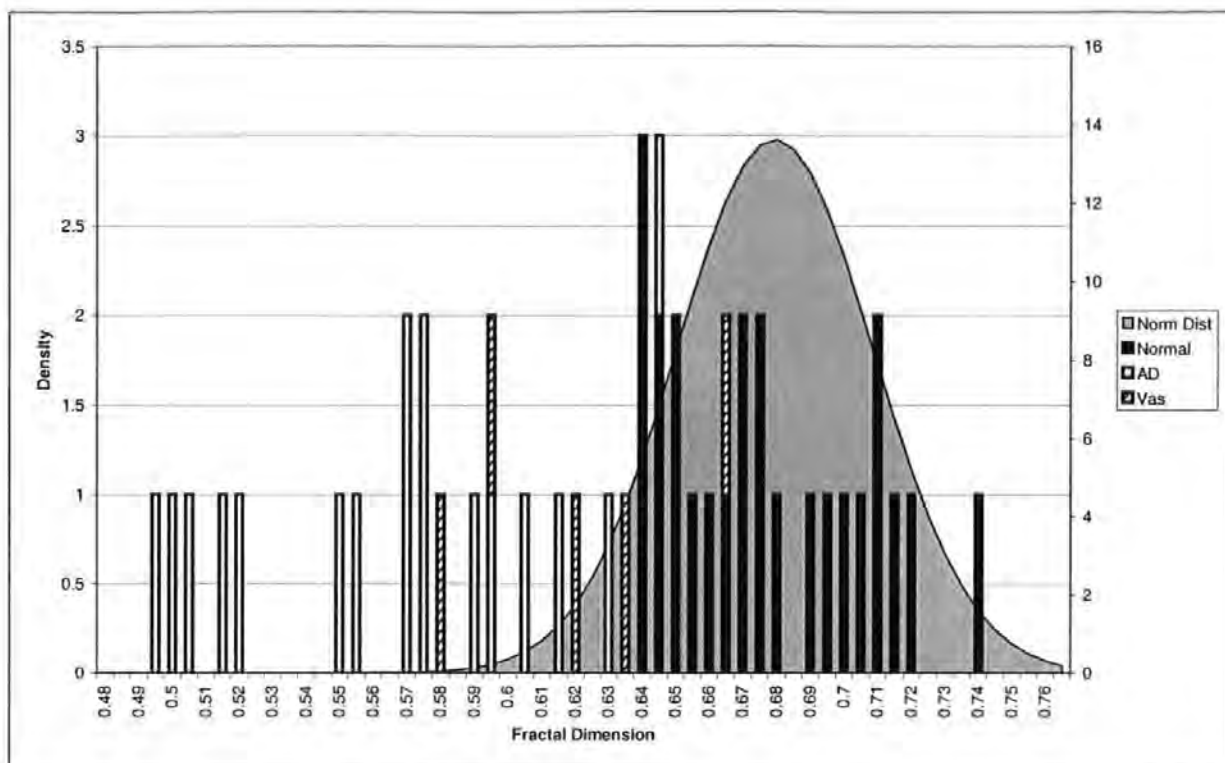
Figure 4-3, Distribution of results from prefered method.

Mean Normal	0.6793
SD Normal	0.0293
Limit of what is considered normal to achieve 99.9% specificity (assuming a Gaussian distribution)	0.5888
Mean AD	0.5684
SD AD	0.0464
Sensitivity to AD (assuming a Gaussian distribution)	67.0%
Mean vascular	0.6207
SD vascular	0.0333
Sensitivity to vascular (assuming a Gaussian distribution)	16.9%

Table 4-7, Summary of results from preferred method applied to evaluation data set.

These results are not as good as had been achieved using the development data and are probably not good enough to form the basis of the required method for detecting early dementia.

To understand the difference between the two data sets we need only look at the salient points given in Table 4-8. These show that the tuned method applied to the development data gives a significantly lower estimated standard deviation of results for the normal subjects: by a factor of 3.6.

117

	Development data set	Evaluation data set
Mean Normal	0.695	0.679
SD Normal	0.008	0.029
Mean AD	0.561	0.568
SD AD	0.042	0.046
Mean vascular	0.593	0.621
SD vascular	0.040	0.033

Table 4-8, Comparison of results from preferred method applied to development and evaluation data sets.

4.3.3 Conclusion

This evaluation has demonstrated the value of a blind test using an independent data set. It has shown that we were in danger of believing results based on too small a set of data, which had itself been used to develop the method.

4.4 Other Methods

4.4.1 Other Fractal Dimension Methods

After the method evaluation, which used the fractal dimension of the zero set of the raw EEG data, the other three alternative fractal measures were applied to the evaluation data set. These results are given in Table 4-9, Table 4-10 and Table 4-11, with a summary of all 4 methods in Table 4-12.

	Normal	Alzheimer's	Vascular
Results	1.2754	1.2152	1.2528
	1.2646	1.2015	1.2663
	1.3447	1.2470	1.2061
	1.3045	1.1921	1.2863
	1.2961	1.2250	1.2238
	1.2875	1.1606	
	1.3012	1.2135	
	1.2705	1.1893	
	1.2942	1.2495	
	1.3190	1.1361	
	1.3154	1.1508	
	1.3106	1.2695	
	1.3318	1.2275	
	1.3356	1.1660	
	1.2829	1.2225	
	1.3011	1.1538	
	1.3591	1.2805	
	1.3052		
	1.3500		
	1.3593		
	1.2713		
	1.3444		
	1.2845		
	1.3189		
Number of samples	24	17	5
Mean	1.3095	1.2059	1.2470
SD	0.0288	0.0427	0.0323

Table 4-9, Adapted Box method applied to assessment data set.

	Normal	Alzheimer's	Vascular
Results	0.6436	0.3281	0.6027
	0.5976	0.5267	0.6007
	0.4148	0.5177	0.4987
	0.3494	0.4104	0.5296
	0.5043	0.5181	0.5365
	0.0982	0.1513	
	0.3595	0.5723	
	0.5806	0.4266	
	0.6274	0.4830	
	0.0897	0.0626	
	0.6831	0.4682	
	0.2599	0.2524	
	0.3276	0.4684	
	0.5425	0.3309	
	0.5973	0.5556	
	0.4779	0.4330	
	0.7157	0.5000	
	0.6429		
	0.6606		
	0.6938		
	0.6408		
	0.6609		
	0.6436		
	0.3530		
Number of samples	24	17	5
Mean	0.5069	0.4121	0.5536
SD	0.1844	0.1438	0.0461

Table 4-10, Zero Set of the auto-correlation function method applied to assessment data set.

	Normal	Alzheimer's	Vascular
Results	1.2510	1.0518	1.1902
	1.1659	1.1171	1.1694
	1.1013	1.1289	1.1026
	1.0647	1.0590	1.1423
	1.1350	1.0884	1.1047
	1.0317	1.0400	
	1.0849	1.1211	
	1.1573	1.0619	
	1.2333	1.0984	
	1.0316	1.0435	
	1.2889	1.0602	
	1.0362	1.0368	
	1.0576	1.0805	
	1.1936	1.0406	
	1.1742	1.1355	
	1.0533	1.0825	
	1.3410	1.1125	
	1.2577		
	1.2364		
	1.2843		
	1.2153		
	1.2450		
	1.2328		
	1.0514		
Number of samples	24	17	5
Mean	1.1635	1.0799	1.1419
SD	0.0958	0.0338	0.0388

Table 4-11, Adapted Box of the auto-correlation function method applied to assessment data set.

Method	Zero Set	Adapted Box	Zero Set of Auto-correlation	Adapted Box of Auto-correlation
Mean Normal	0.6793	1.3095	0.5069	1.1635
SD Normal	0.0293	0.0288	0.1844	0.0958
Limit of what is considered normal to achieve 99.9% specificity	0.5888	1.2206	-0.0630	0.8674
Mean AD	0.5684	1.2059	0.4121	1.0799
SD AD	0.0464	0.0427	0.1438	0.0338
Sensitivity to AD	67.0%	63.5%	0.0%	0.0%
Mean vascular	0.6207	1.2470	0.5536	1.1419
SD vascular	0.0333	0.0323	0.0461	0.0388
Sensitivity to vascular	16.9%	20.7%	0.0%	0.0%

Table 4-12, Summary of assessment results from all methods.

It is clear that these results are incongruous with the previous success of auto correlation based methods. No reason for this could be found and it seems that it may simply have been "good luck". Again, we were in danger of believing results based on too small a set of data, which had itself been used to develop the method.

4.4.2   Subject Specific Measures

Following on from the discussion of subject specific measures and how they may help in the early detection of dementia (see section 3.5), it was decided to extend the analysis by using the evaluation data to better characterise the results from normal/subjects with dementia and to include results from 2 new repeat recordings found in the Deriford data set. V and W are both older normal subjects (time separation 20 days and 42 days respectively).

Record	Raw EEG Data		Auto-correlation of EEG data	
	Zero-set	Adapted Box	Zero-set	Adapted Box
X1	0.690	1.315	0.568	1.041
X2	0.692	1.326	0.684	1.076
X3	0.679	1.313	0.583	1.034
Y1	0.620	1.245	0.608	1.201
Y2	0.604	1.299	0.609	1.082
Y3	0.596	1.218	0.554	1.104
V1	0.635	1.269	0.551	1.131
V2	0.613	1.241	0.528	1.113
W1	0.644	1.275	0.644	1.251
W2	0.653	1.283	0.597	1.174

Table 4-13, Results from young subjects using methods suitable for affine space.

If one considers the variation from sample to sample from the same subject to be equivalent to measurement noise (or short term variability) on the fractal dimension then one may estimate the population standard deviation for a single subject for each measure.

Estimated	Raw EEG Data		Auto-correlation of EEG data	
Population	Zero-set	Adapted Box	Zero-set	Adapted Box
Standard Dev^n	0.016	0.015	0.064	0.064

Table 4-14, Variability of results from young subjects using methods suitable for affine space.

Taking the statistics for the age matched controls and the first recording for each of the young normals (Table 4-15) it may be seen that for all the measures the standard deviation among the group of normals is, as expected, larger than the variation for a single subject (Table 4-14).

Record	Raw EEG Data		Auto-correlation of EEG data	
	Zero-set	Adapted Box	Zero-set	Adapted Box
Mean	0.679	1.310	0.507	1.164
Std Deviation	0.029	0.029	0.184	0.096

Table 4-15, Variability of the Population of Normal Subjects.

The fractal dimension has also been calculated for the subjects with dementia (Table 4-16):

Record	Raw EEG Data		Auto-correlation of EEG data	
	Adapted Box	Zero-set	Adapted Box	Zero-set
Mean AD	1.206	0.568	1.080	0.412
St'd Dev'n AD	0.043	0.046	0.034	0.144
Mean Vascular	1.247	0.621	1.142	0.554
St'd Dev'n Vascular	0.032	0.033	0.039	0.046

Table 4-16, Results from Subjects with dementia.

The graph below (Figure 3-10) summarises the results which were obtained using the zero-set dimension of the raw EEG data and the measured normal variability of the fractal dimension for a single subject as measured on the normals (V, W, X and Y).
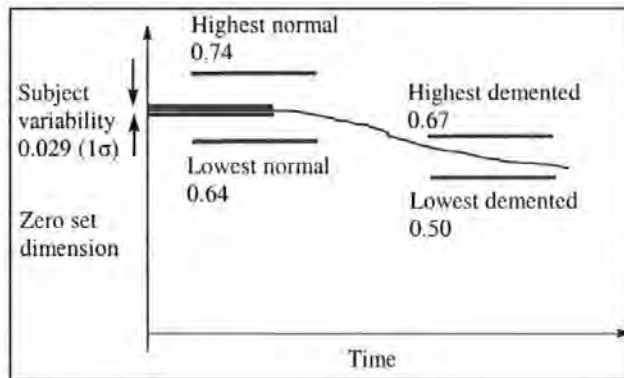
Figure 4-4, Summary of subject specific results showing that this concept could improve early diagnostic efficacy.

The graph demonstrates that the fractal dimension, in this instance, is a good candidate for use in subject specific detection of dementia. This is because the measured fractal dimension of the EEG is generally lower for a subject with dementia than for normal subjects and the variability of a single normal subject's fractal dimension is small in comparison to the variability between members of the set of normals.

4.4.3 Alpha/Theta Ratio

4.4.3.1 Revisiting Results from Development Data

Following on from the discussion of the alpha/theta ratio derived from the fractal dimension (see section 3.6), it was decided to repeat the analysis on the evaluation data set.

To recapitulate: By observation of the signal segments that produce values of fractal dimension it is possible to show that clearly defined signal types, defined in section 2.2.4, transform to certain ranges of values of fractal dimension. Other, less well defined, signals can be classified as having similar fractal dimensions to the clearly defined types and it is possible to determine the density of observations in the Theta, Alpha and Beta type ranges directly from the histogram. These are given, approximately, in Table 4-17.

	Adapted box dimension of raw data or auto-correlation function	Zero-set dimension of raw data or auto-correlation function
Ocular artefacts	Lower than 1.0	Lower than 0.3
Theta	1.0 to 1.2	0.3 to 0.5
Alpha	1.2 to 2.0	0.5 to 1.0
Beta	Above 2.0	Above 1.0

Table 4-17, Approximate mapping of signal type to fractal dimension.

Before analysing the new data using the Alpha/Theta ratio, it was necessary to reanalyse the development data using the new parameterisation. These results are shown below in Table 4-18 through Table 4-21 and summarised in Table 4-22.

Normal who went on to develop Alzheimer's Disease		
	VOL1	0.945
Normal		
	VOL2	1.000
	VOL3	1.000
	VOL4	0.996
	VOL5	0.992
	VOL6	1.000
	VOL7	0.992
	VOL8	0.987
Mean normal		0.995
Std Dev'n Normal		0.005
Limit to achieve 99.9% specificity		0.979
Probable Alzheimer's Disease		
	AD1	0.736
	AD2	0.924
	AD3	0.734
Mean		0.798
Standard Deviation		0.109
Sensitivity		95.1%
Multi-Infarct and Mixed Dementia		
	MID1	0.821
	Mix1	0.748
	MIX2	0.682
	MIX3	0.971
Mean		0.805
Standard Deviation		0.124
Sensitivity		92.0%

Table 4-18, Alpha/theta results from the Zero-Set method applied to the Raw EEG.

Normal who went on to develop Alzheimer's Disease		
	VOL1	0.894
Normal		
	VOL2	0.983
	VOL3	0.915
	VOL4	0.945
	VOL5	0.836
	VOL6	0.971
	VOL7	0.897
	VOL8	0.898
Mean normal		0.921
Std Dev'n Normal		0.051
Limit to achieve 99.9% specificity		0.765
Probable Alzheimer's Disease		
	AD1	0.268
	AD2	0.637
	AD3	0.559
Mean		0.488
Standard Deviation		0.195
Sensitivity		92.2%
Multi-Infarct and Mixed Dementia		
	MID1	0.677
	Mix1	0.346
	MIX2	0.382
	MIX3	0.667
Mean		0.518
Standard Deviation		0.178
Sensitivity		91.7%

Table 4-19, Alpha/theta results from the Zero-Set method applied to the Auto-correlation function.

Normal who went on to develop Alzheimer's Disease		
	VOL1	0.932
Normal		
	VOL2	1.000
	VOL3	0.996
	VOL4	0.987
	VOL5	1.000
	VOL6	1.000
	VOL7	0.996
	VOL8	0.992
Mean normal		0.996
Std Dev'n Normal		0.005
Limit to achieve 99.9% specificity		0.981
Probable Alzheimer's Disease		
	AD1	0.500
	AD2	0.887
	AD3	0.416
Mean		0.601
Standard Deviation		0.251
Sensitivity		93.5%
Multi-Infarct and Mixed Dementia		
	MID1	0.622
	Mix1	0.742
	MIX2	0.338
	MIX3	0.945
Mean		0.662
Standard Deviation		0.254
Sensitivity		89.6%

Table 4-20, Alpha/theta results from the Adapted Box method applied to the Raw EEG.

Normal who went on to develop Alzheimer's Disease		
	VOL1	0.651
Normal		
	VOL2	0.920
	VOL3	0.703
	VOL4	0.752
	VOL5	0.742
	VOL6	0.916
	VOL7	0.798
	VOL8	0.734
Mean normal		0.795
Std Dev'n Normal		0.089
Limit to achieve 99.9% specificity		0.521
Probable Alzheimer's Disease		
	AD1	0.011
	AD2	0.083
	AD3	0.017
Mean		0.037
Standard Deviation		0.040
Sensitivity		100.0%
Multi-Infarct and Mixed Dementia		
	MID1	0.231
	Mix1	0.033
	MIX2	0.000
	MIX3	0.207
Mean		0.118
Standard Deviation		0.118
Sensitivity		100.0%

Table 4-21, Alpha/theta results from the Adapted Box method applied to the Auto-correlation function.

Method	Zero Set	Adapted Box	Zero Set of Auto-correlation	Adapted Box of Auto-correlation
Mean Normal	0.995	0.921	0.996	0.795
SD Normal	0.005	0.051	0.005	0.089
Limit of what is considered normal to achieve 99.9% specificity	0.979	0.765	0.981	0.521
Mean AD	0.798	0.488	0.601	0.037
SD AD	0.109	0.195	0.251	0.040
Sensitivity to AD	95.1%	92.2%	93.5%	100.0%
Mean vascular	0.805	0.518	0.662	0.118
SD vascular	0.124	0.178	0.254	0.118
Sensitivity to vascular	92.0%	91.7%	89.6%	100.0%

Table 4-22, Summary of assessment results from all alpha/theta ratio methods.

As previously noted, this metric (on the limited development data set) seems capable of differentiating control subjects and subjects with dementia with a wide band between the two groups.

4.4.3.2 Alpha / Theta Ratio Applied to the Evaluation Data

The method was repeated on the evaluation data set, which was independent of the tuning of the method. These results are shown in Table 8-9 through Table 8-12 (in Appendix D) and summarised in Table 4-23.

Method	Zero Set	Adapted Box	Zero Set of Auto-correlation	Adapted Box of Auto-correlation
Mean Normal	0.9705	0.9709	0.6597	0.4283
SD Normal	0.0286	0.0388	0.2212	0.2951
Limit of what is considered normal to achieve 99.9% specificity	0.8822	0.8510	-0.0239	-0.4835
Mean AD	0.7848	0.6083	0.4024	0.0562
SD AD	0.1761	0.3003	0.1747	0.0754
Sensitivity to AD	71.0%	79.0%	0.0%	0.0%
Mean vascular	0.9310	0.8731	0.6427	0.2596
SD vascular	0.0799	0.1751	0.1283	0.1803
Sensitivity to vascular	27.1%	45.0%	0.0%	0.0%

Table 4-23, Summary of Alpha/Theta results from all methods.

4.4.3.3 Conclusions Regarding Alpha/Theta Ratio

As with the evaluation of the fractal dimension measures, these results are not as good as had been achieved using the development data. They are probably not good enough to form the basis of the required method for detecting early dementia.

This evaluation has demonstrated the value of a blind test using an independent data set. It has shown that we were in danger of believing results based on too small a set of data, which had itself been used to develop the method.

4.5 Summary

This evaluation has been valuable because it has demonstrated that the performance of the fractal dimension based measures is a strong function of the tuning one applies. From this evaluation it is clear that either of the fractal dimension measures applied to the raw EEG data could be used to separate subjects with dementia from controls but that this separation would have low sensitivity. This is a demonstration of the value of a blind test using an independent data set. It has shown that we were in danger of believing results based on too small a set of data, which had itself been used to develop the method.

Chapter 5. Fundamental Study of the Fractal Nature of the EEG

5.1 The Fundamental Question

It was realised that an implicit assumption was being made during the preceding research. The assumption was that, because the Fractal measures appeared to be able to differentiate (to some extent) between normal subjects and subjects with dementia then the EEG is necessarily fractal in nature. A decision was made to test and attempt to disprove the following hypothesis:

- The Fractal Nature of the EEG contributes to the apparent success of the Fractal based methods.

5.2 Method

Building on the research described in Section 3.9, it was decided to use surrogate data testing. To perform this surrogate data test it is necessary to define a feature which is essential to the EEG being fractal in nature, then modify the recorded EEG data to remove this feature and finally reapply the original fractal based measure to see whether the method works better, similarly or worse than before the feature is removed. The evaluation of whether the performance is better or worse is based on efficacy measured with estimated specificity and sensitivity.

When the feature is removed there are two possible conclusions that will be reached based on how the Method Evaluation Metric changes:

- If the metric gets worse then it is likely that this feature is necessary for both the metric to work and for the hypothesis to be true. Hence, this is weak evidence that the hypothesis is true. It is only weak evidence because the feature removed may be necessary but not sufficient to conclude a fractal nature.

- If the metric is the same or better then there is reasonable evidence that the hypothesis is untrue. That is that the fractal nature of the EEG (should it exist at all) does not contribute to the success of the method.

It was only necessary to remove one feature from the EEG in order to obtain evidence of the hypothesis being untrue. This feature was the structured phase relationships within the data.

The Fourier Transform was applied to obtain phase and magnitude data for all spectral components then the signal was reconstructed with the original magnitude but with the phase data randomised. The resultant signal is non-fractal.

5.3 Results

The fractal dimension measures and Alpha/Theta ratio methods were applied to the EEG data with and without phase randomisation. The results are summarised in Table 5-1 through Table 5-4.

Method	Zero Set	Adapted Box	Zero Set of Auto-correlation	Adapted Box of Auto-correlation
Mean Normal	0.6793	1.3095	0.5069	1.1635
SD Normal	0.0293	0.0288	0.1844	0.0958
Limit of what is considered normal to achieve 99.9% specificity	0.5888	1.2206	-0.0630	0.8674
Mean AD	0.5684	1.2059	0.4121	1.0799
SD AD	0.0464	0.0427	0.1438	0.0338
Sensitivity to AD	67.0%	63.5%	0.0%	0.0%
Mean vascular	0.6207	1.2470	0.5536	1.1419
SD vascular	0.0333	0.0323	0.0461	0.0388
Sensitivity to vascular	16.9%	20.7%	0.0%	0.0%

Table 5-1, Summary of fractal dimension results from all methods (no phase randomisation).

Method	Zero Set	Adapted Box	Zero Set of Auto-correlation	Adapted Box of Auto-correlation
Mean Normal	0.6817	1.3125	0.5991	1.2403
SD Normal	0.0277	0.0284	0.0741	0.0575
Limit of what is considered normal to achieve 99.9% specificity	0.5963	1.2248	0.3703	1.0625
Mean AD	0.5784	1.2139	0.5334	1.1868
SD AD	0.0429	0.0388	0.0504	0.0245
Sensitivity to AD	66.2%	61.2%	0.1%	0.0%
Mean vascular	0.6268	1.2527	0.5897	1.2178
SD vascular	0.0322	0.0309	0.0229	0.0203
Sensitivity to vascular	17.1%	18.4%	0.0%	0.0%

Table 5-2, Summary of fractal dimension results from all methods (with phase randomisation).

Method	Zero Set	Adapted Box	Zero Set of Auto-correlation	Adapted Box of Auto-correlation
Mean Normal	0.9705	0.9709	0.6597	0.4283
SD Normal	0.0286	0.0388	0.2212	0.2951
Limit of what is considered normal to achieve 99.9% specificity	0.8822	0.8510	-0.0239	-0.4835
Mean AD	0.7848	0.6083	0.4024	0.0562
SD AD	0.1761	0.3003	0.1747	0.0754
Sensitivity to AD	71.0%	79.0%	N/A	N/A
Mean vascular	0.9310	0.8731	0.6427	0.2596
SD vascular	0.0799	0.1751	0.1283	0.1803
Sensitivity to vascular	27.1%	45.0%	0.0%	0.0%

Table 5-3, Summary of Alpha/Theta results from all methods (no phase randomisation).

Method	Zero Set	Adapted Box	Zero Set of Auto-correlation	Adapted Box of Auto-correlation
Mean Normal	0.9650	0.9667	0.7377	0.6717
SD Normal	0.0326	0.0331	0.1621	0.1994
Limit of what is considered normal to achieve 99.9% specificity	0.8644	0.8644	0.2369	0.0555
Mean AD	0.8007	0.6434	0.6335	0.4590
SD AD	0.1435	0.2443	0.1138	0.1358
Sensitivity to AD	67.1%	81.7%	0.0%	0.1%
Mean vascular	0.9262	0.8723	0.7441	0.6242
SD vascular	0.0753	0.1464	0.0737	0.1075
Sensitivity to vascular	20.6%	47.8%	0.0%	0.0%

Table 5-4, Summary of Alpha/Theta results from all methods (with phase randomisation).

5.4 Summary

Comparing the results in Table 5-1 with those in Table 5-2 and comparing the results in Table 5-3 with those in Table 5-4, it may be seen that phase randomisation does not cause a significant loss of performance for any of the methods considered. Therefore, it is concluded that the fractal nature of the EEG (should it exist at all) does not contribute to the performance of the fractal dimension methods. From this, it is concluded that the EEG is very unlikely to be a fractal. However, the previous success of the fractal methods is important and is likely to be because they detected a related characteristic of the EEG.

Chapter 6. Development of Two Novel Methods

6.1 Search for an Alternative Metric

The conclusion from the Surrogate Data Testing had a profound effect on the direction of the research. It was recognised that all of the information, which was able to give the (partial) success with fractal dimension measures, was contained within the Power Spectral Density. It was also known from the background research that, despite significant effort over a long period; no spectral based measure had been good enough to use in general clinical practice.

It was decided to tackle this from a different angle and propose methods that shared an important similarity with the fractal measures; we decided to use measures based in the time domain. These were the Allan Variance (which shares features with the adapted box dimension) and the zero-crossing interval distribution (which shares features with the zero-set dimension).

This search for new methods was conducted using just the development data set so that the evaluation data set could be kept in reserve to test any proposed methods.

6.2 Allan Variance

6.2.1 Concept and History

The Allan Variance method [67] of analysing and visualising time domain characteristics of stochastic processes in Gyro theory was investigated. Allan variance is a time-domain analysis technique originally developed to study the frequency stability of oscillators [68]. It can be used to determine the character of the underlying processes that can give rise to data features.

Allan Variance provides a measure of the stability of a signal and the characteristic period of any instability. It may be used as a stand-alone method of data analysis or to complement any of the frequency-domain analysis techniques. The equation describing the measurement of the Allan Variance is given below:

$$\sigma(\tau) = \frac{1}{\tau\sqrt{2}} \cdot RMS\left[\int_{t_0}^{t_0+\tau} \omega(t)dt - \int_{t_0+\tau}^{t_0+2\tau} \omega(t)dt\right].$$ (6.1)

This equation describes the stability of a signal over a time interval, τ. The Allan Variance, $\sigma(\tau)$, is the root mean square of the difference between an integral over a period, τ, and the integral over the next interval of the same length.
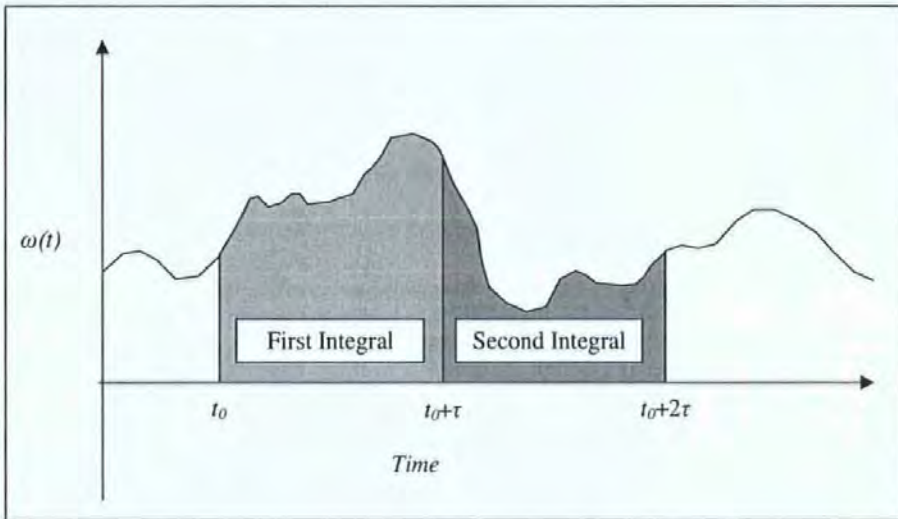
Figure 6-1, A sketch illustrating the Allan Variance method.

Clearly, the Allan Variance contains the same information as the Power Spectral Density; but being in the time domain it emphasises lower frequencies over higher frequencies. This may be an advantage in EEG analysis because, from the fractal dimension, we believe that this emphasis on the time domain may provide visibility of important features for the detection of dementia. The relationship between the Allan Variance and Power Spectral Density is given below:

$$\sigma^2(\tau) = 4\int_0^\infty S(f)\frac{\sin^4(\pi f\tau)}{(\pi f\tau)^2}df .$$ (6.2)

Where $S(f)$ is the power spectral density at frequency f expressed in Hz.

139

6.2.2 Characteristic Plots

In the Allan Variance method of data analysis, instability in the data is assumed to be generated by noise sources of specific types (white, Markov, etc.). The type and size of these noise sources is interpreted from a graph of Allan Variance. The Allan Variance is normally plotted on a log-log scale. To introduce the interpretation of Allan Variance charts it is helpful to plot the Allan Variance charts for well-known signal types and comment on their key characteristics. Plots for white noise, first order Markov and second order Markov processes are given in Figure 6-2, Figure 6-4 and Figure 6-6, respectively. Each has a unity signal power.

Figure 6-2 shows a segment of typical white noise signal (sampled at 128Hz) and Figure 6-3 shows the corresponding Allan variance chart. Notable features are that the gradient is −½, and the right side (corresponding to larger time intervals) has larger measurement noise because less samples of longer duration are available from a finite length of record.

Figure 6-4 shows a segment of a typical first order Markov signal with a time constant of 0.1s and Figure 6-5 shows the corresponding Allan variance chart. Notable features are that there is a peak at 0.1s (the time constant), the gradient above the time constant is -½ and the gradient below the time constant is positive but less than ½.

Figure 6-6 shows a segment of a typical resonant second order Markov signal (resonant frequency 10Hz and damping factor 0.1) and Figure 6-7 shows the corresponding Allan variance chart.
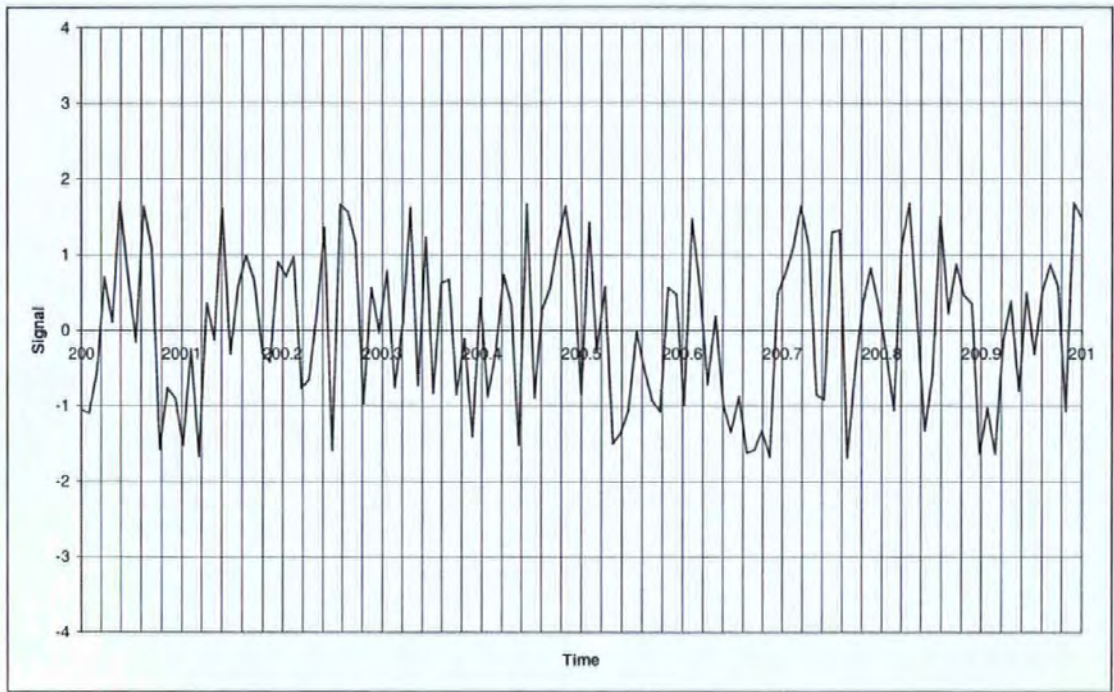
Figure 6-2, White Noise Signal (Uniform Distribution).
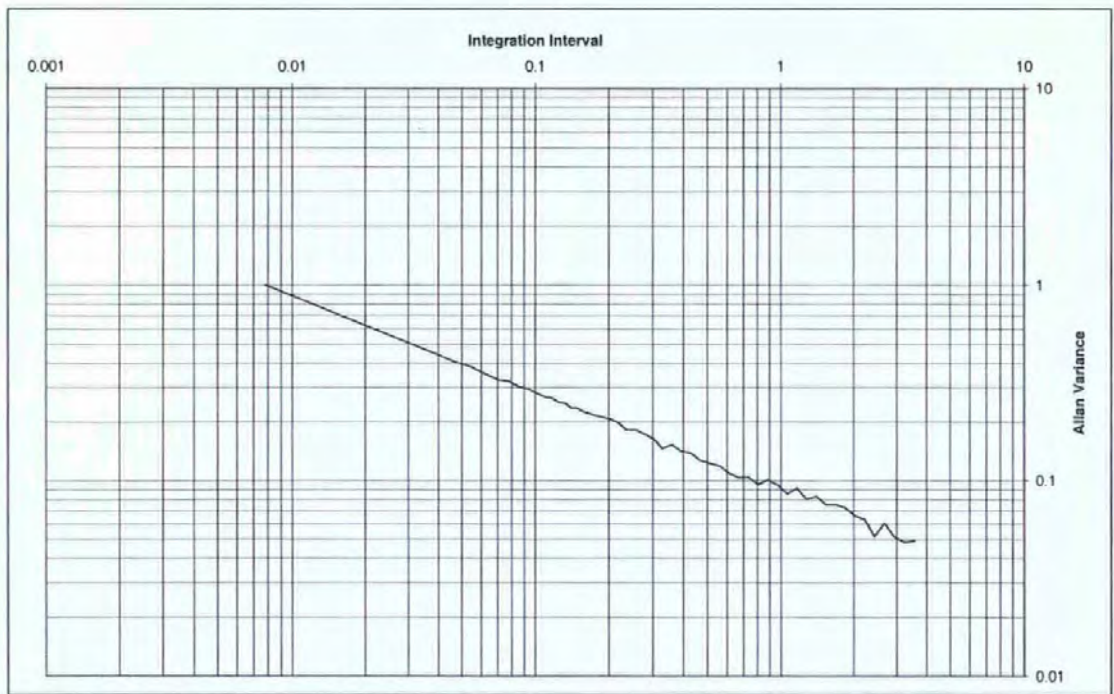
Figure 6-3, Allan Variance Chart of White Noise.

141
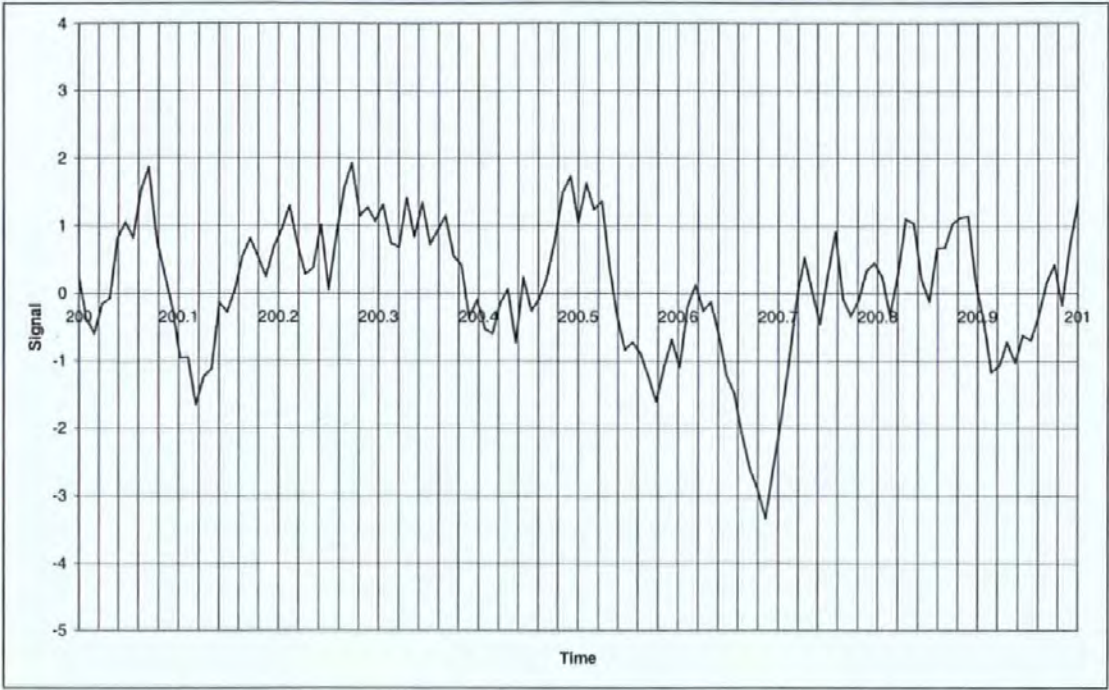
Figure 6-4, First Order Markov Process Signal (Tau = 0.1s).

Figure 6-5, Allan Variance Chart of a First Order Markov Process.

142
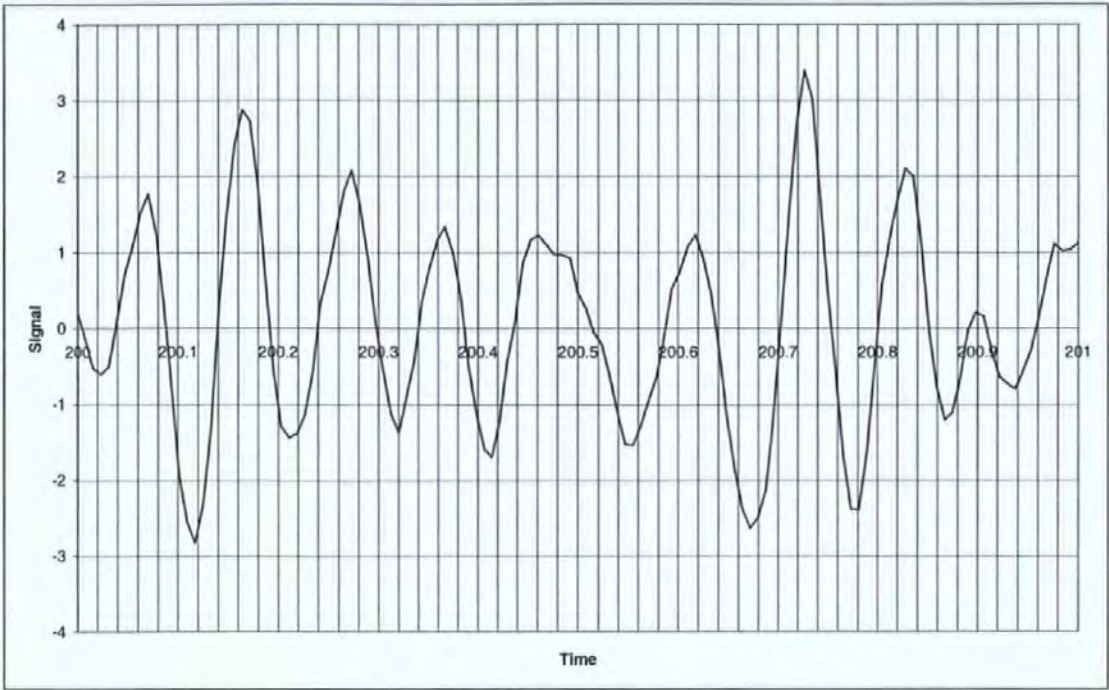
Figure 6-6, Second Order Markov Process (Fn = 10Hz, Zeta = 0.1).
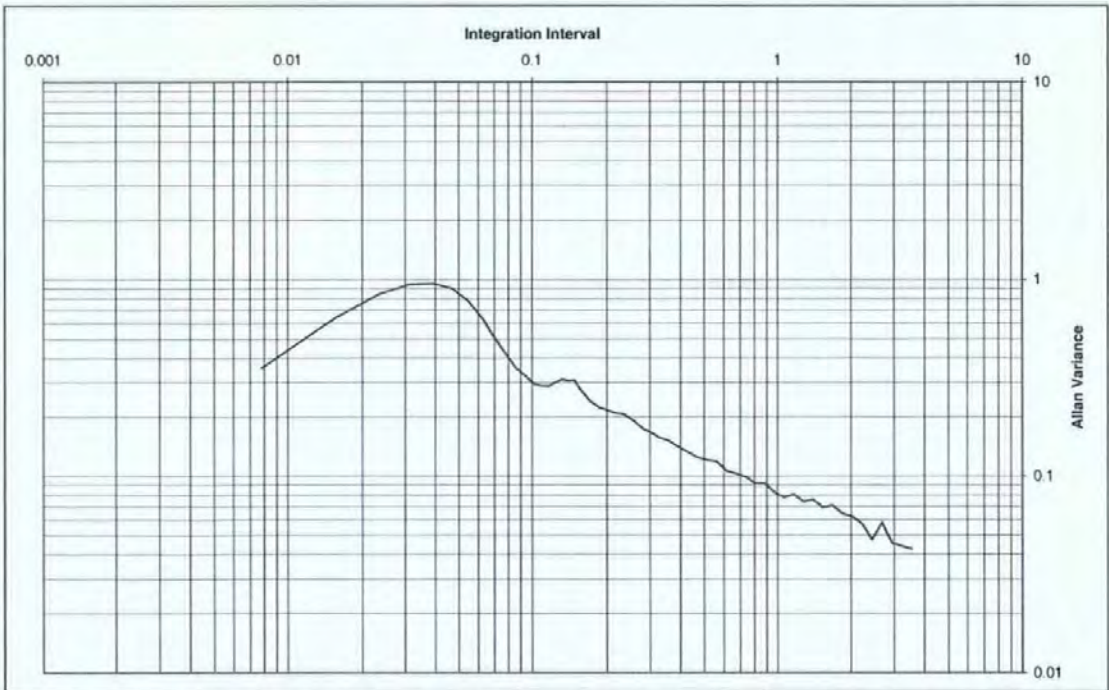
Figure 6-7, Allan Variance Chart of a Second Order Markov Process.

It should be noted that the higher time interval (right) side of the graph is subject to measurement noise because fewer samples will contribute to the estimate of the rms.

It is also important to note that when 2 or more sources of instability are present the largest at any particular τ dominates because the root sum square is used and the Allan Variance is plotted on a log-log scale.

6.2.3　High Frequency Characteristics

There was a concern that 50Hz mains induced and white noise artefacts could distort the Allan Variance. Therefore, a simple 2-zero z-transform filter was applied to the data before the Allan Variance was computed. The two zeros were at 50Hz and 60Hz in order to exclude interference artefacts at UK or USA mains frequencies.

The effect of this filter on noisy data (Channel T4 from subject Vol8) is shown in Figure 6-8; the upper line is without the filter and the lower line is with the filter. The effect of this filter on a record containing 50Hz mains 'hum' (Channel P3 from subject Mix3) is shown in Figure 6-9; again, the upper line is without the filter and the lower line is with the filter.
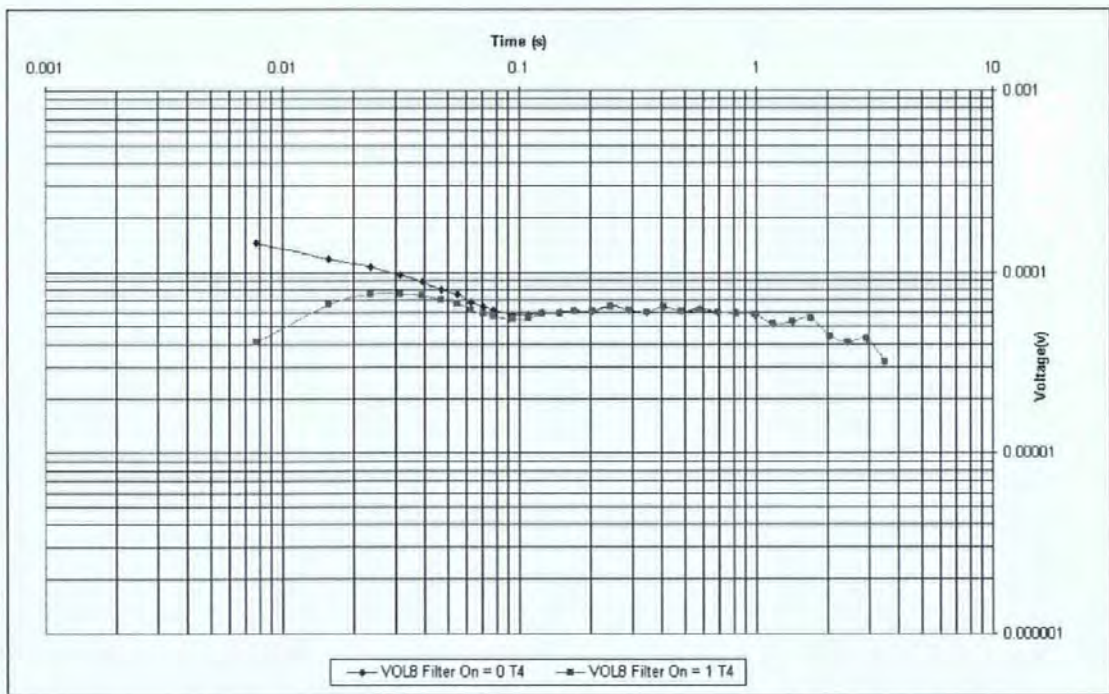
Figure 6-8, Allan Variance plot from noisy data with and without filtering.
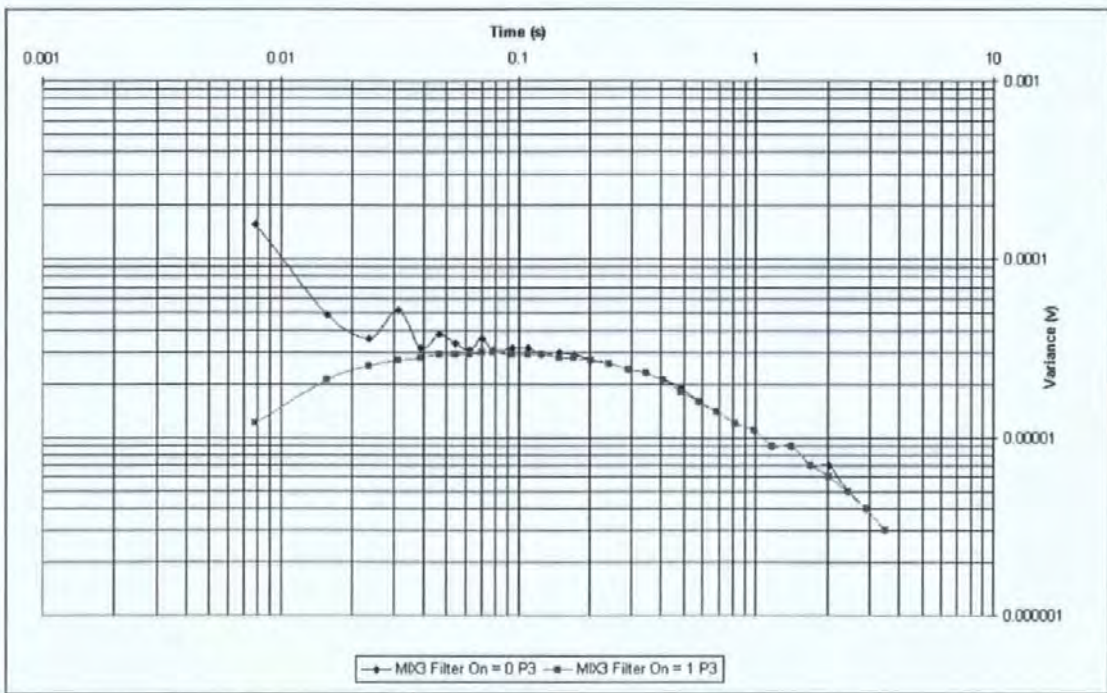
Figure 6-9, Allan Variance plot from 50Hz contaminated data with and without filtering.

6.2.4 Allan Variance plots from normal and Alzheimer's subjects

As this was believed to be the first time that the Allan Variance of the EEG had been investigated, we decided to plot the Allan Variance of bipolar channel pairs as it varies over the scalp and as it varies from normal subjects to subjects with dementia. The development data was used. Each of the following sheets contains 2 graphs; the first is the Allan Variance from a specific area of the scalp for 7 controls and the second is the Allan Variance from the same area of the scalp for 7 subjects with dementia.
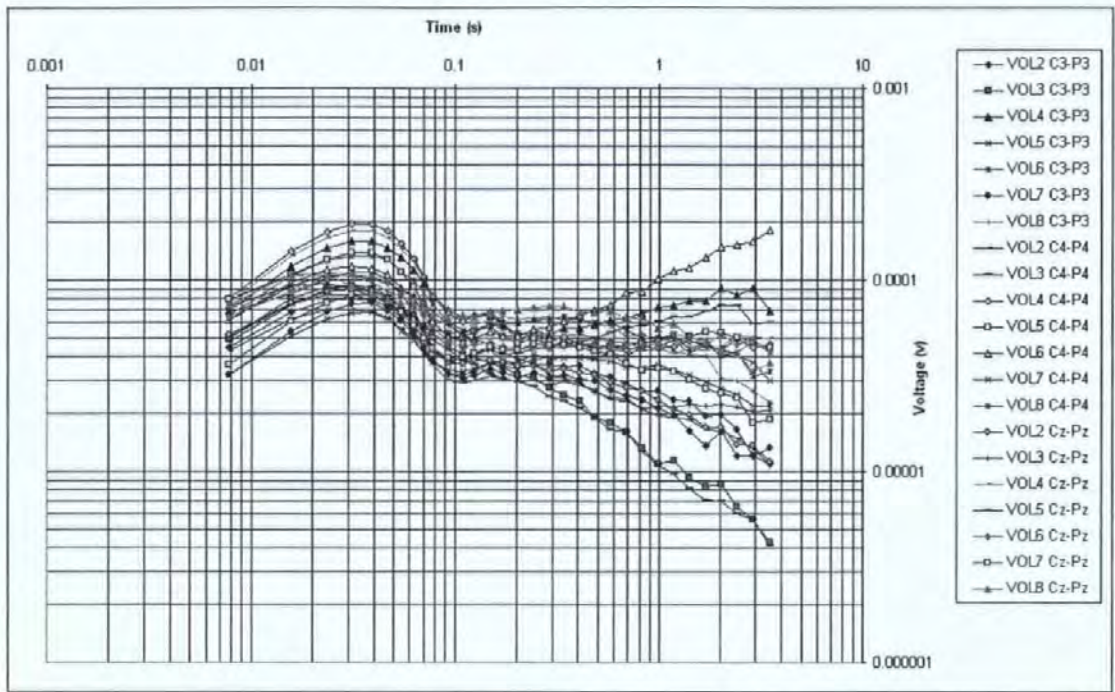
Figure 6-10, Allan Variance plot from Cental-Perietal pair for Normal Subjects.
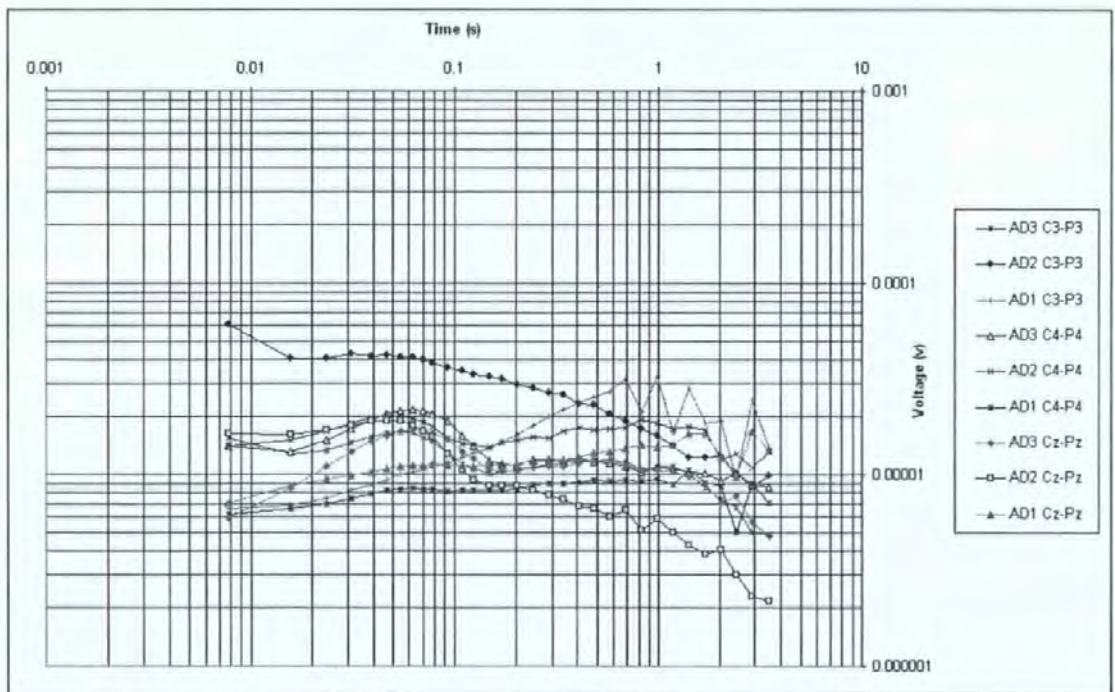
Figure 6-11, Allan Variance plot from Cental-Perietal pair for Alzheimer's Subjects.

146
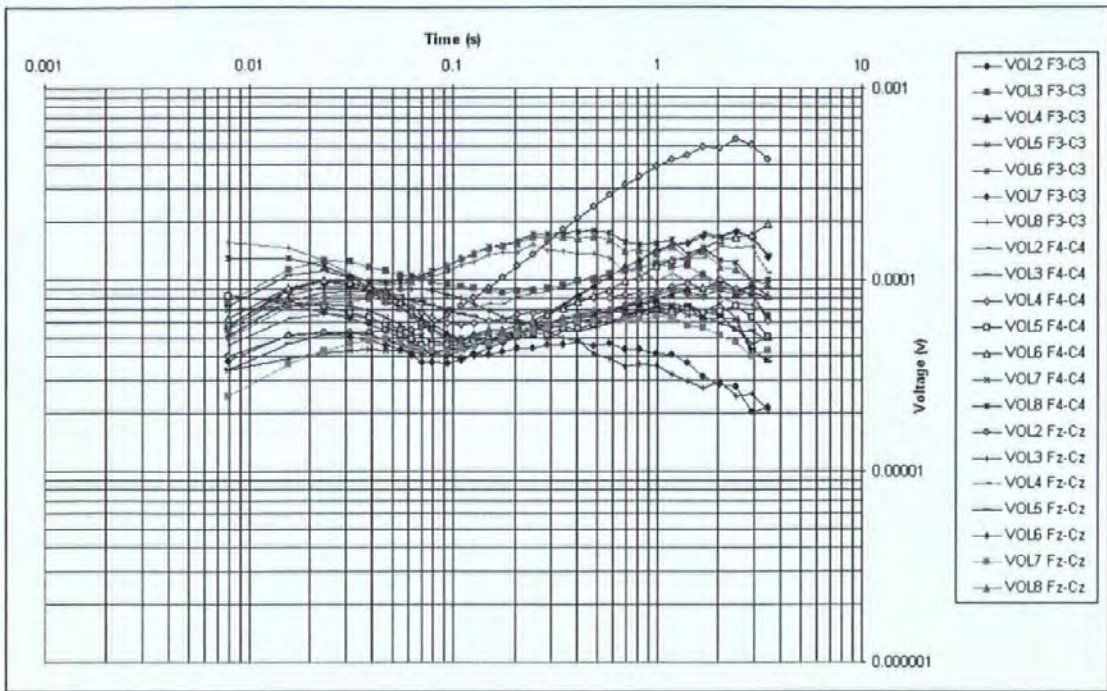
Figure 6-12, Allan Variance plot from Frontal-Central pair for Normal Subjects.
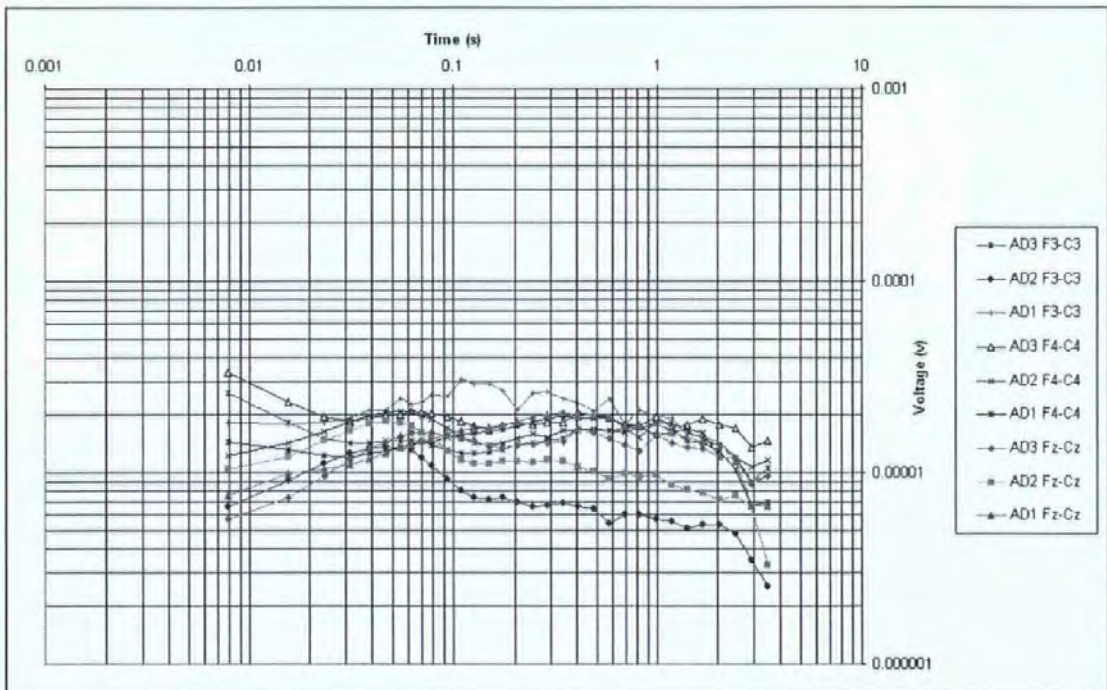
Figure 6-13, Allan Variance plot from Frontal-Central pair for Alzheimer's Subjects.
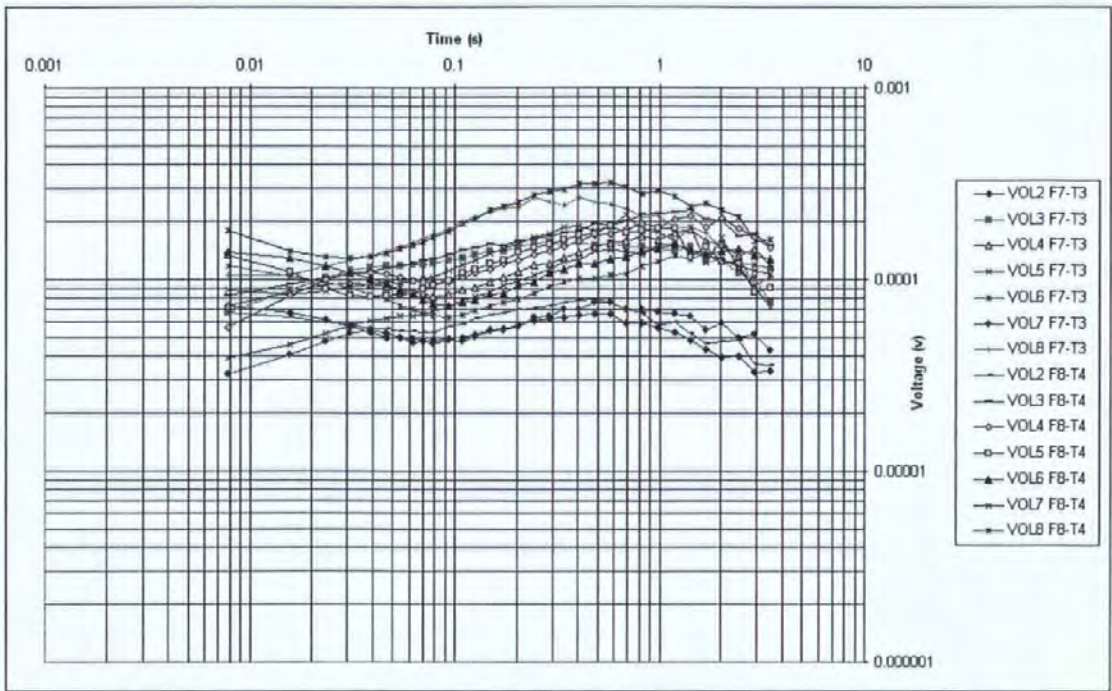
Figure 6-14, Allan Variance plot from Frontal-Temporal pair for Normal Subjects.
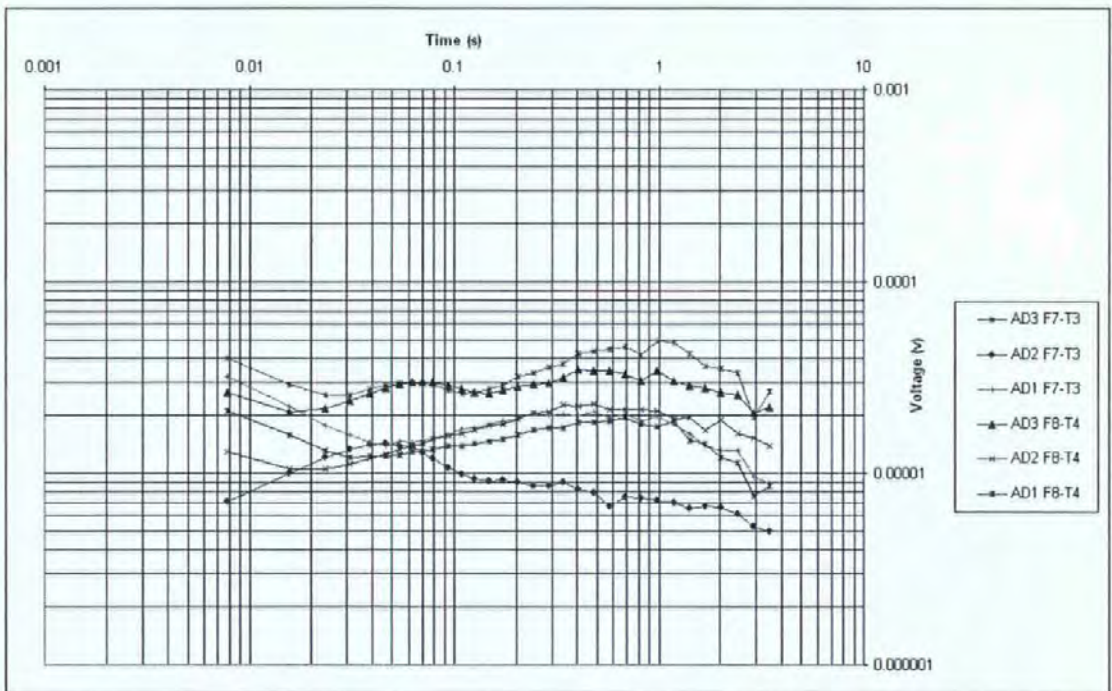
Figure 6-15, Allan Variance plot from Frontal-Temporal pair for Alzheimer's Subjects.
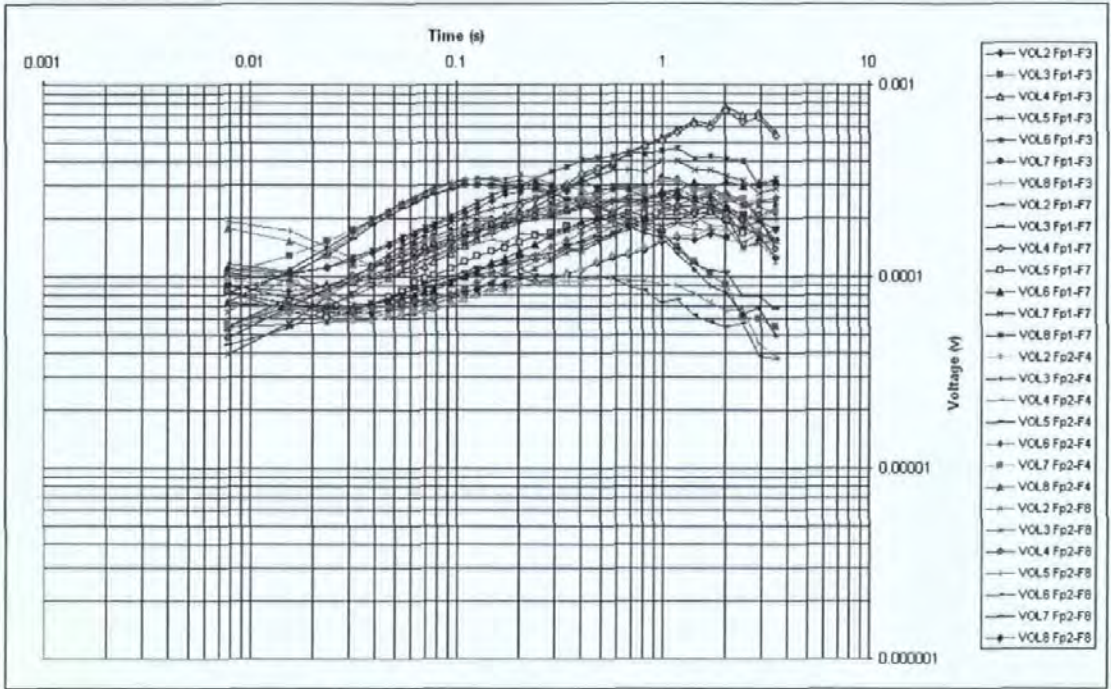
Figure 6-16, Allan Variance plot from Intra-Frontal pair for Normal Subjects.
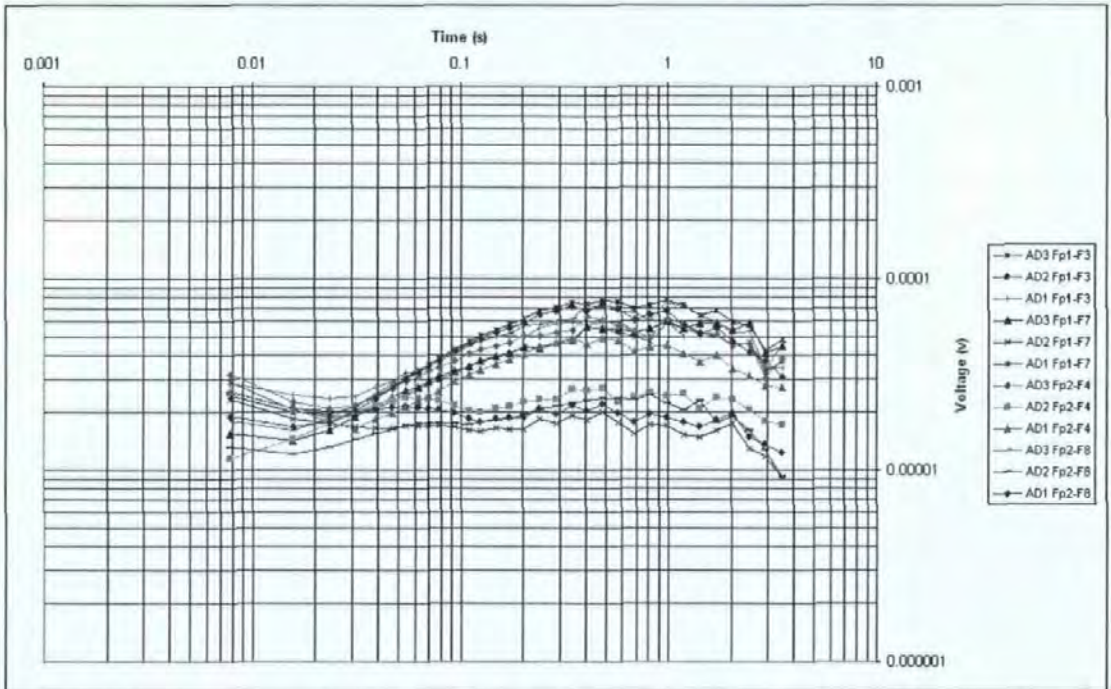
Figure 6-17, Allan Variance plot from Intra-Frontal pair for Alzheimer's Subjects.
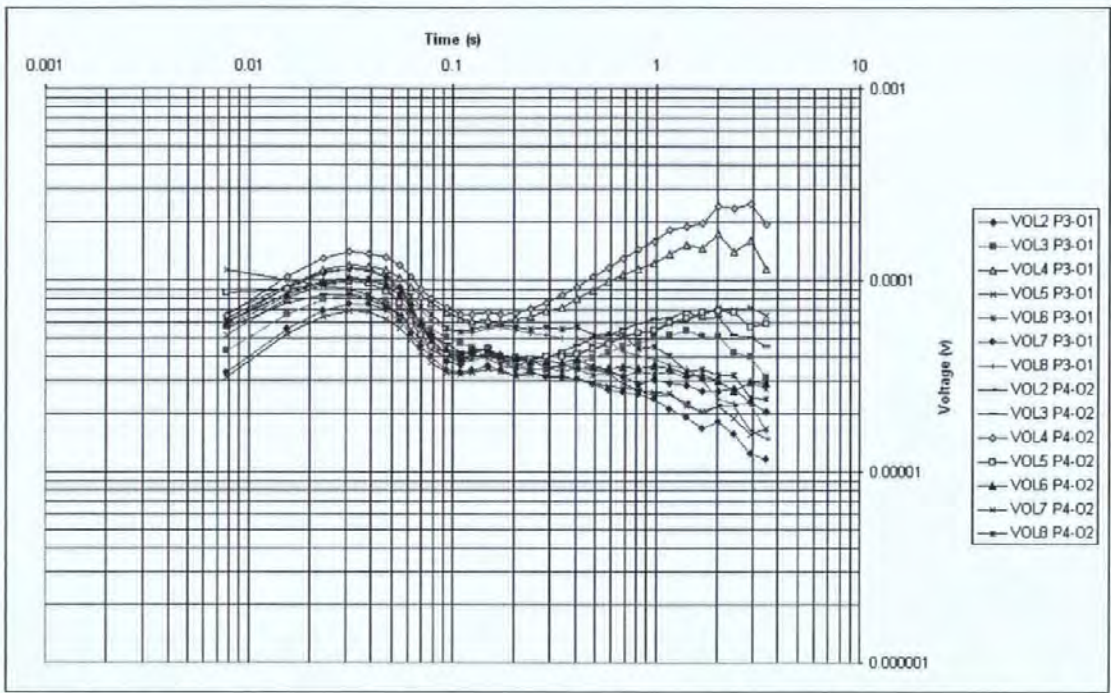
Figure 6-18, Allan Variance plot from Perietal-Occipital pair for Normal Subjects.
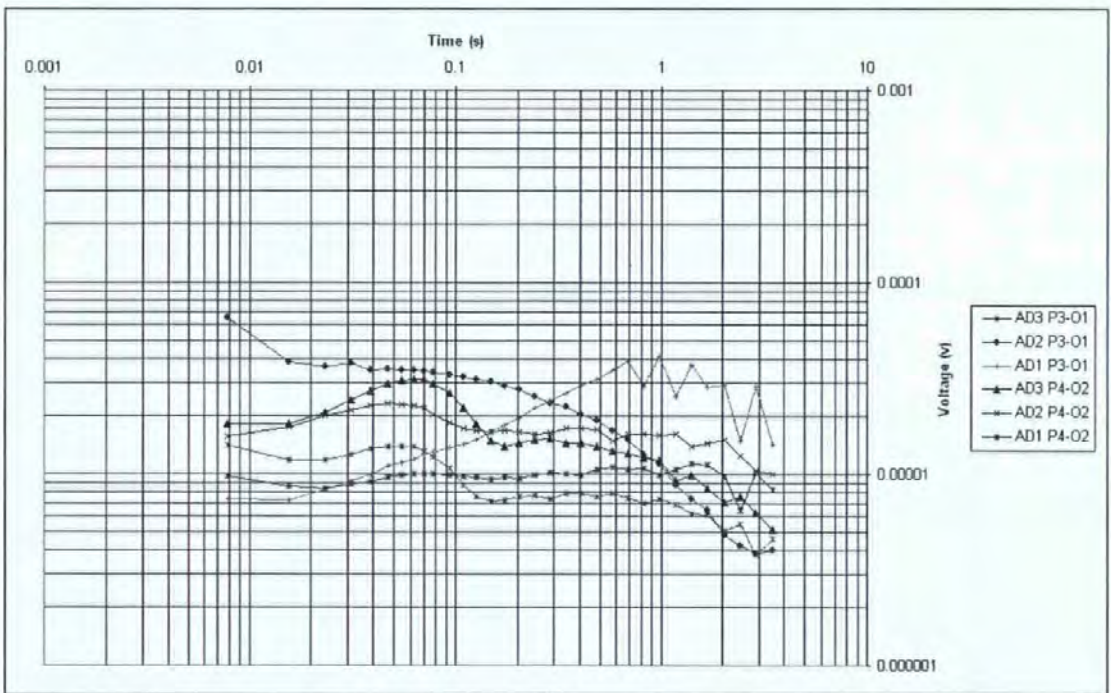
Figure 6-19, Allan Variance plot from Perietal-Occipital pair for Alzheimer's Subjects.
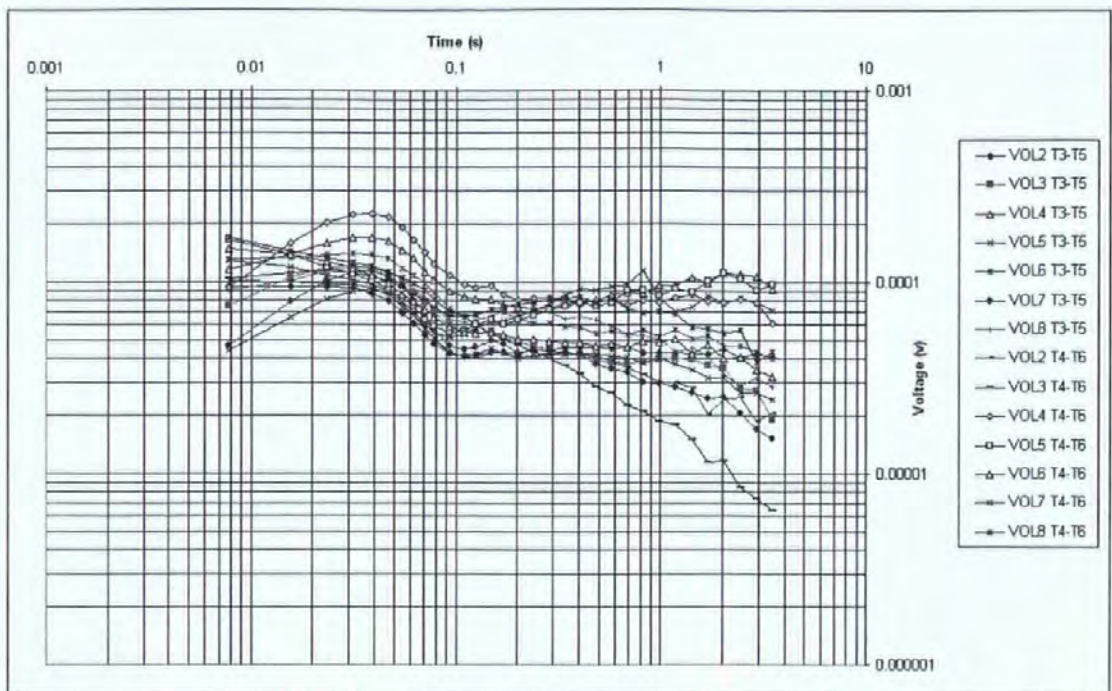
Figure 6-20, Allan Variance plot from Intra-Temporal pair for Normal Subjects.
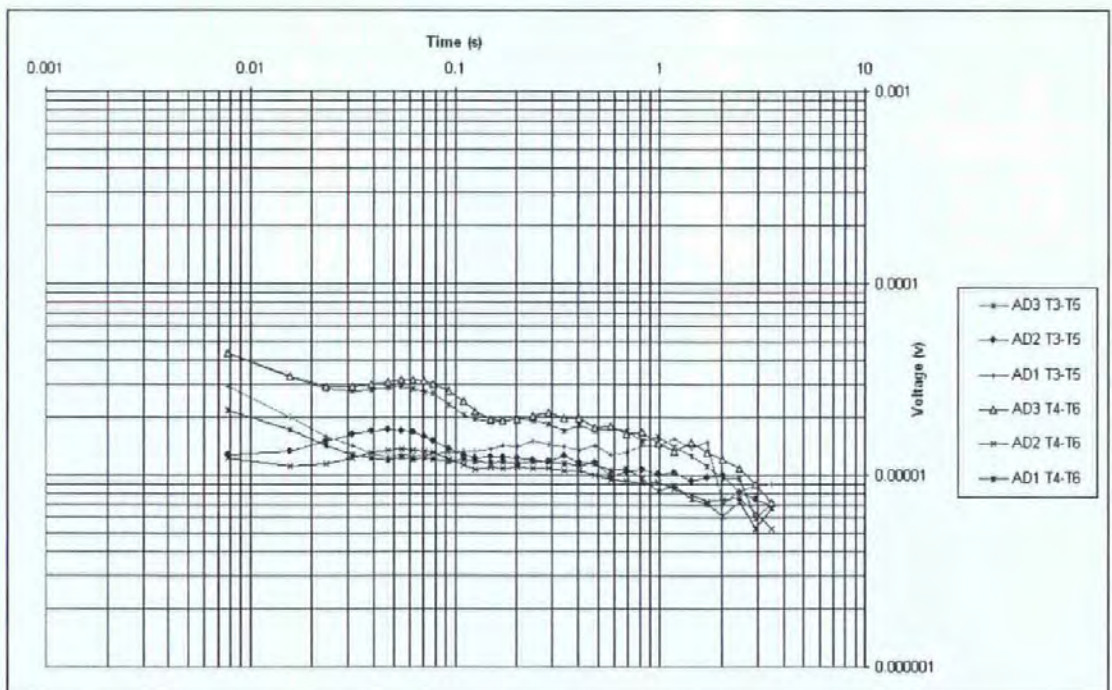
Figure 6-21, Allan Variance plot from Intra-Temporal pair for Alzheimer's Subjects.
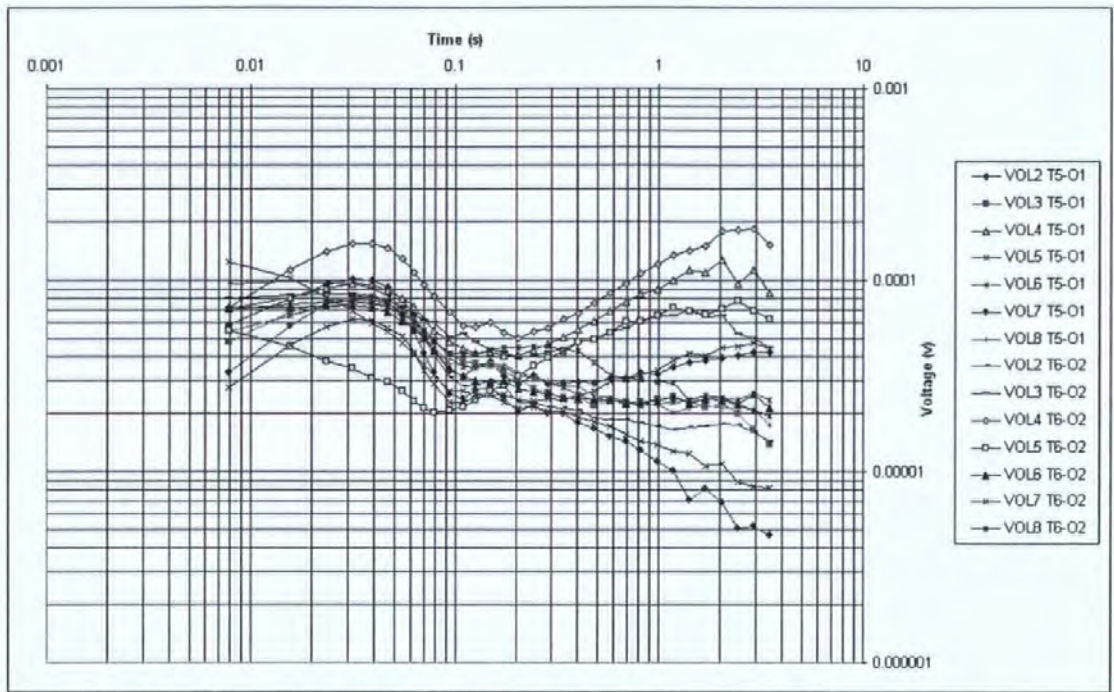
Figure 6-22, Allan Variance plot from Temporal-Occipital pair for Normal Subjects.
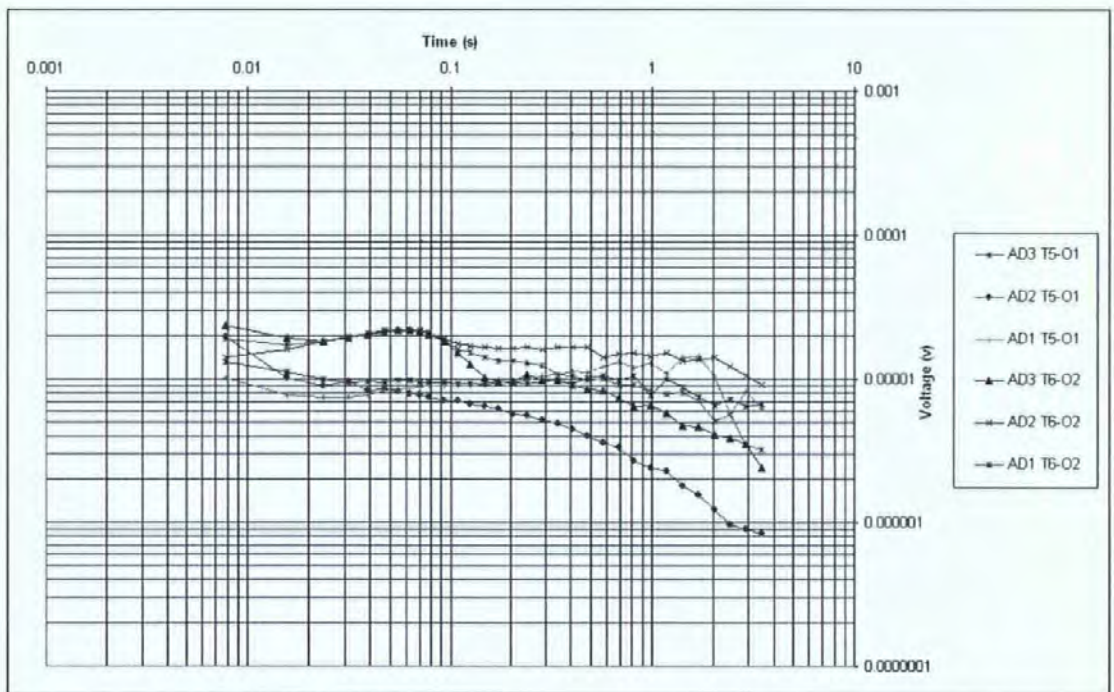
Figure 6-23, Allan Variance plot from Temporal-Occipital pair for Alzheimer's Subjects.

The Allan Variance obtained from normal subjects is most characteristically different from subjects with dementia in the temporal, perietal and occipital regions. This mirrors the findings with fractal dimension (see Section 3.8). In the frontal region, the Allan Variance is less ordered and this is probably because this area is most prone to ocular and other muscular artefacts.

6.2.5 Possible Metric and Results from the Development Data Set

The metric which was taken from the Allan Variance chart to evaluate whether such metrics could be useful was the ratio of the Allan variance at 0.04s (equivalent to approximately 12.5Hz) to the Allan variance at 0.1s (equivalent to 5Hz). This was taken from the Allan variances for the same set of bipolar channels from the rear of the scalp as had been used to evaluate the Fractal measures. Two possibilities present themselves, however. These are to take the minimum across these selected channels and to take the rms across these selected channels. The results for the development data set are given in Table 6-1, Table 6-2 and Table 6-3.

Subject	T3-T5	T4-T6	T5-O1	T6-O2	C3-P3	C4-P4	P3-O1	P4-O2	Cz-Pz	RMS	Min
VOL2	2.040	2.198	2.948	2.898	2.407	2.233	3.034	2.748	2.349	2.563	2.040
VOL3	1.986	1.627	1.965	1.645	1.960	1.806	1.630	1.720	1.719	1.790	1.627
VOL4	1.912	2.108	1.998	2.267	2.289	2.918	1.746	1.902	2.593	2.220	1.746
VOL5	1.877	1.835	2.236	1.477	2.976	2.787	2.119	2.326	2.451	2.276	1.477
VOL6	1.909	1.867	2.010	2.056	2.240	2.275	2.347	2.296	2.203	2.140	1.867
VOL7	2.455	2.153	3.246	2.706	2.325	1.996	2.198	2.077	2.129	2.394	1.996
VOL8	1.882	1.727	2.017	1.807	1.643	1.566	1.814	1.796	1.365	1.745	1.365
Mean										2.161	1.731
Std Dev'n										0.301	0.256
Limit necessary to achieve 99.9% specificity										1.230	0.940

Table 6-1, Allan Variance ratio metric for normal subjects.

| Subject	T3-T5	T4-T6	T5-O1	T6-O2	C3-P3	C4-P4	P3-O1	P4-O2	Cz-Pz	RMS	Min
AD1	0.985	1.039	0.872	1.004	0.770	0.967	0.722	0.919	0.921	0.916	0.722
AD2	1.239	1.082	1.172	1.093	1.134	1.281	1.059	1.236	1.498	1.206	1.059
AD3	1.202	1.090	1.115	1.120	1.210	1.014	1.260	1.033	0.965	1.116	0.965
MID1	1.415	1.189	1.264	1.152	1.301	1.280	1.552	1.373	1.292	1.318	1.152
Mix1	1.578	1.281	1.199	1.074	0.818	0.806	1.205	1.341	0.707	1.145	0.707
MIX2	0.893	0.957	1.118	0.900	0.992	0.963	1.048	0.869	0.947	0.968	0.869
MIX3	1.270	1.100	1.132	1.107	1.048	1.332	1.008	1.382	1.638	1.239	1.008
Mean										1.130	0.926
Std Dev'n										0.144	0.168
Sensitivity with limit necessary to achieve 99.9% specificity										76%	53%

Table 6-2, Allan Variance ratio metric for subjects with dementia.

Subject	T3-T5	T4-T6	T5-O1	T6-O2	C3-P3	C4-P4	P3-O1	P4-O2	Cz-Pz	RMS	Min
VOL1	2.190	1.885	2.017	1.992	1.776	0.941	1.745	1.163	1.486	1.733	0.941

Table 6-3, Allan Variance ratio metric for Vol1.

The sensitivities shown at the bottom of Table 6-2 (76% for Alzheimer's and 53% for vascular disease) was encouraging enough to try this same metric on the evaluation data.

6.2.6 Testing on the Evaluation Data Set

The Allan variance methods (minimum and rms of the ratio from 0.04s to 0.1s) were applied to the evaluation data set and the results are shown in Table 6-4 and Table 6-5.

	Normal	Alzheimer's	Vascular
Results	1.3927	1.0263	1.5256
	1.2146	1.3100	1.7599
	1.9088	0.9516	1.0101
	1.7759	0.9182	1.5820
	1.6366	0.9765	1.1521
	1.5062	0.7493	
	1.3230	0.8215	
	2.0261	1.0787	
	1.4603	1.4039	
	1.4667	1.1662	
	0.8085	1.1002	
	0.9686	0.7071	
	1.8038	0.8364	
	1.9783	0.7870	
	1.7573	1.1011	
	2.2668	1.1343	
	1.6094	0.9276	
	0.9779		
	1.7805		
	1.9148		
	1.1108		
	1.1981		
	1.6463		
	2.5363		
Number of samples	24	17	5
Mean	1.5862	0.9998	1.4059
SD	0.4220	0.1936	0.3130

Table 6-4, Allan Variance ratio metric for evaluation data (Minimum).

	Normal	Alzheimer's	Vascular
Results	1.6174	1.2439	1.7031
	1.9427	1.7665	1.9348
	2.1359	0.9899	1.1025
	2.3002	1.0242	1.9170
	2.1466	1.2272	1.3448
	1.8305	0.8577	
	1.6197	0.8784	
	2.3679	1.2152	
	1.6277	1.5578	
	1.6734	1.3155	
	1.7846	1.2880	
	1.0893	1.0988	
	2.0087	0.9125	
	2.7890	0.8500	
	2.0470	1.2334	
	2.5235	1.2710	
	2.1706	0.9975	
	1.7065		
	2.2306		
	2.6503		
	1.4106		
	1.8367		
	1.7781		
	3.2619		
Number of samples	24	17	5
Mean	2.0229	1.1604	1.6005
SD	0.4756	0.2506	0.3660

Table 6-5, Allan Variance ratio metric for evaluation data (RMS).

6.2.7 Conclusion

If one assumes that the results from a population of normal subjects would fall into a Gaussian distribution then one may estimate the decision-making threshold which determines abnormality (to achieve 99.9% specificity). The mean and standard deviation figures for the normal subjects using the minimum and rms from the Allan variance ratios imply limits to be applied of 0.282 and 0.553 respectively.

If we apply these limits then for the minimum metric the sensitivity to Alzheimer's and the sensitivity to vascular dementia are both estimated to be 0.0%. The rms metric fairs only marginally better with the estimated sensitivity to Alzheimer's of 0.8% and the sensitivity to vascular dementia of 0.2%. These are clearly disappointing results and the Allan variance metrics were discarded. However, it remains true that the Allan variance may provide a new and interesting method to visualise the spectral content of the EEG.

6.3   Zero Crossing Interval Distribution

6.3.1   Introduction

A further novel method that shared some features with the zero-set dimension was proposed. This was the zero-crossing interval distribution (or probability density function). Initially, the research concentrated on the strict zero crossing interval distribution as reported at Como [10]. This was superseded by work, which is reported in this thesis, that deals with the interval between double zero crossings. That is, the interval between a positive to negative transition to the next positive to negative transition.

6.3.2   Mathematical Interpretation of the Fractal Dimension of the Zero Set

This analysis considers the zero-set dimension discussed in Section 3.4.1. Consider a single gap, length g, between two consecutive zero crossings where the second crossing is at the beginning of a line being used to 'cover' the zero-set as illustrated in Figure 6-24. The distance, d, is the interval between the end of one line being used to cover the zero-set and the start of the next.
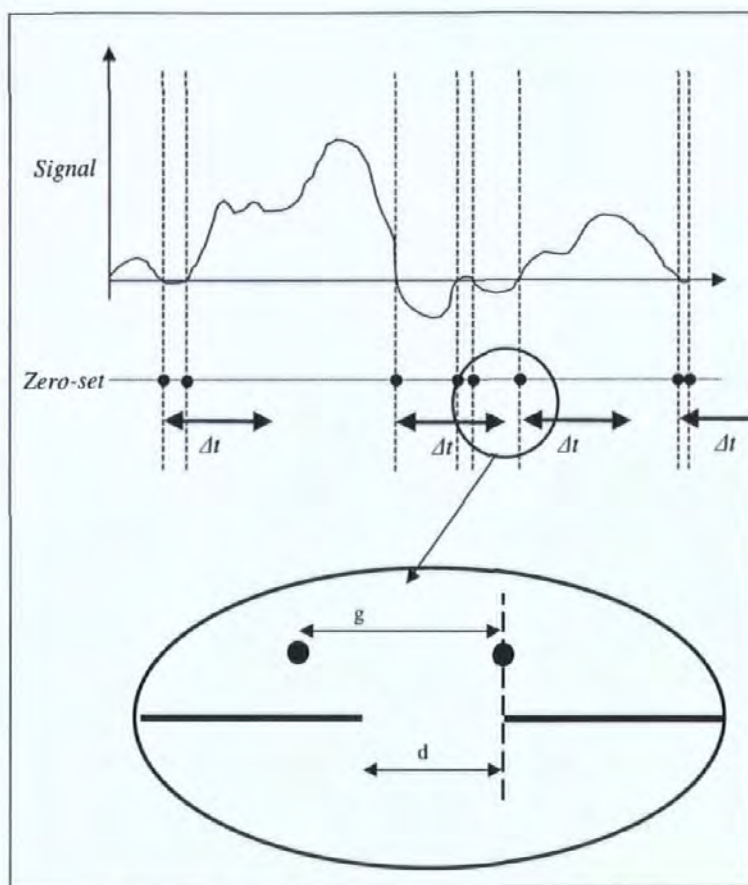
Figure 6-24, A sketch of the Dimension of the Zero-set.

For the zero-set dimension, as applied to quantised signals, both g and d are integer multiples of the sampling period T_s expressed as $g_s T_s$ and $d_s T_s$. Where, g_s and d_s are integers and obey the following inequality:

$$\max(0, g - \Delta t) \le d < g,$$ (6.3)

or,

$$\max\left(0, g_s - \frac{\Delta t}{T_s}\right) \le d_s < g_s.$$ (6.4)

The ratio of the length, Δt, necessary to cover a line gap pair to the interval covered, l, is given by:

$$\frac{\Delta t}{l} = \frac{\Delta t}{d + \Delta t}.$$ (6.5)

157

Thus, the average total length, L, of line segments necessary to cover the zero set for a data set of length L_0 is given by:

$$L(\Delta t) = L_0 \sum_{j=0}^{\infty} \left(P(d_s = j) \frac{\Delta t}{T_s j + \Delta t} \right), \tag{6.6}$$

where $P(d=j)$ is the probability of d being equal to j. And,

$$L(\Delta t) = L_0 \sum_{i=1}^{\infty} \left(P(g_s = i) \cdot \sum_{j=0}^{\infty} \left(P\left(\frac{d_s = j}{g_s = i} \right) \frac{\Delta t}{T_s j + \Delta t} \right) \right). \tag{6.7}$$

If we assume that the distance, d, is equally likely to be in any of the allowable states (and this is reasonable given our demonstration that phase randomisation has no effect) then:

$$L(\Delta t) = L_0 \sum_{i=1}^{\infty} \left(P(g_s = i) \cdot \left(\sum_{j=J}^{i-1} \frac{\Delta t}{(i-J)(T_s j + \Delta t)} \right) \right), \tag{6.8}$$

where,

$$J = \max\left(0, i - \frac{\Delta t}{T_s} \right). \tag{6.9}$$

Thus,

$$L(\Delta t) = L_0 \sum_{i=1}^{\infty} \left(\frac{P(g_s = i)}{(i-J)} \cdot \sum_{j=J}^{i-1} \left(\frac{\Delta t}{(T_s j + \Delta t)} \right) \right), \tag{6.10}$$

and,

$$L(\Delta t) = L_0 \sum_{i=1}^{\infty} \left(\frac{\Delta t \cdot P(g_s = i)}{T_s(i-J)} \cdot \sum_{j=J+\Delta t/T_s}^{i-1+\Delta t/T_s} \left(\frac{1}{j} \right) \right), \tag{6.11}$$

$$L(\Delta t) = L_0 \sum_{i=1}^{\infty} \left(\frac{\Delta t \cdot P(g_s = i)}{T_s(i-J)} \cdot \left(H_{i-1+\Delta t/T_s} - H_{J-1+\Delta t/T_s} \right) \right), \tag{6.12}$$

158

where H_n is the nth Harmonic Number (first order) for $n>0$ and zero for $n=0$.

Equation 6.12 may be recognised to be of the form below. Recall, $P(g_s=i)$ is the Probability Density Function of the zero-crossing interval distribution.

$$L(\Delta t) = L_0 \sum_{i=1}^{\infty} \left(P(g_s = i) K(i, \Delta t) \right) \tag{6.13}$$

K may be plotted as a function of the zero crossing interval, i, and the length of the line being used to cover the zero set:
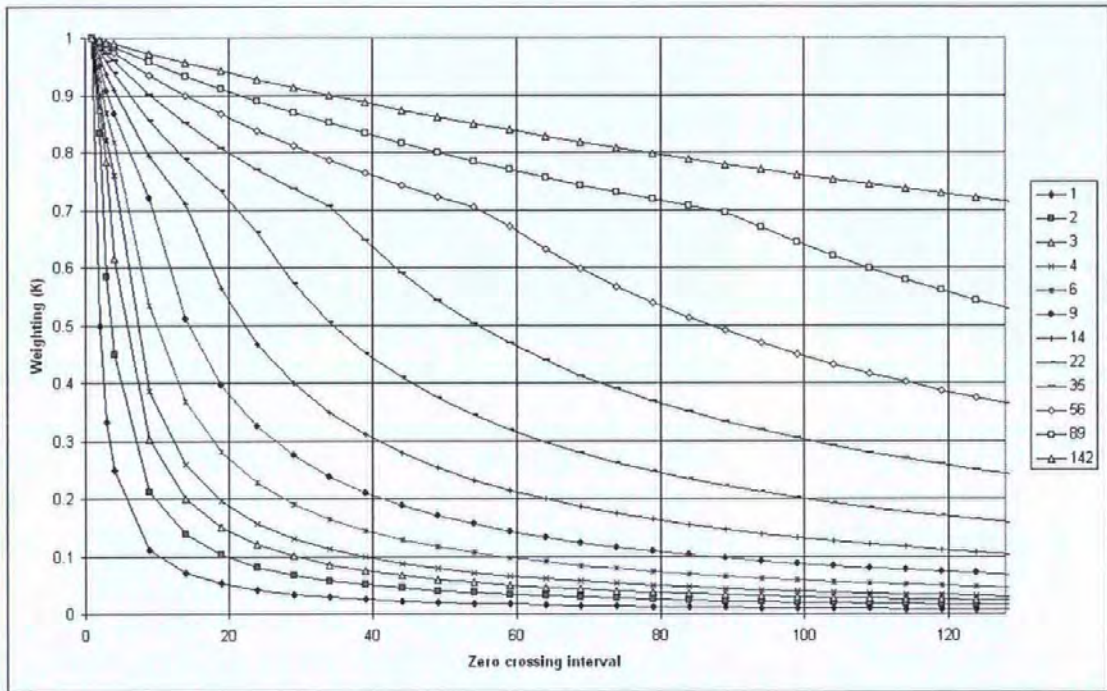
Figure 6-25, Weighting against zero crossing interval for various line lengths.
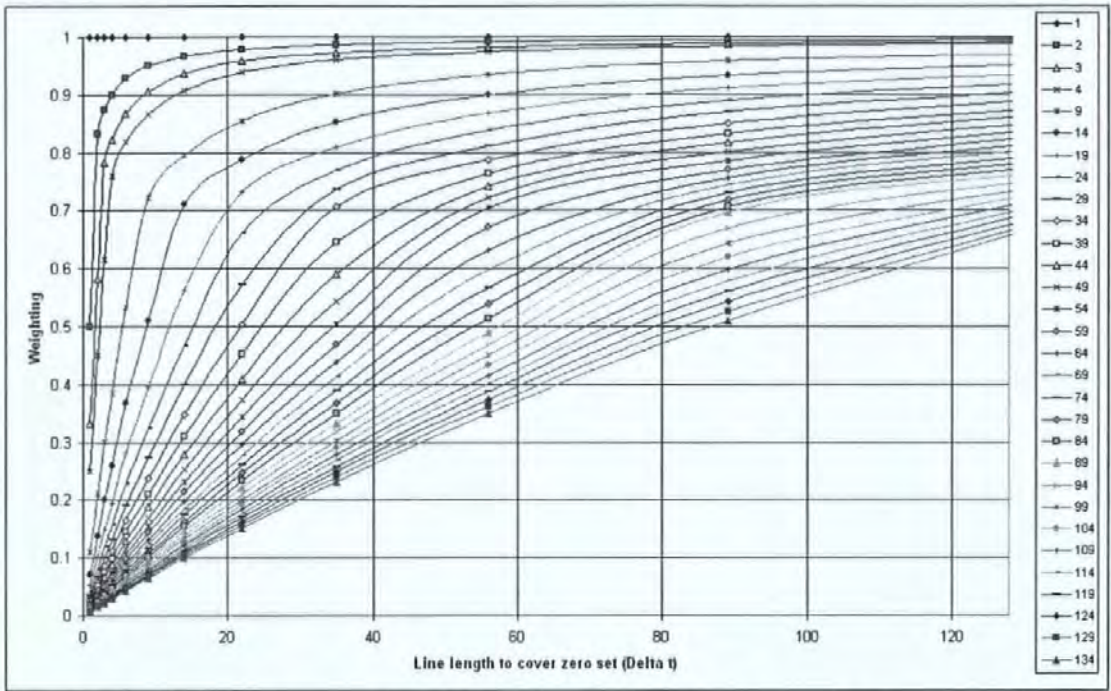
Figure 6-26, Weighting against line length used to cover the zero set for crossing intervals.

To illustrate the effect of the nature of this weighting function it is helpful to plot the line length (L/L_0) against the line length (Δt) for hypothetical PSDs of zero crossing interval which are monotonic. That is $P(g_s=i) = 1$ for $i=g_{so}$ and zero elsewhere.
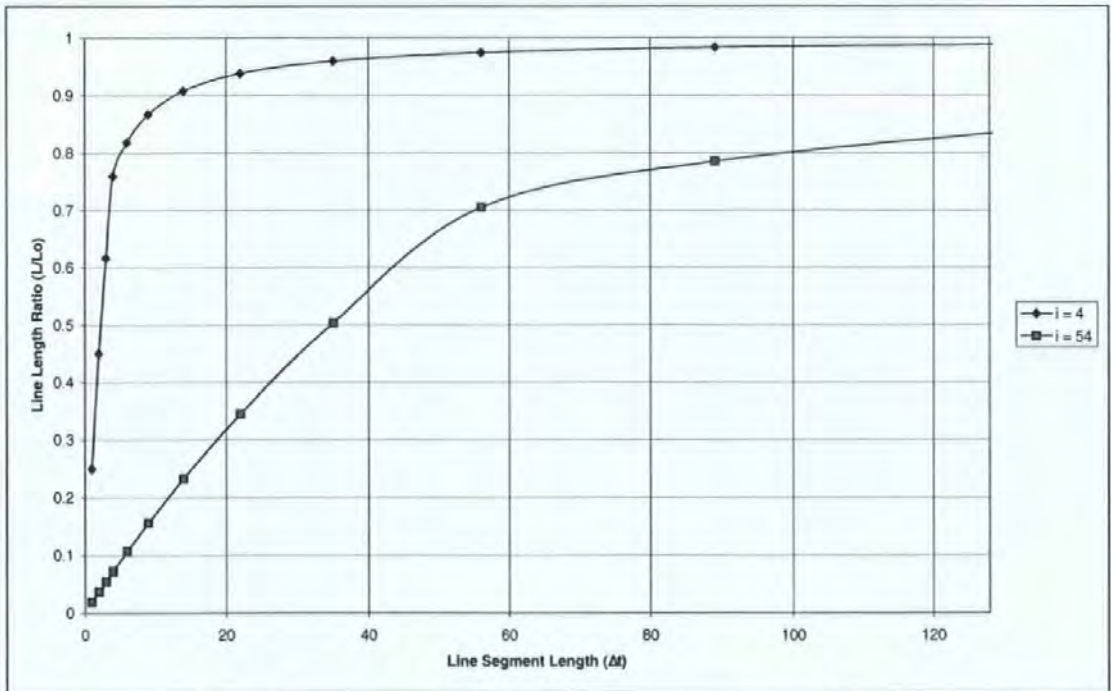
Figure 6-27, Length of line necessary to cover zero set against line segment length.

These curves, when compared to the theoretical curves for fractal dimensions (below) show that longer zero crossing intervals (lower frequencies) tend to give a lower fractal dimension. Hence, it has been shown that the measured fractal dimension of the zero set is a direct function of the zero crossing interval PDF (assuming that phase is random) and that longer zero crossing intervals (lower frequencies) tend to give a lower fractal dimension.
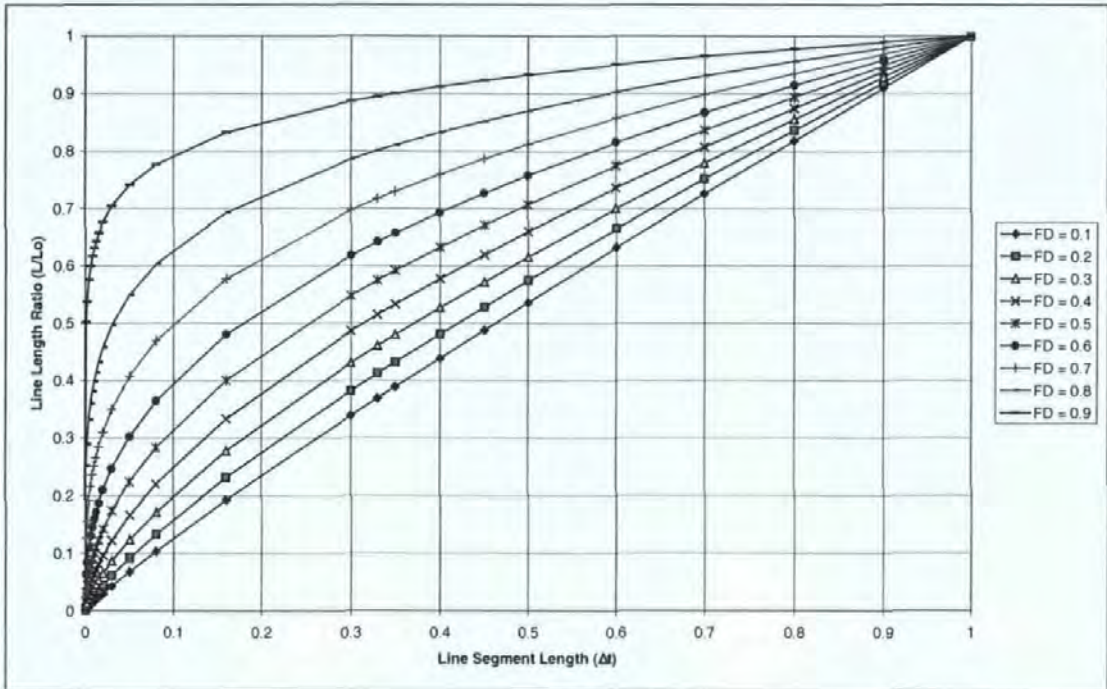
Figure 6-28, Length of line necessary to cover zero set against line segment length.

6.3.3   High Frequency Characteristics

As with the Allan Variance, there was a concern that 50Hz mains induced and white noise artefacts could distort the results. Therefore, the same simple 2-zero z-transform filter was applied to the data before the zero crossing interval distribution was computed (see Section 6.2.3).

6.3.4 Zero Crossing Interval Plots from Normal and Alzheimer's Subjects

As this was believed to be the first time that the zero-crossing interval of the EEG had been investigated in detail, we decided to plot the probability density function (PDF) of bipolar channel pairs over the scalp and as it varies from normal to subjects with dementia. The development data was used. Each of the following sheets contains two graphs; the first is the zero-crossing interval PDF from a specific area of the scalp for 7 controls and the second is the same for 7 subjects with dementia.
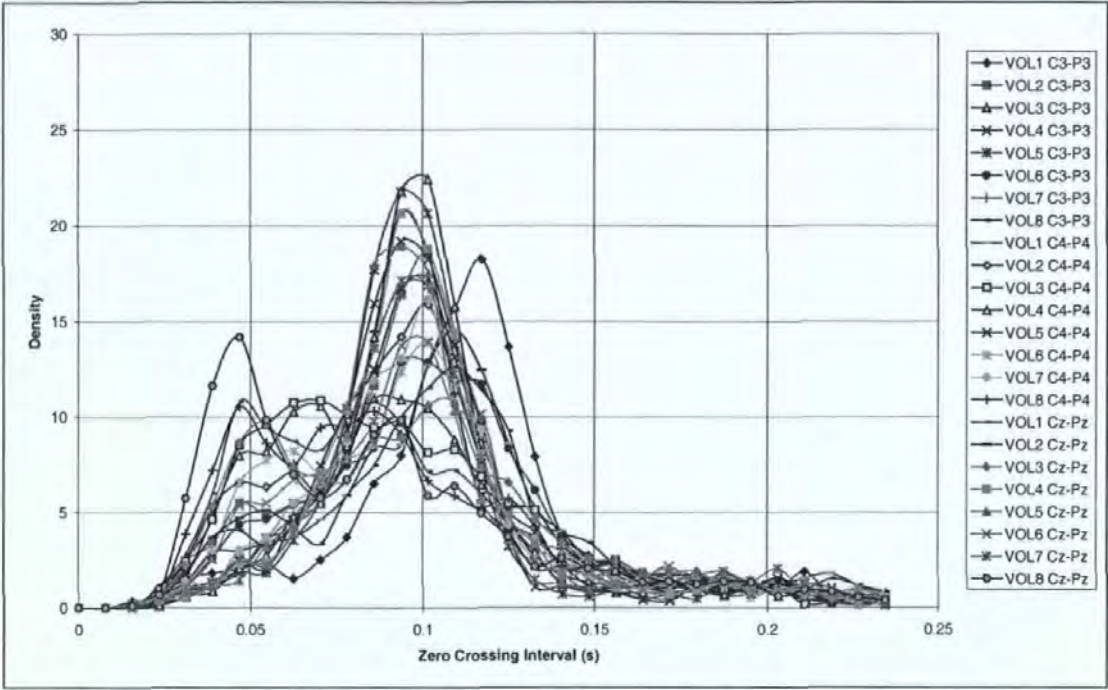
Figure 6-29, Zero-Crossing Interval PDF from Cental-Perietal pair for Normal Subjects.
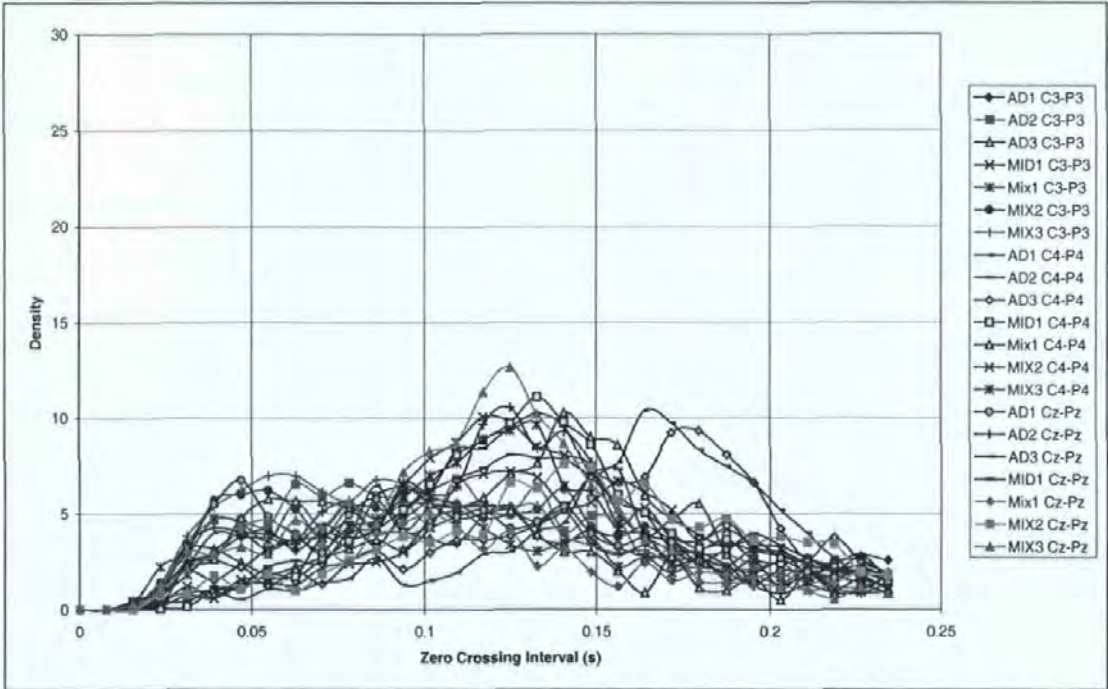
Figure 6-30, Zero-Crossing Interval PDF from Cental-Perietal pair for subjects with dementia.
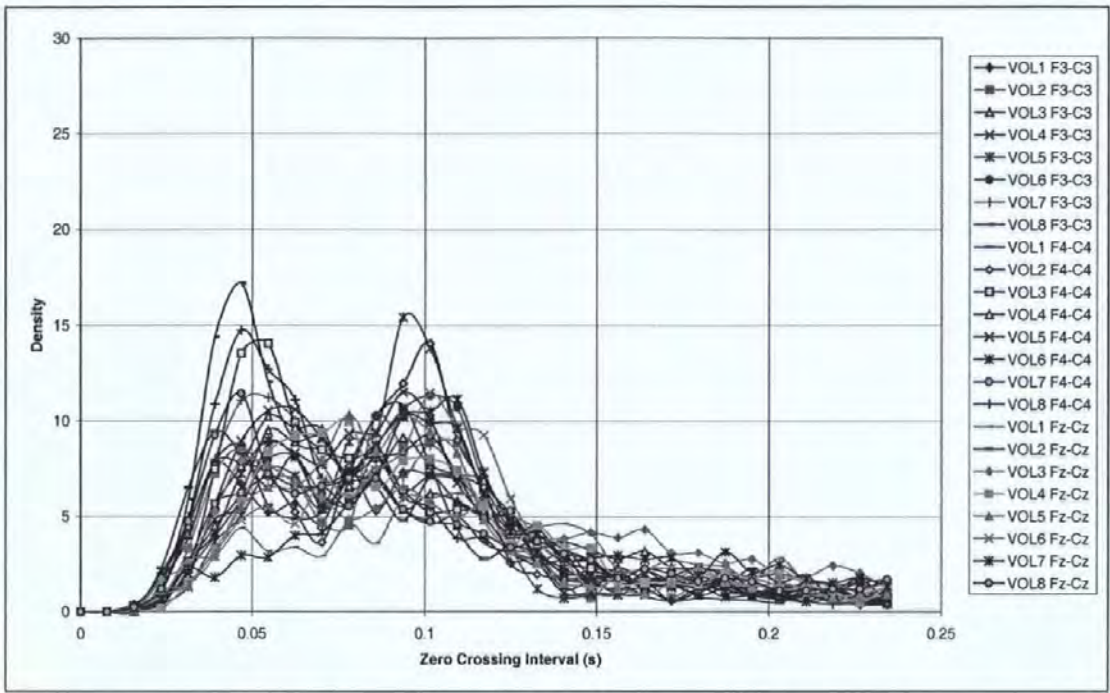
Figure 6-31, Zero-Crossing Interval PDF from Frontal-Central pair for Normal Subjects.
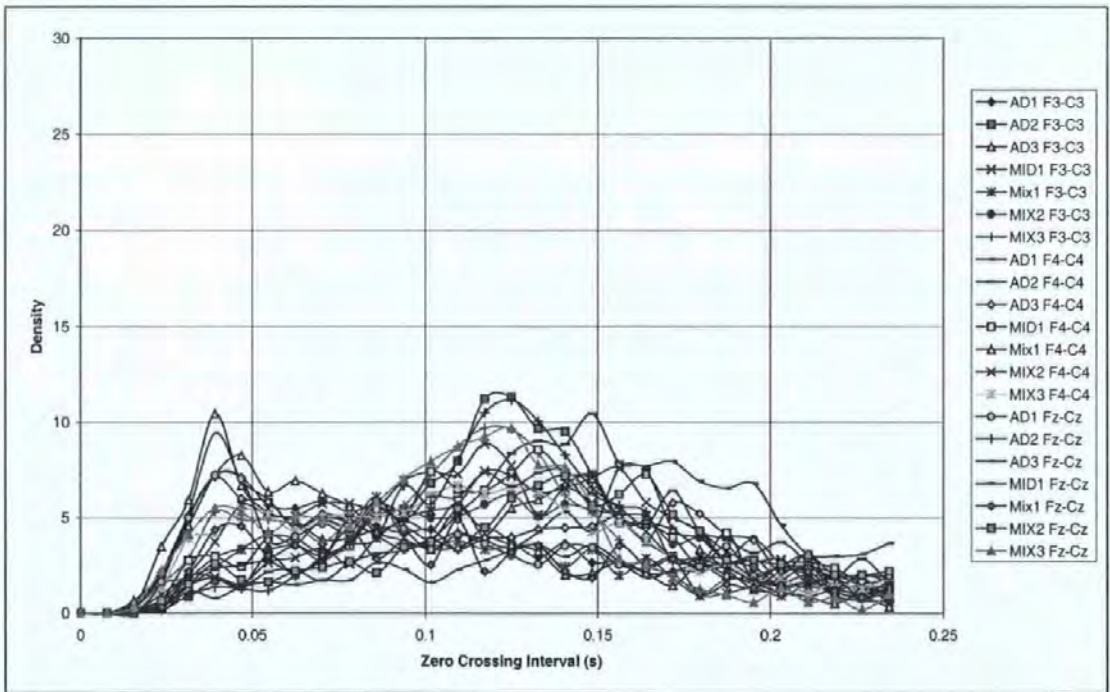
Figure 6-32, Zero-Crossing Interval PDF from Frontal-Central pair for subjects with dementia.
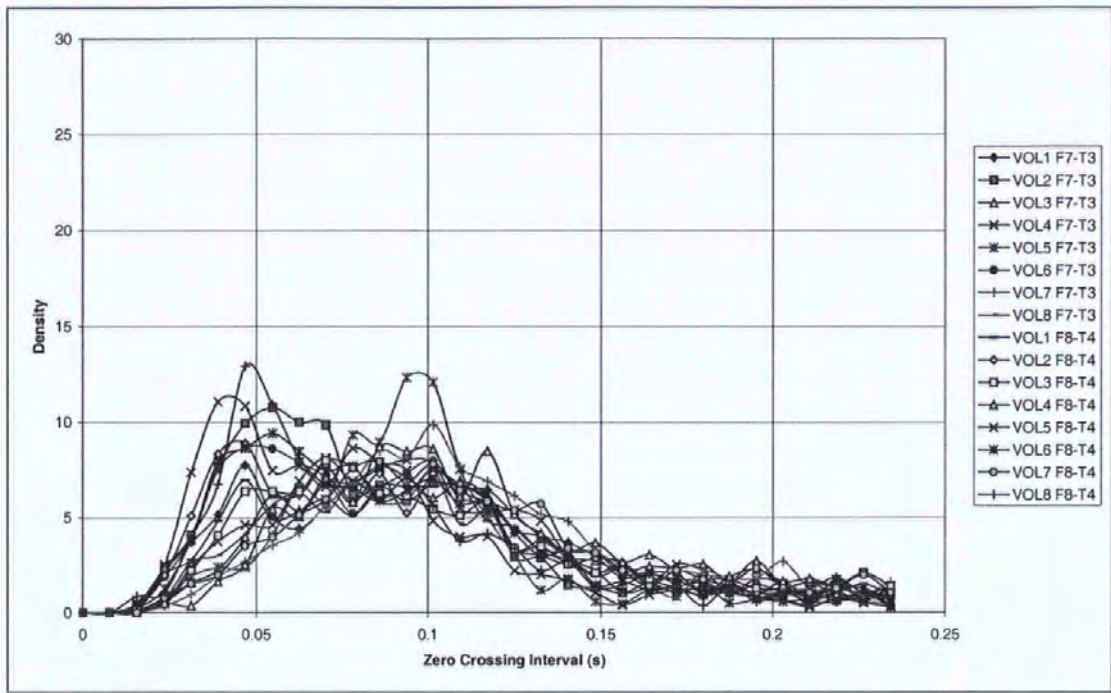
Figure 6-33, Zero-Crossing Interval PDF from Frontal-Temporal pair for Normal Subjects.
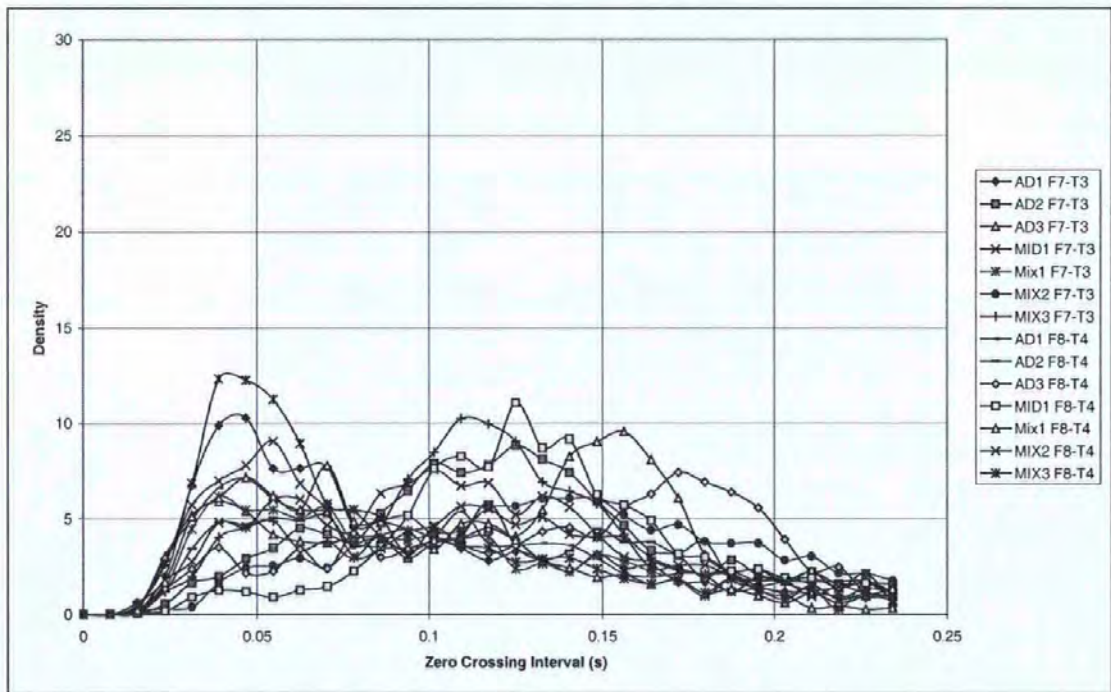
Figure 6-34, Zero-Crossing Interval PDF from Frontal-Temporal pair for subjects with dementia.
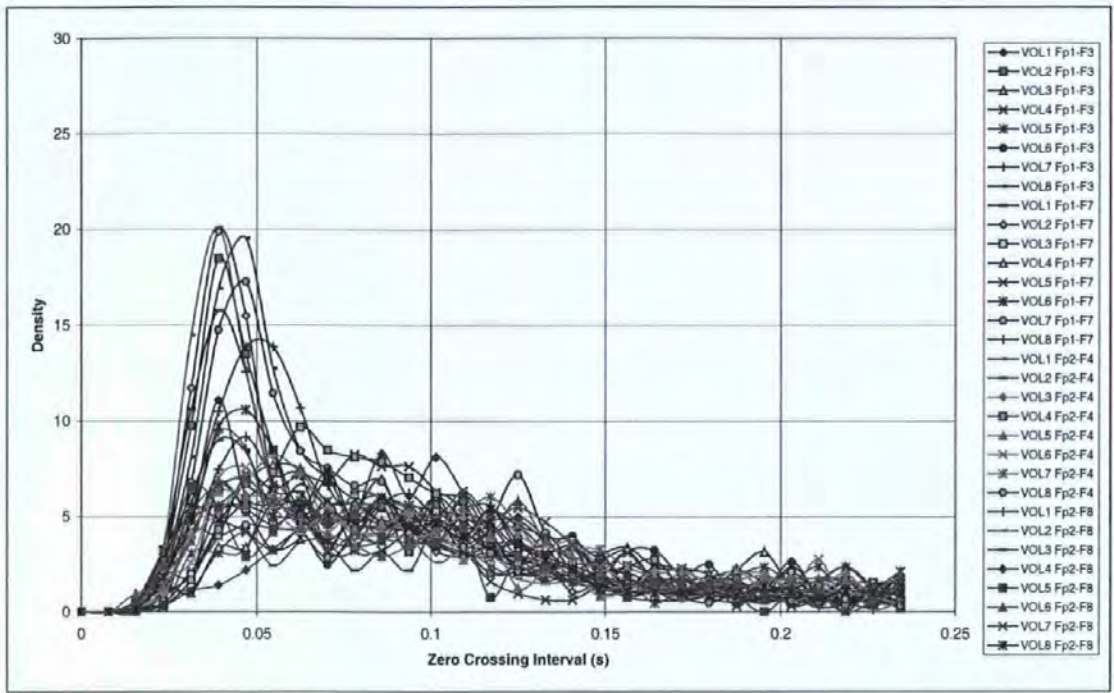
Figure 6-35, Zero-Crossing Interval PDF from Intra-Frontal pair for Normal Subjects.
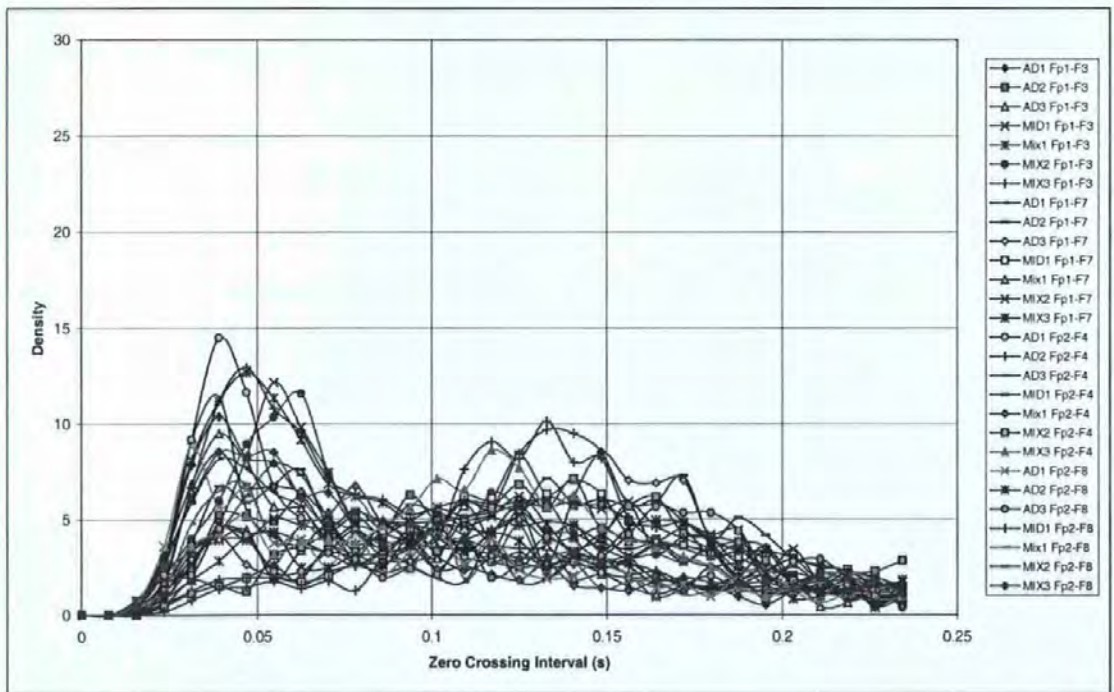
Figure 6-36, Zero-Crossing Interval PDF from Intra-Frontal pair for subjects with dementia.
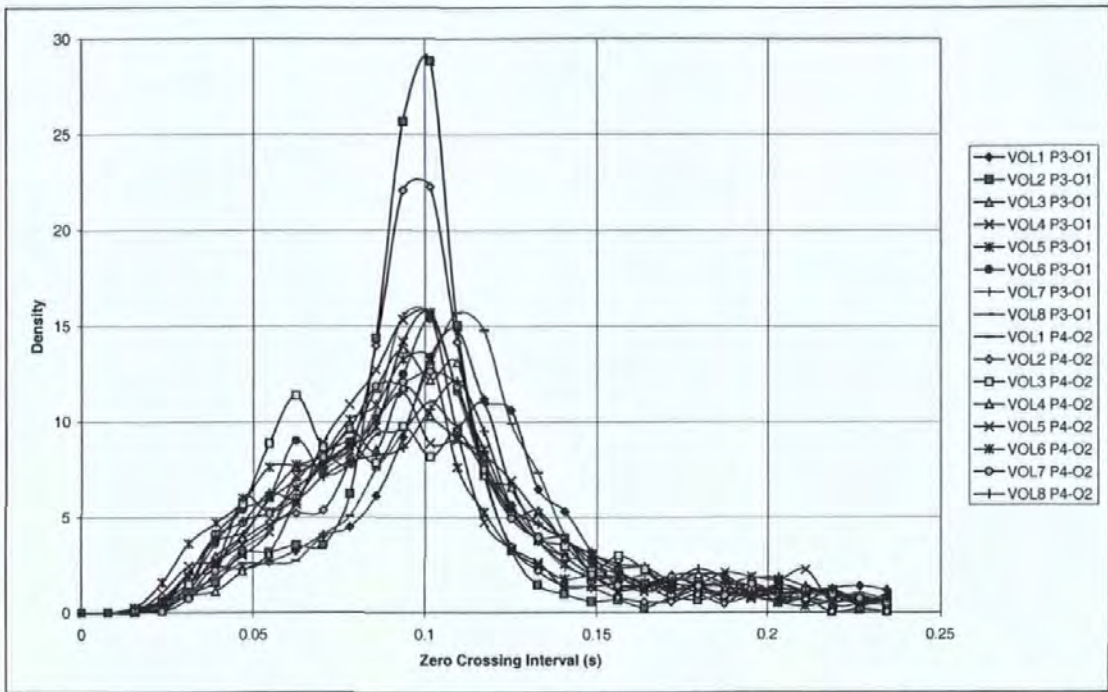
Figure 6-37, Zero-Crossing Interval PDF from Perietal-Occipital pair for Normal Subjects.
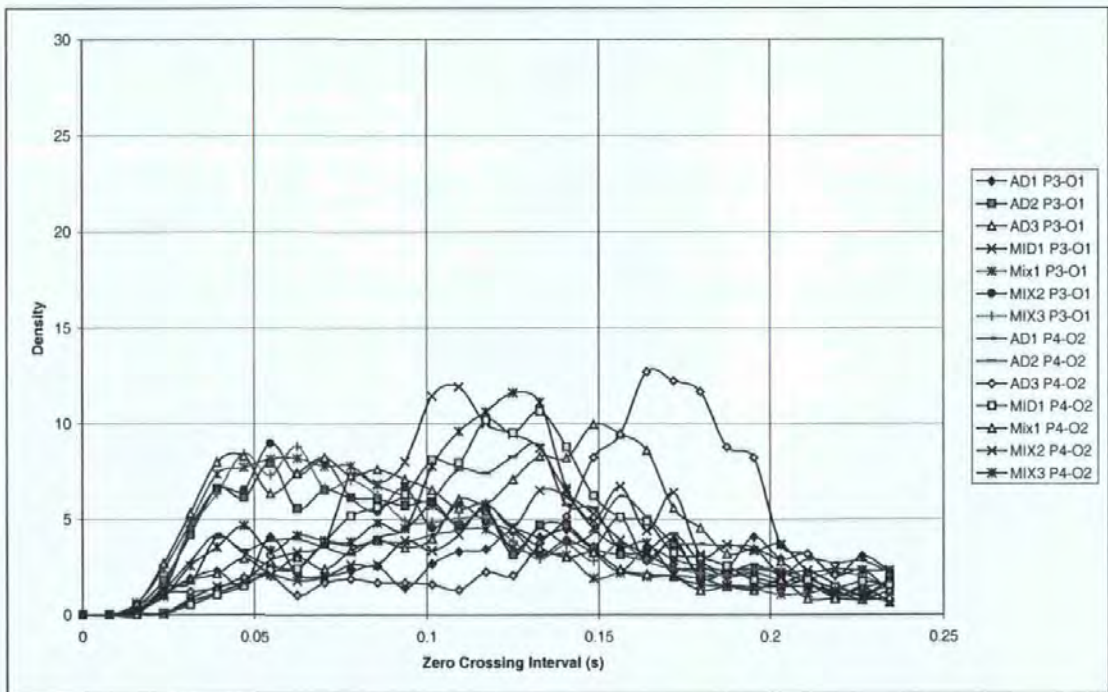
Figure 6-38, Zero-Crossing Interval PDF from Perietal-Occipital pair for subjects with dementia.
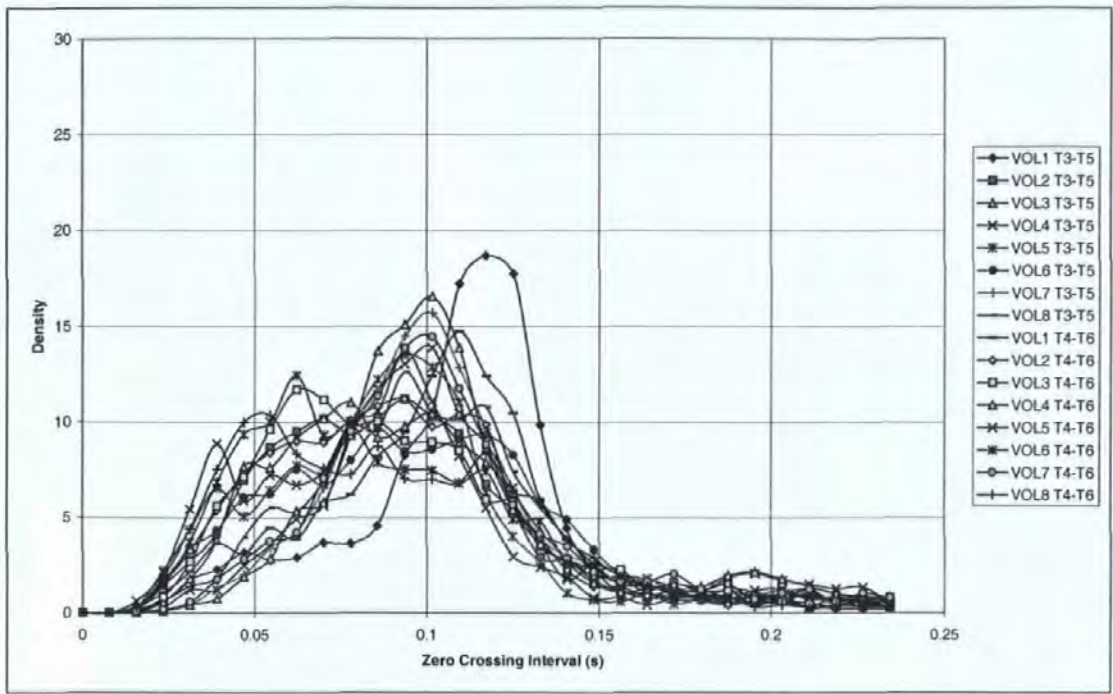
Figure 6-39, Zero-Crossing Interval PDF from Intra-Temporal pair for Normal Subjects.
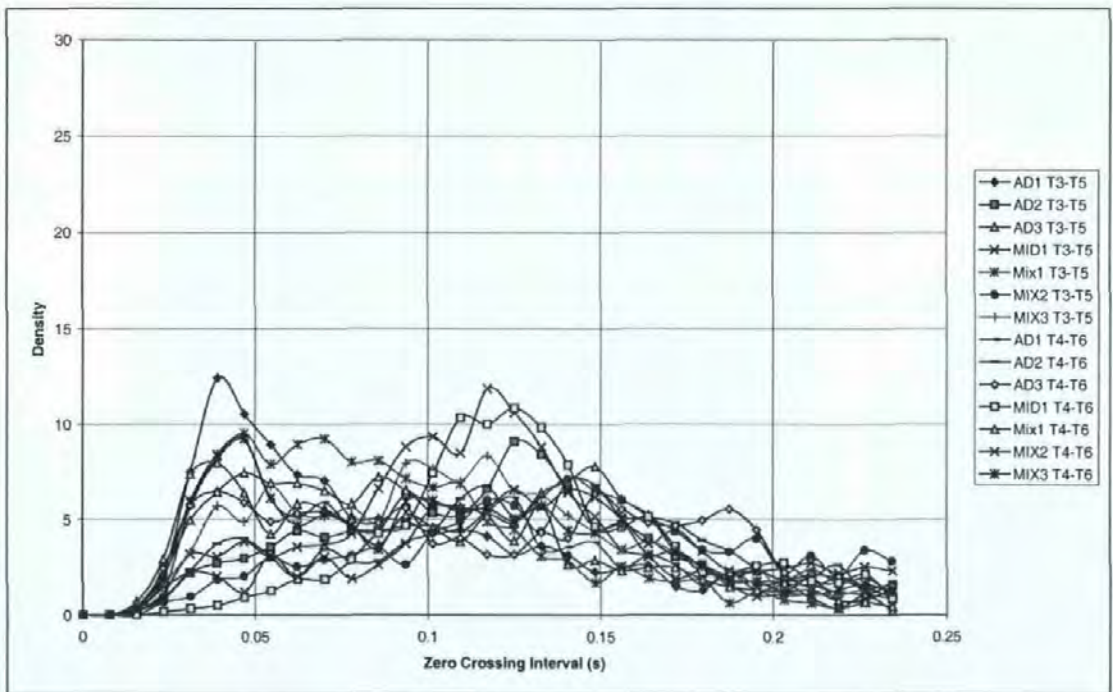
Figure 6-40, Zero-Crossing Interval PDF from Intra-Temporal pair for subjects with dementia.
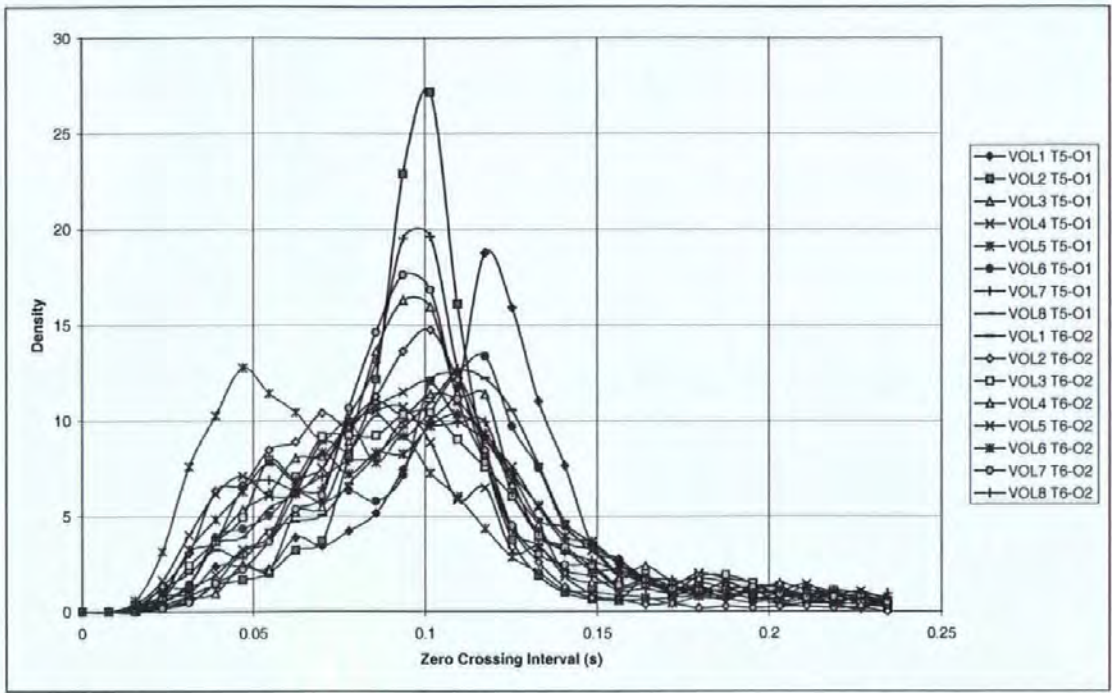
Figure 6-41, Zero-Crossing Interval PDF from Temporal-Occipital pair for Normal Subjects.
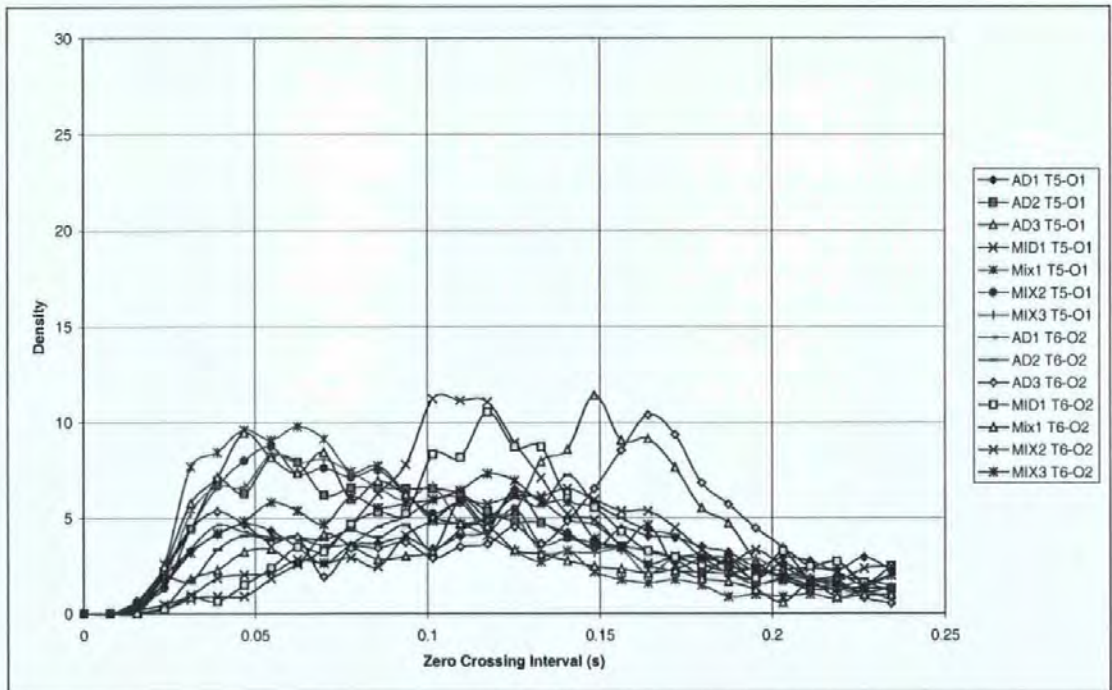
Figure 6-42, Zero-Crossing Interval PDF from Temporal-Occipital pair for subjects with dementia.

169

The plots obtained from normal subjects are most characteristically different from subjects with dementia in the temporal, perietal and occipital regions. This mirrors the findings with fractal dimension (see Section 3.8). In the frontal region, the results are less ordered and this is probably because this area is prone to ocular and other muscular artefacts.

6.3.5 Cumulative Based Metric of Zero Crossing Interval

The first metrics to suggest themselves when looking at the zero crossing interval distribution were cumulative based metrics. If we plot the cumulative density distribution, for bipolar channels at the rear of the scalp, for normals (Figure 6-43) and subjects with dementia (Figure 6-44) then it is clear that the normals have a higher density at lower time intervals. Hence, we evaluated the 75%, 80% and 85% points of the cumulative distribution as a metric. These results are shown in Table 6-7, Table 6-6 and Table 6-8 respectively.
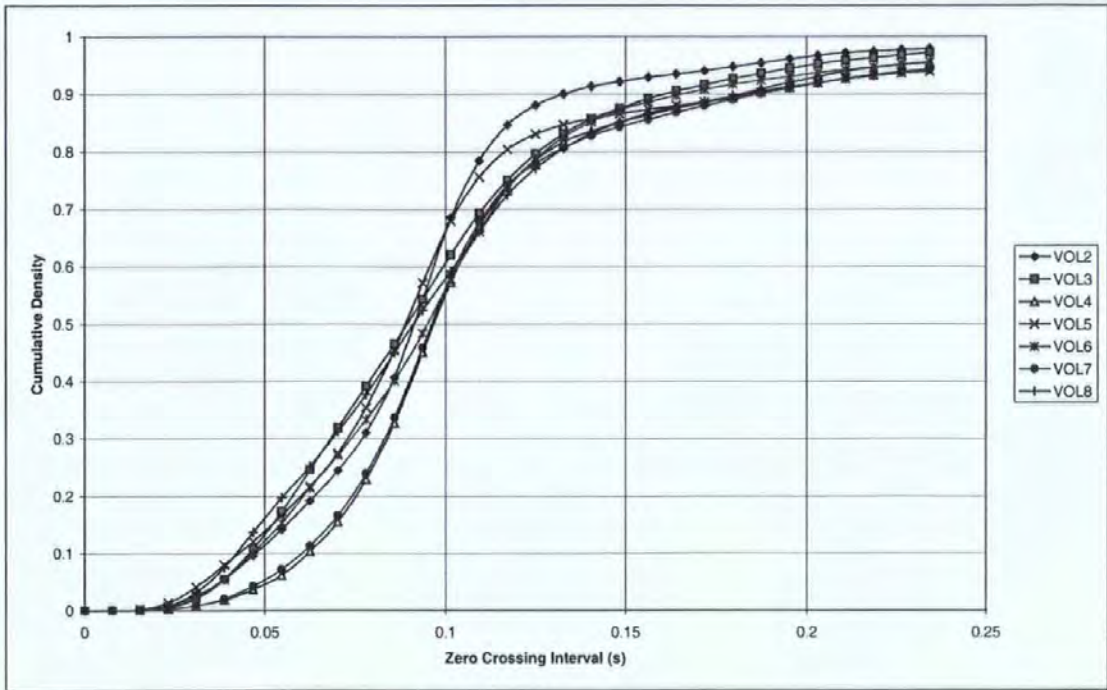
Figure 6-43, Zero crossing interval CDF from normal subjects.
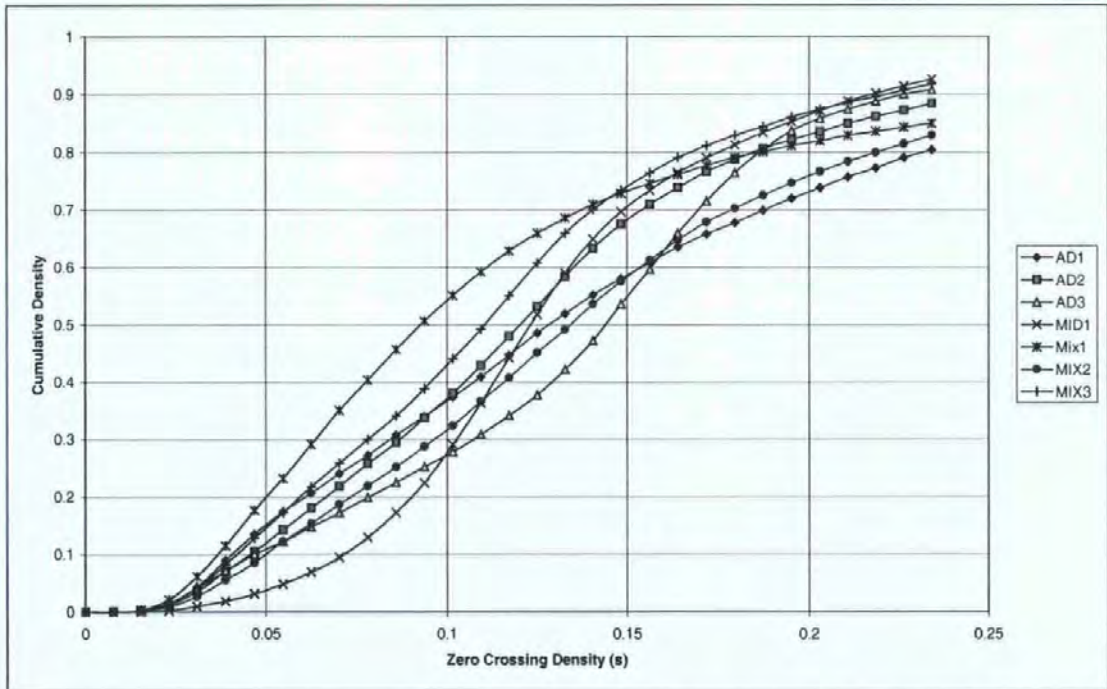
Figure 6-44, Zero crossing interval CDF from subjects with dementia.

Normal who went onto develop Alzheimer's Disease		
	VOL1	0.068
Normal		
	VOL2	0.056
	VOL3	0.058
	VOL4	0.061
	VOL5	0.045
	VOL6	0.052
	VOL7	0.061
	VOL8	0.048
Mean normal		0.055
Std Dev'n Normal		0.006
Limit to achieve 99.9% specificity		0.074
Probable Alzheimer's Disease		
	AD1	0.062
	AD2	0.067
	AD3	0.075
Mean		0.068
Standard Deviation		0.007
Sensitivity		16.0%
Multi-Infarct and Mixed Dementia		
	MID1	0.077
	Mix1	0.055
	MIX2	0.067
	MIX3	0.066
Mean		0.066
Standard Deviation		0.009
Sensitivity		17.5%

Table 6-6, Minimum 80% point of zero-crossing interval CDF over rear of scalp.

Normal who went onto develop Alzheimer's Disease		
	VOL1	0.064
Normal		
	VOL2	0.052
	VOL3	0.053
	VOL4	0.059
	VOL5	0.040
	VOL6	0.046
	VOL7	0.058
	VOL8	0.042
Mean normal		0.050
Std Dev'n Normal		0.007
Limit to achieve 99.9% specificity		0.073
Probable Alzheimer's Disease		
	AD1	0.051
	AD2	0.059
	AD3	0.069
Mean		0.060
Standard Deviation		0.009
Sensitivity		7.8%
Multi-Infarct and Mixed Dementia		
	MID1	0.072
	Mix1	0.048
	MIX2	0.059
	MIX3	0.057
Mean		0.059
Standard Deviation		0.010
Sensitivity		9.1%

Table 6-7, Minimum 75% point of zero-crossing interval CDF over rear of scalp.

Normal who went onto develop Alzheimer's Disease		
	VOL1	0.072
Normal		
	VOL2	0.061
	VOL3	0.065
	VOL4	0.064
	VOL5	0.051
	VOL6	0.059
	VOL7	0.064
	VOL8	0.059
Mean normal		0.060
Std Dev'n Normal		0.005
Limit to achieve 99.9% specificity		0.076
Probable Alzheimer's Disease		
	AD1	0.072
	AD2	0.074
	AD3	0.081
Mean		0.076
Standard Deviation		0.005
Sensitivity		50.8%
Multi-Infarct and Mixed Dementia		
	MID1	0.082
	Mix1	0.063
	MIX2	0.075
	MIX3	0.075
Mean		0.074
Standard Deviation		0.008
Sensitivity		39.8%

Table 6-8, Minimum 85% point of zero-crossing interval CDF over rear of scalp.

6.3.6   Mean Zero Crossing Interval

The next metric tried was the mean zero crossing interval. The overall PDF from which the mean interval is taken (for bipolar channels at the rear of the scalp) is shown in Figure 6-45 for normals and Figure 6-46 for subjects with dementia.
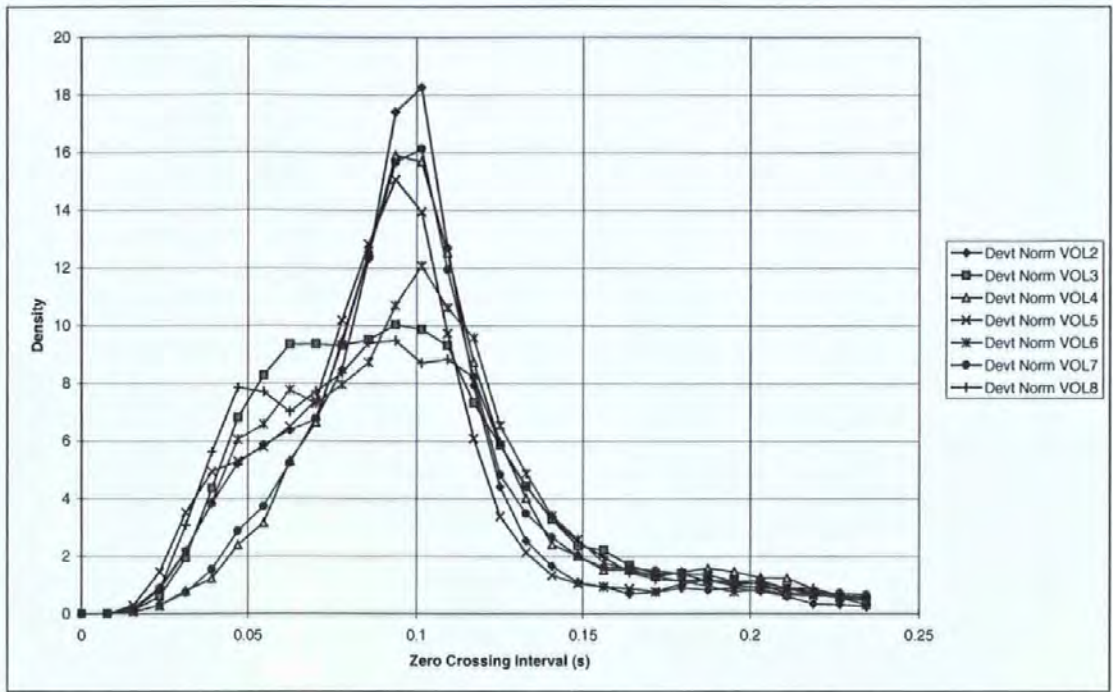
Figure 6-45, Combined zero-crossing PDF from selected channels for normal subjects.
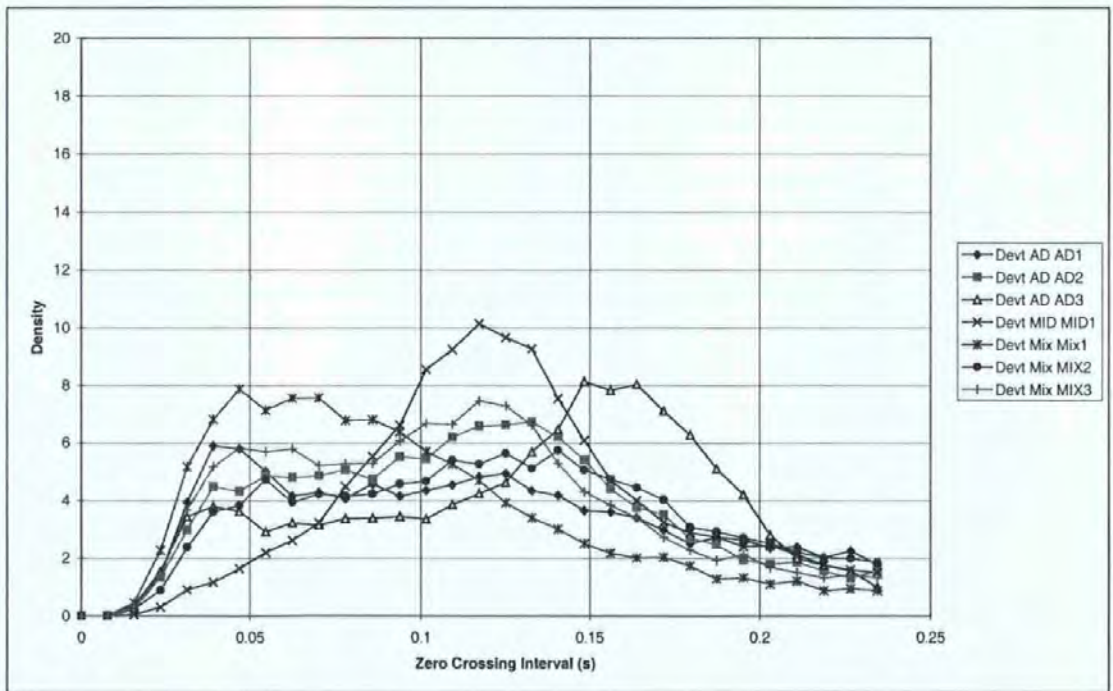
Figure 6-46, Combined zero-crossing PDF from selected channels for subjects with dementia.

The use of the average zero crossing gap was inspired from the mathematics below which attempted to isolate the important feature of the zero-set fractal dimension.

The mean zero crossing interval for the development data set is and the estimated sensitivities are given in Table 6-9.

Normal who went onto develop Alzheimer's Disease		
	VOL1	110
Normal		
	VOL2	95
	VOL3	97
	VOL4	105
	VOL5	93
	VOL6	99
	VOL7	104
	VOL8	96
Mean normal		98
Std Dev'n Normal		4.6
Limit to achieve 99.9% specificity		112
Probable Alzheimer's Disease		
	AD1	115
	AD2	116
	AD3	131
Mean		121
Standard Deviation		9.0
Sensitivity		82.2%
Multi-Infarct and Mixed Dementia		
	MID1	127
	Mix1	95
	Mix2	123
	Mix3	110
Mean		114
Standard Deviation		14.6
Sensitivity		53.4%

Table 6-9, Mean zero-crossing interval over rear of scalp (ms).

6.3.7 Correlation to Normal Zero Crossing Interval Distribution

6.3.7.1 Introduction and the Reference Normal PDF

As the features of the zero crossing interval PDF (Figure 6-45 and Figure 6-46) are complex and it appears that the important features are the position and shapes of peaks that are characteristic of a normal PDF, it was decided to estimate what is normal (with a tolerance) and then compare each signal to it. The mean and standard deviation of the PDF for the set of normals, at each interval was assessed and plotted. This is shown graphically in Figure 6-47, below.
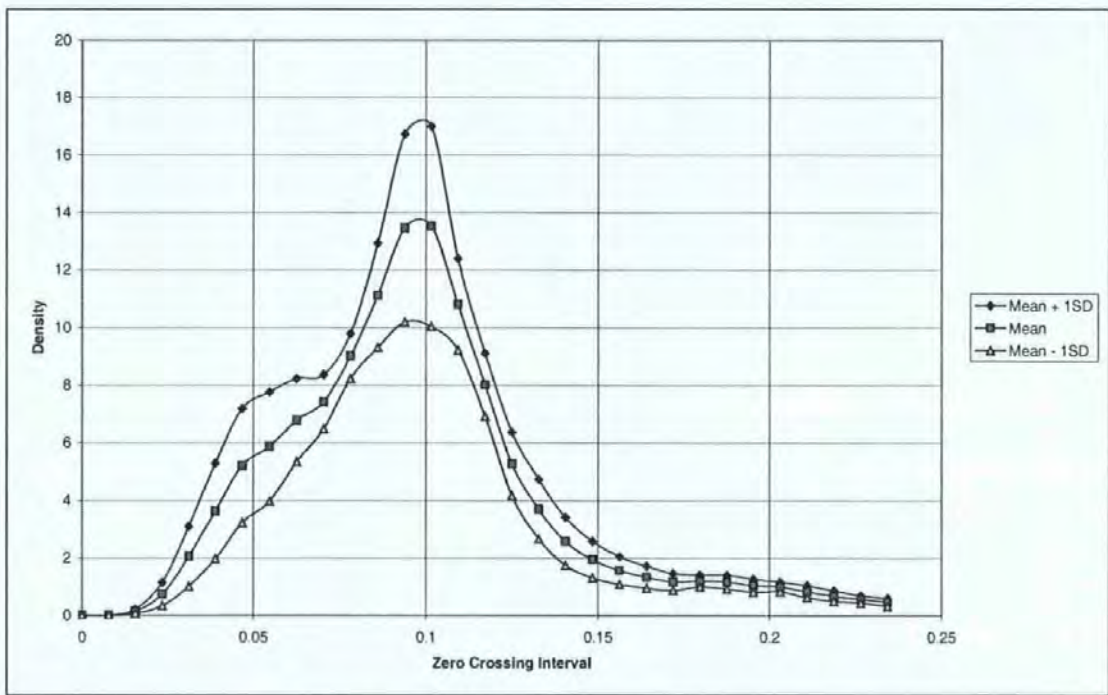
Figure 6-47, Reference zero-crossing PDF for normal subjects.

6.3.7.2 Results using the Development Data Set

Each record from the development data set was compared to this reference curve and the distance from it, at each point, was expressed in standard deviations. The rms of these standard deviations was taken as the error from the complete record. It is noted that other methods exist to compare distributions but these were not applied during this research.

177

Table 6-10, below, shows the results of this comparison and they are encouraging. However, their significance is compromised because they are self-referential. That is, it is not surprising that the normals used to create the standard curve are closest to it. For this reason it is important to repeat this test on the evaluation data, whilst using the standard normal curve from the development data as the reference. This runs contrary to the general rule of reserving the evaluation data set for testing the best of these novel methods and hence avoiding the charge of simply testing enough methods that one was bound to be successful eventually. However, in this instance it was felt that nothing else would provide a sensible measure of the methods' efficacy.

Normal who went onto develop Alzheimer's Disease		
	VOL1	2.4
Normal		
	VOL2	1.1
	VOL3	0.9
	VOL4	1.0
	VOL5	1.1
	VOL6	0.8
	VOL7	0.8
	VOL8	0.8
Mean normal		0.92
Std Dev'n Normal		0.14
Limit to achieve 99.9% specificity		1.36
Probable Alzheimer's Disease		
	AD1	5.2
	AD2	4.3
	AD3	9.2
Mean		6.23
Standard Deviation		2.64
Sensitivity		96.8%
Multi-Infarct and Mixed Dementia		
	MID1	5.1
	Mix1	2.2
	Mix2	5.7
	Mix3	3.5
Mean		4.13
Standard Deviation		1.60
Sensitivity		95.8%

Table 6-10, Difference from standard normal plot.

6.3.7.3   Results using the Evaluation Data Set

Each record from the evaluation data set was compared to the reference curve derived from the development data set and the distance from it, at each point, was expressed in standard deviations. The rms of these standard deviations was taken as the error from the complete record.

Table 6-11, below, shows the results of this comparison and they are contrasted with the results from the development data set in Table 6-12.

	Normal	Alzheimer's	Vascular
Results	1.5	4.4	3.4
	4.0	2.0	4.0
	3.9	3.1	5.1
	1.7	7.2	2.0
	1.3	3.2	2.8
	1.5	6.6	
	1.9	7.6	
	2.7	5.4	
	2.9	3.9	
	2.6	4.0	
	1.5	3.1	
	2.4	3.5	
	1.7	10.9	
	1.6	5.8	
	1.1	3.2	
	3.9	5.8	
	1.0	5.8	
	1.7		
	2.4		
	2.1		
	2.6		
	1.7		
	3.0		
	3.0		
Number of samples	24	17	5
Mean	2.25	5.03	3.44
SD	0.88	2.23	1.18

Table 6-11, Results from metric based on difference from average normal.

	Development data set	Evaluation data set
Average results from normal subjects	2.25	2.25
Standard deviation from normal subjects	0.14	0.88
Limit to achieve 99.9% specificity	1.36	4.98
Average result for Alzheimer's subjects	6.23	5.03
Standard deviation of Alzheimer's subjects	2.64	2.23
Estimated sensitivity to Alzheimer's disease	96.8%	51.0%
Average result for vascular dementia subjects	4.13	3.44
Standard deviation of vascular dementia subjects	1.60	1.18
Estimated sensitivity to vascular dementia	95.8%	9.6%

Table 6-12, Comparison of development and evaluation data results.

From these results, it may be seen that the sensitivities to Alzheimer's disease and (particularly) vascular dementia using the evaluation data (51% and 9.6% respectively) are significantly lower than similar results using the development data (96.8% and 95.8% respectively). This is because the difference of the evaluation data set normals to the development data set normals is large – but not as large as the difference to any of the groups of subjects with dementia. It is felt that this method is unlikely to provide a reliable, sensitive metric to detect dementia. However, it may be worth repeating this experiment in the future with a larger set of development and evaluation data taken with the same recording protocol.

6.3.8 Alpha / Theta Ratio from Zero Crossing Interval

The Alpha/Theta ratio derived from the fractal dimension measures gave some of the better results (see Sections 3.6 and 4.4.3). It was decided to create a similar metric based on the zero crossing interval PDF. The boundaries for each band of activity were chosen after numerical experimentation on the development data set and the boundaries that gave the best results are shown in Table 6-13, below. These experimentally derived boundaries are acceptable given the definitions in Section 2.2.4.

	T (s)	F (Hz)
Beta/Alpha boundary	0.055	18.3
Alpha/Theta boundary	0.125	8.0
Sub Theta boundary	0.234	4.3

Table 6-13, Band boundaries.

The metric used was the ratio of density in the Alpha range to the sum of the densities in the Alpha and Theta ranges. This metric seems (on the development data) capable of differentiating control subjects from subjects with dementia with a wide band between the two groups (see results below, Table 6-14). It should be remembered that the entire recording from each subject was used without any pre-selection of segments that we wish to analyse and that this method is relying on pushing the records from artefacts out of the ranges specified for Alpha and Theta. The estimated sensitivities to Alzheimer's disease and vascular dementia for a specificity of 99.9% are also given in Table 6-14.

Normal who went onto develop Alzheimer's Disease		
	VOL1	0.747
Normal		
	VOL2	0.883
	VOL3	0.780
	VOL4	0.811
	VOL5	0.859
	VOL6	0.790
	VOL7	0.814
	VOL8	0.770
Mean normal		0.815
Std Dev'n Normal		0.042
Limit to achieve 99.9% specificity		0.686
Probable Alzheimer's Disease		
	AD1	0.494
	AD2	0.525
	AD3	0.325
Mean		0.448
Standard Deviation		0.108
Sensitivity		98.7%
Multi-Infarct and Mixed Dementia		
	MID1	0.535
	Mix1	0.691
	Mix2	0.465
	Mix3	0.584
Mean		0.569
Standard Deviation		0.095
Sensitivity		89.2%

Table 6-14, Alpha/theta ratio based on zero crossing interval.

6.3.9 Zero Crossing Interval Sequence

To complete the investigation of the zero crossing interval distribution, it was decided to study the sequence in which the intervals occurred. This would determine, for example, if alpha waves occur in bursts and whether such information could be used as the basis for a metric to detect dementia. Note this method has similarities to the Markov Chain theory, which is exploited in genetics, etc.

To illustrate the method used for this study, consider the typical normal subject Vol2. The two dimensional probability density function (Figure 6-48) was plotted to show the likelihood of a pair of zero-crossing intervals adjacent to one another. The vertical axis in Figure 6-48 is the probability and the two horizontal axes are the first interval and the second interval. From the illustration, it seems (visually) that there is some structure and that an interval typical of an alpha wave (10Hz-12Hz) is more likely to be followed by a similar interval than would be expected from random variation alone. To test this we constructed the two dimensional PDF which would be expected if the sequence were random and taken from the 1D PDF of zero-crossing intervals (Figure 6-49). This 'expected' distribution is shown in Figure 6-50 and the difference between this expected distribution and the actual distribution is shown in Figure 6-51. This difference from what would be expected by a random sequence and the actual sequence has a distinct structure and it confirms that alpha waves occur in bursts. That is an alpha wave is more likely to be followed by another alpha wave than it would be if the sequence of intervals were random.
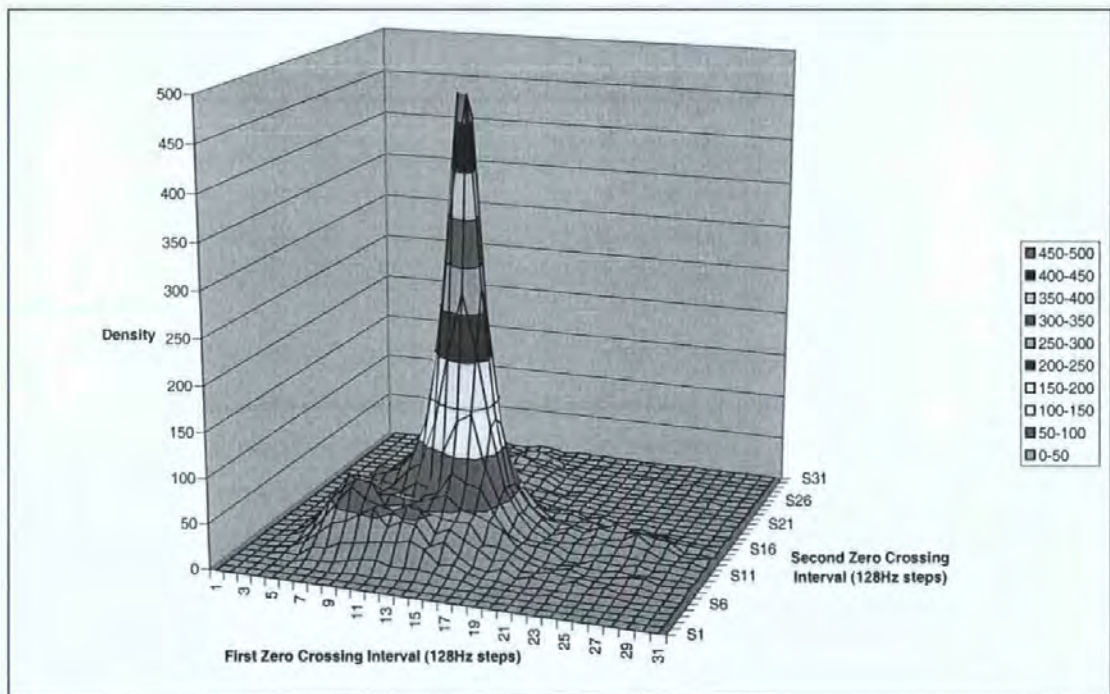
Figure 6-48, Zero-crossing interval sequence for Vol2 (actual).
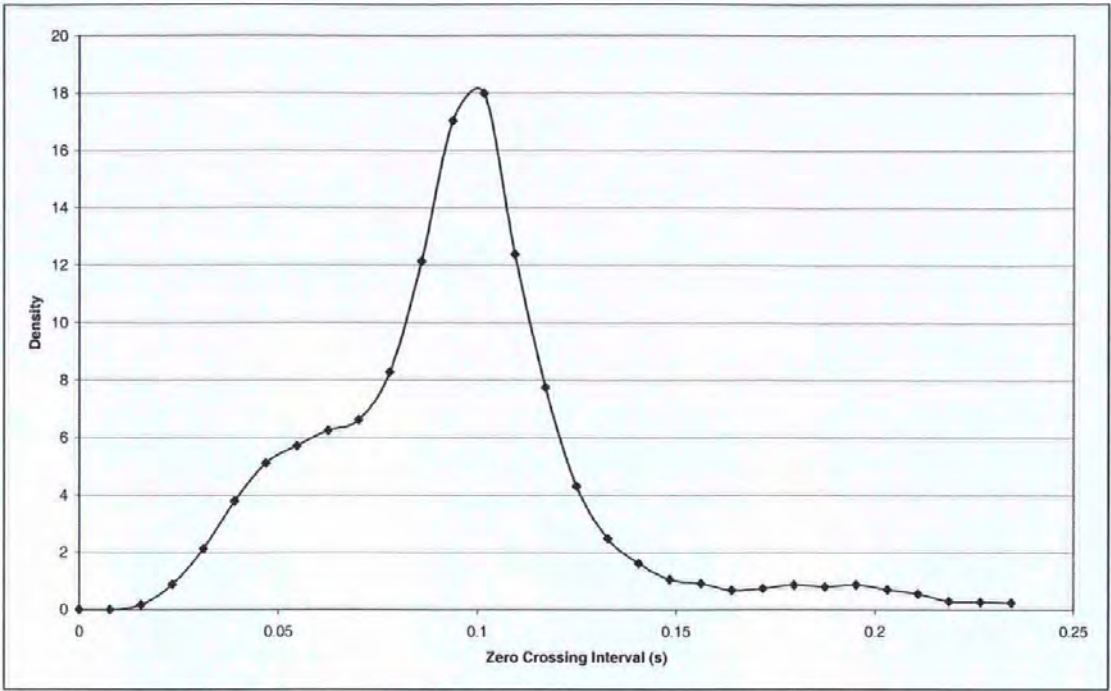
Figure 6-49, Zero-crossing interval sequence for Vol2 (1D).
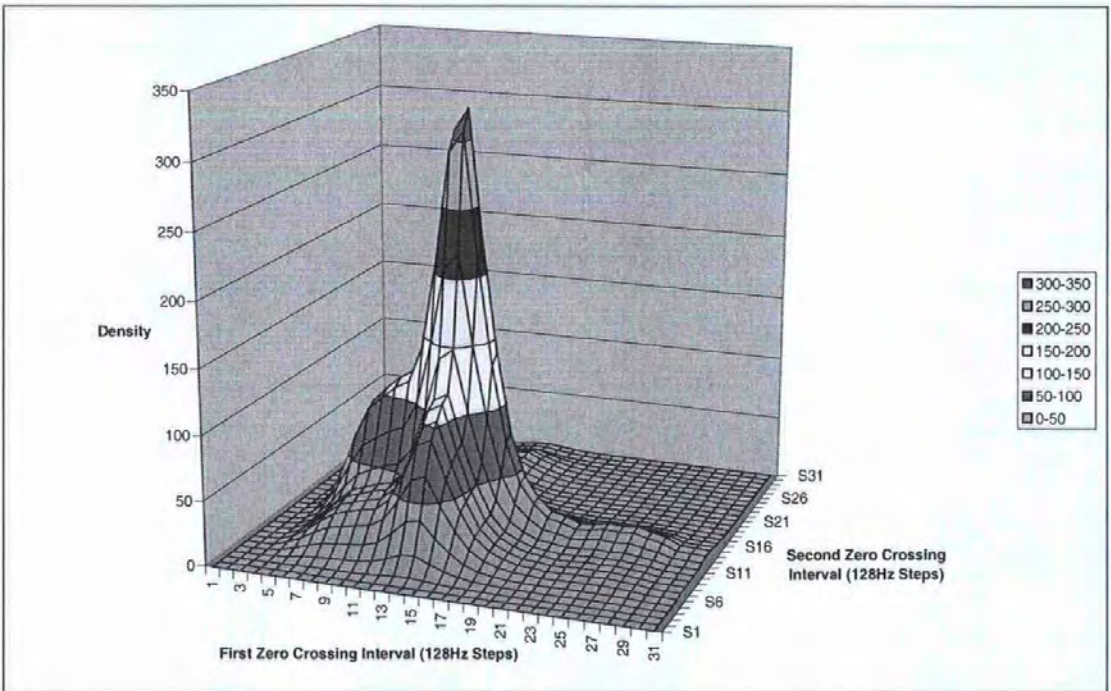
Figure 6-50, Zero-crossing interval sequence for Vol2 (expected).
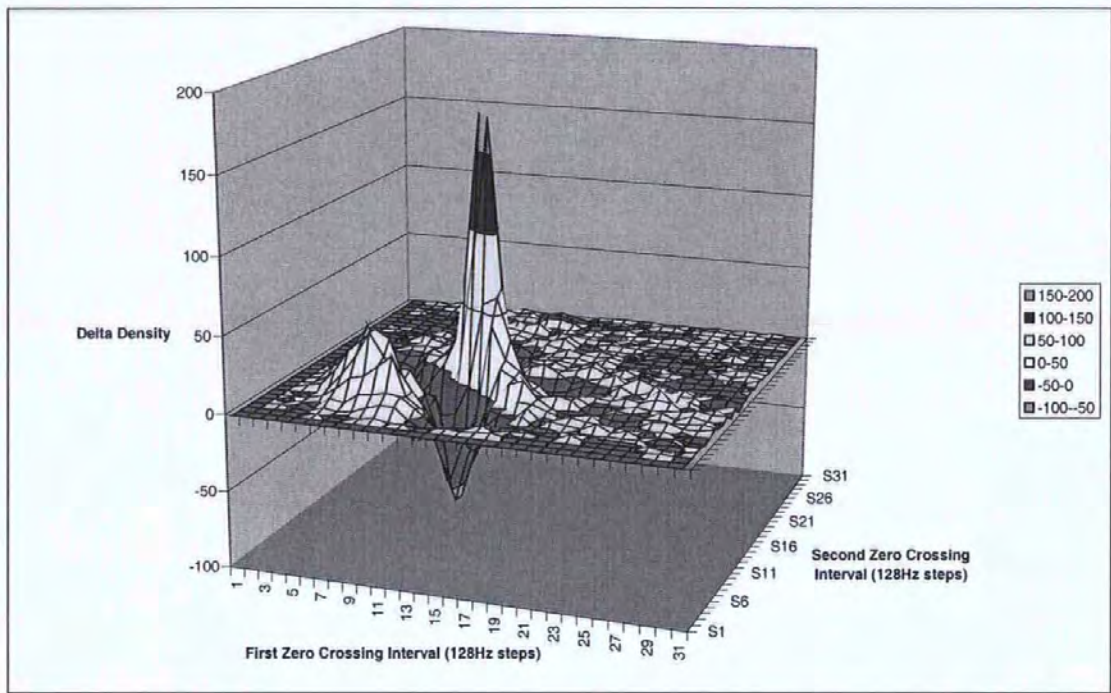
Figure 6-51, Zero-crossing interval sequence for Vol2 (difference).

A similar set of graphs has been produced for each of the subjects in the development data set. Each of the Figures below (Figure 6-52 to Figure 6-66) show the 1D PDF in the top left, the expected 2D PDF in the top right, the actual 2D PDF in the bottom left and finally the difference (actual minus expected) in the bottom right.
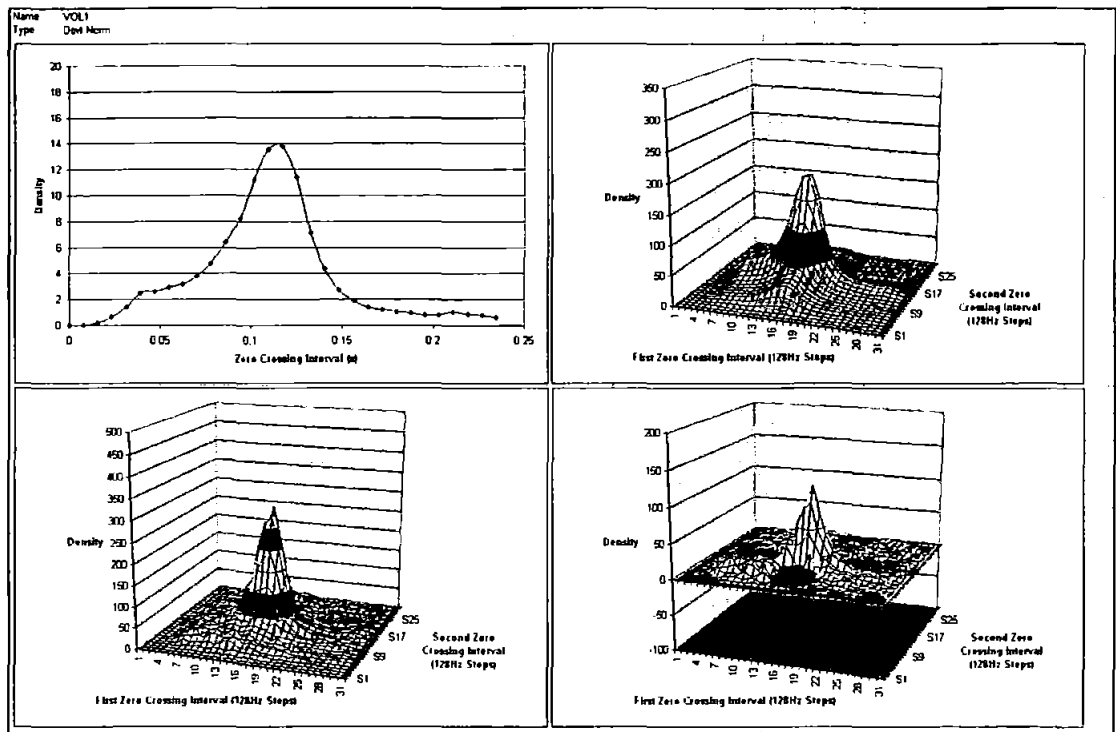
Figure 6-52, Zero-crossing interval sequence for Vol1.
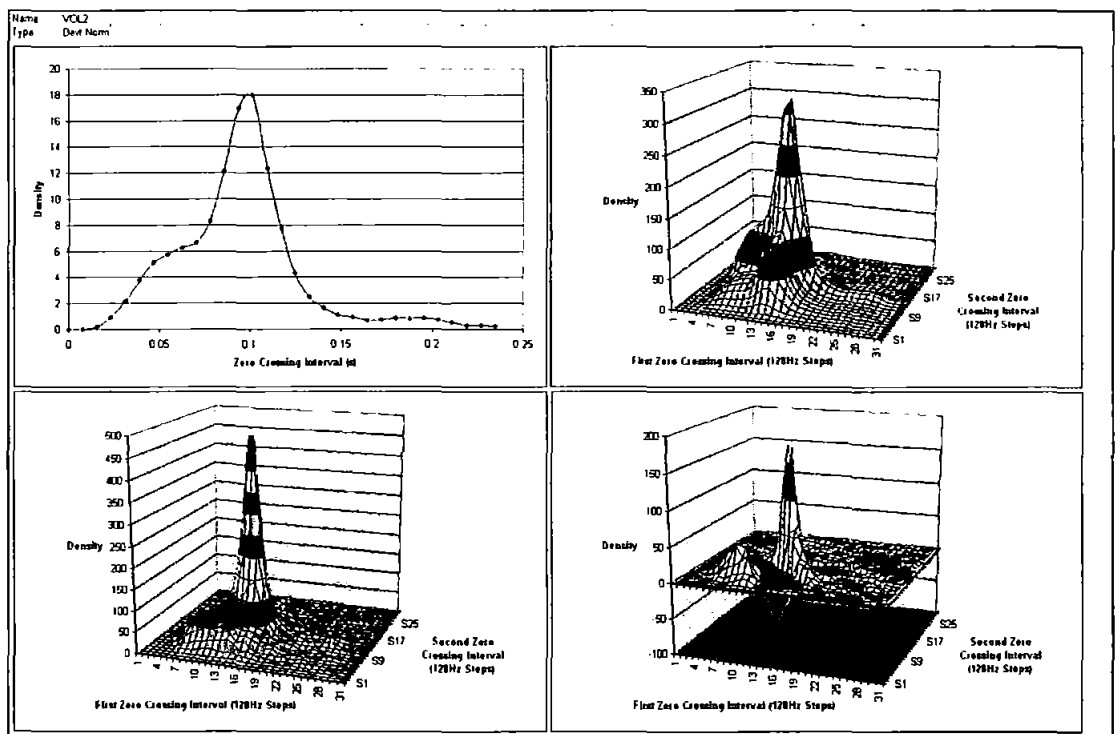
Figure 6-53, Zero-crossing interval sequence for Vol2.
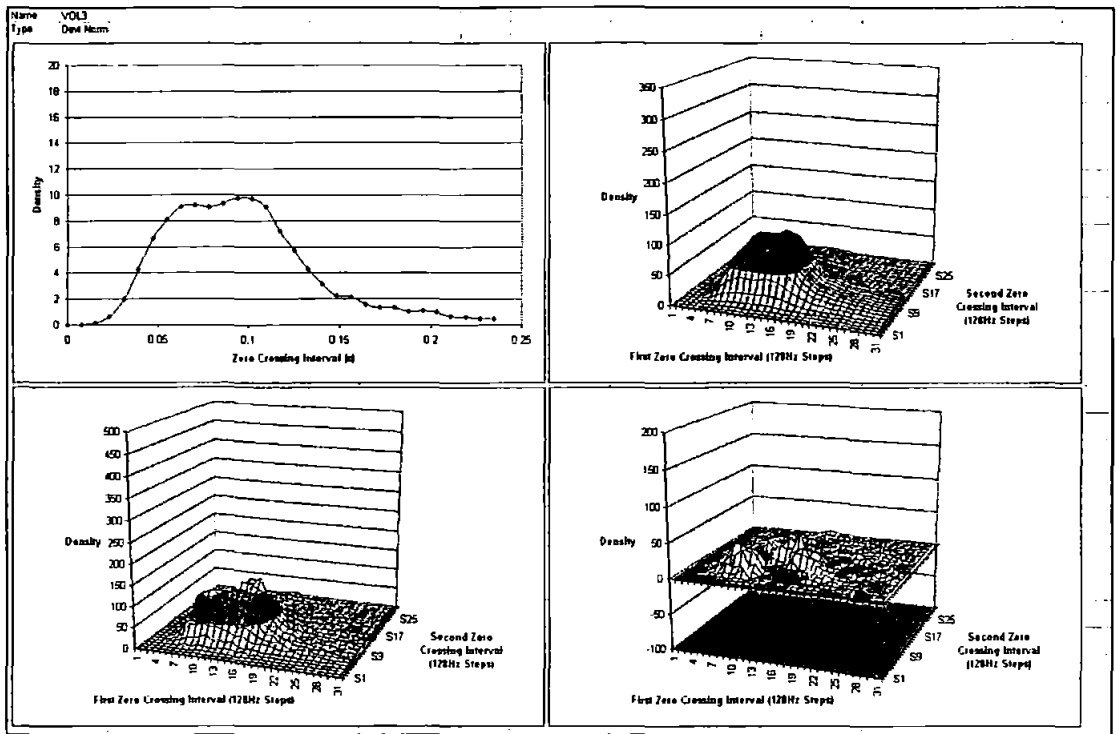
Figure 6-54, Zero-crossing interval sequence for Vol3.
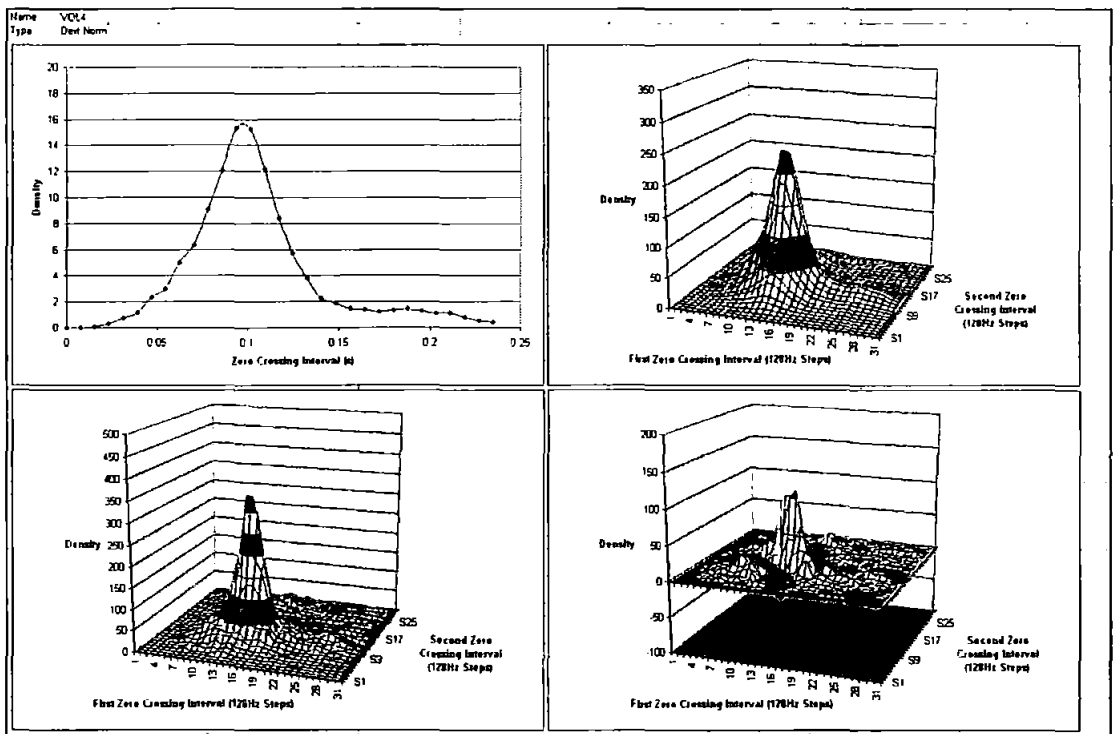
Figure 6-55, Zero-crossing interval sequence for Vol4.
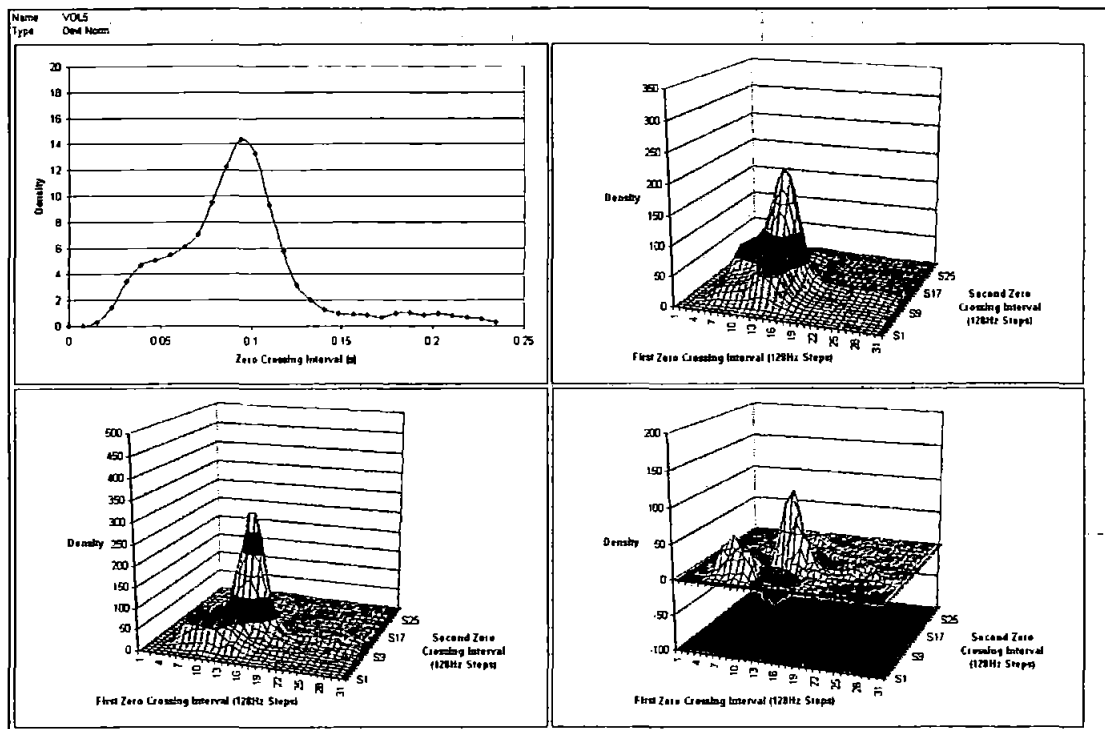
Figure 6-56, Zero-crossing interval sequence for Vol5.
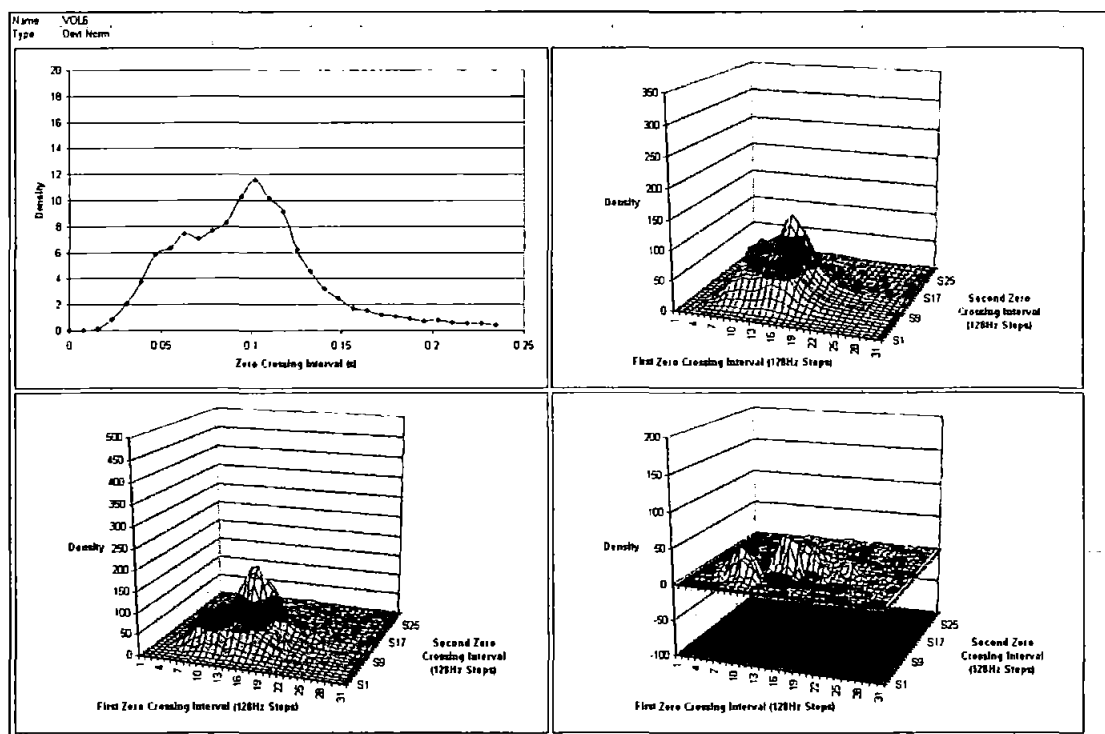
Figure 6-57, Zero-crossing interval sequence for Vol6.
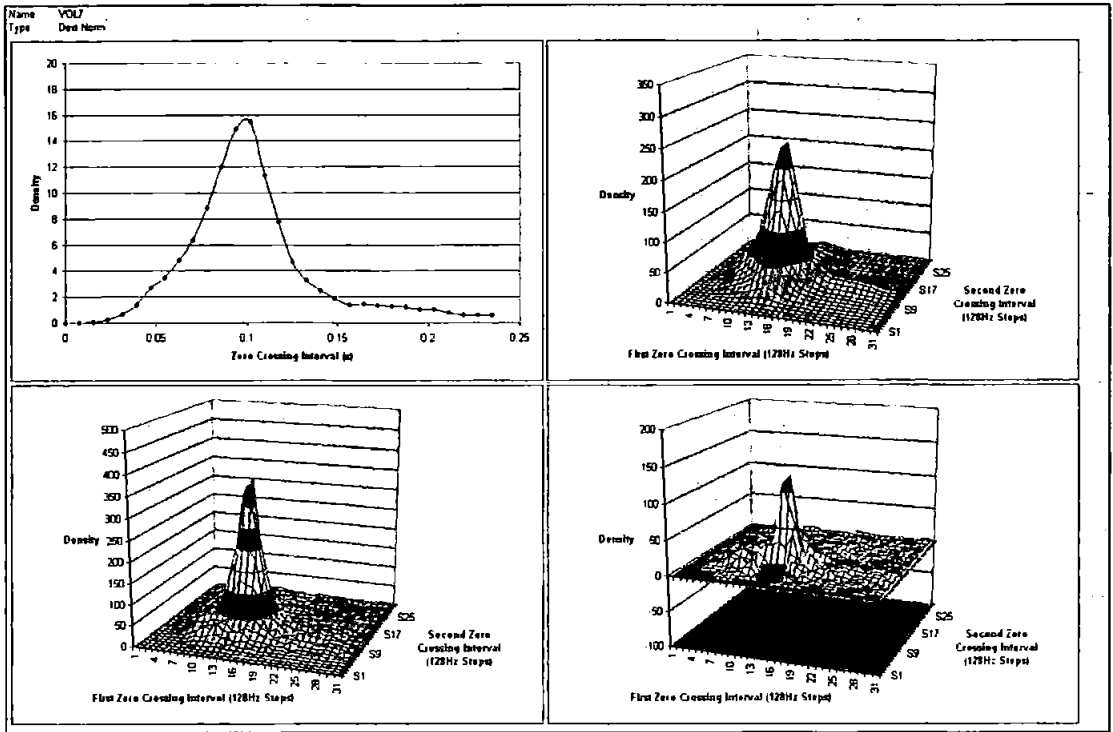
Figure 6-58, Zero-crossing interval sequence for Vol7.
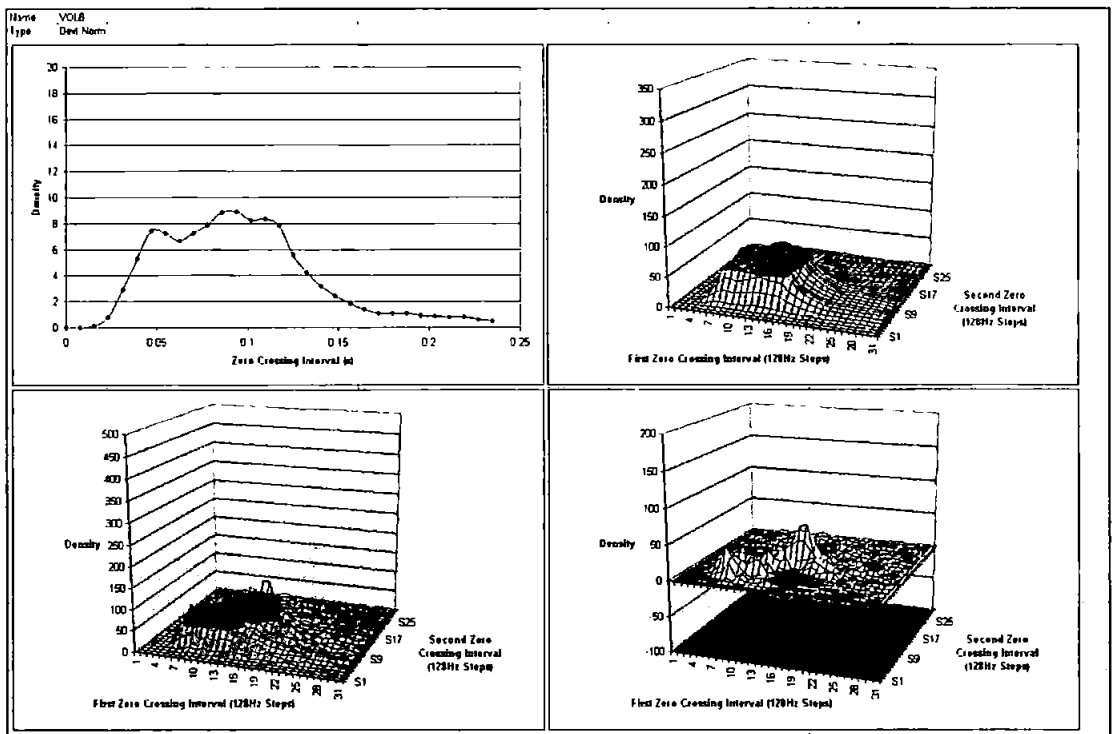
Figure 6-59, Zero-crossing interval sequence for Vol8.
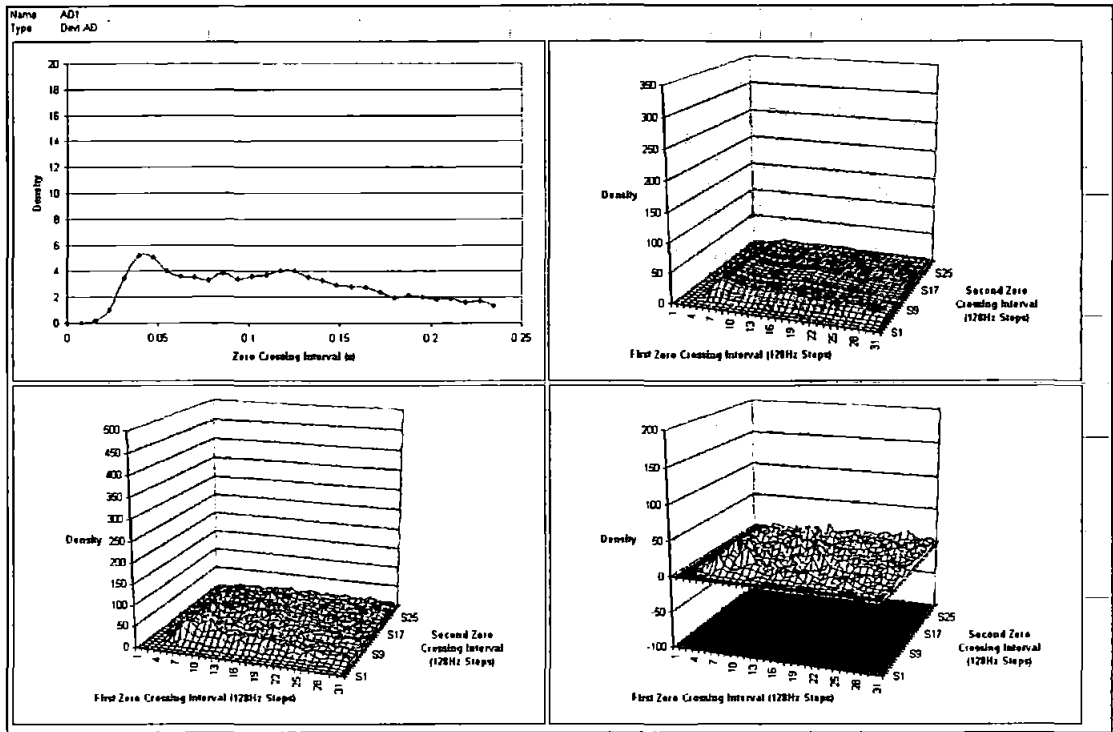
Figure 6-60, Zero-crossing interval sequence for AD1.
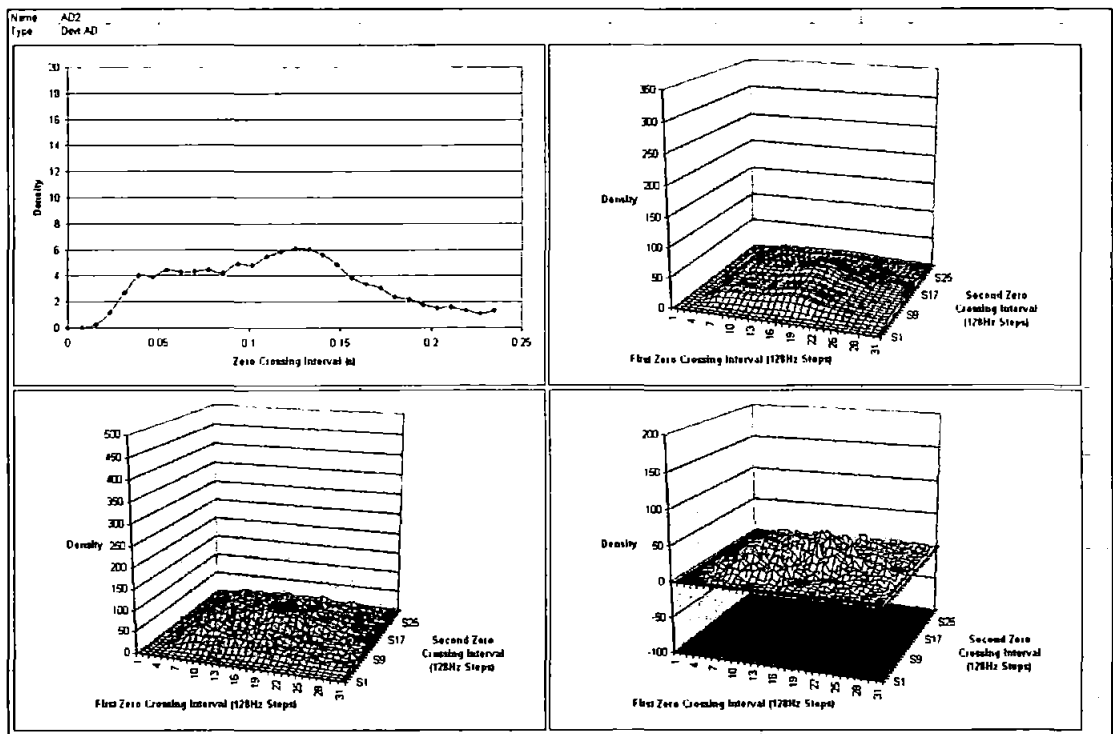
Figure 6-61, Zero-crossing interval sequence for AD2.
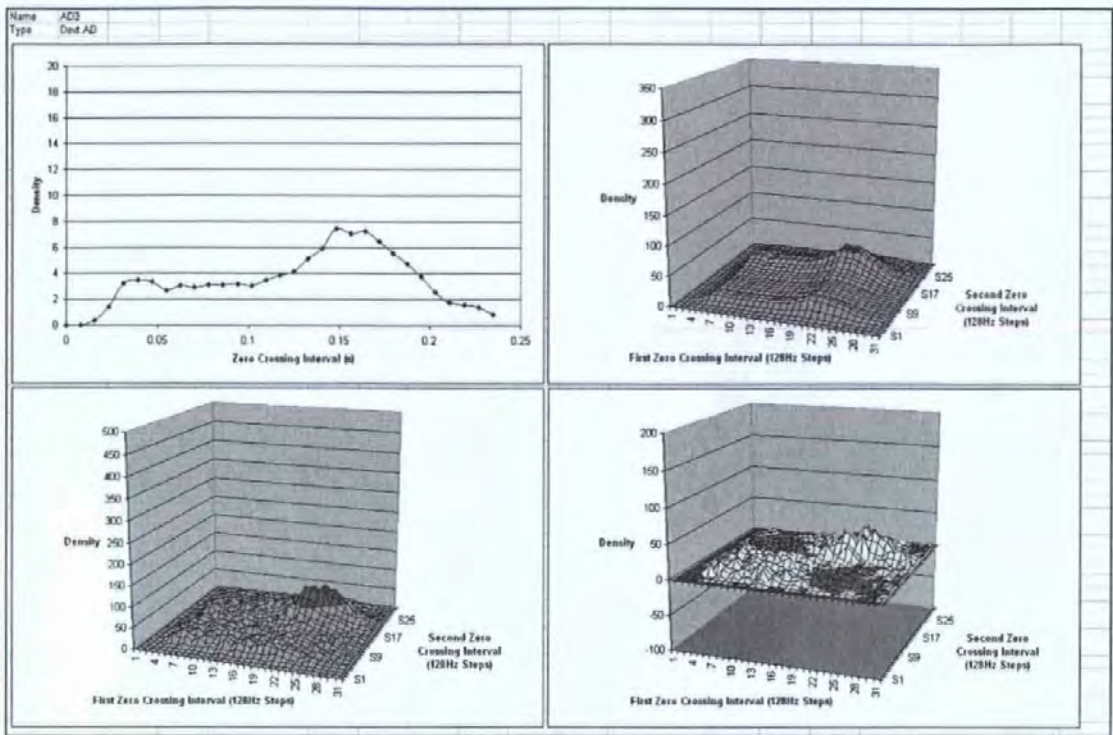
Figure 6-62, Zero-crossing interval sequence for AD3.
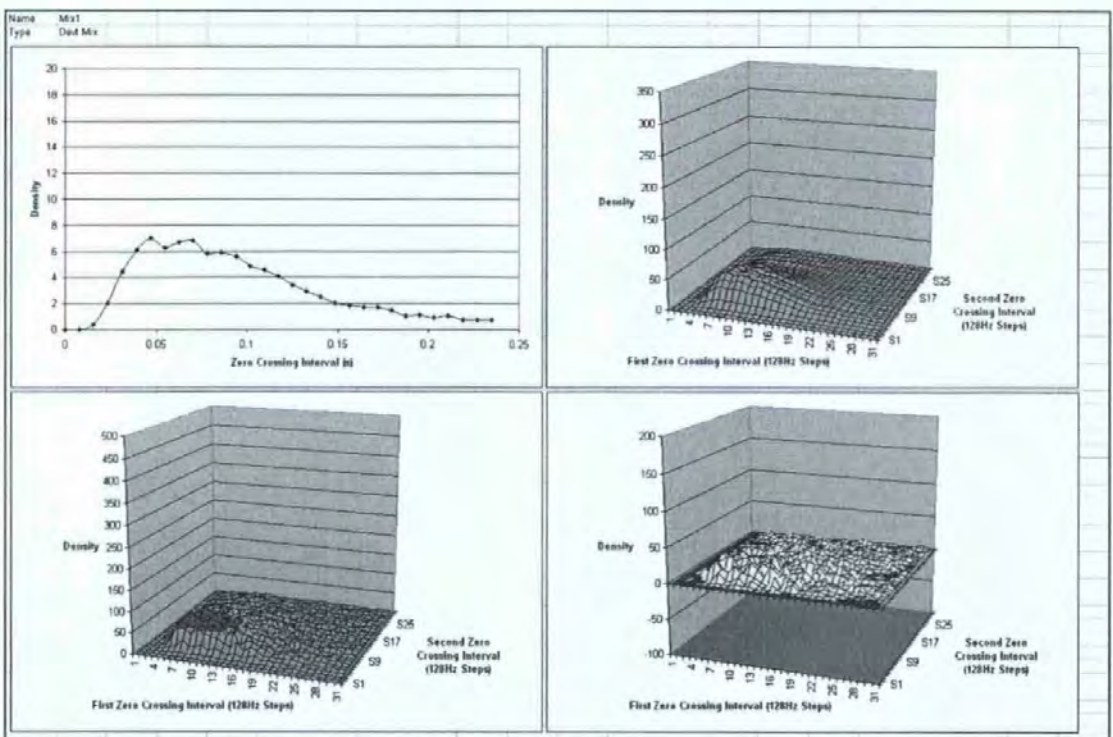
Figure 6-63, Zero-crossing interval sequence for Mix1.

191
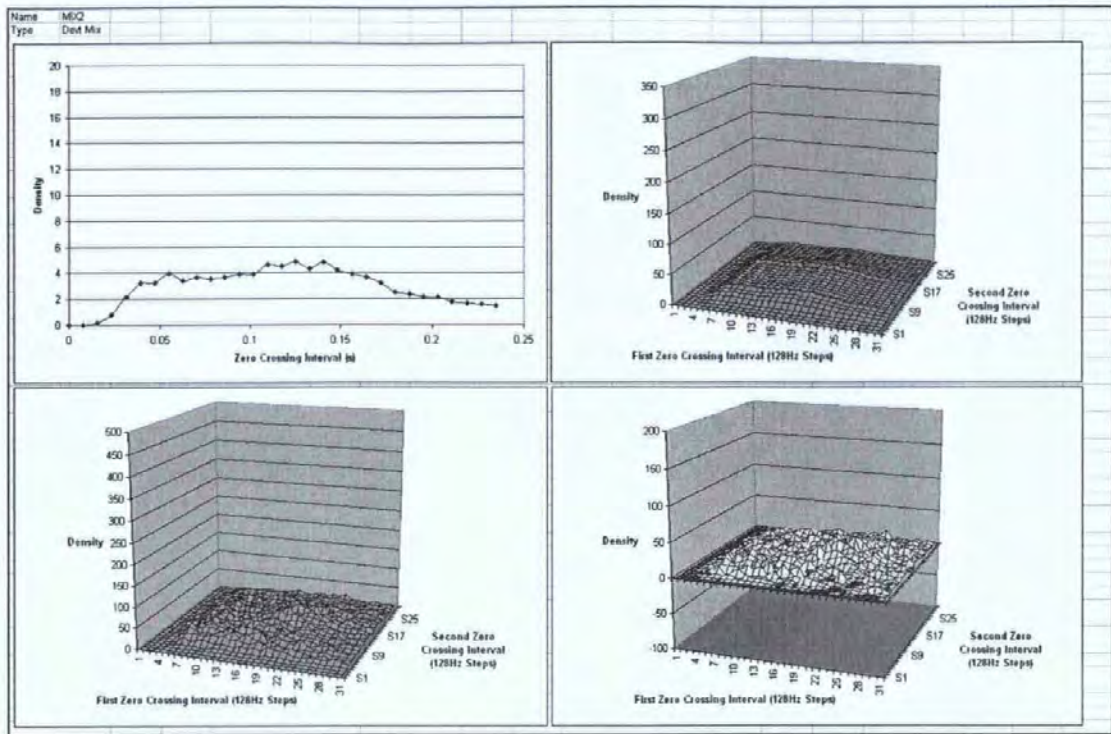
Figure 6-64, Zero-crossing interval sequence for Mix2.
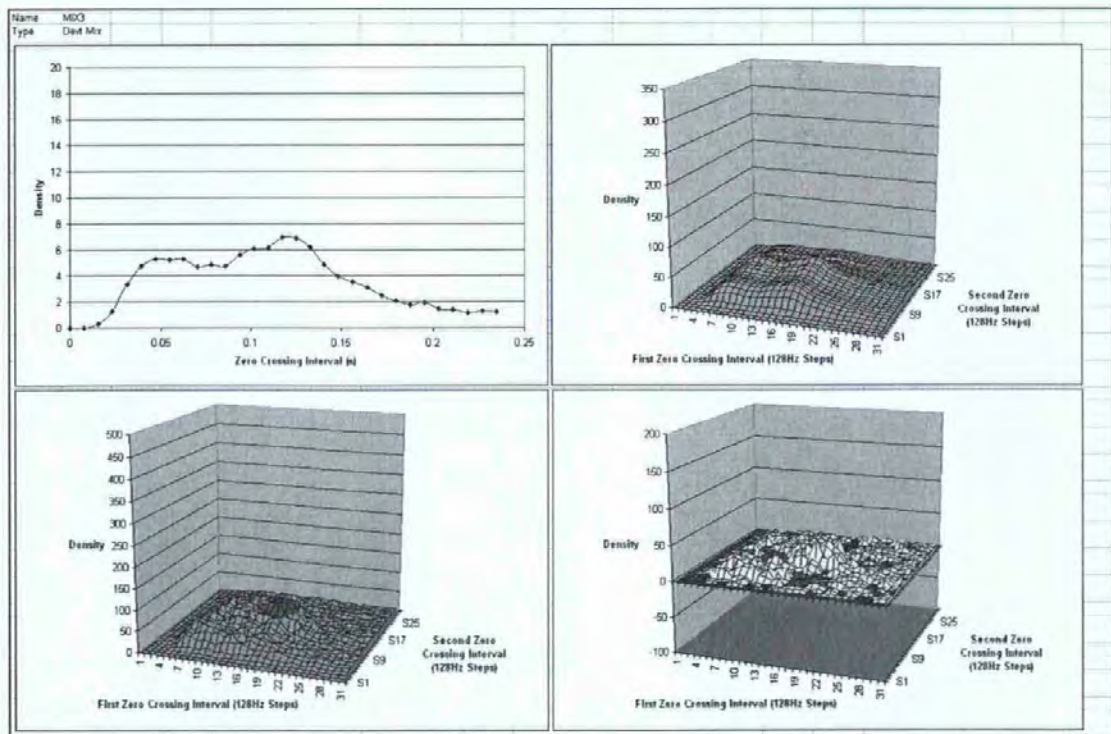
Figure 6-65, Zero-crossing interval sequence for Mix3.
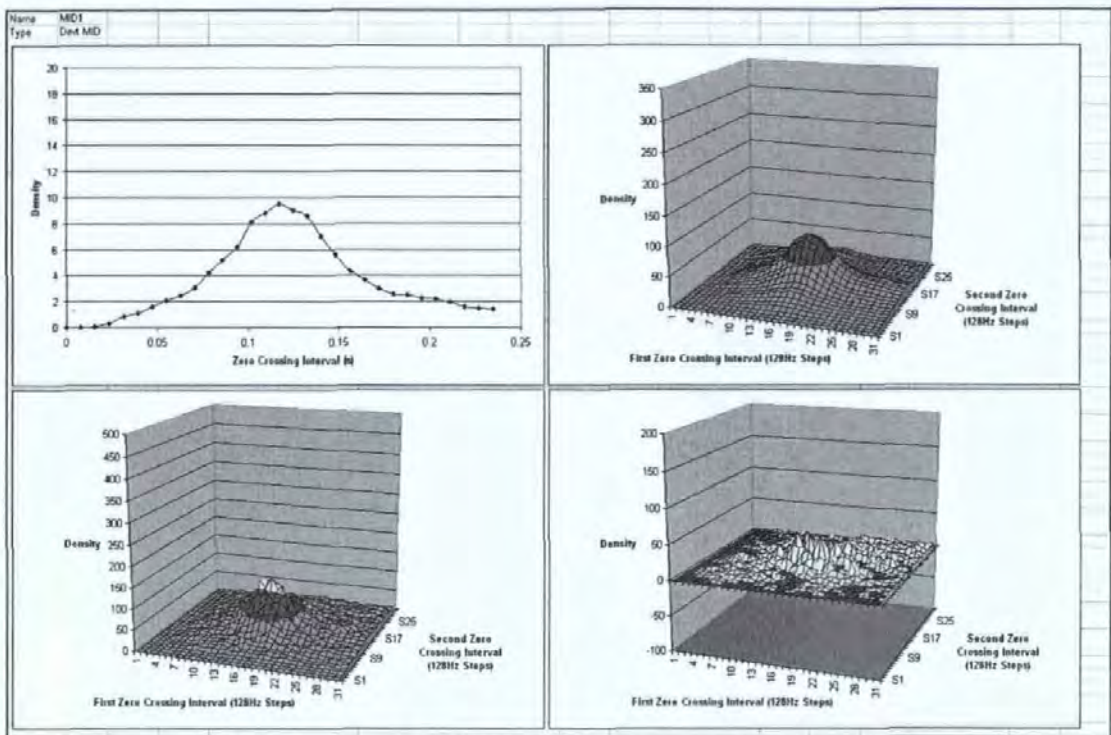
Figure 6-66, Zero-crossing interval sequence for MID1.

From these figures it is possible to conclude that most of the normal subjects show evidence of alpha waves occurring in burst (to a lesser or greater extent), whereas, none of the subjects with dementia shows evidence of alpha waves occurring in bursts. Although this is an interesting way of identifying coherent bursts of alpha waves it was not possible (despite significant work) to convert this into a meaningful metric that could provide differentiation between subjects with dementia and normal subjects.

6.3.10 Testing on the Evaluation Data Set

All of the prospective methods based on the zero crossing interval were compared (Table 6-15) to see which should be tested on the evaluation data set. It should be remembered that these results are from experiments using parameterisation honed to the same development data set. Hence, the need to use independent data (the evaluation data set).

Method	Estimated sensitivity to Alzheimer's	Estimated sensitivity to vascular dementia
80% Cumulative density position	16.0%	17.5%
75% Cumulative density position	7.8%	9.1%
85% Cumulative density position	50.8%	39.8%
Mean zero crossing interval	82.2%	53.4%
Difference from reference normal curve	96.8%	95.8%
Repeat of difference from reference normal curve using evaluation data	51.0%	9.6%
Alpha/Theta ratio based on zero crossing interval	98.7%	89.2%

Table 6-15, Estimated sensitivities for zero crossing interval methods.

The Alpha/Theta ratio metric based on the zero-crossing interval was chosen to test as it showed the most promise. The results of this method applied to the evaluation data set are shown in Table 6-16 and an illustration of the distribution of results is given in Figure 6-67.
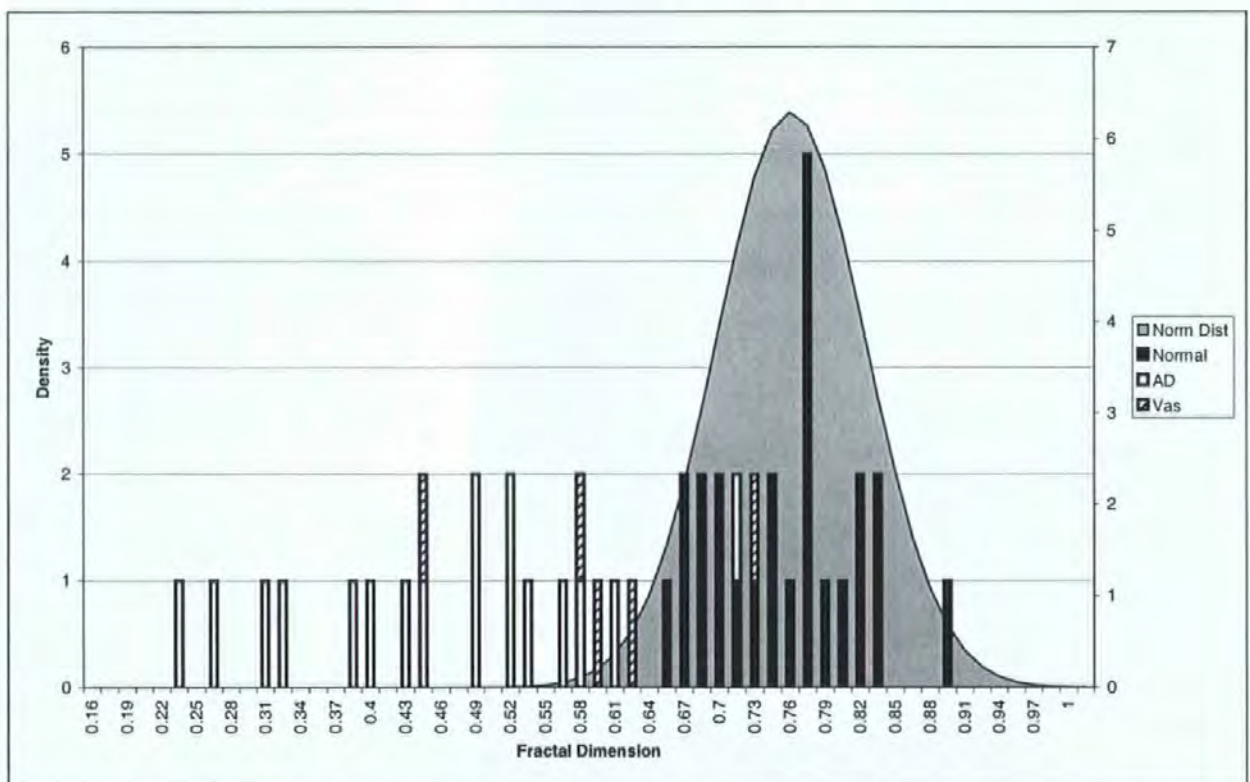
Figure 6-67, Distribution of results from zero crossing interval derived Alpha/Theta ratio.

	Normal	Alzheimer's	Vascular
Results	0.734	0.490	0.608
	0.788	0.727	0.634
	0.716	0.530	0.455
	0.849	0.316	0.742
	0.784	0.531	0.584
	0.796	0.395	
	0.708	0.331	
	0.751	0.440	
	0.710	0.537	
	0.688	0.496	
	0.754	0.621	
	0.658	0.580	
	0.760	0.243	
	0.839	0.269	
	0.810	0.565	
	0.775	0.404	
	0.828	0.445	
	0.779		
	0.690		
	0.825		
	0.672		
	0.783		
	0.672		
	0.900		
Number of samples	24	17	5
Mean	0.761	0.466	0.604
SD	0.063	0.130	0.103

Table 6-16, Results from Alpha/Theta metric based on zero crossing interval.

These results show that, if one were to demand a specificity of 99.9%, then a result would be considered abnormal if it were less than 0.565. This gives an estimated sensitivity to Alzheimer's disease of 77.8% and an estimated sensitivity to vascular (or mixed) dementia of 35.2%.

6.3.11 Comparison to Alpha / Theta Derived from PSD

Having produced an Alpha/Theta ratio metric based on the zero-crossing interval it was important to produce a similar method based on the power spectral density and determine whether similar results could have been produced this way.

For this method, the combined power spectral density was taken from the same electrode pairs (bipolar) as had been used for the preceding methods. The boundaries for each band of activity were chosen after numerical experimentation on the development data set and the boundaries that gave the best results are shown in Table 6-17, below. These experimentally derived boundaries are acceptable given the definitions in Section 2.2.4 and are very similar to the boundaries previously used for the Alpha/Theta ratio based on the zero-crossing interval (Table 6-13).

	F (Hz)
Beta/Alpha boundary	18.0
Alpha/Theta boundary	8.0
Sub Theta boundary	4.0

Table 6-17, Band boundaries.

As before, the metric used was the ratio of density in the Alpha range to the sum of the densities in the Alpha and Theta ranges. The results from the development data set are shown in Table 6-18.

Normal who went onto develop Alzheimer's Disease		
	VOL1	0.635
Normal		
	VOL2	0.767
	VOL3	0.718
	VOL4	0.731
	VOL5	0.791
	VOL6	0.711
	VOL7	0.746
	VOL8	0.714
Mean normal		0.740
Std Dev'n Normal		0.030
Limit to achieve 99.9% specificity		0.646
Probable Alzheimer's Disease		
	AD1	0565
	AD2	0.468
	AD3	0.569
Mean		0.534
Standard Deviation		0.057
Sensitivity		97.5%
Multi-Infarct and Mixed Dementia		
	MID1	0.510
	Mix1	0.669
	Mix2	0.517
	Mix3	0.598
Mean		0.573
Standard Deviation		0.075
Sensitivity		83.2%

Table 6-18, Alpha/theta ratio based on PSD.

The results from applying this method to the evaluation are shown in Table 6-19.

	Normal	Alzheimer's	Vascular
Results	0.672	0.533	0.562
	0.718	0.673	0.565
	0.615	0.559	0.699
	0.773	0.403	0.589
	0.721	0.482	0.604
	0.722	0.472	
	0.660	0.541	
	0.650	0.512	
	0.730	0.589	
	0.635	0.437	
	0.642	0.649	
	0.799	0.598	
	0.741	0.504	
	0.774	0.518	
	0.769	0.544	
	0.665	0.406	
	0.754	0.477	
	0.793		
	0.636		
	0.627		
	0.721		
	0.816		
	0.754		
	0.693		
Number of samples	24	17	5
Mean	0.712	0.523	0.604
SD	0.061	0.076	0.065

Table 6-19, Alpha/Theta metric based on power spectral density.

These results show that, if one were to demand a specificity of 99.9%, then a result would be considered abnormal if it were less than 0.524. This gives an estimated sensitivity to Alzheimer's disease of 50.3% (c.f. 77.8% for alpha/theta ration based on zeros crossing interval) and an estimated sensitivity to vascular (or mixed) dementia of 10.7% (c.f. 35.2% for alpha/theta ration based on zeros crossing interval). Hence, an Alpha/Theta ratio generated from the zero crossing intervals has better performance than the same generated from the power spectral density.

6.3.12 Revisiting Subject Specificity

Given that the best method discovered is the Alpha/Theta ratio based on zero crossing interval distribution, it was decided to check whether the subject specific concept would help with this method. This follows from the discussion of subject specific measures and how they may help in the early detection of dementia (see section 3.5).

Record	ADAPTED BOX
X1	0.814
X2	0.840
X3	0.856
Y1	0.551
Y2	0.581
Y3	0.513
V1	0.553
V2	0.563
W1	0.716
W2	0.788

Table 6-20, Alpha/Theta ratio of Zero Crossing Interval applied to subject specific data.

If one considers the variation from sample to sample from the same subject to be equivalent to measurement noise (or short term variability) on the fractal dimension then one may estimate the population standard deviation for a single subject for each measure: 0.043.

Taking the statistics for the evaluation normals (Mean = 0.761, SD = 0.063) it may be seen that the standard deviation among the group of normals is, as expected, larger than the variation for a single subject (0.043).

The graph below summarises the subject specific results that were obtained using the new metric.
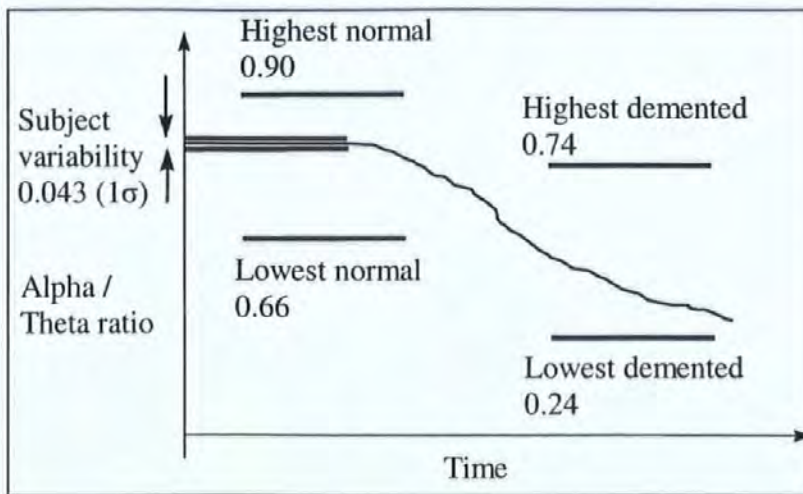
Figure 6-68, Updated subject specific results (illustration).

The graph shows that this method benefits from the use of subject specific interpretation.

6.3.13 Evaluating the Significance of this Novel Method

The Alpha/Theta ratio based on the zero crossing interval distribution is a promising, novel method. It has been shown (on an independent data set) that, if one were to demand a specificity of 99.9%, the estimated sensitivities to early Alzheimer's disease and vascular dementia are 77.8% and 35.2% respectively.

By comparison, the sensitivities, under similar conditions, with the same data and using the best fractal method tested, to early Alzheimer's disease and vascular dementia are 67.0% and 16.9% respectively. In addition, under similar conditions, with the same data and using a standard method (Alpha/Theta ratio based on the power spectral density), the sensitivities to early Alzheimer's disease and vascular dementia are 50.3% and 10.7% respectively.

Therefore, the best novel method (Alpha/Theta ratio based on the zero crossing interval distribution) is better at detecting dementia than either fractal measures or a typical standard method. It should also be remembered that the application of subject specific methodology would improve these results still further.

It is interesting to consider whether this, the best method achieved in this research, is good enough to be of used in clinical practice. Before we consider this question though, we should recall that the data used to test the method was realistic, and independent of the method development:

- The trial data set encompassed various states: awake, drowsy and alert, with periods of eyes closed and open.

- The classification of the records between normal and Alzheimer's disease was taken from the written hospital diagnosis sheets.

- The probable Alzheimer's and vascular subjects were not previously diagnosed and were therefore in the early stages of exhibiting symptoms; in fact some of these subjects were not referred for dementia diagnosis but came in for investigation of seizures et cetera.

- For all records, to avoid the possibility of inadvertently or unconsciously selecting data particularly suitable for analysis a predetermined protocol was applied. Data from 60s to 300s from each record was used. This avoids electrical artefacts, which commonly occur at the beginning of a record, and gives a standard 4 minutes of data to analyse. This segment of data including artefacts was analysed with no á priori selection of elements 'suitable for analysis'. This approach leads to a prediction of the usefulness of the technique, as it would most conveniently be used in practice.

The benefits of introducing this method (subject to a larger scale trial) would be:

- One third of vascular dementia sufferers could be detected earlier and offered the benefit of existing drugs and therapies to extend the symptom free state. Cost of care would also be delayed or reduced.

- Three-quarters of early Alzheimer's disease sufferers could be detected earlier and offered the benefit of new drugs to slow the progression of their disease and extend the symptom free state. Cost of care would also be delayed or reduced.

201

The costs of introducing the method would be mainly felt be GPs who would have to be convinced of the value of the new method. The costs would be:

- The cost of the computer systems deployed in GPs surgeries (PC, software, interface box and electrodes)

- Training for the GPs and some extra time with each patient

- 1 in 1000 normal subjects will be troubled with an unnecessary visit to a hospital Neurophysiology department.

It is not possible to directly equate financial cost and medical resources to relieving patient suffering. However, there is a point at which a technique/therapy/practice becomes viable. I believe, subject to a larger scale trial, that this method provides benefits that outweigh the cost.

6.4 Summary

The surrogate data testing in the preceding chapter showed that all of the information, which was able to give the (partial) success with fractal dimension measures, was contained within the power spectral density. However, it was also known from the background research that, despite significant effort over a long period; no spectral based measure had been good enough to use in general clinical practice. Thus, it was decided to take a different approach and propose methods that were determined by the power spectral density but were in the time domain. These novel methods were the Allan Variance (which shares features with the adapted box dimension) and the zero-crossing interval distribution (which shares features with the zero-set dimension). This search for novel methods was conducted using just the development data set so that the evaluation data set could be kept in reserve to test any proposed methods.

Allan variance is a time-domain analysis technique originally developed to study the frequency stability of oscillators and it can be used to determine the character of the underlying processes that can give rise to data features. After some study of the Allan Variance of the EEG for normal subjects to subjects with dementia, a metric derived from the Allan Variance was proposed. This metric tested on the evaluation data set, the results were very disappointing and the Allan variance metrics were discarded. However, it remains true that the Allan variance may provide a new and interesting method to visualise the spectral content of the EEG.

A novel method that shared some features with the zero-set dimension was proposed. This was the zero-crossing interval distribution (or probability density function). Initially, the research concentrated on the strict zero crossing interval distribution but this was superseded by using the interval between double zero crossings (that is, the interval between a positive to negative transition to the next positive to negative transition). After some mathematical investigation of this concept several metrics were tested on the development data set; the 75%, 80% and 85% points of the cumulative density function, the mean zero crossing interval, the correlation of the zero crossing interval probability function to the mean zero crossing interval probability function for normal subjects, the Alpha/Theta ratio derived from the zero crossing interval PDF and the zero crossing interval sequence.

The best results were obtained with the Alpha/Theta ratio derived from the zero crossing interval PDF and this method was tested against the evaluation data set. These results show that, if one were to demand a specificity of 99.9% the estimated sensitivity to Alzheimer's disease and vascular dementia would be 77.8% and 35.2% respectively. This method was thus shown to be better at detecting dementia than either fractal measures or a typical standard method. It is also noted that applying the subject specific methodology would improve this still further.

The benefits and costs of this method were considered in order to give an opinion on whether this method is good enough to be of used in clinical practice. The significant benefits were that one third of vascular dementia sufferers and three quarters of Alzheimer's disease sufferers could be detected earlier. This gives the opportunity to prescribe drugs and therapies that could extend the symptom free state and reduce/delay the cost of care. The costs would be mainly felt in general practice where new equipment, training and patient contact time would be required. There would also be a false alarm rate and 1 in 1000 normal subjects will be troubled with an unnecessary visit to a hospital Neurophysiology department. Considering this, I formed a personal opinion that, subject to confirmation of the results in a larger scale trial, this method provides benefits that outweigh the cost.

Chapter 7. Review, Conclusions and Future Work

7.1 Review

Improved life expectancy has led to a significant increase in the number of people in the high-risk age groups that will develop Alzheimer's disease and other dementia. Efforts are being made to develop treatments that slow the progress of these diseases. However, unless a sufferer is diagnosed in the early stages the treatments cannot give the maximum benefit. Therefore, there is an urgent need for a practical, decision support tool that will enable the earliest possible detection of dementia within the large at-risk population.

This thesis described the background to the research; the Human EEG, fractals, chaos, complexity, and particularly their application to detecting dementia. The state of the art in automated EEG analysis was also reviewed.

The two main sources of published work on the fractal dimension of the Human EEG that existed before this research were those by Woyshville and Calabrese, and Wu *et al*. These papers were reviewed, particularly from a theoretical standpoint, and numerical experimentation are used to confirm that both methods had shortcomings. There are problems associated with estimating the fractal dimension of shapes, such as the EEG, that exist in affine space.

Two methods, which are appropriate in affine space, were selected from the range of dimension measures found in the literature. The Adapted Box Dimension and Dimension of the Zero Set were each applied to raw EEG data and to the auto-correlation of the EEG data. The results seem to show that all these fractal methods provide metrics that tend to decrease when dementia is present. However, the separation between subjects with dementia and normal subject was not good. It was found that changing controlling constants in the method, such as the segment length, affected the results. Better results were produced by tuning parameters, but this does not represent strong evidence as it is not clear whether the better results occur because the

205

method is tuned to that set of data or because this method of tuning will work in general.

These concerns were the main reason for conducting the evaluation, with a new, independent set of data, described in Chapter 4. This evaluation, with new data, produced mediocre results but it was valuable because it demonstrated that the performance of the fractal dimension based measures is a strong function of the tuning one applies. From the evaluation it was clear fractal measures could be used to separate subjects with dementia from controls but that this separation would have low sensitivity. This evaluation was also a clear demonstration of the value of a blind test using an independent data set and the dangers of taking results from a small a set of data, which had itself been used to develop the method.

Subject specific analysis of the fractal dimension was also proposed. This was shown to be an exciting, interesting and useful candidate for early detection of dementia. Subject specific analysis involves comparing an EEG to those taken previously from the same subject: Looking for trends in indices that arise over time rather than comparing an EEG to what is generally normal within the population. Subject specific EEG techniques were shown more sensitive than group comparison based on the same metric.

It was observed that measurements of fractal dimension over short data segments (2s) produced by clearly defined signal types (alpha wave, etc.) fall into bands. Other, less well defined, signals can be classified as having similar fractal dimensions to the clearly defined types and it is possible to determine the density of observations in the bands associated with Theta, Alpha and Beta activity. A metric, the ratio of observations in the Alpha range to the sum of the total observations in the Alpha and Theta ranges, was tested (on a small data set) and a differentiation between the normal and subjects with dementia was found.

Time evolution of the fractal dimension was also studied and it was found that the fractal dimension is stable and high for the normal subjects except where they become drowsy toward the end of the recording. The subjects with dementia present a generally lower fractal dimension (as noted previously) and the fractal dimension is less stable with time as the normals. It was also noted that subjects with dementia do not seem to enter a drowsy phase before the end of the recording.

The variability of fractal dimension over the scalp was also considered. In particular, it was shown that the efficacy of the fractal dimension based methods to separate normal subjects from those with dementia was better in the posterior region of the head. This is believed to be because the effect of dementia on the EEG is stronger and artefacts are weaker on the scalp at the back of the head.

Inspired by the work of other earlier researchers, the fractal dimension of the auto-correlation function had been used in this research. It was shown that their success was due to the content of the power spectral density and not to the time domain shape of the waveform. When this was discovered the implication that the EEG may not be fractal was not recognised, but this was rectified in later surrogate data testing experiments. These experiments showed that phase randomisation did not cause a significant loss of performance for any of the methods considered. Therefore, it was concluded that the fractal nature of the EEG (should it exist at all) does not contribute to any of the fractal dimension methods and the EEG is very unlikely to be a fractal. Previous success of the fractal methods is still important because it has clearly picked up on a significant feature within the EEG.

The surrogate data testing showed that the information necessary for the fractal dimension measures was contained in the power spectral density. It was also known, however, that despite significant effort over a long period no spectral based measure had been good enough to use in general clinical practice. Because of this, it was decided to take a different approach and propose methods that were determined by the power spectral density but were in the time domain. These novel methods were the Allan Variance and the zero-crossing interval distribution.

The results from Allan variance were very disappointing and the Allan variance metrics were discarded. However, the Allan variance may provide a new and interesting method to visualise the spectral content of the EEG.

Various metrics concerning the zero-crossing interval distribution were tested using the development data set and the best results were obtained using the Alpha/Theta ratio derived from the zero crossing interval PDF. This metric was tested against the evaluation data set and the results show that, if one were to demand a specificity of 99.9% the estimated sensitivity to Alzheimer's disease and vascular dementia would be 77.8% and 35.2% respectively. This method was thus shown to be better at detecting dementia than either fractal measures or a

typical standard method. It is also noted that applying the subject specific methodology would improve this still further. The benefits and costs of this method were considered in order to give an opinion on whether this method is good enough to be of used in clinical practice. The significant benefits were that one third of vascular dementia sufferers and three quarters of Alzheimer's disease sufferers could be detected earlier. This gives the opportunity to prescribe drugs and therapies that could extend the symptom free state and reduce/delay the cost of care. The costs would be mainly felt be in general practice where new equipment, new training and some increased patient contact time would be required. There would also be a false alarm rate and 1 in 1000 normal subjects will be troubled with an unnecessary visit to a hospital Neurophysiology department. Considering this, I formed a personal opinion that, subject to confirmation of the results in a larger scale trial, this method provides benefits that outweigh the cost.

7.2   Future Work

7.2.1   General

This section attempts to answer the question: "Given a further 3 to 5 years what would I do to further the search for a practical method for the early detection of dementia?" This section is also intended to kick-start the process of planning MSc, MPhil and PhD projects that will follow on from this work. Some of this work has already begun under the European collaborative BioPattern project [65].

In the following sections, it is suggested that future work should concentrate on reviewing and drawing together all of the recent parallel strands of investigation into the detection of dementia from the EEG using, for example, ICA, ERP, subject specific analysis or the novel methods described in this paper. The drawing together of these strands could be accomplished using a data fusion method such as Artificial Neural Networks. The future work should also begin to address the lack of large high quality database of serial EEGs from normal subjects, subjects who appear to be in decline and subjects with dementia (confirmed post-mortem). These activities would provide a combined method and a proof of that method's effectiveness. This could lead to use in real situations and benefit to people.

7.2.2 Review and Development

Future research should begin with a review of the current candidate methods for the early detection of dementia from the EEG. Such as:

- Independent Component Analysis;

- Event Related Potentials analysed using Spectral/Bispectral or Wavelet methods;

- Subject specific methods suggested in this Thesis;

- The novel methods suggested in this Thesis;

- Dimensional Complexity;

- Power spectral density ratios.

The next task would be to evaluate whether a data fusion based approach, such as Artificial Neural Networks or Fuzzy Logic, could provide any benefit and then design it. This would need to consider whether the methods are measuring different aspects of dementia related artefacts within the EEG or simply measuring the same thing in different ways. Clearly, if it is the latter then the data fusion will provide little benefit because the information derived from the methods is highly correlated. A consideration would be the amount of data required to test and evaluate several different combinational strategies in a meaningful way. Another concern would be that there is no simple way to choose a data fusion method and hone it for a particular problem; it normally requires a deep expert to derive a method of this class.

7.2.3 Trial and Data Collection

One of the largest barriers to the implementation of an EEG based method for the early detection of dementia is the availability of data. This is because the creation of a large high quality database of serial EEGs from normal subjects, subjects who appear to be in decline and subjects with dementia (confirmed post-mortem) is a significant undertaking in terms of time and resource. Some of this work has already begun under the European collaborative BioPattern project [65].

209

The main issues are:

- Confirming dementia. Many dementias, such as Alzheimer's disease, cannot be confirmed until a post mortem is carried out and this clearly extends the time necessary to collect a significant database of confirmed dementia cases.

- Ethical approval will be required. The ethical approval will only be given if it can be shown that issues such as data security and patient consent have been adequately considered and protected. This is particularly difficult because:

  > Repeated measures (required for subject specific measures) are not required for medical purposes and therefore we are justifying additional (minor) procedures, which are of no direct benefit to the patient concerned.

  > Some of the patients whose consent is required will have dementia – will we be able to rely on consent before the onset of dementia?

  > We will require post-mortems to confirm some types of dementia.

- Sharing the database. The EEG records will be valuable to many researchers and sharing such a large quantify of data on a large (global) scale requires clear planning, security and infrastructure.

I would suggest that once the data has been collected, it should be divided into a development data set and a trial data set. The development data set would be available to the researcher(s) who are developing the combined method. The trial data set would be available to independent researcher(s) who would trial the (well-defined) method in order to preserve its value as a blind trial data set. The number of records required in each data set and the frequency of taking EEGs from individuals needs to be determined.

7.2.4 Implementation

Patient representative groups, general practitioners, clinicians, health care managers, medical equipment suppliers and other interested parties should be engaged at an appropriate time to canvas their support for the introduction of EEG methods for the early detection of dementia.

After consultation and having developed a combined method, it will be necessary to engage a small number of GPs and Hospital facilities in a multi-centre trial. This trial would verify the estimated efficacies of the proposed method and expose any logistical or procedural issues. The potential of Information Technology (eMedicine) to facilitate GP to hospital EEG data transfers in the event of a referral and to facilitate subject specific disease diagnosis would also be assessed. This trial will be required to argue the case for the wider introduction of the method.

7.3 Conclusions

This thesis has produced the following conclusions.

- Previously published methods using the fractal dimension of the EEG are not wholly appropriate. This is because the EEG exists within affine space and conventional methods of estimating fractal dimension cannot be made to work without arbitrary assumptions in affine space.

- There are a number of fractal dimension methods that are appropriate for use with signals that lie in affine space. The performance of these methods is highly dependent on the selection of controlling parameters. The performance of these methods in a blind evaluation was reasonable (if one demands a specificity of 99.9%, the estimated sensitivity to Alzheimer's and vascular dementia is 67% and 17% respectively).

- Although the fractal measures are useful and successful, this is not due to the fractal nature of the EEG. The success is due to the detail of the EEG power spectral density and a natural robustness of the method to artefacts.

- Subject specific methods are an important way to improve the efficacy of metric based methods such as fractal dimension.

- The Allan Variance of the EEG gives an interesting method of visualising the data, however, it has not been possible to produce a metric to separate normal from subjects with dementia.

- Novel methods based on the zero crossing interval distribution are promising; particularly the Alpha/Theta ratio. It has been shown (on an independent data set) that, if one were to demand a specificity of 99.9% the estimated sensitivities to early Alzheimer's disease and vascular dementia are 77.8% and 35.2% respectively.

- It is possible to summarise an EEG recording into a single index and retain information pertinent to the detection of dementia. This is important for subject specific measures.

Chapter 8. References

Note: key references are in **bold** type.

[1] Raleigh V S (1999) World population and health in transition. BMJ, vol. 319, pp. 981-984.

[2] Hendrie H C (1998) Epidemiology of Dementia and Alzheimer's Disease. Am. J. Geriatr. Psychiatry, vol. 6, pp S3-S18.

[3] Kurz A (1998) Benefit of drug treatments for patients with Alzheimer's Disease. Clinician, vol. 16 (5), pp. 7-13.

[4] Cacabelos R (2002) Pharmacogenomics for the treatment of dementia. Ann, Med. vol. 34, pp. 357-379.

[5] Anand R (1998) Rivastigmine - Clinical efficacy and tolerability. Clinician, vol. 16 (5), pp. 14-22.

[6] Fox N C, Crum W R, Scahill R I, Stevens J M, Janssen J C and Rossor M N (2001) Imaging of onset and progression of Alzheimer's disease with voxel-compression mapping of serial magnetic resonance images. Lancet, vol. 358, pp 201-205.

[7] **Henderson G T, Wu P, Ifeachor E C and Wimalaratna H S K (1998) Subject specific variability of the Fractal Dimension of the Human Electroencephalogram. Proc. Third Int. Conf. On Neural Networks and Expert Systems in Medicine and Healthcare, University of Pisa, pp. 322-330.**

[8] **Henderson G T, Ifeachor E C, Wimalaratna H S K, Allen E M and Hudson N R (2000) Prospects for routine detection of dementia using the fractal dimension of the human electroencephalogram. Proc. International Conference on Advances in Medical Signal and Information Processing. IEE Conf. Prob. No. 476, pp. 284-289.**

[9] **Henderson G T, Ifeachor E C, Wimalaratna H S K, Allen E M and Hudson N R (2000) Prospects for routine detection of dementia using the fractal dimension of the human electroencephalogram. IEE Proc.-Sci. Meas. Technol., vol. 147 (6), pp. 321-326.**

[10] **Henderson G T, Ifeachor E C, Wimalaratna H S K, Allen E M and Hudson N R (2002) Electroencephalogram-Based methods for rourine detection of dementia. Proc. IV International Workshop on Biosignal Interpretation, Polytechnic University Milano, pp. 319-322.**

[11] Jasper H H (1958) The Ten-Twenty electrode system of the international federation. Electroencephalogram and Clinical Neurophysiology, vol. 10, pp. 371-375.

[12] Dondey M, Gaches J (1977) Part A, Semiology in Clinical EEG, Handbook of Electroencephalography and Clinical Neurophysiology, Vol. 11.

[13] Ktonas P Y (1981) Automated analysis of abnormal electroencephalograms. CRC Critical reviews in biomedical engineering, Vol. 9, pp 39-97.

[14] Mandelbrot B B (1982) The Fractal Geometry of Nature, W H Freeman, San Francisco.

[15] Addison P S (1997) Fractals and Chaos, Institute of Physics Publishing.

[16] Saupe D, Peitgen H, Jurgens H (1992) Chaos and Fractals New Frontiers of Science, Springer-Verlag.

[17] Gleick J, Chaos-Making a new science http://www.imho.com/grae/chaos/chaosbib.html

[18] Mandelbrot B B (1967) How long is the coast of Britain?, Science vol. 155, pp 636-638.

[19] Metz C E (1978) Basic Principles of ROC Analysis, Seminars in Nuclear Medicine, Vol. VIII, No. 4 (October), pp 283-298.

[20] Tabachnick B G and Fidell L S (1996) Using multivariate statistics (3rd ed.). New York: Harper Collins.

[21] Grass M and Gibbs F (1938) A Fourier transform of the EEG. J. Neurophysiol., Vol. 1, pp 521-526.

[22] Baldock G and Walter W (1946) A new electronic analyser, Electron. Eng., 18, pp 339-342.

[23] Barlow J (1979) Computerised Clinical Electroencephalography in perspective. IEEE Trans. On Biomedical Engineering, Vol. BME-26, No. 7, pp 377-391.

[24] Jansen BH, Bourne J R, Jagannathan V and Ward J W (1981) Evaluation of Slow-waves in Electroencephalogram using Syntactic Shape Analysis. Conf. Proc. IEEE Southeastcon, pp. 406-410.

[25] Gotman J, Skuce D R, Thompson C J, Gloor P, Ives J R and Ray W F (1973) Clinical applications of spectral analysis and extraction of features from electroencephalograms with slow waves in adult patients. Electroencephalography and Clinical Neurophysiology. 35, pp 225-235.

[26] Moretti D V, Babiloni C, Binetti G, Cassetta E, Forno G D, Ferreric F, Ferro R, Lanuzza B, Miniussi C, Nobili F, Rodriguez G, Salinari S and Rossini P M (2004) Individual analysis of EEG frequency and band power in mild Alzheimer's disease. Clinical Neurophysiology, vol. 115, pp. 299-308.

[27] Riddington E, Ifeachor E, Allen E and Mapps D (1996a) Investigation into different methods of fuzzy inference using ROC analysis. Proc. Of the Int. Conf. On Neural Networks and Expert Systems in Medicine and Healthcare, University of Plymouth, pp. 104-111.

[28] **Riddington E, Wu J, Ifeachor E, Allen E and Hudson N (1996b) Knowledge-based enhancements and interpretation of EEG signals. Proc. Of the Int. Conf. On Neural Networks and Expert Systems in Medicine and Healthcare, University of Plymouth, pp. 246-255.**

[29] Haykin S (1994) Neural Networks, a Comprehensive Foundation. ISBN 0 02 352761-7. Macmillan.

[30] **Pritchard W S, Duke D W, Coburn K L, Moore N C, Tucker K A, Jann M W and Hostetler R M (1994) EEG-based, neural-net predictive classification of Alzheimer's disease versus control subjects is augmented by non-linear EEG measures. Electroencephalography and Clinical Neurophysiology, Vol. 91, pp 118-130.**

[31] Wu J, Ifeachor E C, Allen E M and Hudson N.R (1994) A neural network based artefact detection system for EEG signal processing. Proc. Of the Int. Conf. On Neural Networks and Expert Systems in Medicine and Healthcare, University of Plymouth, pp. 257-266.

[32] Rohalova M, Sykacek P, Koska M and Dorffner G (2001) Detection of the EEG Artifacts by the Means of the (Extended) Kalman Filter. Measurement Science Review, Vol. 1, No. 1, pp. 59-62.

[33] Zhou W and Gotman J (2004) Removal of EMG and ECG artefacts from EEG based on wavelet transform and ICA. Proc. of the 26th Annual International Conf. of the IEEE EMBS. pp. 392-395.

[34] Bisset W M (1995) Chaos: a mechanism for human disease. Proc. R. Coll. Physicians Edinb. 25: pp 96-104.

[35] Lipsitz L A and Goldberger A L (1992) Loss of 'complexity' and aging. JAMA, Vol. 267, No 13, pp 1806-1809.

[36] **Pritchard W S and Duke D W (1992) Measuring chaos in the brain: a tutorial review of non-linear dynamical EEG analysis. Intern. J. Neuroscience, Vol. 67, pp. 31-80.**

[37] Pritchard W S and Duke D W (1992) Modulation of EEG dimensional complexity by smoking. Journal of Psychophysiology 6, pp 1-10.

[38] Pritchard W S and Duke D W (1992) Dimensional analysis of no-task human EEG using the Grassberger-Procaccia method. Psychophysiology Vol. 29, No. 2, pp 182-192.

[39] **Pritchard W S, Duke D W and Krieble K (1995) Dimensional analysis of resting human EEG II: Surrogate-data testing indicates nonlinearity but not low-dimensional chaos. Psychophysiology, 32, pp 486-491.**

[40] Brandt M E, Ademaglu A and Pritchard W S (2000) Nonlinear prediction and complexity

of alpha EEG activity. International J. of Bifurcation and Chaos, vol. 10, No. 1, pp. 123-133.

[41] Sugihara G and May R (1990) Nonlinear forecasting as a way of distinguishing chaos from measurement error in time series. Nature Vol. 344, pp734-741.

[42] Woyshville M J and Calabrese J R (1994) Quantification of occipital EEG changes in Alzheimer's Disease utilising a new metric: the fractal dimension. Biol. Psychiatry, Vol. 35, pp 381-387.

[43] Nikias C and Mendel J (1993) Signal processing with higher order spectra. IEEE Signal Processing Magazine, Vol. 10, pp 10-37.

[44] Aspect Medical Systems Inc. (1992) Technology overview: bispectral analysis. P/N 085-005 20.

[45] Aspect Medical Systems Inc. (1994) Technology overview: bispectral index. P/N 1010003 01.

[46] Glass P, Sebel P, Greenwald S and Chamoun N (1994) Quantification of the relative effects of anesthetic agents on the EEG and patient responsiveness to incision. Anesthesiology, Vol. 81, No 3, pp. A407.

[47] Greenwald S, Chaing H H, Devlin P, Smith C, Sigl J and Chamoun N (1994) The Bispectral Index (BIS2.0) as a hypnosis measure. Anesthesiology, Vol. 81 No. 3A, pp. A477.

[48] Kearse L A, Saini V, deBros F and Chamoun N (1991) Bispectral analysis of EEG may predict anesthetic depth during narcotic induction. Anestesiology, Vol. 75, No. 3, pp. A175-A175.

[49] Kearse L A, Manberg P, Chamoun N deBros F and Zaslavsky A (1994) Bispectral analysis of the electroencephalogram correlates with movement to skin incision during propofol/nitrous oxide anesthesia. Anesthesiology, Vol. 81, No. 6, pp 1365-1370.

[50] Lien C A, Berman M, Saini V, Matteo R S, Sharp G J and Chamoun N (1992) The accuracy of the EEG in predicting hemodynamic changes with incision during isoflurane anesthesia. Anesth. Analg. Vol. 74, pp. S187.

[51] Liu J, Singh H, Wu G, Gaines G Y and White P F (1994) Use of the EEG Bispectral Index to predict awakening from general anesthesia. Anesth. Analg. Vol. 78, pp. S254.

[52] Sebel P S, Rampil I, Cork R, White P, Smith N T, Brull S and Chamoun N (1993) Bispectral analysis for monitoring anesthesia - a multicenter study. Anesthesiology, Vol. 79, No. 3, pp. A178.

[53] Sebel P S, Rampil I, Cork R, White P F, Smith N T, Glass P, Jopling M and Chamoun N (1994) Bispectral Analysis (BIS) for monitoring anesthesia: comparison of anesthetic techniques. Anesthesiology, Vol. 81, No. 3A, pp. A1488.

[54] Vernon J, Bowles S Sebel P S and Chamoun N (1992) EEG Bispectrum predicts movement at incision during isoflurane or propofol anesthesia. Anesthesiology, Vol. 77, No. 3, pp. A502.

[55] Ungureanu M, Bigan C, Strungaru R and Lazarescu (2004) Independent Component Analysis Applied in Biomedical Signal Processing. Measurement Science Review, Vol. 4, Sect. 2, pp. 1-8.

[56] Hoya T, Hori G, Bakardjian H, Nishimura T, Suzuki T, Miyawaki Y, Funase A and Cao J (2003) Classification of Single Trial EEG Signals by a Combined Principal and Independent Component Analysis and Probabilistic Neural Network Approach. 4th International Symposium on ICA and Blind Signal Separation. pp. 197-202.

[57] Wada Y, Nanbu Y, Jiang Z, Koshimo Y, Yamaguchi N and Hashimoto T (1997) Electroencephalographic Abnormalities in Patients with Presenile Dementia of the Alzheimer Type: Quantitative Analysis at Rest and during Photic Stimulation. Biol. Psychiatry, Vol. 41, pp. 217-225.

[58] Tanaka H, Koenig T, Pascual-Marqui R D, Hirata K, Kochi K and Lehmann D (2000) Event-Related Potential and EEG Measures in Parkinson's Disease without and with Dementia. Dement. Geriatr. Cogn. Disord., Vol. 11, pp. 39-45.

[59] Bianchi A M, Molteni S C, Panzica F, Visani E, Franceschetti S and Cerutti S (2004) Spectral and Bispectral Analysis of the EEG Rhythms in Basal Conditions and During Photic Stimulation. Proc. of the 26th Annual International Conf. of the IEEE EMBS. pp. 574-577.

[60] Durka P J (2003) From Wavelets to Adaptive Approximations: Time-frequency Parametrization of EEG. BioMedical Engineering OnLine. www.biomedical-engineering-online.com/content/2/1/1.

[61] Wu P, Ifeachor E C, Allen E M, Wimalaratna H S K and Hudson N R (1996) Statistical quantitative EEG features in differentiation of demented patients from normal controls. Proc. Of the Int. Conf. On Neural Networks and Expert Systems in Medicine and Healthcare, University of Plymouth, pp. 366-375.

[62] Mandelbrot B B (1984) Fractals in physics: Squig clusters, diffusion, fractal measures and the unicity of fractal dimensionality, J. Stat. Phys. Vol. 34, pp 895-930.

[63] Voss R F (1988) Fractals in nature: from characterisation to simulation, The Science Of Fractal Images, Springer-Verlag, Berlin, pp 21-70.

[64] Wu P, Ifeachor E C, Allen E M, Wimalaratna H S K and Hudson N R (1996) Subject Specific Features: A Feasibility Study, Proc. of the Int. Conf. On Neural Networks and Expert Systems in Medicine and Healthcare, University of Plymouth, 339-345.

[65] **Ifeachor E C, Outram N J, Henderson G T, Wimalaratna H S K, Hudson N, Sneyd R, Dong C and Bigan C (2004) Non-linear methods for biopattern analysis: role and challenges, Proc. of the 26th annual international conf. of the IEEE EMBS.**

[66] Bayat A (2002) Bioinformatics. BMJ, Vol. 324, pp. 1018-1022.

[67] IEEE Specification Format Guide and Test Procedure for Interferometric Single-Axis Fibre Optic Gyros, Annex C (1995) An overview of the Allan Variance method of IFOG noise analysis, Document No. P952/D21, pp. 60-70.

[68] Allan D W (1966) Statistics of atomic frequency standards. Proc. IEEE, vol. 54, No. 2, pp. 221-230.

Appendix A.   Source Code from Wu's Work

This is the original code used by Wu in his research [61].

```
void complex() {

    int a, b;
    float temp, correlate[257];
    float DCtemp[7];

    for(a=0;a<=6;a++)
      {
          DCtemp[a]=0.0;
      }
    for(a=0;a<=256;a++)
      {
          correlate[a]=0.0;
      }

    temp=0.0;
    for(a=0;a<=255;a++)
      {
          if (temp<fabs(x[a]))
                temp=fabs(x[a]);
      }
    for(a=0;a<=255;a++)
      {
          x[a]=64.0*x[a]/(temp+0.0000001);
      }

    for(a=0;a<=255;a++)
      {
          correlate[a]=0.0;
          for(b=0;b<=255-a;b++)
            {
                correlate[a]=correlate[a]+x[b]*x[a+b];
            }
      }

    temp=0.0;
    for(a=0;a<=255;a++)
      {
          if (temp<fabs(correlate[a])) temp=fabs(correlate[a]);
      }
    for(a=0;a<=255;a++)
      {
          x[a]=300.0*correlate[a]/(temp+0.0000001);
      }

    x[256]=x[255];

    for(a=0;a<=255;a++)
      {
          DCtemp[1]=DCtemp[1]+sqrt((x[a]-x[a+1])*(x[a]-
                    x[a+1])+1.0);
      }
    for(a=0;a<=255;a=a+4)
      {
          DCtemp[2]=DCtemp[2]+sqrt((x[a]-x[a+4])*(x[a]-
                    x[a+4])+16.0);
      }
    for(a=0;a<=255;a=a+8)
      {
          DCtemp[3]=DCtemp[3]+sqrt((x[a]-x[a+8])*(x[a]-
                    x[a+8])+64.0);
      }
    for(a=0;a<=255;a=a+16)
      {
          DCtemp[4]=DCtemp[4]+sqrt((x[a]-x[a+16])*(x[a]-
                    x[a+16])+16.0*16.0);
      }
    for(a=0;a<=255;a=a+32)
      {
          DCtemp[5]=DCtemp[5]+sqrt((x[a]-x[a+32])*(x[a]-
                    x[a+32])+32.0*32.0);
      }
    for(a=0;a<=255;a=a+64)
```

```
{
    DCtemp[6]=DCtemp[6]+sqrt((x[a]-x[a+64])*(x[a]-
            x[a+64])+64.0*64.0);
}

for (a=2;a<=6;a++)
  {
    DCtemp[a]=1.0-(log(DCtemp[a])-
                    log(DCtemp[1]))/log(pow(2,a)));
  }

temp=0.0;
for (a=2;a<=5;a++)
  {
    for (b=a+1;b<=6;b++)
      {
        if (DCtemp[a]>DCtemp[b])
          {
              temp=DCtemp[a];
              DCtemp[a]=DCtemp[b];
              DCtemp[b]=temp;
          }
          else
          {
          }
      }
  }

DCBand[0][1]=(DCtemp[3]+DCtemp[4]+DCtemp[5])/3.0;

}
```

Appendix B.   Early Software Overview

The early software, described in this appendix, was written in Borland Turbo C++ V4.5 (later software is described in Appendix C). The software provides a data visualisation front end, spectral analysis and fractal dimension analysis. There are approximately 170,000 source lines of code. Several side-builds implement other analysis methods such as Innovation Statistics analysis.

The main user interface for the software is shown below:
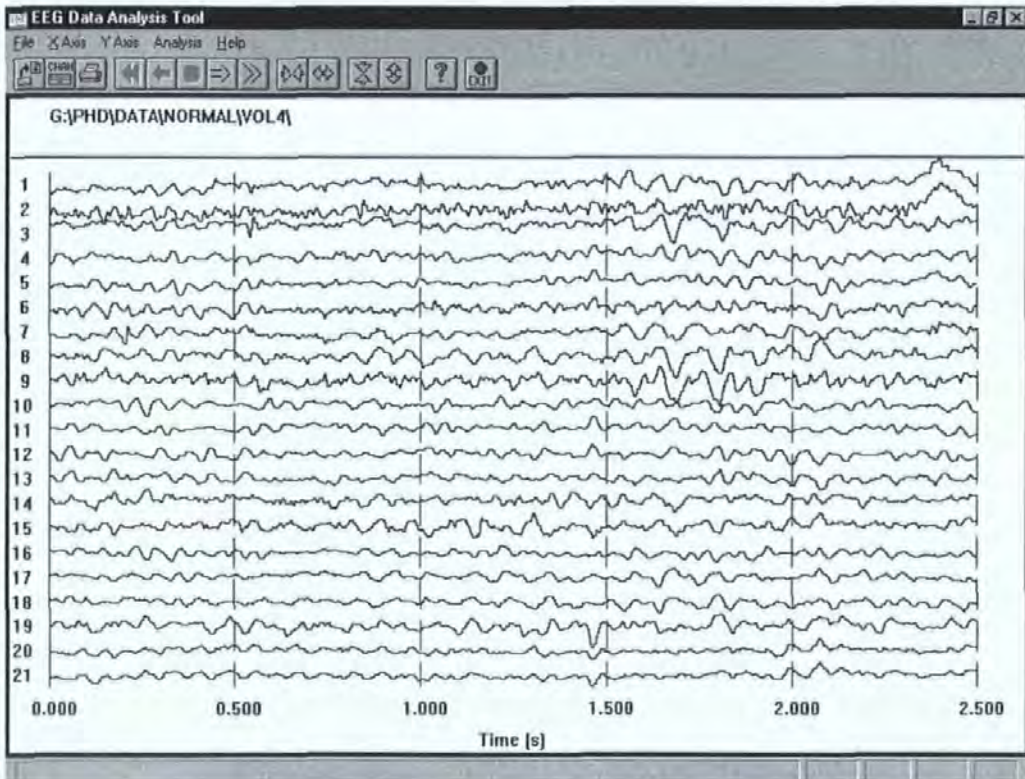
This interface is written as a dialog client, and is derived from the predefined TDialog class. All of the functions available on the tool bar may be accessed from the menu system.

The following functions are available from the menu and/or the short cut icons in the main build of software:

Icon	Menu selection	Effect
	File : • Load...	Displays a dialog to select and load EEG data
	• Change Channel	Displays a dialog to select which channels to display and analysis
	• Print	Prints the currently displayed screen of EEG data
	• Configure Printer	Displays printer setup dialog
	• Exit	Exits the application
	X Axis : • Forward	Steps forward through the EEG data
	• Back	Steps back though the EEG data
	• Play : Forward	Runs forward through the EEG data
	• Play : Backward	Runs in reverse through the EEG data
	• Play : Stop	Stops the EEG display running forward or reverse
	• Zoom Out	Expands the time (X) axis scaling
	• Zoom In	Reduces the time (X) axis scaling
	Y Axis : • Zoom Out	Expands the voltage (Y) axis scaling
	• Zoom In	Reduces the voltage (Y) axis scaling
	Analysis : • Set Analysis Range	Displays a dialog that allows the user to select the EEG data range to analyse
M	• Cycle Montage	Changes the EEG montage cyclically from "Original recorded montage" to "Common average montage" to "Common reference montage" and back to "Original recorded montage" again
	• Fractal Dimension	Calculates and displays the Adapted Box Dimension and Dimension of the Zero-Set for both raw EEG data and the autocorrelation of EEG data for the currently selected data file, channels and analysis range
	• All Files FD	Calculates and displays the Adapted Box Dimension and Dimension of the Zero-Set for both raw EEG data and the autocorrelation of EEG data for all channels of all data files. Results are written to a file for manual analysis. This is effectively a batch process.
	• Hunt FD	As "All Files FD" but used stored Histograms rather than recalculating them
	• Analyse Sequence Of FD	Stub ready for Hidden Markov Model analysis for fractal dimension sequence
	• Mean Holo Fn	Calculates and displays the cross-bicoherence of the EEG data for the currently selected data file, channels and analysis range
	• Spectrum	Calculates and displays the spectrum of the EEG data for the currently selected data file, channels and analysis range
	• Statistics	Calculates and displays the mean and standard deviation of the EEG data for the currently selected data file, channels and analysis range
	• Allan Variance	Calculates and displays the Allan Variance Chart of the EEG data for the currently selected data file, channels and analysis range
?	Help: • Contents	Displays help on using this application (not up to date)
	• Using Help	Displays standard help on using windows help
	• About	Displays a windows "About" box

Channel selection, analysis range selection and analysis are performed in Modal Child Windows (based on the TDialog client class), which are displayed for the user to observe results or input preferences. The following table describes the files that are included in the build:

Filename	Function
Allan.h	Calculates and displays Allan chart of the raw EEG data
Channel.cpp	Displays TDialog that allows user to select channels for display and analysis
Channel.h	Header file to provide interface to channel.cpp
EEG.EXE	Compiled executable code
EEG.hpj	Compiled windows help file
Eeg_data.cpp	Provides interface to eeg data files as EEG class
Eeg_data.h	Header file to provide interface to EEG class
fft.cpp	Defined functions for the FFT (Fast Fourier Transform) class
fft.h	Header file to provide interface to the FFT class
Fractal.cpp	Calculates and displays Adapted Box Dimension and Dimension of the Zero-Set for both raw EEG data and the autocorrelation of EEG data. Has the ability to store histograms for further analysis.
Fractal.h	Header file to provide interface to fractal.cpp
Mainhelp.rtf	Defines help to be displayed to user (Not up to date)
Meanholo.cpp	Calculates and displays the cross bicoherence of the EEG
Meanholo.h	Header file to provide interface to meanholo.cpp
Nlyssabd.cpp	Dialog client to display 'About' dialog box (Auto-created by Turbo C++)
Nlyssabd.h	Header file to provide interface to nlyssabd.cpp
Nlyssapp.cpp	Application code (Auto-generated by Turbo C++)
Nlyssapp.def	Windows definition file (Code/Data type, Heap/Stack size etc.)
Nlyssapp.h	Header file to provide interface to nlyssapp.h
Nlyssapp.rc	Resource code file (menu, bitmaps, etc.)
Nlyssapp.rh	Resource header file provides access to nlyssapp.rc
Nlytdlgc.cpp	Main TDialog client for event response (user interface code)
Nlytdlgc.h	Header file to provide interface to nlytdlgc.cpp
range.h	Displays TDialog that allows user to select data range for display and analysis
Spectrum.h	Calculates and displays the spectrum of the data using the Fast Fourier Transform
stats.h	Calculates and displays mean and standard deviation of data
Toolbar.rtf	Defines toolbar help to be displayed to user (Not up to date)
Wprint.cpp	Printer interface
Wprint.h	Header file to provide interface to wprint.cpp

The code that performs the fractal dimension calculation is available on CDROM.

Appendix C.   Later Software Overview

The later software, described in this appendix, was written in Microsoft Visual C++. The change of compiler was necessary in order to be compatible with the EEG logging software from Biologic. The software provides a data visualisation front end, spectral analysis and fractal dimension analysis.

The main user interface for the software is shown below:

Appendix D. Detailed, Supporting Results

This section contains tables of detailed results that have been moved from the main body of the thesis to ease reading.

The following four tables (Table 8-1 through Table 8-4) show fractal dimension of the zero-set of the cross-correlation function (between channels) for comparison to the fractal dimension of the zero-set of the auto-correlation. These results were used in the discussion of the question "what is the meaning of the fractal dimension of an auto-correlation function?" as reported in section 3.9.2.

	Ch 1	Ch 2	Ch 3	Ch 4	Ch 5	Ch 6	Ch 7	Ch 8	Ch 9	Ch 10
Ch 1	0.415	0.545	0.416	0.560	0.523	0.476	0.401	0.483	0.519	0.542
Ch 2	0.530	0.531	0.448	0.418	0.525	0.534	0.173	0.448	0.494	0.570
Ch 3	0.518	0.418	0.463	0.471	0.530	0.523	0.428	0.467	0.524	0.528
Ch 4	0.481	0.472	0.512	0.547	0.557	0.571	0.477	0.554	0.532	0.580
Ch 5	0.549	0.500	0.491	0.557	0.551	0.520	0.550	0.554	0.553	0.560
Ch 6	0.526	0.515	0.519	0.544	0.543	0.553	0.547	0.547	0.543	0.570
Ch 7	0.436	0.371	0.467	0.472	0.554	0.528	0.514	0.487	0.529	0.490
Ch 8	0.452	0.481	0.516	0.534	0.526	0.550	0.532	0.544	0.555	0.557
Ch 9	0.507	0.297	0.503	0.556	0.551	0.571	0.523	0.559	0.572	0.594
Ch 10	0.474	0.585	0.548	0.569	0.565	0.590	0.560	0.582	0.574	0.637
Ch 11	0.471	0.488	0.461	0.469	0.540	0.534	0.464	0.514	0.575	0.544
Ch 12	0.556	0.477	0.552	0.571	0.607	0.587	0.547	0.585	0.576	0.601
Ch 13	0.560	0.443	0.530	0.556	0.548	0.570	0.540	0.543	0.559	0.560
Ch 14	0.560	0.541	0.437	0.536	0.538	0.551	0.514	0.538	0.561	0.576
Ch 15	0.524	0.527	0.515	0.542	0.540	0.546	0.527	0.556	0.553	0.597
Ch 16	0.546	0.539	0.537	0.576	0.575	0.556	0.547	0.553	0.571	0.558
Ch 17	0.340	0.473	0.495	0.552	0.560	0.547	0.453	0.484	0.539	0.554
Ch 18	0.548	0.548	0.527	0.581	0.562	0.600	0.526	0.577	0.586	0.650
Ch 19	0.564	0.551	0.505	0.552	0.574	0.579	0.513	0.583	0.562	0.623
Ch 20	0.546	0.532	0.534	0.572	0.558	0.556	0.510	0.555	0.558	0.561
Ch 21	0.541	0.529	0.483	0.561	0.551	0.559	0.537	0.564	0.564	0.569

Table 8-1: Fractal dimension of the cross-correlation for Vol3 (Part 1).

	Ch 11	Ch 12	Ch 13	Ch 14	Ch 15	Ch 16	Ch 17	Ch 18	Ch 19	Ch 20	Ch 21
Ch 1	0.486	0.547	0.398	0.532	0.535	0.534	0.482	0.579	0.449	0.546	0.511
Ch 2	0.459	0.529	0.526	0.513	0.492	0.542	0.473	0.545	0.540	0.549	0.547
Ch 3	0.541	0.526	0.532	0.483	0.517	0.534	0.416	0.508	0.536	0.521	0.512
Ch 4	0.525	0.556	0.575	0.560	0.571	0.552	0.571	0.580	0.550	0.528	0.591
Ch 5	0.562	0.574	0.564	0.553	0.546	0.555	0.542	0.554	0.566	0.549	0.555
Ch 6	0.582	0.572	0.580	0.550	0.562	0.562	0.527	0.585	0.562	0.551	0.574
Ch 7	0.513	0.550	0.519	0.503	0.515	0.540	0.506	0.541	0.525	0.517	0.526
Ch 8	0.498	0.545	0.559	0.544	0.549	0.561	0.489	0.570	0.545	0.546	0.565
Ch 9	0.527	0.583	0.571	0.535	0.559	0.567	0.509	0.577	0.579	0.557	0.568
Ch 10	0.557	0.640	0.593	0.550	0.596	0.580	0.556	0.609	0.568	0.566	0.586
Ch 11	0.493	0.586	0.536	0.535	0.543	0.564	0.421	0.602	0.556	0.562	0.561
Ch 12	0.573	0.666	0.620	0.566	0.586	0.590	0.600	0.622	0.600	0.585	0.604
Ch 13	0.541	0.583	0.570	0.552	0.565	0.549	0.543	0.572	0.559	0.560	0.556
Ch 14	0.549	0.578	0.555	0.556	0.550	0.555	0.531	0.556	0.563	0.553	0.560
Ch 15	0.534	0.599	0.563	0.555	0.560	0.571	0.551	0.586	0.582	0.562	0.566
Ch 16	0.576	0.603	0.571	0.551	0.573	0.568	0.536	0.589	0.575	0.579	0.563
Ch 17	0.501	0.552	0.564	0.499	0.557	0.553	0.504	0.542	0.509	0.547	0.541
Ch 18	0.587	0.638	0.580	0.570	0.592	0.595	0.568	0.606	0.580	0.594	0.590
Ch 19	0.544	0.616	0.584	0.570	0.586	0.568	0.497	0.581	0.590	0.569	0.576
Ch 20	0.542	0.571	0.561	0.556	0.564	0.558	0.548	0.580	0.562	0.564	0.553
Ch 21	0.562	0.613	0.572	0.563	0.584	0.566	0.548	0.576	0.565	0.569	0.568

Table 8-2: Fractal dimension of the cross-correlation for Vol3 (Part 2).

Table 8-3; Fractal dimension of the cross-correlation for AD3 (Part 1).

	Ch 1	Ch 2	Ch 3	Ch 4	Ch 5	Ch 6	Ch 7	Ch 8	Ch 9	Ch 10
Ch 1	0.310	0.289	0.308	0.313	0.298	0.321	0.289	0.309	0.303	0.302
Ch 2	0.294	0.295	0.302	0.309	0.292	0.307	0.309	0.306	0.308	0.298
Ch 3	0.315	0.301	0.307	0.311	0.301	0.412	0.315	0.316	0.320	0.311
Ch 4	0.303	0.302	0.315	0.396	0.300	0.614	0.412	0.311	0.319	0.310
Ch 5	0.301	0.292	0.310	0.302	0.299	0.333	0.294	0.305	0.311	0.305
Ch 6	0.315	0.345	0.463	0.582	0.319	0.785	0.479	0.323	0.398	0.428
Ch 7	0.304	0.304	0.320	0.335	0.304	0.561	0.313	0.311	0.331	0.313
Ch 8	0.305	0.307	0.314	0.317	0.312	0.324	0.308	0.301	0.309	0.302
Ch 9	0.304	0.318	0.331	0.325	0.312	0.552	0.337	0.305	0.309	0.314
Ch 10	0.305	0.309	0.318	0.316	0.300	0.435	0.333	0.303	0.308	0.308
Ch 11	0.305	0.301	0.304	0.308	0.306	0.330	0.296	0.312	0.306	0.308
Ch 12	0.312	0.322	0.311	0.345	0.312	0.495	0.323	0.308	0.321	0.305
Ch 13	0.287	0.286	0.295	0.322	0.304	0.348	0.299	0.309	0.336	0.312
Ch 14	0.284	0.293	0.302	0.304	0.298	0.322	0.318	0.312	0.298	0.315
Ch 15	0.294	0.304	0.316	0.318	0.301	0.353	0.319	0.310	0.314	0.314
Ch 16	0.305	0.305	0.318	0.317	0.307	0.321	0.317	0.308	0.313	0.307
Ch 17	0.305	0.296	0.299	0.303	0.301	0.301	0.306	0.304	0.311	0.300
Ch 18	0.306	0.299	0.296	0.307	0.302	0.313	0.307	0.306	0.305	0.300
Ch 19	0.335	0.303	0.322	0.340	0.314	0.492	0.369	0.312	0.324	0.310
Ch 20	0.303	0.300	0.302	0.309	0.316	0.349	0.311	0.319	0.317	0.314
Ch 21	0.307	0.324	0.313	0.320	0.293	0.493	0.358	0.331	0.343	0.330

	Ch 11	Ch 12	Ch 13	Ch 14	Ch 15	Ch 16	Ch 17	Ch 18	Ch 19	Ch 20	Ch 21
Ch 1	0.302	0.313	0.299	0.296	0.305	0.308	0.301	0.301	0.297	0.304	0.304
Ch 2	0.287	0.300	0.303	0.295	0.311	0.305	0.300	0.300	0.309	0.298	0.301
Ch 3	0.317	0.312	0.303	0.312	0.309	0.309	0.300	0.303	0.317	0.312	0.328
Ch 4	0.309	0.326	0.303	0.309	0.312	0.309	0.308	0.303	0.333	0.312	0.416
Ch 5	0.308	0.299	0.304	0.299	0.311	0.303	0.298	0.302	0.301	0.304	0.304
Ch 6	0.338	0.520	0.320	0.382	0.324	0.315	0.314	0.327	0.509	0.366	0.497
Ch 7	0.294	0.351	0.325	0.300	0.314	0.314	0.298	0.306	0.318	0.325	0.324
Ch 8	0.305	0.315	0.310	0.318	0.307	0.304	0.313	0.303	0.311	0.308	0.314
Ch 9	0.323	0.330	0.327	0.319	0.312	0.311	0.307	0.299	0.337	0.317	0.335
Ch 10	0.308	0.313	0.307	0.304	0.308	0.312	0.302	0.308	0.313	0.312	0.316
Ch 11	0.304	0.310	0.305	0.301	0.316	0.305	0.302	0.301	0.308	0.305	0.318
Ch 12	0.326	0.309	0.287	0.303	0.308	0.311	0.294	0.295	0.329	0.303	0.349
Ch 13	0.310	0.308	0.300	0.290	0.315	0.310	0.295	0.306	0.302	0.305	0.324
Ch 14	0.304	0.295	0.297	0.299	0.307	0.309	0.295	0.296	0.305	0.309	0.299
Ch 15	0.300	0.313	0.319	0.308	0.310	0.308	0.312	0.305	0.314	0.313	0.315
Ch 16	0.311	0.330	0.305	0.312	0.308	0.312	0.303	0.303	0.308	0.315	0.313
Ch 17	0.303	0.303	0.303	0.299	0.303	0.305	0.302	0.299	0.311	0.306	0.298
Ch 18	0.305	0.303	0.300	0.293	0.306	0.305	0.301	0.299	0.302	0.296	0.292
Ch 19	0.303	0.332	0.300	0.282	0.318	0.310	0.311	0.303	0.336	0.318	0.351
Ch 20	0.302	0.314	0.315	0.308	0.314	0.309	0.299	0.304	0.328	0.309	0.326
Ch 21	0.295	0.320	0.312	0.310	0.320	0.312	0.303	0.312	0.298	0.312	0.312

Table 8-4: Fractal dimension of the cross-correlation for AD3 (Part 2).

The following four tables (Table 8-5 through Table 8-8) show fractal dimension of the zero-set of the time-incoherent cross-correlation function (between channels) for comparison to the fractal dimension of the zero-set of the auto-correlation. These results were used in the discussion of the question "what is the meaning of the fractal dimension of an auto-correlation function?" as reported in section 3.9.3.

	Ch 1	Ch 2	Ch 3	Ch 4	Ch 5	Ch 6	Ch 7	Ch 8	Ch 9	Ch 10
Ch 1	0.461	0.163	0.283	0.490	0.457	0.499	0.501	0.523	0.436	0.398
Ch 2	0.165	0.145	0.457	0.406	0.431	0.522	0.190	0.465	0.517	0.550
Ch 3	0.463	0.485	0.426	0.548	0.462	0.435	0.370	0.499	0.488	0.499
Ch 4	0.378	0.517	0.490	0.549	0.501	0.580	0.523	0.538	0.585	0.600
Ch 5	0.398	0.533	0.532	0.524	0.536	0.552	0.540	0.545	0.560	0.555
Ch 6	0.529	0.334	0.518	0.566	0.563	0.565	0.525	0.559	0.566	0.605
Ch 7	0.190	0.278	0.387	0.508	0.489	0.526	0.444	0.517	0.487	0.517
Ch 8	0.522	0.462	0.500	0.530	0.542	0.519	0.504	0.543	0.554	0.564
Ch 9	0.558	0.551	0.524	0.528	0.546	0.562	0.513	0.540	0.562	0.567
Ch 10	0.546	0.546	0.525	0.567	0.593	0.607	0.574	0.568	0.590	0.637
Ch 11	0.566	0.492	0.471	0.509	0.505	0.549	0.442	0.510	0.520	0.588
Ch 12	0.567	0.567	0.594	0.601	0.620	0.629	0.539	0.592	0.623	0.640
Ch 13	0.534	0.513	0.512	0.562	0.562	0.559	0.500	0.544	0.578	0.612
Ch 14	0.556	0.431	0.475	0.532	0.532	0.543	0.486	0.551	0.557	0.569
Ch 15	0.550	0.530	0.551	0.565	0.556	0.554	0.543	0.547	0.588	0.600
Ch 16	0.539	0.511	0.553	0.558	0.554	0.562	0.540	0.551	0.572	0.573
Ch 17	0.497	0.519	0.461	0.519	0.553	0.526	0.477	0.517	0.558	0.514
Ch 18	0.542	0.523	0.541	0.598	0.594	0.602	0.504	0.566	0.580	0.626
Ch 19	0.546	0.494	0.518	0.584	0.567	0.565	0.505	0.554	0.563	0.600
Ch 20	0.537	0.534	0.524	0.558	0.559	0.556	0.499	0.558	0.554	0.567
Ch 21	0.525	0.489	0.509	0.518	0.553	0.567	0.518	0.563	0.553	0.602

Table 8-5: Fractal dimension of the Time-Incoherent cross-correlation for Vol3 (Part 1).

	Ch 11	Ch 12	Ch 13	Ch 14	Ch 15	Ch 16	Ch 17	Ch 18	Ch 19	Ch 20	Ch 21
Ch 1	0.419	0.516	0.486	0.509	0.477	0.522	0.437	0.531	0.403	0.547	0.400
Ch 2	0.545	0.500	0.456	0.403	0.417	0.527	0.393	0.421	0.429	0.504	0.326
Ch 3	0.436	0.516	0.499	0.450	0.528	0.513	0.468	0.507	0.515	0.362	0.527
Ch 4	0.507	0.600	0.552	0.549	0.580	0.559	0.508	0.585	0.569	0.528	0.561
Ch 5	0.541	0.594	0.565	0.553	0.566	0.555	0.467	0.587	0.545	0.545	0.562
Ch 6	0.569	0.598	0.561	0.553	0.556	0.561	0.495	0.577	0.576	0.566	0.589
Ch 7	0.509	0.541	0.524	0.505	0.493	0.522	0.496	0.528	0.538	0.520	0.502
Ch 8	0.512	0.597	0.559	0.529	0.562	0.559	0.511	0.550	0.542	0.543	0.568
Ch 9	0.600	0.590	0.557	0.554	0.563	0.556	0.548	0.584	0.567	0.579	0.586
Ch 10	0.541	0.639	0.618	0.591	0.601	0.564	0.536	0.615	0.609	0.575	0.592
Ch 11	0.496	0.579	0.561	0.540	0.530	0.546	0.503	0.541	0.541	0.576	0.561
Ch 12	0.592	0.663	0.619	0.599	0.600	0.607	0.573	0.627	0.631	0.586	0.627
Ch 13	0.533	0.596	0.567	0.572	0.580	0.547	0.552	0.576	0.568	0.559	0.559
Ch 14	0.551	0.581	0.565	0.539	0.559	0.560	0.536	0.562	0.548	0.547	0.549
Ch 15	0.561	0.599	0.579	0.564	0.563	0.571	0.551	0.604	0.574	0.559	0.562
Ch 16	0.581	0.586	0.574	0.560	0.580	0.569	0.547	0.582	0.577	0.565	0.556
Ch 17	0.465	0.522	0.523	0.515	0.552	0.550	0.499	0.580	0.540	0.535	0.505
Ch 18	0.602	0.646	0.590	0.582	0.594	0.589	0.568	0.640	0.598	0.589	0.599
Ch 19	0.562	0.615	0.564	0.558	0.587	0.568	0.542	0.597	0.584	0.566	0.565
Ch 20	0.525	0.594	0.565	0.553	0.561	0.564	0.557	0.600	0.564	0.565	0.536
Ch 21	0.550	0.595	0.575	0.575	0.570	0.558	0.539	0.592	0.579	0.559	0.566

Table 8-6: Fractal dimension of the Time-Incoherent cross-correlation for Vol3 (Part 2).

Table 8-7; Fractal dimension of the Time-Incoherent cross-correlation for AD3 (Part 1).

	Ch 1	Ch 2	Ch 3	Ch 4	Ch 5	Ch 6	Ch 7	Ch 8	Ch 9	Ch 10
Ch 1	0.259	0.301	0.305	0.307	0.292	0.277	0.307	0.304	0.301	0.304
Ch 2	0.302	0.280	0.307	0.303	0.312	0.303	0.294	0.306	0.307	0.312
Ch 3	0.312	0.295	0.323	0.300	0.310	0.356	0.318	0.313	0.328	0.315
Ch 4	0.326	0.305	0.312	0.335	0.304	0.328	0.314	0.309	0.313	0.318
Ch 5	0.293	0.303	0.297	0.298	0.300	0.308	0.307	0.311	0.301	0.304
Ch 6	0.339	0.421	0.357	0.503	0.325	0.380	0.317	0.320	0.473	0.333
Ch 7	0.305	0.303	0.315	0.317	0.315	0.316	0.318	0.317	0.326	0.317
Ch 8	0.314	0.308	0.314	0.312	0.309	0.315	0.316	0.306	0.312	0.319
Ch 9	0.307	0.311	0.326	0.304	0.319	0.323	0.326	0.308	0.313	0.324
Ch 10	0.307	0.327	0.307	0.306	0.305	0.311	0.314	0.308	0.311	0.311
Ch 11	0.302	0.301	0.307	0.307	0.295	0.303	0.305	0.311	0.316	0.307
Ch 12	0.306	0.319	0.321	0.378	0.299	0.318	0.325	0.309	0.313	0.314
Ch 13	0.293	0.298	0.306	0.321	0.298	0.364	0.294	0.312	0.320	0.312
Ch 14	0.301	0.295	0.305	0.313	0.305	0.326	0.312	0.312	0.307	0.309
Ch 15	0.317	0.314	0.304	0.313	0.307	0.316	0.313	0.306	0.308	0.311
Ch 16	0.312	0.314	0.309	0.311	0.309	0.315	0.302	0.308	0.315	0.310
Ch 17	0.298	0.305	0.311	0.305	0.307	0.312	0.297	0.305	0.307	0.303
Ch 18	0.304	0.303	0.301	0.303	0.301	0.297	0.295	0.305	0.308	0.299
Ch 19	0.287	0.313	0.320	0.328	0.308	0.339	0.312	0.321	0.367	0.310
Ch 20	0.296	0.314	0.322	0.304	0.299	0.307	0.314	0.311	0.322	0.308
Ch 21	0.297	0.300	0.318	0.331	0.306	0.316	0.341	0.315	0.329	0.319

Table 8-8: Fractal dimension of the Time-Incoherent cross-correlation for AD3 (Part 2).

	Ch 11	Ch 12	Ch 13	Ch 14	Ch 15	Ch 16	Ch 17	Ch 18	Ch 19	Ch 20	Ch 21
Ch 1	0.283	0.286	0.292	0.310	0.305	0.311	0.304	0.297	0.308	0.303	0.300
Ch 2	0.310	0.308	0.304	0.295	0.301	0.316	0.295	0.304	0.306	0.295	0.311
Ch 3	0.323	0.316	0.312	0.299	0.312	0.306	0.303	0.298	0.308	0.310	0.349
Ch 4	0.311	0.323	0.329	0.301	0.316	0.311	0.309	0.307	0.326	0.317	0.377
Ch 5	0.295	0.296	0.300	0.307	0.308	0.304	0.310	0.303	0.301	0.308	0.306
Ch 6	0.347	0.463	0.447	0.311	0.330	0.340	0.369	0.310	0.659	0.340	0.509
Ch 7	0.311	0.335	0.319	0.315	0.318	0.311	0.291	0.299	0.335	0.309	0.346
Ch 8	0.310	0.308	0.312	0.314	0.309	0.305	0.305	0.312	0.311	0.314	0.314
Ch 9	0.321	0.320	0.315	0.319	0.311	0.313	0.304	0.312	0.342	0.325	0.320
Ch 10	0.312	0.310	0.309	0.304	0.309	0.317	0.311	0.303	0.316	0.309	0.313
Ch 11	0.300	0.305	0.316	0.303	0.304	0.309	0.305	0.306	0.313	0.307	0.311
Ch 12	0.306	0.316	0.325	0.313	0.315	0.314	0.297	0.308	0.322	0.306	0.370
Ch 13	0.300	0.310	0.306	0.307	0.323	0.313	0.299	0.304	0.304	0.339	0.335
Ch 14	0.309	0.309	0.300	0.297	0.313	0.315	0.302	0.305	0.316	0.310	0.325
Ch 15	0.308	0.317	0.316	0.305	0.313	0.316	0.310	0.306	0.308	0.324	0.321
Ch 16	0.308	0.310	0.319	0.303	0.319	0.313	0.317	0.312	0.312	0.313	0.327
Ch 17	0.301	0.307	0.302	0.301	0.308	0.301	0.303	0.300	0.304	0.308	0.314
Ch 18	0.300	0.304	0.306	0.297	0.304	0.307	0.300	0.298	0.305	0.297	0.307
Ch 19	0.321	0.315	0.330	0.313	0.314	0.328	0.298	0.302	0.338	0.315	0.363
Ch 20	0.297	0.322	0.304	0.307	0.316	0.309	0.303	0.311	0.326	0.314	0.321
Ch 21	0.303	0.333	0.329	0.340	0.311	0.317	0.302	0.310	0.407	0.311	0.411

The following four tables (Table 8-9 through Table 8-12) show the alpha/beta ratio derived from the fractal dimension measures described in section 4.4.3.2 applied to the evaluation data set.

	Normal	Alzheimer's	Vascular
Results	0.9916	0.8233	0.9874
	0.9580	0.8069	0.9916
	0.9916	0.9622	0.8069
	0.9280	0.7542	0.9748
	0.9703	0.9283	0.8945
	0.9068	0.5848	
	0.9538	0.9030	
	0.9790	0.7342	
	1.0000	0.9359	
	0.9440	0.4670	
	0.9873	0.5551	
	0.8918	0.9538	
	0.9958	0.9034	
	0.9916	0.5516	
	0.9872	0.9286	
	0.9706	0.5628	
	1.0000	0.9874	
	0.9706		
	0.9580		
	0.9916		
	0.9748		
	0.9916		
	0.9790		
	0.9790		
Number of samples	24	17	5
Mean	0.9705	0.7848	0.9310
SD	0.0286	0.1761	0.0799

Table 8-9, Alpha/Theta results from the Zero-Set method applied to the Raw EEG.

	Normal	Alzheimer's	Vascular
Results	0.9156	0.2761	0.8113
	0.7422	0.6398	0.6989
	0.5328	0.5979	0.4728
	0.4681	0.3519	0.6591
	0.5652	0.5026	0.5714
	0.1707	0.2065	
	0.4167	0.6995	
	0.6927	0.3750	
	0.9615	0.4516	
	0.3393	0.2000	
	0.9318	0.3795	
	0.4255	0.1875	
	0.4063	0.3353	
	0.6082	0.1441	
	0.6946	0.6631	
	0.4956	0.3523	
	0.9565	0.4787	
	0.8350		
	0.7957		
	0.9074		
	0.7854		
	0.7867		
	0.8429		
	0.5575		
Number of samples	24	17	5
Mean	0.6597	0.4024	0.6427
SD	0.2212	0.1747	0.1283

Table 8-10, Alpha/Theta results from the Zero-Set method applied to the Auto-correlation function.

	Normal	Alzheimer's	Vascular
Results	0.9832	0.7059	0.9706
	0.9496	0.5294	0.9790
	0.9958	0.9160	0.5756
	0.9580	0.5294	0.9874
	0.9874	0.8193	0.8529
	0.9496	0.3489	
	0.9580	0.8025	
	0.9790	0.4958	
	1.0000	0.8908	
	0.9538	0.1441	
	0.9873	0.1429	
	0.8067	0.9622	
	1.0000	0.8109	
	0.9958	0.3008	
	0.9622	0.8151	
	0.9580	0.1483	
	1.0000	0.9790	
	0.9790		
	0.9832		
	0.9916		
	0.9706		
	0.9916		
	0.9748		
	0.9874		
Number of samples	24	17	5
Mean	0.9709	0.6083	0.8731
SD	0.0388	0.3003	0.1751

Table 8-11, Alpha/Theta results from the Adapted Box method applied to the Raw EEG.

	Normal	Alzheimer's	Vascular
Results	0.7679	0.0155	0.4515
	0.2979	0.1342	0.3803
	0.2247	0.2712	0.0651
	0.1571	0.0000	0.3305
	0.2183	0.0381	0.0705
	0.0198	0.0054	
	0.1556	0.1556	
	0.3305	0.0140	
	0.8277	0.0448	
	0.0744	0.0000	
	0.8326	0.0090	
	0.0744	0.0286	
	0.1076	0.0221	
	0.4538	0.0000	
	0.3915	0.1135	
	0.1717	0.0000	
	0.9286	0.1034	
	0.6769		
	0.6157		
	0.8376		
	0.5636		
	0.7009		
	0.6580		
	0.1921		
Number of samples	24	17	5
Mean	0.4283	0.0562	0.2596
SD	0.2951	0.0754	0.1803

Table 8-12, Alpha/Theta results from the Adapted Box method applied to the Auto-correlation function.